Archives of Endocrinology and Metabolism

ISSN 2359-4292

OFFICIAL JOURNAL OF THE BRAZILIAN SOCIETY OF ENDOCRINOLOGY AND METABOLISM

Vol. 70 – No. 02 – April 2026

editorial

Obesity in Brazil: 214 million reasons to act
Bruno Halpern, Maria Edna de Melo

originals

Higher consumption of ultra-processed foods is associated with disordered eating symptoms and low-quality diet in adults with obesity
Carolina Machado Favaron, Marcos Mônico-Neto, Hanna Karen Moreira Antunes, Lia Rita Azeredo Bittencourt, Thales Delmondes Galvão, Sergio Tufik, Raquel Munhoz da Silveira Campos

Extracellular vesicles related to familial hypercholesterolemia
Júnea P. de P. Silvino, Cinthia E. Jannes, Rodrigo M. C. Pestana, Lucas P. de P. Silvino, Iêda de F. O. Silva, Andréa Teixeira-Carvalho, Karina B. Gomes

Intact and bioactive PTH values are strongly correlated in kidney transplant recipients
Tábata Carolina Faria Nascimento de Assis, Humberto Campos Clemente, Daniel Borges Drumond, Leandro Junior Lucca, Miguel Moyses-Neto, Francisco José Albuquerque de Paula, Elen Almeida Romão

Accuracy of clinical risk factor-based models as a screening test for detecting gestational diabetes mellitus in a low-resource setting
Olayinka Comfort Senbanjo, Fatimat Motunrayo Akinlusi, Kabiru Afolarin Rabiu

MicroRNAs miR-29a-3p and miR-192-5p: promising urinary biomarkers for kidney function loss
Cristine Dieter, Eliandra Girardi, Marcia Puñales, Daisy Crispim,

Differences in the aggressiveness of familial versus sporadic non-medullary thyroid cancer: An unresolved controversy
Fabíola Yukiko Miasaki, Teresa Cristina Santos Cavalcanti, Hans Graf, Edna Teruko Kimura, Peter Andreas Kopp, Gisah Amaral de Carvalho

Non-invasive detection of metastatic papillary thyroid carcinoma after radical surgery using salivary metabolomic biomarkers
Fei Yu, Jingya Pan, Liuting Zhang, Shaohua Li, Chuan Zhang, Jingjing Fu, Peng Zhou, Jun Wang, Xiaochen Yao, Yudan Ni, Ailing Zhang, Qingle Meng, Rui Yang, Lei Xu, Feng Wang, Jianhua Wang, Liang Shi

Comparative diagnostic accuracy of the triglyceride/HDL-c ratio and lipid accumulation product index for the early detection of metabolic syndrome among adults with obesity in Indonesia: findings from the 2023 Health Survey
Alya Ayu Alvitananda, Etika Ratna Noer, Ahmad Syauqy, Edward Kurnia Setiawan Limijadi, Adriyan Pramono

Evaluation of breast calcification, calcification characteristics, and BI-RADS categories in patients with primary hyperparathyroidism
Fatma Dilek Dellal Kahramanca, Sevgul Faki, Ekin Yigit Koroglu, Arzu Ozsoy, Ahmet Dirikoc, Oya Topaloglu, Reyhan Ersoy, Bekir Cakir

Evaluation of three inflammation-associated blood indices for predicting malignancy in thyroid nodules
Merve Çatak, Bülent Koca, Zeynep Çetin, Özden Özdemir BAŞER

The decline of iodine therapy in the treatment of Graves' disease in a hospital center: a 20-year analysis
Isabela Busto Silva, Gisah Amaral de Carvalho, Fabíola Yukiko Miasaki, João Pedro Ignotti de Almeida, Matheus Pessini Sousa, Caio Pereira Mueller, Hans Graf, Mariana Driesel Bertolin, Cléo Otaviano Mesa Júnior

Role of insulin-regulated aminopeptidase as potential biomarker in insulin resistant polycystic ovary syndrome patients
Osman Köse, Koray Gök, Elif Köse, Sezen Irmak Gözükara, Abdullah Tüten, Mehmet Sühha Bostancı

case reports

Immunotherapy response in microsatellite-stable poorly differentiated thyroid carcinoma with mismatch repair deficiency and high tumor mutational burden
João Henrique Feldmann, João Felipe Feldmann, Cassio Murilo Hidalgo-Filho, Gustavo Luis Contado Alves, Sérgio Gonçalves, Gilberto de Castro Júnior

From amenorrhea to pregnancy: spontaneous recovery of the female athlete triad during the COVID-19 pandemic
Eduardo Medeiros Ferreira da Gama, Francisco de Paula Paranhos-Neto, Miguel Madeira, Laura Maria Carvalho Mendonça, Maria Lucia Fleiuss Farias

Identification of a novel *THRB* mutation causing thyroid hormone resistance syndrome
Jing Yang, Chuan Wang, Li Quan, Sheng Jiang

brief communication

Challenging the recessive paradigm of Mahvash disease: heterozygous phenotypes from a novel splice-site variant
Francisco Martínez Bugallo, Gema García de la Rosa, Carol Prieto-Morín

letters to the editor

Comment on suspicious for malignancy cytology: nuclear characteristics deserve special attention in reported cytology analysis – real-world scenario cohort in thyroidology
Ilker Sengul, Demet Sengul

Response to the letter to the editor: Appraisal of suspicious for malignancy cytology: nuclear characteristics deserve special attention in reported cytology analysis – real-world scenario cohort in thyroidology
Fabiane Carvalho Macedo, Ricardo Luiz Costantin Delfim, Fernanda Vaisman

Comment on the "Evaluation of sensory loss in the feet and associated factors in ambulatory patients with diabetes: a cross-sectional study"
Han Gao

SBEM
Sociedade Brasileira de Endocrinologia e Metabologia

Archives of Endocrinology and Metabolism

OFFICIAL JOURNAL OF THE BRAZILIAN SOCIETY OF ENDOCRINOLOGY AND METABOLISM

Editorial supervisor: Roselaine Monteiro
roselaine@endocrino.org.br

Rua Botucatu, 572 – conjunto 83 – 04023-062 – São Paulo, SP
Telefax: (11) 5575-0311 / 5082-4788

Online submission / Electronic publishing
www.aem-sbem.com • www.scielo.br/abem

SANTANA
Serviços Editoriais
sfsantana3@gmail.com.br

Indexed in Biological Abstracts, Index Medicus, Latindex, Lilacs, MedLine, PubMed, SciELO, Scopus, ISI-Web of Science

BRAZILIAN ARCHIVES OF ENDOCRINOLOGY AND METABOLISM
Brazilian Society of Endocrinology and Metabolism – São Paulo, SP:
Brazilian Society of Endocrinology and Metabolism, volume 5, 1955-
Six issues/year
Continued from: Brazilian Archives of Endocrinology (v. 1-4), 1951-1955
ISSN 2359-4292 (online issues)

1. Endocrinology – journals 2. Metabolism – journals
I. Brazilian Society of Endocrinology and Metabolism II. Brazilian Medical Association

CDU 612.43 Endocrinology
CDU 612.015.3 Metabolism

Archives of Endocrinology and Metabolism

OFFICIAL JOURNAL OF THE BRAZILIAN SOCIETY OF ENDOCRINOLOGY AND METABOLISM

Archives of endocrinology and metabolism Official journal of **SBEM** – Brazilian Society of Endocrinology and Metabolism (Department of the Brazilian Medical Association), **SBD** – Brazilian Diabetes Society, **ABESO** – Brazilian Association for the Study of Obesity and Metabolic Syndrome

2024-2026



EDITOR-IN-CHIEF
Cesar Luiz Boguszewski (PR)

DEPUTY EDITORS
Madson Queiroz de Almeida (SP)
Marcio C. Mancini (SP)

ASSOCIATED EDITORS
Celia Regina Nogueira (SP)
Davi Casale Aragon (SP)
Fernanda Vaisman Balieiro (RJ)
João Roberto de Sá (SP)
Jose A. Sgarbi (SP)
Josivan Gomes de Lima (RN)
Larissa Garcia Gomes (SP)
Leandro Kasuki (RJ)
Letícia F. Gontijo Silveira (MG)
Luiz Claudio Gonçalves de Castro (DF)
Madson Queiroz de Almeida (SP)
Marcelo A. Mori (SP)
Marcio C. Mancini (SP)
Marcio W. Lauria (MG)
Maria Candida Barisson (SP)
Maria Tereza Nunes (SP)
Mario José Abdalla Saad (SP)
Marise Lazaretti-Castro (SP)
Melanie Rodacki (RJ)
Miguel Madeira (RJ)
Rodrigo de Oliveira Moreira (RJ)
Sonir R. Antonini (SP)
Simone van de Sande Lee (SC)
Vania dos Santos Nunes-Nogueira (SP)

EDITORIAL COMMISSION
Alexandre Hohl (SC)
Ana Amélia Hoff (SP)
Andrea Glezer (SP)
Ayrton Custódio Moreira (SP)
Berenice B. Mendonça (SP)
Caroline k Kramer (Toronto)
Catarina Brasil d'Alva (SP)
Dalisbor Marcelo Weber da Silva (PR)
Daisy Crispim Moreira (RS)
Décio Laks Eizirik (Brussels)
Edna Nakandakare (SP)
Edna T. Kimura (SP)
Eduardo Coelho Machado (RS)
Fabio Vasconcellos Comim (MG)
Flávia Amanda Costa Barbosa (SP)
Flavio Hojaij (SP)
Gabriela Heiden Teló (RS)
Gil Guerra-Júnior (SP)
Gisah M. do Amaral (PR)
Hermelinda Cordeiro Pedrosa (DF)
Isabela Judith Benseñor (SP)
Itamar de Souza Santos (SP)
Janice Sepúlveda Reis (MG)
José Augusto Sgarbi (SP)
Julio Z. Abucham (SP)
Luis Henrique Santos Canani (RS)
Luiz Eduardo Armondi Wildemberg (RJ)
Manoel Ricardo Alves Martins (CE)
Marcos Tadashi Kakitani Toyoshima (SP)
Marilia de Brito Gomes (RJ)
Margaret Cristina da Silva Boguszewski (PR)
Melissa Premaor (MG)
Michele Drehmer (RS)
Roberta Cobas (RJ)
Sandra R. G. Ferreira (SP)
Simone Van den Sande Lee (SC)
Sergio Atala Did (SP)
Suemi Marui (SP)
Tânia Aparecida Sanchez Bachega (SP)
Victória Borba (PR)

COORDINATORS OF THE SBEM DEPARTMENTS
ADRENAL AND HYPERTENSION
Flávia Amanda Costa Barbosa (SP)

BASIC ENDOCRINOLOGY
Maria Tereza Nunes (SP)

DIABETES MELLITUS
Ruy Lyra da Silva Filho (PE)

DYSLIPIDEMIA AND ATHEROSCLEROSIS
Márcio Weissheimer Lauria (MG)

ENDOCRINOLOGY OF SPORT AND EXERCISE
Andréa Messias Britto Fioretti (SP)

WOMEN ENDOCRINOLOGY, ANDROLOGY AND TRANSGENERITY
Tayane Muniz Fighera (RS)

PEDIATRIC ENDOCRINOLOGY
Luiz Cláudio Gonçalves de Castro (DF)

BONE AND MINERAL METABOLISM
Francisco José Albuquerque de Paula (SP)

NEUROENDOCRINOLOGY
Andrea Glezer (SP)

OBESITY
Fábio Rogério Trujilho (BA)

THYROID
Rafael Selbach Scheffel (RS)

REPRESENTATIVES OF COLLABORATING SOCIETIES

SBD
Ruy Lyra da Silva Filho (PE)

ABESO
Fábio Rogério Trujilho (BA)

FOUNDER
Waldemar Berardinelli (RJ)

EDITORS-IN-CHIEF, EDITORIAL OFFICE*
1951-1955
Waldemar Berardinelli (RJ)
Thales Martins (RJ)

1957-1972
Clementino Fraga Filho (RJ)

1964-1966*
Luiz Carlos Lobo (RJ)

1966-1968*
Pedro Collett-Solberg (RJ)

1969-1972*
João Gabriel H. Cordeiro (RJ)

1978-1982
Armando de Aguiar Pupo (SP)

1983-1990
Antônio Roberto Chacra (SP)

1991-1994
Rui M. de Barros Maciel (SP)

1995-2006
Claudio Elias Kater (SP)

2007-2010
Edna T. Kimura (SP)

2011-2014
Sergio Atala Dib (SP)

2015-2022
Marcello D. Bronstein (SP)

2022-2023
Beatriz D'Agord Schaan (RS)

SBEM
Sociedade Brasileira de Endocrinologia e Metabologia

Sociedade Brasileira de Endocrinologia e Metabologia

2025-2026



NEUTON DORNELAS GOMES (DF)
President



KAREN FAGGIONI DE MARCA SEIDEL (RJ)
President-Elect



FLÁVIA COIMBRA PONTES MAIA (MG)
Executive Secretary



FÁBIO FERREIRA MOURA (PE)
Treasurer-General



MARISE LAZARETTI CASTRO (SP)
Scientific Director



CLAYTON LUIZ DORNELLES MACEDO (RS)
Director of Communications

SCIENTIFIC DEPARTMENTS – 2025/2026

ACCESS THE WEBSITE

ADRENAL AND HYPERTENSION

Coordinator: Flávia Amanda Costa Barbosa (SP)
Subcoordinator: Adriane Maria Rodrigues (PR)
Directors: Aline Barbosa Moraes (RJ)
Leonardo Vieira Neto (RJ)
Maria Candida Barisson Villares Fragoso (SP)
Rafael Buck Giorgi (SP)
Thaís Castanheira de Freitas Resende (GO)

ACCESS THE WEBSITE

BASIC ENDOCRINOLOGY

Coordinator: Maria Tereza Nunes (SP)
Subcoordinator: Luciani Renata Silveira de Carvalho (SP)
Directors: Carolina Ferraz da Silva (SP)
Lucas Leite Cunha (SP)
Manuela Giuliani Marcondes Rocha Braz (SP)
Milena Gurgel Teles Bezerra (CE)
Rafael Loch Batista (SP)

ACCESS THE WEBSITE

DIABETES MELLITUS

Coordinator: Ruy Lyra da Silva Filho (PE)
Subcoordinator: Saulo Cavalcanti da Silva (MG)
Directors: Fernando Valente (SP)
João Modesto Filho (PB)
Marcello Casaccia Bertoluci (RS)
Rodrigo de Oliveira Moreira (RJ)
Wellington Santana da Silva Junior (PI)

ACCESS THE WEBSITE

DYSLIPIDEMIA AND ATHEROSCLEROSIS

Coordinator: Márcio Weissheimer Lauria (MG)
Subcoordinator: Renan Magalhães Montenegro Junior (CE)
Directors: Joaquim Custódio da Silva Junior (BA)
Joana Rodrigues Dantas Vezzani (RJ)
Lúcia Helena Oliveira Cordeiro (PE)
Marcello Casaccia Bertoluci (RS)
Maria Helane Costa Gurgel Castelo (CE)

ACCESS THE WEBSITE

ENDOCRINOLOGY OF SPORT AND EXERCISE

Coordinator: Andréa Messias Britto Fioretti (SP)
Subcoordinator: Rogério Friedman (RS)
Directors: Alexis Dourado Guedes (BA)
Cristina da Silva Schreiber de Oliveira (SC)
Cristiano Roberto Grimaldi Barcellos (SP)
Fúlvio Clemo Santos Tomaselli (SC)
João Carlos Ramos-Dias (SP)

ACCESS THE WEBSITE

WOMEN ENDOCRINOLOGY, ANDROLOGY AND TRANSGENERITY

Coordinator: Tayane Muniz Fighera (RS)
Subcoordinator: Poli Mara Spritze (RS)
Directors: Alexandre Hohl (SC)
Elaine Maria Frade Costa (SP)
Fábio Vasconcellos Comim (MG)
Marcelo Fernando Ronsoni (SC)
Thyciara Fontenele Marques (CE)

ACCESS THE WEBSITE

PEDIATRIC ENDOCRINOLOGY

Coordinator: Luiz Cláudio Gonçalves de Castro (DF)
Subcoordinator: Sonir Roberto Rauber Antonini (SP)
Directors: Ana Pinheiro Machado Canton (SP)
Gil Guerra Júnior (SP)
Jacqueline Rosângela de Araújo (PE)
Margaret Cristina da Silva Boguszewski (PR)
Nathália Lisboa Rosa Almeida Gomes (MG)

ACCESS THE WEBSITE

BONE AND MINERAL METABOLISM

Coordinator: Francisco José Albuquerque de Paula (SP)
Subcoordinator: Narriane Chaves Pereira de Holanda (PB)
Directors: Bárbara Campolina Carvalho Silva (MG)
Catarina Brasil d'Alva (CE)
Érico Higino Carvalho (PE)
Leonardo Costa Bandeira e Farias (PE)
Victória Zeghbi Cochenski Borba (PR)

ACCESS THE WEBSITE

NEUROENDOCRINOLOGY

Coordinator: Andrea Glezer (SP)
Subcoordinator: Vania dos Santos Nunes Nogueira (SP)
Directors: Beatriz Santana Soares Rocha (MG)
Guilherme Alcides Flôres Soares Rollin (RS)
Leandro Kasuki Jomori de Pinho (RJ)
Manoel Ricardo Alves Martins (CE)
Paula Condé Lamparelli Elias (SP)

ACCESS THE WEBSITE

OBESITY

Coordinator: Fábio Rogério Trujilho (BA)
Subcoordinator: Cynthia Melissa Valério (RJ)
Directors: Bruno Halpern (SP)
Cintia Cercato (SP)
Fernando Gerchman (RS)
Simone Van de Sande Lee (SC)
Thaisa Dourado Guedes Trujilho (BA)

ACCESS THE WEBSITE

THYROID

Coordinator: Rafael Selbach Scheffel (RS)
Subcoordinator: Cléo Otaviano Mesa Júnior (PR)
Directors: Adriano Namo Cury (SP)
Caroline Serrano do Nascimento (SP)
Fernanda Vaisman Balieiro (RJ)
Raquel Andrade de Siqueira (GO)
Susan Chow Lindsey (SP)

PERMANENT COMMISSIONS - 2025/2026

SCIENTIFIC COMMITTEE

Coordinator: Sergio Setsuo Maeda (SP)

Members

Ana Cláudia Latronico (SP)
Caroline Serrano (SP)
Cintia Cercato (SP)
Daniela Espíndola (GO)
Fernanda Vaisman (RJ)
Fernando Giuffrida (BA)
Josivan Lima (RN)
Mônica de Oliveira (PE)
Rodrigo Lamounier (MG)
Sonir Roberto Antonini (SP)
Carolina Garcia Soares Leães (RS)

Members – Local Scientific Committee

Cristiane Leitão (RS)
Fernando Gerchman (RS)
Rafael Selbach Scheffel (RS)
Polimara Spritzer (RS)

COMMITTEE FOR DIVERSITY, EQUITY, AND INCLUSION (CDEI)

Coordinator: Luciana Mattos Barros Oliveira (BA)

Members

Amanda de Araujo Laudier (RJ)
Erik Trovão Diniz (PE)
Flavia Amanda Costa Barbosa (SP)
Lia Lousada (CE)
Andreza Cristina Oliveira Berlink (BA)

COMMITTEE ON THE HISTORY OF ENDOCRINOLOGY AND METABOLISM (CHEM)

Coordinator: Henrique de Lacerda Suplicy (PR)

Members

Cláudio Elias Kater (SP)
Adriana Costa e Forti (CE)
Mauro Antônio Czepielewski (RS)

CAMPAIGN COMMITTEE (CC)

Members

Mateus Dornelles Severo (RS)
Georgia Martina Chichelero (RS)
Rafael Buck Giorgi (SP)
Leonardo Barbi Walter (RS)
Wellington Santana da Silva Junior (MA)
Mariana Guerra Paulino Guerra (ES)
Ximene Antunes (RJ)

PROFESSIONAL ETHICS AND DEFENCE COMMITTEE (CDP)

Coordinator: Ana Karina de Melo Bezerra Sodré (CE)

Members

Adauto Versiani Ramos (MG)
Adriano Namo Cury (SP)
Maria Augusta Karas Zella (PR)

CONTINUING MEDICAL EDUCATION COMMITTEE (CEMC)

Coordinator: Manoel Martins (CE)

Members

Milena Gurgel Teles (CE)
Carolina Castro Porto Silva Janovsky (SP)
André Gonçalves (PI)
Larissa Garcia Gomes (SP)

ENVIRONMENTAL ENDOCRINOLOGY COMMITTEE (CEA)

Coordinator: Elaine Maria Frade Costa (SP)

Members

Eveline Gadelha Pereira Fontenele (CE)
Maria Tereza Nunes (SP)
Caroline Serrano (SP)
Luiz Cláudio Castro (DF)

RARE ENDOCRINE DISEASES COMMITTEE (ENDO-RARAS)

Coordinator: Fernanda Azevedo Correa (Switzerland)

Members

José Viana Lima Junior (SP)
Nathalia Lisboa (MG)
Berenice Bilharinho de Mendonça (SP)
Luiz Cláudio Castro (DF)
Margaret Boguszewski (PR)
Renata Scalco (SP)

BYLAWS AND REGULATORY AFFAIRS COMMITTEE

Coordinator: Rui Monteiro de Barros Maciel (SP)

Members

Paulo Augusto Carvalho Miranda (MG)
Alana Abrantes Nogueira de Pontes (PB)
Rafael Selbach Scheffel (RS)
Paulo Lacativa (RJ)

ETHICS COMMITTEE (CE)

Inspector General: Diana Viegas Martins (BA)
Deputy Coordinator: Luciana Antunes de Almeida Secchi (MS)
1st Board Member: Itairan da Silva Terres (SC)
2nd Board Member: Angela Maria Spinola e Castro (SP)
Member: Marília Gabriela Zanier Gomes (GO)

MEDICAL TRAINING IN ENDOCRINOLOGY AND METABOLISM COMMITTEE

Coordinator: Milena Coelho Fernandes Caldato (PA)

Members

Marcia Helena Soares Costa (RJ)
Luciana Ansaneli Naves (DF)
Rafael Buck Giorgi (SP)

INSTITUTIONAL RELATIONS AND PUBLIC POLICY COMMITTEE

Coordinator: João Lindolfo Cunha Borges (DF)

Members

Maria Edna de Melo (SP)

COMMITTEE FOR THE PROMOTION OF NEW LEADERSHIP (CVNL)

Coordinator: Victoria Rodrigues Granja Alencar (PE)

Members

Leonardo Barbi Walter (RS)
Antonio Bentes de Figueiredo Junior (SP)
Isabella Santiago de Melo Miranda (DF)
Raquel Beatriz Gonçalves Muniz (RJ)

SPECIALIST TITLE IN ENDOCRINOLOGY AND METABOLISM COMMITTEE

Coordinator: Rodrigo de Oliveira Moreira (RJ)
Deputy Coordinator: Maria Edna de Melo (SP)

Members

Margaret de Castro (SP)
Miguel Madeira (RJ)
Monike Lourenço Dias Rodrigues (GO)
Marcelo Fernando Ronsoni (SC)
Cléo Otaviano Mesa Júnior (PR)

INTERNATIONAL COMMITTEE (CI)

Coordinator: Paulo Augusto Carvalho Miranda (MG)

Members

Ana Luiza Maia (RS)
Luciana Ansaneli Naves (DF)
Madson Queiroz de Almeida (SP)
Junia R.O.L Sweizer (Germany)

TEMPORARY COMMITTEE ON ARTIFICIAL INTELLIGENCE AND TECHNOLOGIES IN ENDOCRINOLOGY AND METABOLISM (CIATEM)

Coordinator: Marcio Krakauer (SP)

Members

Walmir Ferreira Coutinho (RJ)
Edson Perrotti Santos (AL)
Felipe Henning Gaia Duarte (SP)
Milena Gurgel Teles Bezerra (CE)

Archives of Endocrinology and Metabolism
ISSN 2359-4292
OFFICIAL JOURNAL OF THE BRAZILIAN SOCIETY OF ENDOCRINOLOGY AND METABOLISM

editorial

Obesity in Brazil: 214 million reasons to act

Bruno Halpern[1,2,3]
https://orcid.org/0000-0003-0973-5065

Maria Edna de Melo[2,3]
https://orcid.org/0000-0002-1216-7532

[1] World Obesity Federation (WOF), London, UK
[2] Grupo de Obesidade, Departamento de Endocrinologia, Universidade de São Paulo, São Paulo, SP, Brasil
[3] Departamento de Advocacy, Associação Brasileira para o Estudo da Obesidade e Síndrome Metabólica (ABESO), São Paulo, SP, Brasil

World Obesity Day was established by the World Obesity Federation in 2015 and, since 2020, has been celebrated on March 4th as a strategy to raise awareness of the importance of unified actions to tackle the obesity epidemic, which is continuously growing worldwide, with no signs of reduction (1,2). This increase has been more rapid in low- and middle-income countries and, within countries, has been disproportionately higher among vulnerable populations and younger individuals (1,2).

In 2026, the campaign motto is "8 billion reasons to act", referring to the current world population. Why is that? The World Obesity Federation (WOF) Atlas shows that, at this very moment, half of humanity lives with overweight or obesity, including more than one billion people with obesity itself (3). However, discussing and acting on obesity is a matter that concerns everyone. Obesity is associated with more than 200 diseases, increased disability and mortality, and major impairment in quality of life (2,4). Its impact extends beyond those who live with the disease, affecting society as a whole. As an example, the obesity epidemic imposes a substantial economic burden through direct healthcare costs and indirect costs such as work absenteeism (5), and it also impacts climate change and sustainability (6). Furthermore, providing healthy environments for people living with chronic diseases — especially children — is a human right that should be defended collectively.

In Brazil, as expected, the scenario is extremely concerning. The 2025 World Obesity Atlas showed that, for the first time, more than 30% of the population has obesity and 68% has at least overweight (3). According to WOF data from 2024, the projected annual growth rate in prevalence is 1.8% (7). Among children and adolescents, it is estimated that, in the absence of effective interventions, half will have excess weight by 2050 (7). Even under highly optimistic prevention scenarios, prevalence is expected to continue rising in the coming years and decades (8).

What can be done? First and foremost, it is essential to recognize that the obesity crisis requires actions in both prevention and treatment, not one instead of the other (2).

Brazil has one of the most internationally recognized and awarded Food-Based Dietary Guidelines, with a strong recommendation for "eating real food" and reducing the consumption of ultra-processed foods (UPFs) (9). For context, the concept of UPFs derives from the NOVA classification, developed in Brazil and now widely adopted internationally (10). High UPFs consumption has been repeatedly associated with at least 32 adverse health outcomes, far beyond obesity alone (10,11). In this issue of *Archives of Endocrinology and Metabolism*, Favaron and cols. provide cross-sectional evidence that adds to this body of literature (12). The authors show that a higher proportion of calories from UPFs is associated with poorer diet quality and more disordered eating patterns, including bulimia. Individuals in the highest tertile of

Received on Jan/22/2026
Accepted on Jan/26/2026
DOI: 10.20945/2359-4292-2026-0009

Correspondence to:
Bruno Halpern
brunohalpern@hotmail.com

Editor in Chief:
Cesar Luiz Boguszewski
https://orcid.org/0000-0001-7285-7941

This is an open-access article distributed under the terms of the Creative Commons Attribution License

Copyright© AE&M all rights reserved.

UPFs intake presented higher scores for binge eating and bulimia symptoms, as well as greater emotional, external, and uncontrolled eating, and lower intake of minimally processed foods and protein. These findings suggest that UPFs may not only worsen nutritional quality but also be linked to neurobehavioral mechanisms that favor loss of control over eating, reinforcing maladaptive eating behaviors in obesity. Although similar associations have been described previously (13), a more comprehensive understanding of the relationship between UPFs, mental health, and disordered eating is still lacking. Nevertheless, the available data support the need for more active public actions to reduce UPFs consumption in Brazil.

However, implementing dietary guidelines and reducing UPFs intake is particularly challenging in vulnerable populations, in whom social and economic determinants strongly influence food choices (2,14). Unprocessed foods are often more expensive, whereas UPFs are cheap, ubiquitous, heavily marketed in traditional and social media, and easy to consume, requiring little or no preparation (10,14). As has already occurred in the United States and the United Kingdom, where UPFs account for approximately 60% of total dietary intake, the traditional Brazilian diet — based on home cooking and time for food preparation — is gradually being replaced by ultra-processed products (14). In Brazil, UPFs already contribute more than 20% of total energy intake, and this proportion is increasing every year (15).

Therefore, policies for obesity and other non-communicable diseases should prioritize structural public actions that increase the likelihood of healthy eating, rather than relying solely on generic recommendations for "better choices" without providing realistic conditions for change (2).

In 2022, the World Health Organization (WHO) launched the Acceleration Plan to Stop Obesity, and Brazil was identified as one of the front-runner countries (16). As with all health interventions, obesity prevention strategies should be guided by scientific evidence, not by opinion. The WHO highlights several policies that should be implemented, including taxation of sugar-sweetened beverages (SSBs) (16). During the Brazilian tax reform, taxation of UPFs was proposed; however, in 2024, an excise tax was approved only for soft drinks, after intense political debate and strong industry lobbying, not without many turnarounds. Considering the broad health impact of UPFs and the physiology of human eating behavior, which predisposes individuals to overconsume these products, fiscal policies should target far more than SSBs alone. Importantly, such strategies should not only increase taxes on unhealthy products — which could disproportionately affect vulnerable groups — but also reduce the cost of healthy foods, particularly fruits, vegetables, whole grains, and high-quality protein sources (16). The recent revision of the "*Cesta Básica*" (basic food basket — a list of essential foods for a minimum diet) introduced tax exemptions or reductions for some healthier foods; however, not all included items can be considered nutritionally adequate. Thus, although the tax reform represents a step forward, it remains modest and insufficient to produce a substantial population-level health impact (8).

The WHO also recommends additional measures, such as restricting the marketing of unhealthy foods, especially to children and adolescents; improving front-of-package labeling; strengthening school nutrition policies; and modifying the built environment to reduce physical inactivity (2,16). Several of these strategies have been partially implemented in Brazil, but their effectiveness has been limited. For example, the rapid growth of social media use among younger populations has not been accompanied by adequate regulation of food marketing on digital platforms, a challenge that extends beyond Brazil (17).

An integrated and unified strategy addressing all these fronts simultaneously is essential, as isolated measures are unlikely to be effective, particularly given the food industry's capacity to rapidly adapt and circumvent regulations (14).

The WOF is currently conducting the MAPPS II programme, which explores the perceptions and experiences of healthcare professionals, policymakers, and people living with obesity regarding existing policies, gaps, and priorities. This initiative aims to strengthen obesity prevention and care through improved evidence generation, coalition building, and policy engagement.

Copyright© AE&M all rights reserved.

Nevertheless, even the most effective prevention strategies will not solve the problem for those who already live with obesity, just as condom distribution alone does not address the needs of people already living with HIV (2). Therefore, advocacy for people living with obesity (PlwO) is crucial, despite the barriers imposed by structural stigma. In Brazil, ABESO has advanced this agenda by creating a "Lived Experience" Department and promoting the inclusion of PlwO in public health discussions and decision-making spaces.

Within the Brazilian Unified Health System (SUS), the only available treatment for obesity is bariatric surgery. Although highly effective and associated with substantial improvements in health and quality of life, it is restricted to individuals with severe obesity (class III or class II with comorbidities), is not scalable, and is offered to fewer than 10,000 patients per year, resulting in extremely long waiting lists. Moreover, surgery is indicated only after failure of clinical treatment, despite the fact that structured clinical care is largely unavailable. Postoperative nutritional supplementation is also not routinely provided, despite the known risk of micronutrient deficiencies (18).

Over the years, several proposals to incorporate obesity medications into the public system have been submitted, many led by ABESO, but all were rejected by the National Committee for Health Technology Incorporation (CONITEC), even in the presence of robust cost-effectiveness data. Non-pharmacological standards of care are also scarce, and the situation is aggravated by the lack of formal education in obesity within health professional training programs. As a result, most healthcare professionals, including physicians, graduate without adequate training in obesity, limiting their ability to provide effective and non-stigmatizing care.

With the growing evidence of the broad health benefits of modern obesity treatments — well beyond weight loss — and the publication of the WHO Guidelines on glucagon-like peptide-1 (GLP-1) receptor agonists for obesity (19), it is inevitable that pharmacological therapy will eventually be incorporated into SUS, at least for selected populations. This should occur sooner rather than later. The obesity crisis is not a problem of the future (2,3); it has been a reality for decades, and in Brazil alone there are more than 214 million reasons to act now.

Disclosure: Bruno Halpern has served as a consultant for Novo Nordisk, AstraZeneca, Merck, Eli-Lilly, Boehringer Ingelheim and Currax and gave paid lectures for Novo Nordisk, Eli-Lilly, Merck, Boehringer Ingelheim and Novartis. He is President-Elect of the World Obesity Federation and vice-president of ABESO, both unpaid works. Maria Edna de Melo has been on speakers' bureaus for EMS, Novo Nordisk, Merck; has received support for attending meetings and/or traveling from Novo Nordisk; has participated on advisory boards for Brace Pharma and Merck and works on the Advocacy Department of ABESO, unpaid.

Data availability: datasets related to this article will be available upon request to the corresponding author.

REFERENCES

1. GBD 2021 Adult BMI Collaborators. Global, regional, and national prevalence of adult overweight and obesity, 1990-2021, with forecasts to 2050: a forecasting study for the Global Burden of Disease Study 2021. Lancet. 2025 Mar 8;405(10481):813-838. doi: 10.1016/S0140-6736(25)00355-1.
2. Chandiwana N, Barquera S, Baur L, Buse K, Halford J, Halpern B, Jackson-Morris A, Mbanya JC, Nece P, Ralston J. Obesity is a disease: global health policy must catch up. Lancet Glob Health. 2025 Oct;13(10):e1659-e1660. doi: 10.1016/S2214-109X(25)00275-X.
3. World Obesity Federation. World Obesity Atlas 2025. London: World Obesity Federation; 2025.
4. GBD 2015 Obesity Collaborators; Afshin A, Forouzanfar MH, Reitsma MB, Sur P, Estep K, Lee A, et al. Health Effects of Overweight and Obesity in 195 Countries over 25 Years. N Engl J Med. 2017 Jul 6;377(1):13-27. doi: 10.1056/NEJMoa1614362.
5. Okunogbe A, Nugent R, Spencer G, Powis J, Ralston J, Wilding J. Economic impacts of overweight and obesity: current and future estimates for 161 countries. BMJ Glob Health. 2022 Sep;7(9):e009773. doi: 10.1136/bmjgh-2022-009773.
6. Swinburn BA, Kraak VI, Allender S, Atkins VJ, et al. The Global Syndemic of Obesity, Undernutrition, and Climate Change: The Lancet Commission report. Lancet. 2019
7. World Obesity Federation. World Obesity Atlas 2024. London: World Obesity Federation; 2024.
8. Nilson EAF, Gianicchi B, Ferrari G, Rezende LFM. The projected burden of non-communicable diseases attributable to overweight in Brazil from 2021 to 2030. Sci Rep. 2022 Dec 28;12(1):22483. doi: 10.1038/s41598-022-26739-1.
9. Brasil. Ministério da Saúde. Secretaria de Atenção à Saúde. Departamento de Atenção Básica. Guia alimentar para a população brasileira [Internet]. 2nd ed. Brasília: Ministério da Saúde; 2014 [cited 2026 Jan 21].
10. Monteiro CA, Louzada ML, Steele-Martinez E, Cannon G, Andrade GC, Baker P, et al. Ultra-processed foods and human health: the main thesis and the evidence. Lancet. 2025 Dec 6;406(10520):2667-2684. doi: 10.1016/S0140-6736(25)01565-X.
11. Lane MM, Gamage E, Du S, Ashtree DN, McGuinness AJ, Gauci S, et al. Ultra-processed food exposure and adverse health outcomes: umbrella review of epidemiological meta-analyses. BMJ. 2024 Feb 28;384:e077310. doi: 10.1136/bmj-2023-077310.
12. Favaron CM, Mônico-Neto M, Antunes HKM, Bittencourt LRA, Galvão TD, Tufik S. Higher consumption of ultra-processed foods is associated with disordered eating symptoms and low-quality diet in adults with obesity. Arch Endocrinol Metab. 2026;70(2):1-11, e260010. doi: 10.20945/2359-4292-2026-0010.

Copyright© AE&M all rights reserved.

13. Pereira T, Mocellin MC, Curioni C. Association between ultraprocessed foods consumption, eating disorders, food addiction and body image: a systematic review. BMJ Open. 2024 Dec 20;14(12):e091223. doi: 10.1136/bmjopen-2024-091223.
14. Popkin BM, Barquera S, Corvalan C, Hofman KJ, Monteiro C, Ng SW, Swart EC, Taillie LS. Towards unified and impactful policies to reduce ultra-processed food consumption and promote healthier eating. Lancet Diabetes Endocrinol. 2021 Jul;9(7):462-470. doi: 10.1016/S2213-8587(21)00078-4.
15. Louzada MLDC, Cruz GLD, Silva KAAN, Grassi AGF, Andrade GC, Rauber F, et al. Consumption of ultra-processed foods in Brazil: distribution and temporal evolution 2008-2018. Rev Saude Publica. 2023 Apr 14;57:12. doi: 10.11606/s1518-8787.2023057004744.
16. World Health Organization. WHO acceleration plan to stop obesity. Geneva: World Health Organization; 2023.
17. Mc Carthy CM, de Vries R, Mackenbach JD. The influence of unhealthy food and beverage marketing through social media and advergaming on diet-related outcomes in children-A systematic review. Obes Rev. 2022 Jun;23(6):e13441. doi: 10.1111/obr.13441.
18. Lingvay I, Cohen RV, Roux CWL, Sumithran P. Obesity in adults. Lancet. 2024 Sep 7;404(10456):972-987. doi: 10.1016/S0140-6736(24)01210-8.
19. Celletti F, Farrar J, De Regil L. World Health Organization Guideline on the Use and Indications of Glucagon-Like Peptide-1 Therapies for the Treatment of Obesity in Adults. JAMA. 2025 Dec 1. doi: 10.1001/jama.2025.24288

Copyright© AE&M all rights reserved.

Archives of Endocrinology and Metabolism
ISSN 2359-4292
OFFICIAL JOURNAL OF THE BRAZILIAN SOCIETY OF ENDOCRINOLOGY AND METABOLISM

original

Higher consumption of ultra-processed foods is associated with disordered eating symptoms and low-quality diet in adults with obesity

Carolina Machado Favaron[1]
https://orcid.org/0000-0003-4051-747X

Lia Rita Azeredo Bittencourt[3]
https://orcid.org/0000-0001-7738-0927

Raquel Munhoz da Silveira Campos[1]
https://orcid.org/0000-0001-6132-4349

Marcos Mônico-Neto[1,2]
https://orcid.org/0000-0002-9515-1260

Thales Delmondes Galvão[2]
https://orcid.org/0000-0003-2605-0797

Hanna Karen Moreira Antunes[1,3]
https://orcid.org/0000-0001-6648-0957

Sergio Tufik[3]
https://orcid.org/0000-0002-3804-8865

[1] Programa de Pós-graduação Interdisciplinar em Ciências da Saúde, Universidade Federal de São Paulo, Santos, SP, Brasil
[2] BariMais — Medicina Integrada, São Paulo, SP, Brasil
[3] Programa de Pós-graduação em Psicobiologia, Universidade Federal de São Paulo, São Paulo, SP, Brasil

ABSTRACT

Objective: This study aims to evaluate ultra-processed food consumption and eating behavior in adults with obesity. **Subjects and methods:** A cross-sectional study with 77 volunteers from São Paulo, Brazil. Food consumption was assessed using three 24-hour dietary recalls, classified by using the NOVA classification system, and the Diet Quality Index was also evaluated. Eating behavior and symptoms of binge eating and bulimia were assessed using the Bulimic Investigatory Test Edinburgh (BITE), the Dutch Eating Behaviour Questionnaire (DEBQ), and the Three Factor Eating Questionnaire (TFEQ-21). **Results:** The average BMI of the sample was 39.14 kg/m² ± 5.57, and the median caloric intake was 1661 kcal (756.07–4774.40), with a macronutrient distribution of 48% carbohydrates, 32% fat, and 20% protein. Volunteers were divided into tertiles of calories ingested from ultra-processed foods (%): 1st < 24.10% (n = 25); 2nd between 24.10%–35.40% (n = 26); and the 3rd > 35.40% (n = 26). The sample showed intermediate diet quality (43.08 ± 10.17), while the 3rd tertile presented a low-quality diet (37 ± 10), differing from other groups (p = 0.001; p = 0.003). All groups showed intermediate BITE scores (19,6 ± 9,8), an indicator of unusual eating behavior. The third tertile had a higher symptom score than the first tertile (p = 0.008). In the association analysis, the consumption of ultra-processed foods was positively associated with the presence of binge eating and bulimia symptoms (p = 0.018), emotional (p = 0.001) and external eating (p = 0.001) as assessed by the DEBQ, and emotional (p = 0.008) and uncontrolled eating (p = 0.006) as assessed by the TFEQ-21. In contrast, diet quality was negatively associated with the consumption of ultra-processed foods (p < 0.001). **Conclusion:** Our findings suggest that higher consumption of ultra-processed foods by volunteers with obesity may be associated with higher scores for unusual eating behavior, symptoms of binge eating, and bulimia, in addition to augmented emotional, external and uncontrolled eating, and lower diet quality scores.

Keywords: Obesity; ultra-processed foods; feeding and eating disorders; binge eating disorder; bulimia

INTRODUCTION

Nutritional transition is known to occur primarily in developing countries due to social, cultural, demographic, and economic factors. It is characterized by a reduction in infectious diseases and malnutrition cases, and an increase in obesity and non-communicable diseases, particularly driven by changes in dietary patterns with an increased consumption of foods rich in fats, especially of animal origin, sugar, and processed foods (1-3).

Currently, these foods can be defined by their degree of processing using the NOVA classification system, which categorizes ultra-processed foods as formulations prepared via various industrial techniques and the inclusion of food additives to increasing palatability, such as high-fructose corn syrup and hydrogenated oils, contributing to high fat and sugar content in these products (4).

Received on July/4/2025
Accepted on Dec/8/2025
DOI: 10.20945/2359-4292-2026-0010

Correspondence to:
Marcos Mônico-Neto
Programa de Pós-graduação Interdisciplinar em Ciências da Saúde,
Universidade Federal de São Paulo, Santos, SP, Brasil
Rua Silva Jardim, 136, térreo
11015020 – Santos, SP, Brasil
marcosmoniconeto@gmail.com

Associated editor:
Marcio C. Mancini
https://orcid.org/0000-0003-1278-0406

This is an open-access article distributed under the terms of the Creative Commons Attribution License

Copyright© AE&M all rights reserved.

High consumption of these foods has been associated with an increased prevalence of overweight and obesity (5-8), cardiovascular and cerebrovascular diseases (7,8), type 2 diabetes mellitus (9), metabolic syndrome (7,8,10), depression (7,8,11), anxiety (11), and a higher risk of all-cause mortality (7,8,12,13). Additionally, there is also evidence of these foods having the capacity to induce changes in eating behavior, triggering compulsive overeating (14).

Eating disorders can occur in individuals with obesity and is associated with a higher risk of social and health implications, in addition to compromising the outcome of interventions focused on body weight management (15,16). The etiology of eating disorders is multifactorial, involving environmental influences, such as body dissatisfaction and family stress, along with biological factors, such as hormonal changes in the neuroendocrine control of food consumption (17).

Recently, the association between the consumption of ultra-processed foods and the risk of symptoms related to eating disorders has been investigated (18). It is believed that the consumption of ultra-processed foods may trigger changes in endocrine and neurobiological pathways that regulate eating behavior, compromising conditions related to eating disorders. It is suggested that guidance on the exclusion of these foods could contribute to the effectiveness of conventional obesity treatment (19,20). To test this hypothesis, a cross-sectional study was conducted to assess the consumption of ultra-processed foods and the presence of eating disorder symptoms in individuals with obesity, as well as to improve the understanding of the factors that may worsen obesity and its comorbidities, and to support the development of more effective interventions that consider food processing and diet quality in obesity treatment.

SUBJECTS AND METHODS

Population

The volunteers were recruited via social media and from a private health service specializing in the clinical and surgical treatment of obesity, located in the city of São Paulo, SP, Brazil. For inclusion criteria, we considered adults of both sexes, aged 18 to 59, with a diagnosis of obesity assessed by Body Mass Index (BMI) ≥ 30 kg/m². Exclusion criteria included pregnancy; volunteers undergoing pharmacological treatment for body weight loss; use of corticosteroids or antiepileptic drugs; history of renal or cardiac disease; alcohol abuse; smoking; diagnosis of obesity secondary to genetic disorders; or the presence of eating disorders.

Data collection occurred between September 2021 and August 2023. After initial contact and the volunteer´s consent, an interview was conducted to provide information about the study, assess eligibility, and apply the anamnesis questionnaire. Subsequently, the volunteers were scheduled for the study protocol assessments, which included anthropometric measurements and nutritional evaluation.

Were included 77 individuals with severe obesity (BMI: 39.14 kg/m² ± 5.57), of both sexes (77.90% female participants and 22.10% male), aged 36 ± 8 years, body mass of 106.2 kg (± 18.7), and height of 1.64 m (± 0.08).

This study was conducted according to the principles of the Declaration of Helsinki and was approved by the Research Ethics Committee of UNIFESP (CAAE: 36548020.0.0000.5505), with the Brazilian clinical trials registration number RBR-103k2gpz/ 2021. All procedures were explained to the volunteers, and they all provided their written consent.

Anthropometric measurements

All subjects' body mass (kg) and height (m) were measured in the morning after a 12-hour fast and with them wearing minimum clothing, without shoes or accessories (such as watches or earrings). Body weight was assessed using the BOD POD® Body Composition System (Life Measurement Instruments, Concord, CA), which has a maximum capacity of 250 kg and a sensitivity of 10 g. The equipment was calibrated before each assessment according to the manufacturer's instructions. Height was measured using a Standard Sanny® stadiometer (capacity up to 220 cm).

The body mass index (BMI) was calculated by dividing the weight by height squared (kg/m²). For classification purposes, the cutoff points established by the World Health Organization (21) were used, defining class 1 obesity as BMI ≥ 30 kg/m², class 2 obesity as BMI ≥ 35 kg/m², and class 3 obesity as BMI ≥ 40 kg/m².

Copyright© ACE&M all rights reserved.

All assessments were conducted by the same researcher, who had been previously trained.

Nutritional assessment

Dietary consumption assessment

Dietary consumption data were based on the mean of three 24-hour dietary recalls on non-consecutive days, with one day of the weekend. The 24-hour recalls were applied considering the multiple-pass method, consisting of: 1. Quick and uninterrupted listing of food and drinks; 2. Review of forgotten foods; 3. Time and occasion of food consumption; 4. Details and description of the quantities consumed; 5. Final review (22). Participants had access to reference photographs of utensils (such as spoons and cups) to assist in estimating portion sizes, with the aim of improving the accuracy of dietary data collection. The dietary data were analyzed using the Nutrabem® software, which uses as its database the *Tabela Brasileira de Composição de Alimentos* (TACO) and the Database of Nutrients from the U.S. Department of Agriculture (USDA) (23). The classification of foods based on the extent and purpose of industrial processing was carried out using the NOVA classification system (4). All foods were listed and culinary preparations were evaluated individually. For homemade or artisanal preparations, the recipes were deconstructed into standardized ingredients by the software, and the components were listed. For preparations classified as industrial formulations, such as ready-to-eat meals, fast food, mass-produced packaged breads, and flavored yogurt, the labeling was analyzed, and the foods were entered without separating their ingredients; subsequently, all foods were allocated into groups according to their processing. Foods that did not fit perfectly into any category were classified in consensus with other researchers. Data collection for the 24-hour dietary recalls and the classification process according to the NOVA system was conducted by a trained researcher, following established guidelines (24).

The diet quality index was also assessed using the "Diet Quality Index associated with the Digital Food Guide (DQI-DFG)", developed based on guidelines from the Department of Nutrition of the Harvard School of Public Health, with adjustments made to reflect the dietary habits of the Brazilian population. The index classifies foods into two groups: moderation components – foods that can be harmful if consumed in excess: sugar and sweets, dairy drinks and sweetened yogurts, processed meats and bovine and pork meat, refined grains and flours, some cereals and potatoes, crackers and snacks, and processed fat; and adequacy components – foods that are sources of nutrients and bioactive compounds: fruits and vegetables, leafy vegetables, cereals and whole grains, tubers and roots, poultry, fish and eggs, legumes, nuts, oils and fats, and dairy products. Each food group receives a score according to the portion consumed relative to a reference range. The final score ranging from 0 to 100: < 40 points is a low-quality diet; between 40 and 70 points, intermediate quality diet; and > 70 points, good quality diet (25).

Eating behavior assessment

Eating behavior was assessed using self-administered questionnaires, applied online through the Google Forms® platform. The internal consistency of each questionnaire was evaluated using Cronbach's α and McDonald's ω coefficients. Values ≥ 0.70 were considered indicative of good internal consistency (26).

- **Bulimic Investigatory Test Edinburgh (BITE):** consisting of 33 items divided into two scales that assess symptoms and severity of bulimia or binge eating. The symptom scale comprises 30 questions ("yes"/"no") designed to investigate the presence of bulimic symptoms. For items 1, 13, 21, 23, and 31, one point is assigned for a "no" response, whereas all other items are scored for "yes". A total score ≥ 20 may suggest the presence of binge eating and bulimia nervosa, while intermediate scores between 10 and 19, suggest unusual eating behavior without all the diagnostic criteria for bulimia or binge eating, but should be investigated considering the risk of early stages of eating disorders. The severity scale includes three questions that assess the intensity and frequency of binge eating and purging behaviors. A score > 5 are considered significant, and scores ≥ 10 indicate high severity (27). The Brazilian version was translated by Cordás & Hochgraf (1993) (28). Cronbach's α: 0.79 and McDonald´s ω: 0.82.

Copyright© ACE&M all rights reserved.

- **Dutch Eating Behaviour Questionnaire (DEBQ):** comprising 33 questions divided into three subscales that address restrained eating (10 questions), external eating (10 questions), and emotional eating (13 questions), subdivided into emotional eating in response to diffuse or clearly labeled emotions. The questions are answered on a 5-point Likert scale, ranging from never, rarely, sometimes, often, to very often. The mean score of each subscale is calculated. The subscale with the highest score represents the predominant eating style. The DEBQ was translated and validated for the Brazilian population by Moreira and cols. (2017) (29). Cronbach's α: 0.91 and McDonald´s ω: 0.92.
- **The Three Factor Eating Questionnaire (TFEQ-21):** composed of 21 questions that assess cognitive restraint (6 questions), emotional eating (6 questions), and uncontrolled eating (9 questions). The response format varies from 1 to 4 points. Subsequently, the mean score of each evaluated eating behavior dimension was calculated and converted to a 0–100 scale. The higher score in an analyzed dimension indicates the predominance of that eating style. It was translated and applied to a Brazilian sample by Natacci & Ferreira Júnior (2011) (30). Cronbach's α: 0.80 and McDonald's ω: 0.82.

Statistical analyses and sample size

For statistical analysis, the STATISTICA program (StatSoft — South America; São Paulo — Brazil; version 7.0 for Windows) was used. The value considered for statistically significant change was set at $\alpha < 0.05$. The normality of the data was assessed using the Shapiro-Wilk test. Parametric variables were expressed as mean ± standard deviation (mean ± SD), and non-parametric variables were expressed as median values (minimum and maximum). In group comparisons, one-way ANOVA tests were applied to BMI, symptom subscale (BITE), external and restrained eating subscale (DEBQ), cognitive restraint and uncontrolled eating subscale (TFEQ-21), followed by the application of the post hoc Tukey test when assessing parametric variables. Non-parametric variables, including body weight, severity subscale (BITE), emotional eating subscale (DEBQ) and emotional eating subscale (TFEQ-21), were analyzed using the Kruskal-Wallis and Mann-Whitney tests. Association analyses were performed using the Generalized Linear Model (GzLM), with the SPSS software version 21.0 (SPSS Inc., Chicago, Illinois, USA), and applying the appropriate distribution (gamma or linear) as determined by the Akaike Information Criterion (AIC). The p-values were reported along with β coefficients and confidence intervals.

For the sample size calculation, the G*Power 3.0.10 analysis program was used, adopting the multiple linear regression test. We considered a significance level of 5%, a test power of 95%, and an effect size of 0.15. The calculated sample size was 74 volunteers. Additionally, to determine the sample size, a previous study published with a similar sample to the one proposed in the present investigation was considered (27).

RESULTS

Seventy-seven volunteers of both sexes were evaluated, with the majority being female (77.9%), with a mean age of 36 years (±8.7), body weight of 106.2 kg (±18.7), height of 1.64 m (±0.08), and a clinical diagnosis of class 2 obesity (BMI: 39.14 kg/m² ±5.57). For the investigation of our outcomes, the sample was divided into three groups based on the tertile of ultra-processed food calorie intake (%), with the first tertile consuming less than 24.10% of total calories from ultra-processed foods (n = 25); the second tertile consuming between 24.10% and 35.40% (n = 26); and the third tertile consuming above 35.40% of calories from ultra-processed foods (n = 26). Considering the variables of body weight and BMI, no differences were observed between the evaluated groups.

The presence and severity of binge eating and bulimia symptoms were assessed using the Bulimic Investigatory Test Edinburgh (BITE) questionnaire. In the sample, 24.7% of the participants presented normal eating behavior scores, 51.9% had a medium score, suggesting the presence of unusual eating behavior, and 23.4% had high scores, indicating binge eating with possible presence of bulimia. Regarding the severity subscale, 46.8% showed no severity of

Copyright© AE&M all rights reserved.

symptoms, 40.3% had clinically significant symptoms, and 13% exhibited a high degree of severity.

Although the average of the tertile groups did not reach the cutoff point that suggests the presence of an eating disorder, all groups had scores consistent with unusual eating behavior. In the symptoms subscale, it was identified that the third tertile group had a higher score value when compared to the first tertile group (p=0.008). There was no difference between the groups based on the severity subscale (**Table 1**).

When evaluating eating styles associated with restrained, external, and emotional eating using the Dutch Eating Behaviour Questionnaire (DEBQ), it was observed that 37.8% of the sample had higher scores for external eating, 36.5% for emotional eating, and 25.7% for restrained eating. The third tertile group showed higher values for emotional and external eating variables compared to the first tertile group (p = 0.005; p = 0.004, respectively) and the second tertile group (p = 0.0003; p = 0.007, respectively) (**Table 1**).

Furthermore, when analyzing factors associated with emotional eating, cognitive restraint, and uncontrolled eating according to the Three Factor Eating Questionnaire (TFEQ-21), it was identified that 52% had higher scores on the emotional eating subscale, 29.3% for cognitive restraint, and 18.7% for uncontrolled eating. It was observed that the third tertile group showed higher scores for emotional eating (first tertile p = 0.002; second tertile p=0.0009) and uncontrolled eating (first tertile p = 0.024; second tertile p = 0.048) when compared with the other groups (**Table 1**). For the other variables presented in **Table 1**, no significant differences were found between the groups investigated.

In the evaluation according to the Diet Quality Index–DQI-DFG, it was observed that the total sample presented a score intermediate quality diet (43 ± 10), as well as the first tertile (46.75 ± 8.72) and second tertile groups (45 ± 8). However, the third tertile group presented low-quality diet classification (37 ± 10), with a significant difference when compared to the first and second tertile groups (p = 0.001; p = 0.003, respectively) (**Table 2**).

In the analysis of dietary intake, the median caloric consumption was 1661 kcal (756.07–4774.40), and the distribution according to the NOVA classification of 48% (±14) of unprocessed or minimally processed foods, 7% (1–33) of processed culinary ingredients, 11% (±8) of processed foods, and 32% (±15) of ultra-processed foods (**Table 2**).

Analyzing dietary intake, there was a difference in total caloric consumption between the second and the third tertile groups (p = 0.0002). In the evaluation of the NOVA classification, the first tertile group showed higher consumption of unprocessed and minimally

Table 1. Presence of binge eating and bulimia symptoms according to BITE, emotional, external, and restrained eating according to DEQB, and cognitive restraint, emotional eating, and uncontrolled eating according to TFEQ-21 in adults with obesity based on the tertile of ultra-processed food consumption

Variables	All (n = 77)	1st tertile (n = 25)	2nd tertile (n = 26)	3rd tertile (n = 26)
Bulimic Investigatory Test Edinburgh				
Symptom subscale	14.50 ± 6.13	11.88 ± 5.75	14.62 ± 5.76	16.90 ± 6.01[A]
Severity subscale*	5 (0–22)	5 (0–14)	5 (0–18)	5.50 (0–22)
Dutch Eating Behaviour Questionnaire				
Emotional eating*	3.08 (1–5)	2.77 (1–4.69)	2.69 (1.23–4.62)	3.62 (2.46–5)[A,B]
External eating	3.28 ± 0.71	3.06 ± 0.69	3.10 ± 0.63	3.67 ± 0.66[A,B]
Restrained eating	2.78 ± 0.52	2.85 ± 0.52	2.90 ± 0.53	2.60 ± 0.46
The Three Factor Eating Questionnaire				
Emotional eating (0–100)*	61 (0–100)	56 (0–94)	44.50 (0–83)	75 (39–100)[A,B]
Cognitive restraint (0–100)	46.30 ± 14.30	48.60 ± 17.20	48.81 ± 11.39	41.90 ± 13.56
Uncontrolled eating (0–100)	46.60 ± 21.70	40.30 ± 21.80	42.38 ± 19.99	56.30 ± 20.26[A,B]

BITE: Bulimic Investigatory Test Edinburgh; DEBQ: Dutch Eating Behaviour Questionnaire; TFEQ-21: The Three Factor Eating Questionnaire.
[A]Statistical significance of the1st tertile; [B]Statistical significance of the 2nd tertile; *Non-parametric data expressed in median (minimum and maximum values); parametric data expressed in mean and standard deviation.
ANOVA with post hoc Tukey test (parametric data); Kruskal-Wallis test (non-parametric data).

Copyright© ACE&M all rights reserved.

processed foods compared to the second (p = 0.002) and the third tertiles (p = 0.0001). There was also a difference between the second and the third tertiles (p = 0.0001). Additionally, the first and the second tertile groups had a higher proportion of processed culinary ingredients compared to the third tertile group (p = 0.0005 and p = 0.0006, respectively) (**Table 2**).

In the consumption of ultra-processed foods, it is possible to observe that the third tertile group had a higher contribution of these foods to caloric intake compared to the first (p = 0.0001) and the second tertile groups (p = 0.0001). The second tertile group also had a higher intake when compared to the first tertile group (p = 0.0001) (**Table 2**).

Considering the assessment of macronutrient intake, the average protein intake in the total sample was 20% (±4), lipid intake was 32% (±5), and carbohydrate intake was 48% (±7). In the analysis separated by tertile, it was observed that the third tertile group had a lower total protein intake compared to the first (p = 0.0001) and the second tertile groups (p = 0.001). There was no difference in the average intake of total lipids and carbohydrates between the groups (**Table 2**).

The association analysis reinforces the previous findings. It was observed that the consumption of ultra-processed foods was positively associated with the symptom subscale of binge eating and bulimia (p = 0.018, β = 0.008, 1.001 – 1.015 95% IC). Additionally, a positive association was found between ultra-processed food consumption, emotional eating (p = 0.001, β = 0.008, 1.003 – 1.014 95% IC) and external eating (p = 0.001, β = 0.005, 1.002 – 1.008 95% IC) according to the DEBQ; as well as with emotional eating (p = 0.008, β = 0.007, 1.002 – 1.013 95% IC) and uncontrolled eating (p = 0.006, β = 0.006, 1.002 – 1.010 95% IC), as assessed by the TFEQ-21. We also identified that the higher consumption of ultra-processed foods was associated with lower Diet Quality Index scores (p < 0.001, β = -0.008, 0.988 – 0.995 95% IC) (**Table 3**).

DISCUSSION

The results of this study suggest positive association between higher consumption of ultra-processed foods and the presence of binge eating and bulimia symptoms, as well as higher scores for emotional eating, external eating, and uncontrolled eating. We also find that the group of volunteers with a higher consumption of ultra-processed foods exhibited higher scores for unusual eating behavior.

The high availability and easy access to ultra-processed foods may contribute to the worsening of obesity, not only due to its caloric content but also its potential neurobiological and metabolic effects, exacerbating symptoms of eating disorders and unusual eating behavior (19). So far, few studies have investigated the possible association between the consumption of ultra-processed foods and eating disorders in adults (18,31). In previous investigations, the analysis of data from a cohort of French adults identified that an increase in the consumption of ultra-processed

Table 2. Nutritional profile according to the tertile of ultra-processed food consumption in adults with obesity

Variables	All (n = 77)	1st tertile (n = 25)	2nd tertile (n = 26)	3rd tertile (n = 26)
DQI-DFG	43.08 ± 10.17	47 ± 9	46 ± 9	37 ± 10[A,B]
Total caloric intake (kcal)*	1661 (756–4774)	1667 (756–2623)	1432 (1001–2312)	2114 (1139–4774)[B]
Unprocessed foods (% kcal)	49 ± 14	60 ± 14	52 ± 8[A]	37 ± 11[A,B]
Processed culinary ingredients (% kcal)*	7 (1–33)	8 (3–33)	8 (3–17)	4 (1–13)[A,B]
Processed foods (% kcal)	11 ± 8	14 ± 9	9 ± 5	9 ± 7
ultra-processed foods (% kcal)	32 ± 15	17 ± 7	30 ± 3[A]	49 ± 11[A,B]
Protein (%)	20 ± 4	22 ± 4	21 ± 4	17 ± 3[A,B]
Fat (%)	32 ± 5	32 ± 5	32 ± 5	23 ± 11
Carbohydrate (%)	48 ± 7	47 ± 7	49 ± 8	49 ± 6

DQI-DFG: Diet Quality Index associated with the Digital Food Guide. Cut-off points: < 40 points: low quality diet; 40-70 points: intermediate quality diet; > 70 points: good quality diet; [A]Statistical significance of the1st tertile; [B]Statistical significance of the 2nd tertile; *Non-parametric data expressed in median (minimum and maximum values); parametric data expressed in mean and standard deviation.
ANOVA with post hoc Tukey test (parametric data); Kruskal-Wallis test (non-parametric data).

Copyright© ABE&M all rights reserved.

Table 3. Association between the presence and severity of binge eating and bulimia symptoms according to BITE, eating styles according to DEQB and TFEQ-21, Diet Quality Index (DQI-DFG) and consumption of ultra-processed foods (%)

Dependent variable	β	Wald	Exp (B)	(95% CI)	p-value
Bulimic Investigatory Test Edinburgh					
Symptom subscale	0.008	5.567	1.008	(1.001–1.015)	**0.018**
Severity subscale	0.009	2.858	1.009	(0.999–1.020)	0.91
Dutch Eating Behaviour Questionnaire					
Emotional eating	0.008	10.355	1.008	(1.003–1.014)	**0.001**
External eating	0.005	11.997	1.005	(1.002–1.008)	**0.001**
Restrained eating	-0.003	6.789	0.997	(0.994–0.999)	0.09
Three-Factor Eating Questionnaire					
Emotional Eating	0.007	7.005	1.007	(1.002–1.013)	**0.008**
Cognitive Restraint	-0.002	3.402	0.998	(0.995–1)	0.065
Uncontrolled Eating	0.006	7.627	1.006	(1.002–1.010)	**0.006**
Diet Quality Index	-0.008	22.435	0.992	(0.988–0.995)	**0.000002**

BITE: Bulimic Investigatory Test Edinburgh; DEBQ: Dutch Eating Behaviour Questionnaire; TFEQ-21: The Three Factor Eating Questionnaire; DQI-DFG: Diet Quality Index associated with the Digital Food Guide.

Generalized Linear Model (GzLM). The consumption of ultra-processed foods (%) was used as the independent variable. Statistical significance $p \leq 0.05$.

foods was associated with a 21% higher risk of Binge Eating Disorder (BED) and 8% of bulimia nervosa (BN) (18).

To our knowledge, there have been no previous studies examining the consumption of ultra-processed foods and symptoms of binge eating and bulimia in a clinical sample of adults with obesity. Our findings support the hypothesis that the consumption of ultra-processed foods may negatively impact the eating behavior of individuals with obesity.

We observed a higher prevalence of women in our sample, which is consistent with studies showing that women are more likely than men to seek clinical and surgical treatment for obesity (32,33).

In the investigated sample, 23.4% of volunteers presented scores consistent with binge eating symptoms with probable presence of bulimia, and unusual eating behavior was observed in 51.9% of the individuals assessed. In a systematic review study that evaluated the presence of eating disorders in the general population, the prevalence of BED was found to be 2.3% for women and 0.3% for men, while the prevalence of bulimia was 1.5% for women and 0.1% for men (34). In individuals with obesity, the prevalence of BED can vary from 9.5% to 40.6% (35), corroborating our results.

Our findings are similar to the study by Erden Aki and cols. (2022) (36), who evaluated 465 patients with obesity who were candidates for bariatric surgery. In their study, 23.6% of the investigated sample achieved scores indicative of binge eating, and 57.8% presented unusual eating behavior according to the BITE instrument. In the analysis of tertile groups, volunteers with a higher consumption of ultra-processed foods had higher scores for unusual eating behavior. The consumption of palatable foods can impair eating control and produce behaviors similar to dependence on these foods, due to the high fat and sugar content, which leads to excessive consumption and worsening obesity (37).

Non-homeostatic control of food intake, also referred to as "hedonic hunger", is defined as food consumption in the absence of physiological hunger signals, driven by pleasure, and is accentuated in individuals with obesity compared to individuals without obesity. This behavior is mediated by environmental and cognitive factors, such as learning and memory, and is influenced by the action of brain's reward systems through dopamine release, being activated by the intake of palatable foods with high sugar and fat content, such as ultra-processed foods (38-41).

Eating behavior patterns of individuals are known as eating styles and can be divided into three dimensions: restrained eating, characterized by intentional food restriction aimed at body weight control; external eating, when the presence of food can trigger

Copyright© AE&M all rights reserved.

excessive food intake; and emotional eating, in which emotional components such as stress, fear, anxiety, and even depression can influence food choices and preference for palatable foods, especially those with high sugar content (42-44).

In our study, it was observed that individuals with a higher consumption of ultra-processed foods had higher scores for emotional and external eating. In the study conducted by Erden Aki and cols. (2022) (36), a similar result was observed, in which participants had higher average scores for the emotional and external eating subscales. Corroborating, a study with 121 participants with obesity, Benzerouk and cols. (2020) (45) found that participants with binge eating symptoms exhibited elevated emotional and external eating, suggesting that individuals with binge eating tendencies may use palatable foods to compensate for negative feelings or to cope with distress. In addition, in our study, it was found that volunteers in the third tertile of ultra-processed food consumption scored higher in the emotional eating domains than the others; additionally, in the food disinhibition subscale, individuals in the third tertile scored higher than those in the first and second tertiles.

Aymes and cols. (2022) (46) evaluated 2,237 patients with obesity and 403 participants without obesity. Through the application of the TFEQ-21, it was identified that all three scores of eating behavior were higher in individuals with obesity compared to the control group. Additionally, the authors observed that dimensions of food disinhibition and emotional eating were associated with obesogenic eating habits, such as eating at night or in front of the television or stopping eating due to gastric fullness compared to a feeling of satiation. Moreover, in the study by Jeffers and cols. (2019) (47), the presence of a negative effect, such as emotional eating, increased susceptibility to hunger, and eating disinhibition, was associated with a higher likelihood of consuming foods high in sugar. Improvement in emotional eating behavior may contribute to the body weight loss process (48).

Considering the assessment of dietary intake, the average caloric contribution of unprocessed and minimally processed foods in the total sample was 49% ± 14, and for ultra-processed foods, it was 32% ± 15. Although the consumption of unprocessed foods is similar to that of the Brazilian population (53.25%), the intake of calories from ultra-processed foods exceeds the population's consumption (19.69%) (49). In an analysis of a community sample from Rio de Janeiro, Brazil, the consumption of hyperpalatable foods by volunteers with BED was 63%, and for BN, it was 44% (50). In individuals with obesity, Lopes Pinto and cols. (2019) (51) identified that the consumption of ultra-processed foods was 27.2%, while unprocessed and minimally processed foods accounted for 55.7% of daily calory intake.

The high consumption of ultra-processed foods is related with a low-quality diet, characterized by high intake of total and saturated fats, low intake of proteins, fibers, and micronutrients such as magnesium, potassium, zinc, and vitamins C, D, B12, and niacin (52). In an analysis of data from the *Inquérito Nacional de Alimentação* (INA — National Food Survey) 2017–2018 (53), the recommended fruits and vegetables consumption (≥ 400g/day) was observed in only 12.9% of respondents. In accordance with previous studies, our research found an association between the consumption of ultra-processed foods and low diet quality.

In the assessment of dietary macronutrient intake considering the NOVA classification system, volunteers with a higher consumption of ultra-processed foods showed a lower intake of unprocessed and minimally processed foods in their diet. They also had a lower total protein intake. Corroborating our findings, in the study by Martini and cols. (2021) (52), the consumption of ultra-processed foods was inversely correlated with the total protein intake in the highest tertile. For each one point increase in the energy contribution from ultra-processed foods, a reduction of 0.07% in total protein intake was observed. A similar result was identified in the study by Bielemann and cols. (2015) (54), in which there was a tendency to reduce daily protein intake with increasing consumption of ultra-processed foods. In a clinical trial in which volunteers were subjected to both an ultra-processed and an unprocessed diet, an increase in carbohydrate and lipid intake from ultra-processed foods was observed, but not in protein intake. There was a slight

Copyright© AE&M all rights reserved.

decrease in protein intake compared to the unprocessed diet (55).

Reinforcing our findings, data from the *Pesquisa de Orçamentos Familiares* (POF – Consumer Expenditure Survey) 2008–2009 (56) indicate an inverse correlation between the acquisition and consumption of vegetables and of ultra-processed foods, demonstrating the ability of ultra-processed foods to replace the intake of healthier foods. The consumption of fruits and vegetables can reduce the risk of diseases, such as cardiovascular disease, coronary heart disease, stroke, cancer, and all-cause mortality due to the presence of fiber, micronutrients, e.g., vitamins and minerals, and bioactive compounds, such as polyphenols (57). The consumption of these foods also impacts mental health, reducing the risk of psychological distress and depression (58). Reinforcing the benefits of consuming whole foods for health, the World Health Organization (WHO) (59) recommends a daily intake of ≥ 400g or five servings of fruits and vegetables per day.

We recognize that this study has certain limitations. Although our findings suggest a possible association between ultra-processed food consumption and eating disorder symptoms, reinforcing previous research, the cross-sectional design and the use of a clinical sample from a single urban center limit the extrapolation of the results to the general population. Future longitudinal studies involving more diverse samples could strengthen these results.

In the dietary intake analysis, the use of the mean of 24-hour dietary recalls, although widely used, may be considered a limitation, as it does not completely eliminate intra-individual variability and may underestimate or overestimate actual food intake, especially among individuals with obesity. Furthermore, the use of self-reported data, both in eating behavior questionnaires and the dietary recalls, may not accurately reflect reality due to potential biases such as social desirability and volunteers' memory recall.

However, the questionnaires demonstrated good internal reliability and the application of the instruments was conducted with the aim of minimizing this effect. Additionally, the instrument was not validated for the NOVA classification system, requiring researcher's to accurately perform the classification.

In conclusion, based on our findings, more than half of the individuals with obesity presented unusual eating behavior, with the group of volunteers showing higher consumption of ultra-processed foods also displaying higher scores for unusual eating behavior, emotional eating, external eating, and uncontrolled eating. Regarding dietary intake, these volunteers had low-quality diet and lower total protein intake.

Therefore, we suggest that the treatment of individuals with obesity should consider diet quality along with the eating behavior dimensions that may reinforce unhealthy food choices. In this context, it is essential to encourage the consumption of unprocessed and minimally processed foods and to reduce the intake of ultra-processed foods, in addition to establishing public policies that promote healthier food systems and access to adequate nutrition. These policies should include incentives for the production and distribution of healthy foods, the regulation of ultra-processed food advertising, and clear nutritional labeling, which may support healthier food choices.

Author contributions: CMF, MMN and RMSC substantially contributed to the conception or design of the work. All the authors contributed to the acquisition, analysis, or interpretation of data for the work; CMF and RMSC drafted the manuscript; All authors have read and approved the final version submitted and take public responsibility for all aspects of the work.

Funding: *Fundação Coordenação de Aperfeiçoamento de Pessoal de Nível Superior (CAPES)*, *Associação Fundo de Incentivo à Pesquisa (AFIP)* and *Fundação de Amparo à Pesquisa do Estado de São Paulo (FAPESP 2018/15921-8)*.

Acknowledgments: *Fundação Coordenação de Aperfeiçoamento de Pessoal de Nível Superior (CAPES)*, *Associação Fundo de Incentivo à Pesquisa (AFIP)* and *Fundação de Amparo à Pesquisa do Estado de São Paulo (FAPESP)*.

Disclosure: no potential conflict of interest relevant to this article was reported.

Data availability: datasets related to this article will be available upon request to the corresponding author.

REFERENCES

1. Popkin BM. Global nutrition dynamics: the world is shifting rapidly toward a diet linked with noncommunicable diseases. Am J Clin Nutr. 2006 Aug;84(2):289-98. doi: 10.1093/ajcn/84.1.289.
2. Batal M, Steinhouse L, Delisle H. The nutrition transition and the double burden of malnutrition. Med Sante Trop. 2018 Nov 1;28(4):345-350. English. doi: 10.1684/mst.2018.0831.
3. Kac G, Pérez-Escamilla R. Nutrition transition and obesity prevention through the life-course. Int J Obes Suppl. 2013 Jun;3(Suppl 1):S6-8. doi: 10.1038/ijosup.2013.3.

Copyright© AE&M all rights reserved.

4. Monteiro CA, Cannon G, Levy RB, Moubarac JC, Louzada ML, Rauber F, et al. Ultra-processed foods: what they are and how to identify them. Public Health Nutr. 2019 Apr;22(5):936-941. doi: 10.1017/S1368980018003762.
5. Canhada SL, Luft VC, Giatti L, Duncan BB, Chor D, Fonseca MJMD, et al. Ultra-processed foods, incident overweight and obesity, and longitudinal changes in weight and waist circumference: the Brazilian Longitudinal Study of Adult Health (ELSA-Brasil). Public Health Nutr. 2020 Apr;23(6):1076-1086. doi: 10.1017/S1368980019002854.
6. Silva FM, Giatti L, de Figueiredo RC, Molina MDCB, de Oliveira Cardoso L, Duncan BB, et al. Consumption of ultra-processed food and obesity: cross sectional results from the Brazilian Longitudinal Study of Adult Health (ELSA-Brasil) cohort (2008-2010). Public Health Nutr. 2018 Aug;21(12):2271-2279. doi: 10.1017/S1368980018000861.
7. Pagliai G, Dinu M, Madarena MP, Bonaccio M, Iacoviello L, Sofi F. Consumption of ultra-processed foods and health status: a systematic review and meta-analysis. Br J Nutr. 2021 Feb 14;125(3):308-318. doi: 10.1017/S0007114520002688.
8. Lane MM, Davis JA, Beattie S, Gómez-Donoso C, Loughman A, O'Neil A, et al. Ultraprocessed food and chronic noncommunicable diseases: A systematic review and meta-analysis of 43 observational studies. Obes Rev. 2021 Mar;22(3):e13146. doi: 10.1111/obr.13146.
9. Moradi S, Hojjati Kermani MA, Bagheri R, Mohammadi H, Jayedi A, et al. Ultra-Processed Food Consumption and Adult Diabetes Risk: A Systematic Review and Dose-Response Meta-Analysis. Nutrients. 2021 Dec 9;13(12):4410. doi: 10.3390/nu13124410.
10. Martínez Steele E, Juul F, Neri D, Rauber F, Monteiro CA. Dietary share of ultra-processed foods and metabolic syndrome in the US adult population. Prev Med. 2019 Aug;125:40-48. doi: 10.1016/j.ypmed.2019.05.004.
11. Lane MM, Gamage E, Travica N, Dissanayaka T, Ashtree DN, Gauci S, et al. Ultra-Processed Food Consumption and Mental Health: A Systematic Review and Meta-Analysis of Observational Studies. Nutrients. 2022 Jun 21;14(13):2568. doi: 10.3390/nu14132568.
12. Suksatan W, Moradi S, Naeini F, Bagheri R, Mohammadi H, Talebi S, et al. Ultra-Processed Food Consumption and Adult Mortality Risk: A Systematic Review and Dose-Response Meta-Analysis of 207,291 Participants. Nutrients. 2021 Dec 30;14(1):174. doi: 10.3390/nu14010174.
13. Schnabel L, Kesse-Guyot E, Allès B, Touvier M, Srour B, Hercberg S, et al. Association Between Ultraprocessed Food Consumption and Risk of Mortality Among Middle-aged Adults in France. JAMA Intern Med. 2019 Apr 1;179(4):490-498. doi: 10.1001/jamainternmed.2018.7289.
14. Lowe MR, Butryn ML. Hedonic hunger: a new dimension of appetite? Physiol Behav. 2007 Jul 24;91(4):432-9. doi: 10.1016/j.physbeh.2007.04.006.
15. Udo T, Grilo CM. Prevalence and Correlates of DSM-5-Defined Eating Disorders in a Nationally Representative Sample of U.S. Adults. Biol Psychiatry. 2018 Sep 1;84(5):345-354. doi: 10.1016/j.biopsych.2018.03.014.
16. Pacanowski CR, Senso MM, Oriogun K, Crain AL, Sherwood NE. Binge eating behavior and weight loss maintenance over a 2-year period. J Obes. 2014;2014:249315. doi: 10.1155/2014/249315.
17. Harrington BC, Jimerson M, Haxton C, Jimerson DC. Initial evaluation, diagnosis, and treatment of anorexia nervosa and bulimia nervosa. Am Fam Physician. 2015 Jan 1;91(1):46-52. PMID: 25591200.
18. Figueiredo N, Kose J, Srour B, Julia C, Kesse-Guyot E, Péneau S, et al. Ultra-processed food intake and eating disorders: Cross-sectional associations among French adults. J Behav Addict. 2022 Apr 4;11(2):588-599. doi: 10.1556/2006.2022.00009.
19. Ayton A, Ibrahim A. The Western diet: a blind spot of eating disorder research?-a narrative review and recommendations for treatment and research. Nutr Rev. 2020 Jul 1;78(7):579-596. doi: 10.1093/nutrit/nuz089.
20. Mathes WF, Brownley KA, Mo X, Bulik CM. The biology of binge eating. Appetite. 2009 Jun;52(3):545-553. doi: 10.1016/j.appet.2009.03.005.
21. Obesity: preventing and managing the global epidemic. Report of a WHO consultation. World Health Organ Tech Rep Ser. 2000;894:i-xii, 1-253. PMID: 11234459.
22. Conway JM, Ingwersen LA, Vinyard BT, Moshfegh AJ. Effectiveness of the US Department of Agriculture 5-step multiple-pass method in assessing food intake in obese and nonobese women. Am J Clin Nutr. 2003 May;77(5):1171-8. doi: 10.1093/ajcn/77.5.1171.
23. Caivano S, Domente SMA, Anunciato T. NutraBem Pro [Internet]. Instituto NutraBem; 2009 [cited 2020 Aug]. Available from: https://nutrabem.unifesp.br/.
24. Martinez-Steele E, Khandpur N, Batis C, Bes-Rastrollo M, Bonaccio M, Cediel G, et al. Best practices for applying the Nova food classification system. Nat Food. 2023 Jun;4(6):445-448. doi: 10.1038/s43016-023-00779-w.
25. Caivano S, Colugnati FAB, Domene SMA. Diet Quality Index associated with Digital Food Guide: update and validation. Cad Saude Publica. 2019 Sep 16;35(9):e00043419. doi: 10.1590/0102-311X00043419.
26. Terwee CB, Bot SD, de Boer MR, van der Windt DA, Knol DL, Dekker J, et al. Quality criteria were proposed for measurement properties of health status questionnaires. J Clin Epidemiol. 2007 Jan;60(1):34-42. doi: 10.1016/j.jclinepi.2006.03.012.
27. Henderson M, Freeman CP. A self-rating scale for bulimia. The 'BITE'. Br J Psychiatry. 1987 Jan;150:18-24. doi: 10.1192/bjp.150.1.18.
28. Cordás TA, Hochgraf PB. O "BITE": instrumento para avaliação da bulimia nervosa – versão para o português (The "BITE": tool for evaluation of bulimia nervosa – Portuguese version). J Bras. Psiquiatr. 1993;42:141-4.
29. Moreira GSX, Mota DCL, Lorenzato L, Kakeshita IS, Costa TMB, Almeida SS. Translation Procedures for Cross-Cultural Adaptation of the Dutch Eating Behavior Questionnaire (DEBQ) to Brazil. Aval Psicol. 2017;16:426-35. doi: 10.15689/ap.2017.1604.12793.
30. Natacci LC, Ferreira Júnior M. The three factor eating questionnaire – R21: tradução para o português e aplicação em mulheres brasileiras (The three factor eating questionnaire – R21: translation and administration to Brazilian women). Rev Nutr. 2011;24:383-94. doi: 10.1590/S1415-52732011000300002.
31. Ayton A, Ibrahim A, Dugan J, Galvin E, Wright OW. Ultra-processed foods and binge eating: A retrospective observational study. Nutrition. 2021 Apr;84:111023. doi: 10.1016/j.nut.2020.111023.
32. Cooper AJ, Gupta SR, Moustafa AF, Chao AM. Sex/Gender Differences in Obesity Prevalence, Comorbidities, and Treatment. Curr Obes Rep. 2021 Dec;10(4):458-466. doi: 10.1007/s13679-021-00453-x.
33. Silva LB, Quadros LG, Campos JM, Boas MLV, Marchesini JC, Ferraz AAB, et al. Brazilian national bariatric registry - pilot study. Rev Col Bras Cir. 2023 Mar 10;50:e20233382. doi: 10.1590/0100-6991e-20233382-en.
34. Galmiche M, Déchelotte P, Lambert G, Tavolacci MP. Prevalence of eating disorders over the 2000-2018 period: a systematic literature review. Am J Clin Nutr. 2019 May 1;109(5):1402-1413. doi: 10.1093/ajcn/nqy342.
35. Kops NL, Vivan MA, Fülber ER, Fleuri M, Fagundes J, Friedman R. Preoperative Binge Eating and Weight Loss After Bariatric Surgery: A Systematic Review and Meta-analysis. Obes Surg. 2021 Mar;31(3):1239-1248. doi: 10.1007/s11695-020-05124-9.
36. Erden Aki ŞÖ, Yıldız Mİ, Kamış GZ, Aytulun A, Karakaya J, Işıklı S. Relationship of depression, impulsivity, distress intolerance and coping styles with maladaptive eating patterns in bariatric candidates. Eat Weight Disord. 2022 Dec;27(8):3351-3366. doi: 10.1007/s40519-022-01465-9.
37. Schulte EM, Avena NM, Gearhardt AN. Which foods may be addictive? The roles of processing, fat content, and glycemic load. PLoS One. 2015 Feb 18;10(2):e0117959. doi: 10.1371/journal.pone.0117959.
38. Liu CM, Kanoski SE. Homeostatic and non-homeostatic controls of feeding behavior: Distinct vs. common neural systems. Physiol Behav. 2018 Sep 1;193(Pt B):223-231. doi: 10.1016/j.physbeh.2018.02.011.
39. Stice E, Yokum S. Gain in Body Fat Is Associated with Increased Striatal Response to Palatable Food Cues, whereas Body Fat Stability Is Associated with Decreased Striatal Response. J Neurosci. 2016 Jun 29;36(26):6949-56. doi: 10.1523/JNEUROSCI.4365-15.2016.

Copyright© AE&M all rights reserved.

40. Schulte EM, Avena NM, Gearhardt AN. Which foods may be addictive? The roles of processing, fat content, and glycemic load. PLoS One. 2015 Feb 18;10(2):e0117959. doi: 10.1371/journal.pone.0117959.
41. Stice E, Yokum S, Blum K, Bohon C. Weight gain is associated with reduced striatal response to palatable food. J Neurosci. 2010 Sep 29;30(39):13105-9. doi: 10.1523/JNEUROSCI.2105-10.2010.
42. Santos MM, Moura PS, Flauzino PA, Alvarenga MS, Arruda SPM, Carioca AAF. Eating behavior and body image in health sciences university students. J Bras Psiquiatr. 2021;70(2):126-33. doi: 10.1590/0047-2085000000308.
43. Viana V. Psicologia, saúde e nutrição: Contributo para o estudo do comportamento alimentar. Análise Psicológica. 2002;20(4):611-24.
44. Jacques A, Chaaya N, Beecher K, Ali SA, Belmer A, Bartlett S. The impact of sugar consumption on stress driven, emotional and addictive behaviors. Neurosci Biobehav Rev. 2019 Aug;103:178-199. doi: 10.1016/j.neubiorev.2019.05.021.
45. Benzerouk F, Djerada Z, Bertin E, Barrière S, Gierski F, Kaladjian A. Contributions of Emotional Overload, Emotion Dysregulation, and Impulsivity to Eating Patterns in Obese Patients with Binge Eating Disorder and Seeking Bariatric Surgery. Nutrients. 2020 Oct 12;12(10):3099. doi: 10.3390/nu12103099.
46. Aymes E, Lisembard G, Dallongeville J, Rousseaux J, Dumont MP, Amouyel P, et al. Identification of several eating habits that mediate the association between eating behaviors and the risk of obesity. Obes Sci Pract. 2022 Mar 3;8(5):585-594. doi: 10.1002/osp4.593.
47. Jeffers AJ, Mason TB, Benotsch EG. Psychological eating factors, affect, and ecological momentary assessed diet quality. Eat Weight Disord. 2020 Oct;25(5):1151-1159. doi: 10.1007/s40519-019-00743-3.
48. Braden A, Flatt SW, Boutelle KN, Strong D, Sherwood NE, Rock CL. Emotional eating is associated with weight loss success among adults enrolled in a weight loss program. J Behav Med. 2016 Aug;39(4):727-32. doi: 10.1007/s10865-016-9728-8.
49. Louzada MLDC, Cruz GLD, Silva KAAN, Grassi AGF, Andrade GC, Rauber F, et al. Consumption of ultra-processed foods in Brazil: distribution and temporal evolution 2008-2018. Rev Saude Publica. 2023 Apr 14;57:12. doi: 10.11606/s1518-8787.2023057004744.
50. Moraes CEF, Hay P, Sichieri R, Fazzino TL, Mourilhe C, Appolinario JC. Hyperpalatable Foods Consumption in a Representative Sample of the General Population in Brazil: Differences of Binge and Non-Binge Eating Meals. Behav Sci (Basel). 2023 Feb 9;13(2):149. doi: 10.3390/bs13020149.
51. Lopes Pinto S, da Silva DCG, Bressan J. Absolute and Relative Changes in Ultra-processed Food Consumption and Dietary Antioxidants in Severely Obese Adults 3 Months After Roux-en-Y Gastric Bypass. Obes Surg. 2019 Jun;29(6):1810-1815. doi: 10.1007/s11695-019-03749-z.
52. Martini D, Godos J, Bonaccio M, Vitaglione P, Grosso G. Ultra-Processed Foods and Nutritional Dietary Profile: A Meta-Analysis of Nationally Representative Samples. Nutrients. 2021 Sep 27;13(10):3390. doi: 10.3390/nu13103390.
53. Romeiro ACT, Brito FDSB, Dos Santos DM, da Costa ES, Curioni CC, Adegboye ARA. Diet quality and consumption of ultra-processed foods according to age groups in Brazil: insights from the National Dietary Survey 2017-2018. Br J Nutr. 2025 Sep 14;134(5):413-424. doi: 10.1017/S000711452510411X.
54. Bielemann RM, Motta JV, Minten GC, Horta BL, Gigante DP. Consumption of ultra-processed foods and their impact on the diet of young adults. Rev Saude Publica. 2015;49:28. doi: 10.1590/s0034-8910.2015049005572.
55. Hall KD, Ayuketah A, Brychta R, Cai H, Cassimatis T, Chen KY, et al. Ultra-Processed Diets Cause Excess Calorie Intake and Weight Gain: An Inpatient Randomized Controlled Trial of Ad Libitum Food Intake. Cell Metab. 2019 Jul 2;30(1):67-77.e3. doi: 10.1016/j.cmet.2019.05.008. Epub 2019 May 16. Erratum in: Cell Metab. 2019 Jul 2;30(1):226. doi: 10.1016/j.cmet.2019.05.020.
56. Canella DS, Louzada MLDC, Claro RM, Costa JC, Bandoni DH, Levy RB, et al. Consumption of vegetables and their relation with ultra-processed foods in Brazil. Rev Saude Publica. 2018;52:50. doi: 10.11606/s1518-8787.2018052000111.
57. Aune D, Giovannucci E, Boffetta P, Fadnes LT, Keum N, Norat T, et al. Fruit and vegetable intake and the risk of cardiovascular disease, total cancer and all-cause mortality-a systematic review and dose-response meta-analysis of prospective studies. Int J Epidemiol. 2017 Jun 1;46(3):1029-1056. doi: 10.1093/ije/dyw319.
58. Głąbska D, Guzek D, Groele B, Gutkowska K. Fruit and Vegetable Intake and Mental Health in Adults: A Systematic Review. Nutrients. 2020 Jan 1;12(1):115. doi: 10.3390/nu12010115.
59. World Health Organization; Food and Agriculture Organization of the United Nations. Diet, nutrition and the prevention of chronic diseases: report of a joint WHO/FAO expert consultation. Geneva: World Health Organization; 2002.

Copyright© AE&M all rights reserved.

Archives of Endocrinology and Metabolism
ISSN 2359-4292
OFFICIAL JOURNAL OF THE BRAZILIAN SOCIETY OF ENDOCRINOLOGY AND METABOLISM

original

Extracellular vesicles related to familial hypercholesterolemia

Júnea P. de P. Silvino[1]
https://orcid.org/0000-0001-8024-5486

Cinthia E. Jannes[2]
https://orcid.org/0000-0002-8791-642X

Rodrigo M. C. Pestana[1]
https://orcid.org/0000-0003-2713-9726

Lucas P. de P. Silvino[1]
https://orcid.org/0009-0000-5424-3639

Iêda de F. O. Silva[3]
https://orcid.org/0000-0002-1843-2632

Andréa Teixeira-Carvalho[4]
https://orcid.org/0000-0003-2814-5183

Karina B. Gomes[1,3]
https://orcid.org/0000-0002-6870-2063

[1] Faculdade de Medicina, Universidade Federal de Minas Gerais, Belo Horizonte, MG, Brasil
[2] Laboratório de Genética do Instituto do Coração (InCor), Universidade de São Paulo, São Paulo, SP, Brasil
[3] Faculdade de Farmácia, Universidade Federal de Minas Gerais, Belo Horizonte, MG, Brasil
[4] Centro de Pesquisas René Rachou, Belo Horizonte, MG, Brasil

ABSTRACT

Objective: This study aimed to evaluate extracellular vesicles (EVs) in a group of carriers of familial hypercholesterolemia (FH)-related genetic variants compared to those in family members without FH. **Subjects and methods**: Annexin V-positive EVs (PS^+-EVs), cardiomyocyte-derived EVs (CardioEVs), endothelial cell-derived EVs (EEVs), platelet-derived EVs (PEVs) and tissue factor-expressing EVs (TFEVs) were evaluated to compare individuals with FH and genetic variants (n = 16) and non-FH patients without genetic variants (n = 16). **Results**: Increased numbers of PS^+-EVs, CardioEVs, EEVs and TFEVs were observed in the group c arrying genetic variants. Furthermore, patients with FH who did not use statins had higher counts of these same EVs than non-FH patients who did not use statins. These EVs were significantly correlated with low-density lipoprotein cholesterol (LDL-c) levels. **Conclusion**: The data suggest that EVs are related to FH and that their cellular origins could be related to cardiovascular complications commonly observed in this disease.

Keywords: Familial hypercholesterolemia; genetic variants; extracellular vesicles; cardiovascular disease

INTRODUCTION

Familial hypercholesterolemia (FH) is an autosomal dominant disease characterized by the presence of variants in genes related to the metabolism of low-density lipoprotein cholesterol (LDL-c). Chronic elevation of LDL-c levels predisposes patients to the risk of premature cardiovascular disease development (1-3). FH can be caused by variants located mainly in the genes encoding the low-density lipoprotein receptor (*LDLR*), apolipoprotein B (*APOB*) and proprotein convertase subtilisin/kexin type 9 (*PCSK9*), with more than 2,900 genetic alterations associated with the disease (4). FH can present multiple phenotypes because of different molecular etiologies and additional genetic factors (5), but the risk of coronary artery disease (CAD) is greater among carriers of pathogenic variants of FH (6).

The pathophysiology of atherosclerosis begins with endothelial injury, which is mediated by a cascade of intra- and intercellular signaling events that shape cellular behavior within vessels and the inflammatory response (7). The main complication resulting from this process is acute coronary syndrome, which is observed more frequently in patients with FH, including young people (8). Thus, identifying plasma markers related to the atherosclerotic process, endothelial injury, and cardiac dysfunction that can identify these outcomes early in patients with FH is highly desirable.

Extracellular vesicles (EVs) 0.1–1.0 µm in diameter, also known as microparticles (MPs), originate from cell

Received on Apr/23/2025
Accepted on Oct/1/2025
DOI: 10.20945/2359-4292-2026-0022

Correspondence to:
Karina Braga Gomes
Faculdade de Farmácia,
Universidade Federal de Minas Gerais
Avenida Antônio Carlos, 6627, Pampulha
31270-901 – Belo Horizonte, MG, Brasil
karinabgb@gmail.com

Associated editor:
Josivan Gomes de Lima
https://orcid.org/0000-0002-1627-7018

This is an open-access article distributed under the terms of the Creative Commons Attribution License

Copyright© ACE&M all rights reserved.

membranes in response to cell activation or apoptosis. Cells may be activated in response to diverse stress stimuli, leading to the initiation of apoptosis or alternative cellular pathways. Such activation represents a critical step for subsequent functional outcomes, including differentiation, proliferation, and programmed cell death. Unlike EVs, exosomes have endosomal origins and are vesicular bodies with membranes composed of a lipid bilayer (30–150 nm in diameter) and are released through the plasma membrane. The initial step of EV formation consists of membrane remodeling via bubble formation and an increase in intracellular calcium levels, resulting in a rearrangement of the phospholipid layer and the exposure of phosphatidylserine. Concomitant with the loss of membrane asymmetry, calcium-sensitive enzymes are activated and promote the cleavage of cytoskeletal filaments, leading to the formation of membrane blebs and the release of EVs (9,10). EVs arise from various cell types and can be released under the influence of cytokines, thrombin, endotoxins or physical stimuli, as well as shear stress or hypoxia (11). Moreover, EVs carry markers on their surfaces that enable identification of the cell of origin.

This study aimed to evaluate PS^{+}-EVs and EVs related to cardiovascular diseases — EVs from cardiomyocytes, endothelium, platelets and EVs that express tissue factor (TF) — in individuals carrying FH-related genetic variants and to compare them with those in a control group.

SUBJECTS AND METHODS

Study population

In this study, 32 individuals were included — 16 FH patients and 16 controls — assisted by the Itinerant Hipercol Brazil program of Instituto do Coração (InCor), Brazil (12). This program aims to investigate the presence of genetic variants in populations with a high prevalence of dyslipidemia, according to information collected by local medical assistance, with an active search for index cases (ICs) based on medical records and cholesterol tests conducted in laboratories for the clinical analysis of local health units.

Individuals in the case group were diagnosed according to the clinical criteria of the Dutch Lipid Clinic Network (DLCN) (13). Individuals with scores of > 8 points were diagnosed as definitive FH, those with 6–8 points were diagnosed as probable FH, and those with 3–5 points were diagnosed as possible FH. Those with scores < 3 were considered to have no FH (FH-absent). All ICs presented LDL-c levels ≥ 210 mg/dL (adults) or ≥ 190 mg/dL (patient age: < 18 years). First- and second-degree relatives without genetic variants in the evaluated genes, who did not meet the DLCN criteria and whose lifestyle and diet were the same as their affected relatives, were included as controls (**Figure 1**). Individuals with hepatic or hematological diseases, descompensated diabetes mellitus (HbA1c > 7.0%), obesity (BMI > 30 kg/m² for adults and BMI Z score > +2 for children), inflammatory and thyroid diseases, and triglyceride levels > 400 mg/dL and who were HIV carriers were excluded from both groups.

Genetic characterization was performed as described in our previous study (14), with the *LDLR* (Gene ID: 3949), *APOB* (Gene ID: 338), *PCSK9* (Gene ID: 255738), *LDLRAP1* (Gene ID: 26119), *LIPA* (Gene ID: 3988), *STAP1* (Gene ID: 26228), *APOE* (Gene ID: 348), *ABCG5* (Gene ID: 64240) and *ABCG8* (Gene ID: 64241) genes sequenced by performing next-generation sequencing (NGS) of samples from ICs. The samples of individuals for whom no variants were observed through NGS analysis were also subjected to the multiplex ligation probe amplification (MLPA) technique to track copy number variants (CNVs) in the *LDLR* gene. DNA sequencing of family members was performed using the Sanger sequencing method after the patient's genetic variant was characterized. Thus, those carrying genetic variants in at least one of the investigated genes were considered to have FH and included in the case group.

Ethical aspects

The present study was approved by the Research Ethics Committee of the UFMG (COEP-UFMG) (CAAE-76387417.6.0000.5149) and by the Ethics Committee of the University of São Paulo (CAAPesqprotocolo100594212.0.1001.0068) and was conducted in accordance with the ethical guidelines of the 1975 Declaration of Helsinki. All participants or their legally acceptable representatives signed written informed consent forms.

Copyright© ACE&M all rights reserved.

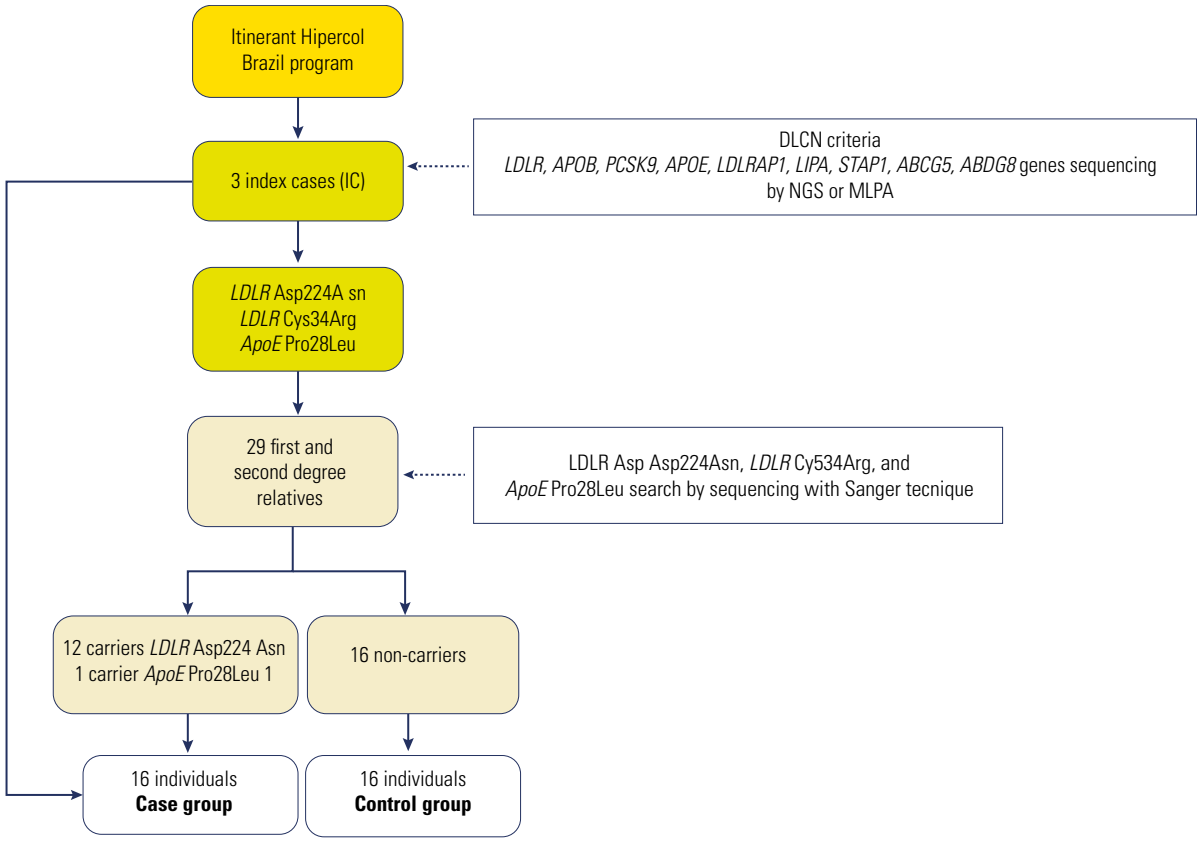


Figure 1. Selection of individuals with Familial Hypercholesterolemia (FH).

From the Itinerant Hipercol Brazil program, three index cases (ICs) were selected based on Dutch criteria and were sequenced in nine genes related to FH by NGS or MLPA. After the genetic variant detected in ICs (Asp224Asn and Cys34Arg in LDLR gene, Pro28Leu in APOE gene), 1st and 2nd degree relatives were included, in a total 29 individuals were sequenced by the Sanger technique to search the variant detected in ICs. 13 individuals carrying the genetic variants (12 in LDLR gene Asp224Asn and one in APOE gene Pro28Leu) and three IC formed the case group; 16 individuals not carrying the genetic variants formed the control group.

Sample collection and processing

Blood samples (5.0 mL) were collected through venipuncture in sodium citrate (3.2%) tubes in a vacuum system with a maximum tourniquet time of 1 min. Prior to blood collection, patients fasted for 8–12 h. Platelet-poor plasma (PPP) was prepared as follows: 1) the sample was centrifuged at 3,500 rpm for 15 min; 2) the upper 2/3 of the supernatant was transferred to a new tube, and centrifugation was again carried out at 3,500 rpm for 15 min; and 3) only the upper two-thirds of the supernatant were distributed in 500 µL aliquots in polypropylene tubes and stored at -80 °C until the EV assays were conducted.

Quantification and characterization of extracellular vesicles

EV analysis was performed through flow cytometry as previously described (15). The antibodies and fluorochromes used in this panel were anti-caveolin-3-Alexa Fluor 647 (cardiomyocytes), anti-CD41a-PE-Cy7 (platelets), and anti-CD142-PE (tissue factor). Annexin V-eFluor450 was used to label EVs that expressed phosphatidylserine (PS) on their surfaces (PS^+-EVs). The results of the phenotyping panel are summarized in **Table S1 (Supplementary data)**.

Prior to the EV quantification assay, an EV-rich suspension was obtained. The PPP was thawed at 37 °C and centrifuged at 1,300 rpm for 5 min to obtain platelet-free plasma (PFP). Afterward, the supernatant was aspirated and diluted (1:3) in citrate phosphate-buffered saline (PBS) containing heparin (1 µg/mL). This solution was then centrifuged at 15,000 rpm for 90 min at 15 °C (at low deceleration). The resultant EV pellet was then resuspended in 100 µL of 10× annexin V binding buffer® (Thermo Fisher Scientific, San Diego, USA) to produce an EV-rich suspension.

Copyright© AE&M all rights reserved.

A "fluorescence minus one" control, which is a sample without the labeling of a particular antibody-fluorochrome, was used before the analysis. The labeling and analysis process was designed for multiparametric analysis in a single tube. Aliquots of 100 µL of EV-rich suspension were transferred to polypropylene bottles. The antibody-fluorochromes were subsequently added in the following order: 2.5 µL of Annexin V-eFluor450, 2.0 µL of anti-caveolin-3-AlexaFluor647, 1.0 µL of CD41a-PE-Cy7, and 2.0 µL of CD142-PE. A 30-min incubation (at room temperature) step was performed after each addition of the antibody-fluorochrome, followed by a wash step with PBS-saline, and centrifugation (1,500 rpm for 20 min at 4 ℃) was carried out to separate and discard the supernatant. The resuspension was performed with 10× annexin V binding buffer. These critical steps were performed in the dark as much as possible. Three aliquots were used as internal controls: an aliquot containing only the buffer and lacking antibody-fluorochromes and EVs, a second aliquot containing the buffer and Annexin V-eFluor450 and lacking EVs, and a third aliquot containing the buffer and EVs and lacking Annexin V-eFluor450.

EVs were detected in a CytoflexS® (Beckman Coulter Inc., Brea, USA) and gated on the basis of their forward (FSC) and side (SSC) scatter distributions of calibration microbeads (Flow Cytometry Submicron Particle Size Reference Kit®, Thermo Fisher Scientific), which provide six sizes of green-fluorescent beads: 0.1 µm, 0.2 µm, 0.5 µm, 1.0 µm and 2.0 µm in diameter. The sample flow rate was 30 µL/min, and the cytometer was programmed to operate at a high flow rate for 60 s for each sample (50,000 events). The CytoflexS® has a volumetric sample injection system that allows absolute particle counting. Analysis was performed using FlowJo® software (Tree Star). The gating strategy applied is shown in **Figure 2**.

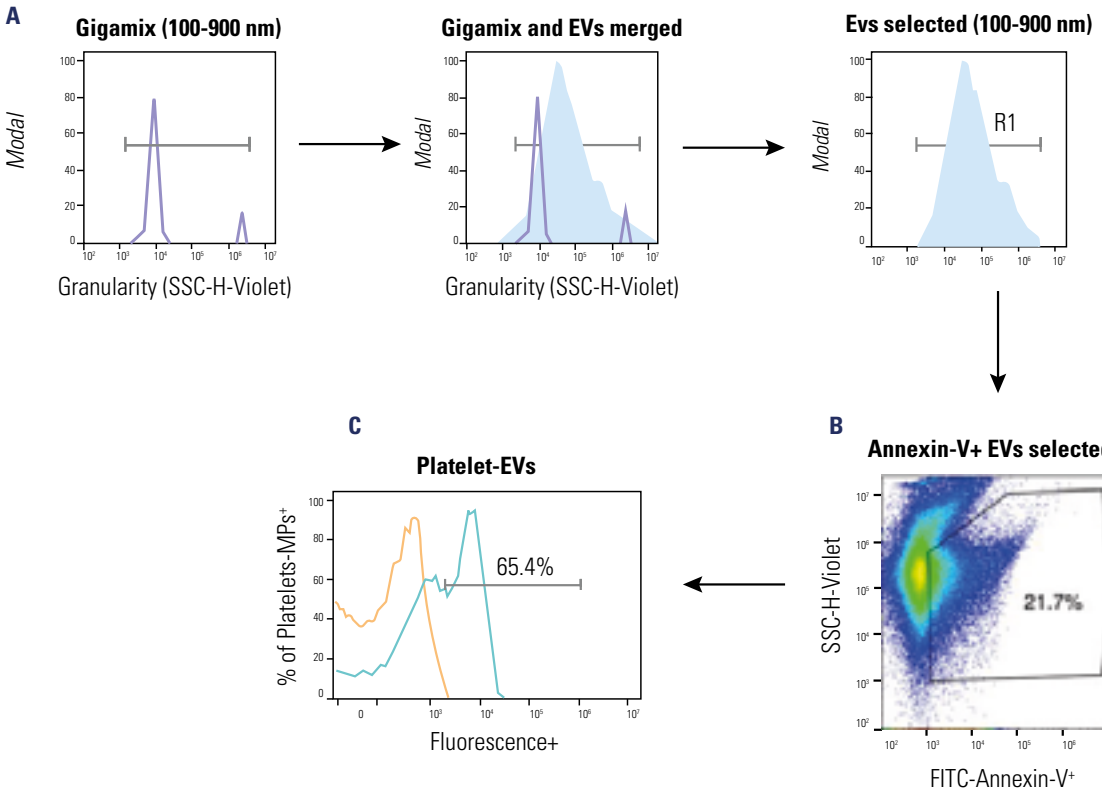


Figure 2. Representative strategies for the Immunophenotyping of Extracellular vesicles (EVs) by flow cytometry.

(**A**) One-dimensional granularity histograms (violet SSC-A) were constructed for the selection of gigamix beads ranging from 100 to 900 nm. Merging one-dimensional Gigamix and MP histograms allow the selection of EVs from 100 to 900 nm (R1). (**B**) Two-dimensional plot of FITC-Annexin V vs. granularity (SSC-H-Violet) with EVs (100 and 900 nm) selected the positivity region for FITC-Annexin V. (**C**) Histograms are used for the quantification of the percentage of phenotype-specific EVs in the samples.

Copyright© AE&M all rights reserved.

LDL-c and lipoprotein(a) (Lp(a)) quantification

The LDL-c values, obtained from medical records, were evaluated under individual baseline conditions, that is, without treatment. However, in FH patients receiving lipid-lowering treatment (13 patients from the case group), baseline LDL-c was estimated using conversion factors reported in the literature according to Foody and cols. (16) and Ballantyne and cols. (17).

Serum Lp(a) was quantified using the Atellica CH® diagnostic kit, which is based on the turbidimetry method, and an Atellica Siemens Healthineers® analyzer.

Statistical analysis

To calculate the sample size, we considered a type I error (α) of 0.05 and a type II error (β) of 0.20 (80% power). On the basis of a pilot analysis, we adopted a standardized effect magnitude of 0.8, considering the number of PS^+-EVs as the main variable. On this basis, 15 patients were required in each group. Statistical analysis was performed using the R Platform version 4.2.2 program. Qualitative variables are described as absolute and relative frequencies of their categories, and quantitative variables are described as measures of central tendency (medians and interquartile ranges (IQRs), or means ± standard deviations). The normality test applied was the Shapiro–Wilk test. The association between qualitative variables was tested using the chi-square test, with p values calculated via Monte Carlo simulation when necessary. Comparisons of the central tendency of quantitative variables between groups were performed using Student's *t* test or the Mann–Whitney test for the two groups. Correlation analysis was performed using the Spearman test. The significance level adopted was 5%, with a statistical power of 95%.

RESULTS

The case group consisted of 14 individuals carrying genetic variants in the *LDLR* gene (13 with Asp224Asn, a pathogenic variant; and one with Cys34Arg, a probable pathogenic variant) and two individuals with genetic variants in the *APOE* gene (both carrying Pro28Leu, a variant with uncertain significance) (14). The other 16 relatives were not carriers of these genetic variants and were classified into the control group.

Carriers of genetic variants presented with a corneal arch (12%), xanthoma or xanthelasma (23%), and these characteristics were not observed in noncarriers. Age, Lp(a) level, sex, frequency of diabetes mellitus, systemic arterial hypertension, history of cardiovascular disease and smoking status did not significantly differ between the groups ($p > 0.05$ for all). However, body mass index (BMI) was higher in the group carrying genetic variants, and LDL-c levels, as expected, were also higher in this group, as the LDL-c level is a diagnostic criterion for FH ($p = 0.025$ and $p < 0.001$, respectively). The clinical and demographic characteristics of the case and control groups are summarized in **Table 1**.

Patients with FH who carried genetic variants had higher counts of PS^+-EVs ($p = 0.040$; **Figure 3A**), CardioEVs ($p = 0.010$; **Figure 3B**), EEVs ($p = 0.010$; **Figure 3C**) and TFEVs ($p = 0.010$; **Figure 3D**) than family members without FH and noncarriers did, regardless of age or sex. No significant difference in the number of PEVs was detected between the groups ($p = 0.060$; **Figure 3E**).

Table 1. Clinical and demographic characterization of carrier and non-carrier groups of genetic variants related to familial hypercholesterolemia

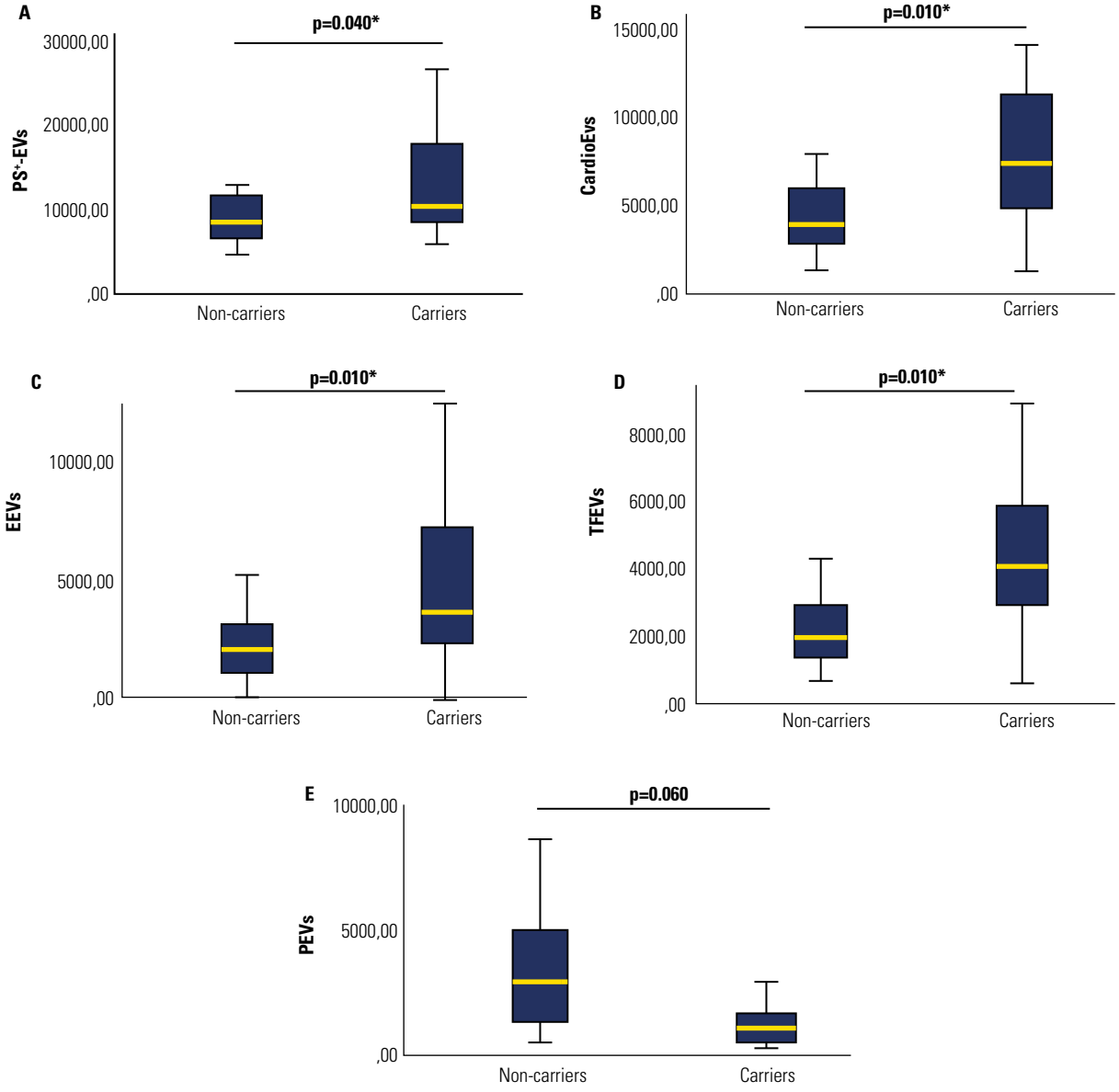
Variables	Non-carriers (n = 16)	Carriers (n = 16)	P value
LDL-c (mmol/L)	3.6 ± 0.9	7.6 ± 2.1	<0.001*
Lp(a) (mmol/L)	0.3 (0.2-0.57)	0.5 (0.2-1.24)	0.216
Age (years)	31.9 ± 21.7	43.6 ± 12.2	0.064
Gender (%)			
Male	20	24	0.810
Female	80	76	
BMI (kg/m²)	21.7 ± 5.5	26.3± 5.2	0.025*
Corneal arch (%)	0	12	–
Xanthomas/Xanthelasma (%)	0	23	–
CVD history (%)	6.7	5.9	0.927
Diabetes mellitus (%)	0	0	1.000
Hypertension (%)	13.3	23.5	0.659
Smoking (%)			
Non-smokers	100	88.2	
Ex-smokers#	0	5.9	0.390
Smokers	0	5.9	

Continuous variables expressed as median (interquartile range – 25th-75th) or mean ± standard deviation, categorical variables expressed as frequency. Data not normally distributed were compared by Mann–Whitney U test. Data normally distributed were compared by Student T-test.

BMI: Body Mass Index; CVD: cardiovascular disease.

*Significant $p < 0.05$. #Up to 1 year before collection.

Copyright© ACE&M all rights reserved.



EVs: extracellular vesicles; PS+-EVs: EVs marked with AnnexinV-eFluor450; CardioEVs: EVs derived from cardiomyocytes; EEVs: EVs derived from endothelial cells; TFEVs: EVs that express tissue factor in surface; PEVs: EVs derived from platelets. Data not normally distributed were expressed as median (25^{th}-75^{th}) and compared by Mann–Whitney U test. *Significant $p < 0.05$.

Figure 3. Comparison of extracellular vesicles count (EVs/μL) between carriers and non-carriers of genetic variants related to Familial Hypercholesterolemia. **A**) PS^+-EVs, **B**) CardioEVs, **C**) EEVs, **D**) TFEVs, **E**) PEVs.

Age was not correlated with EV counts. In contrast, BMI was weakly correlated with CardioEV counts ($p = 0.352$, $p = 0.048$). A significant and positive correlation was observed between LDL-c levels and counts of PS^+-EVs ($p = 0.500$; $p = 0.004$), CardioEVs ($p = 0.509$; $p = 0.030$), EEVs ($p = 0.618$; $p < 0.001$) and TFEVs ($p = 0.623$; $p < 0.001$) in both groups. No correlation was observed between the PEV count and LDL-c level ($p = -0.326$; $p = 0.068$). Interestingly, the PS^+-EV count was also significantly correlated with Lp(a) levels ($p = 0.360$; $p = 0.043$).

Higher counts of total PS+-EVs were observed in the group of individuals with FH who did not use statins than in individuals without FH and who did not use these drugs ($p = 0.020$) (**Figure 4A**). Similarly, higher CardioEV and TFEV counts were observed in the group of individuals with FH than in the group of individuals without FH, both of whom did not use statins ($p = 0.020$ for both) (**Figures 4B and 4C**). Individuals with FH had higher EEV counts than individuals without FH did; neither group used statins ($p < 0.001$) (**Figure 4D**). Additionally, in the group of variant carriers with FH,

Copyright© AE&M all rights reserved.

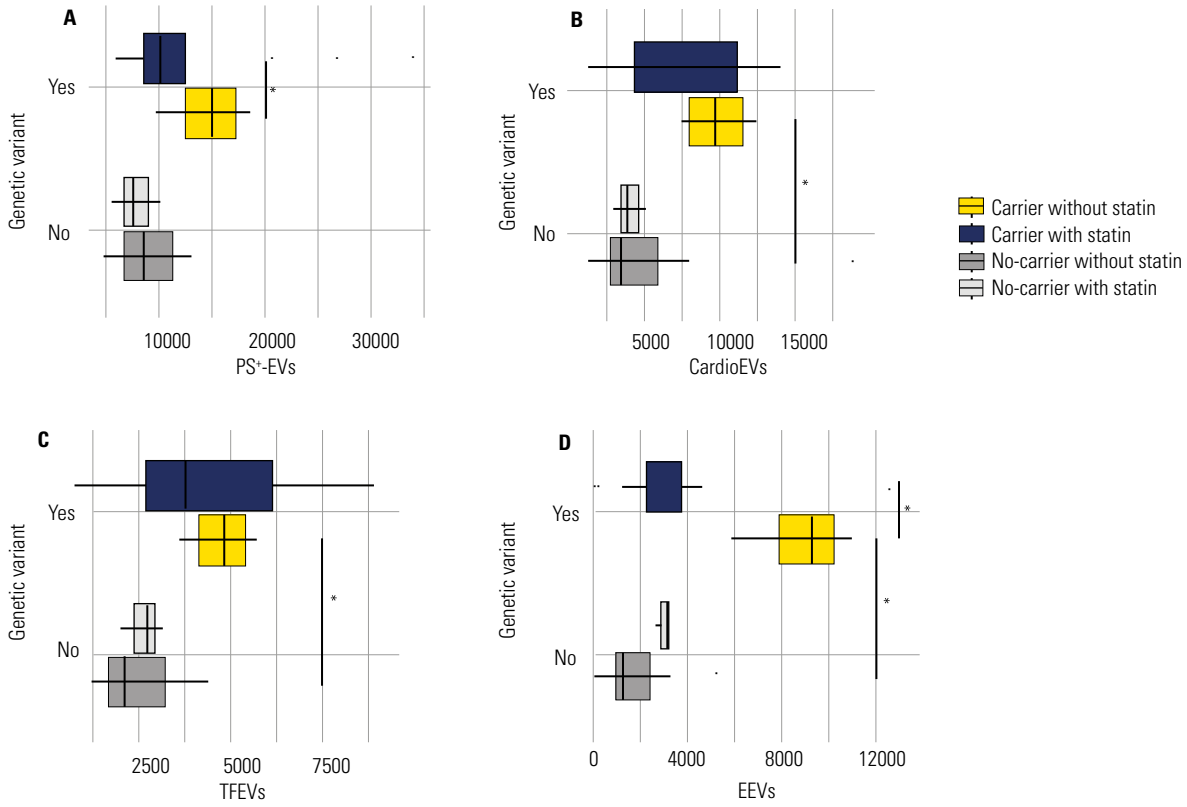


Figure 4. Comparison of extracellular vesicles count (EVs/µL) between carriers and non-carriers of genetic variants according to statin use. **A)** PS⁺-EVs: EVs marked with AnnexinV-eFluor450; **B)** CardioEVs: EVs derived from cardiomyocytes; **C)** TFEVs: EVs that express tissue factor in surface; **D)** EEVs: EVs derived from endothelial cells. *Significant $p < 0.05$.

individuals who were not using statins had higher EEV counts than those who were using this drug did ($p = 0.010$) (**Figure 4D**). PEV counts did not significantly differ between carriers of genetic variants with FH and noncarriers because of the use of statins ($p > 0.050$ for all comparisons; data not shown).

DISCUSSION

In this study, 32 individuals were evaluated, 16 of whom were carriers of genetic variants related to FH, and 16 of whom were 1st- and 2nd-degree family members who were not carriers of the variants found in family clusters. Higher numbers of PS⁺-EVs, CardioEVs, EEVs and TFEVs were observed in the group with FH than in the group without FH. In addition, higher counts were observed among individuals with FH who did not use statins, which suggests that these drugs may play a regulatory role in the release of EVs, either by directly reducing cell activation or injury or by reducing LDL-c levels. In fact, EV counts were positively correlated with LDL-c levels. It is also important to emphasize the correlation of PS⁺-EVs with Lp(a), a marker that is related to FH (18).

Hypercholesterolemia is related to increased oxidative stress. This oxidative stress predisposes individuals to increased accumulation of oxidized LDL cholesterol (oxLDL-C), which interacts with the CD36 receptor. Nielsen and cols. (19) reported that elevated oxLDL-C levels induce proinflammatory monocytes and increase the release of monocyte-derived EVs in subjects with heterozygous FH, particularly in the presence of Achilles tendon xanthomas (ATX). The same group reported that total microvesicles (MVs) and monocyte-, endothelial-, erythrocyte-, and tissue factor-positive cell-derived MVs were significantly greater in FH patients than in controls. In addition, counts of CD36+ MVs derived from endothelial cells and monocytes were significantly higher in FH patients, and oxLDL-C levels predicted all the investigated cell-specific CD36+ MVs in FH patients with ATX (20).

Chen and cols. (21) analyzed the role of PS⁺-EVs in the atherosclerotic process and suggested that they

Copyright© ACE&M all rights reserved.

may induce endothelial dysfunction, vascular inflammation, coagulation, thrombosis, and calcification through their protein components and noncoding RNAs, which may promote atherosclerosis. EVs may represent important pathways of intercellular communication and act as messengers, accelerating the atherosclerosis process, and may become diagnostic biomarkers in the treatment of atherosclerotic disease. In fact, a greater number of EVs with reduced expression of microRNAs, related to protective factors, was demonstrated in human coronary artery smooth muscle cells from patients with FH than in those from control individuals (22).

When EVs were characterized according to cell origin, we observed that the number of CardioEVs was significantly greater in the FH group than in the non-FH group. To the best of our knowledge, this is the first study to evaluate the relationship between CardioEVs and FH. Although cardiomyocytes are not considered typical secretory cells, their EVs can be released because of cellular activation, hypoxia, apoptosis, injury and inflammation, conditions that cooccur with coronary artery disease early in individuals with FH (23,24). A recent study from our group revealed that the number of cardiomyocyte-derived EVs was relatively greater in patients with breast cancer who developed cardiotoxicity secondary to doxorubicin chemotherapy. A positive correlation with serum NT-proBNP levels was also found, which suggests that CardioEVs are involved in the pathophysiology of cardiac cell injury (25).

EEV counts were higher in the group of individuals with FH than in individuals without FH. In addition, in individuals with FH, the number of nonusers of statins was greater than that in individuals with FH and those using statins, corroborating the hypothesis that statins reduce endothelial damage and, consequently, the release of EEVs. EVs originating from endothelial cells are suggestive of vascular pathologies, as they are cellular responses to an activated, compromised and damaged endothelium. Therefore, EEVs are a predictive marker of vascular health (26). Studies have shown a significant increase in the number of circulating EEVs in association with coronary artery disease, suggesting that this elevation is not only related to coronary endothelial dysfunction but is also associated with an increased risk of major cardiovascular events (27,28). Interestingly, EEVs can also promote cell survival, exert anti-inflammatory effects, counteract coagulation processes, or induce endothelial regeneration (29).

The number of EVs carrying cellular markers of different circulating cellular origins (platelets, endothelial cells, and leukocytes) was significantly lower in hypercholesterolemic patients on statin-based lipid-lowering therapy than in untreated hypercholesterolemic patients, in addition to a reduction in the number of platelets, activated inflammatory cells and tissue factor (30). Furthermore, the effect of lipid-lowering therapy on EV clearance is cumulative over time, and patients receiving statin treatment had significantly lower numbers of EVs carrying activated cell markers, indicating that statins protect against cell activation-related vascular disorders (30). Another study comparing two groups, one in which atorvastatin 10 mg was used and the other in which atorvastatin 40 mg was used, revealed a reduction in the number of circulating EEVs and an increase in the number of circulating endothelial cell progenitor cells in patients with ischemic cardiomyopathy compared with those in the group in which atorvastatin 10 mg was used. The effect was independent of the decrease in lipids, LDLox and ultrasensitive C-reactive protein (us-CRP) (31), indicating that the benefit of statin treatment in FH patients goes beyond its effect on lowering LDL-c levels.

In the analysis of EVs that express tissue factor (TFEVs), higher counts were observed in individuals with FH who carry genetic variants. Tissue factor is highly expressed in atherosclerotic plaques, and it is upregulated by LDLox (32). By analyzing TFEVs in relation to lipid-lowering treatment with statins in an animal model, a study was conducted to assess whether simvastatin can inhibit tissue factor production in monocytes from hypercholesterolemic animals, considering that hypercholesterolemia can produce a procoagulant state. Simvastatin treatment reduced LDLox levels and, consequently, decreased monocyte tissue factor expression and TFEV activity, reducing the prothrombotic state (33).

Cardiomyocytes and cardiac fibroblasts constitutively express high levels of TF. Beyond its role in

Copyright© ACE&M all rights reserved.

maintaining systemic hemostatic balance, TF is essential for cardiac hemostasis and acts as a protective barrier against intracardiac bleeding and hemorrhage. Experimental models with reduced TF expression have increased mortality, likely because extensive fibrosis predisposes patients to malignant arrhythmias and sudden death. Furthermore, TF expression and activity are markedly elevated in the myocardium following ischemia–reperfusion injury (34). These findings corroborate our results, in which TFEV and CardioEV counts were both increased in the FH group, suggesting a physiological relationship.

In the evaluation of PEVs, no significant difference was observed between the groups regarding the presence of FH/genetic variants. Platelets play a central role in primary hemostasis because of aggregation and secondary hemostasis because of their procoagulant properties (35). The FH patients in our study were young (mean age of 43.6 years) and possibly had incipient thrombus in atheromatous plaques, a condition observed in patients with more advanced processes.

This study has several limitations, mainly the limited sample size. In addition, genetic variants in other uninvestigated genes related to LDL metabolism may be present in family members classified as noncarriers. Moreover, characterization using other atherosclerotic biomarkers, such as pulse wave velocity, carotid and femoral plaques, and coronary artery calcification, is lacking. Considering that BMI was correlated with CardioEVs, other studies should investigate the mechanism related to these variables. Therefore, only 1st- and 2nd-degree relatives were included as controls, which may lead to the underestimation of differences and limit generalizability.

Statin use by FH patients also affects the expression of molecules on EVs, in addition to their production. Mobarrez and cols. (36) reported that atorvastatin reduces thrombin generation and the expression of TF, glycoprotein IIIa and P-selectin on PEVs in patients with peripheral vascular disease. In agreement with these findings, Tehrani and cols. (37) reported reduced expression of glycoprotein IIIa, P-selectin and TF on PEVs in patients with type 1 diabetes mellitus and dyslipidemia. Finally, Almquist and cols. (38) reported that simvastatin reduced the expression of P-selectin, TF and CD40L on PEVs and of TF on monocyte-derived EVs in patients with diabetes mellitus and chronic kidney disease. Consequently, future studies including FH patients before statin treatment should be conducted to evaluate the effect of genetic variants related to FH on EV count.

In conclusion, EVs have increasingly been recognized as promising candidates for both diagnostic and therapeutic applications. Beyond their potential utility as biomarkers of pathological processes and as vehicles for targeted interventions, EVs may further contribute to elucidating the impact of diverse confounding variables on disease mechanisms and clinical outcomes in FH patients. Our findings suggest that EVs are related to FH, since the counts of PS^{+}-EVs, cardioEVs, EEVs, and TFEVs, which are involved in the atherosclerosis process, were greater in individuals with FH and may be related to cardiovascular outcomes in these patients. However, considering the limitations of our study, we consider that these preliminary results should be validated in a large population with different lifestyles and genetic characteristics.

Funding: *Fundação de Amparo à Pesquisa do Estado de Minas Gerais* (Fapemig).

Acknowledgements: ATC and KBG are grateful to *Conselho Nacional de Desenvolvimento Científico e Tecnológico* – Brazil (CNPq) for the Research Fellowship (PQ).

Disclosure: no potential conflict of interest relevant to this article was reported.

Data availability: datasets related to this article will be available upon request to the corresponding author.

REFERENCES

1. Nordestgaard BG, Chapman MJ, Humphries SE, Ginsberg HN, Masana L, Descamps OS, et al.; European Atherosclerosis Society Consensus Panel. Familial hypercholesterolaemia is underdiagnosed and undertreated in the general population: guidance for clinicians to prevent coronary heart disease: consensus statement of the European Atherosclerosis Society. Eur Heart J. 2013 Dec;34(45):3478-90a. doi: 10.1093/eurheartj/eht273. Epub 2013 Aug 15. Erratum in: Eur Heart J. 2020 Dec 14;41(47):4517. doi: 10.1093/eurheartj/ehaa166.
2. Silva PR, Jannes CE, Marsiglia JD, Krieger JE, Santos RD, Pereira AC. Predictors of cardiovascular events after one year of molecular screening for Familial hypercholesterolemia. Atherosclerosis. 2016 Jul;250:144-50. doi: 10.1016/j.atherosclerosis.2016.05.023.
3. Scicali R, Di Pino A, Platania R, Purrazzo G, Ferrara V, Giannone A, et al. Detecting familial hypercholesterolemia by serum lipid profile screening in a hospital setting: Clinical, genetic and atherosclerotic burden profile. Nutr Metab Cardiovasc Dis. 2018 Jan;28(1):35-43.

Copyright© AE&M all rights reserved.

4. Iacocca MA, Chora JR, Carrié A, Freiberger T, Leigh SE, Defesche JC, et al.; ClinGen FH Variant Curation Expert Panel. ClinVar database of global familial hypercholesterolemia-associated DNA variants. Hum Mutat. 2018 Nov;39(11):1631-1640. doi: 10.1002/humu.23634.
5. Sturm AC, Knowles JW, Gidding SS, Ahmad ZS, Ahmed CD, Ballantyne CM, et al.; Convened by the Familial Hypercholesterolemia Foundation. Clinical Genetic Testing for Familial Hypercholesterolemia: JACC Scientific Expert Panel. J Am Coll Cardiol. 2018 Aug 7;72(6):662-680. doi: 10.1016/j.jacc.2018.05.044.
6. Khera AV, Won HH, Peloso GM, Lawson KS, Bartz TM, Deng X, van Leeuwen EM, Natarajan P, Emdin CA, Bick AG, Morrison AC, Brody JA, Gupta N, Nomura A, Kessler T, Duga S, Bis JC, van Duijn CM, Cupples LA, Psaty B, Rader DJ, et al. Diagnostic Yield and Clinical Utility of Sequencing Familial Hypercholesterolemia Genes in Patients With Severe Hypercholesterolemia. J Am Coll Cardiol. 2016 Jun 7;67(22):2578-89. doi: 10.1016/j.jacc.2016.03.520.
7. Mundi S, Massaro M, Scoditti E, Carluccio MA, van Hinsbergh VWM, Iruela-Arispe ML, et al. Endothelial permeability, LDL deposition, and cardiovascular risk factors-a review. Cardiovasc Res. 2018 Jan 1;114(1):35-52. doi: 10.1093/cvr/cvx226.
8. da Luz PL, Chagas P, Dourado M, et al. Endothelium in atherosclerosis: plaque formation and its complications. In: Endothelium and cardiovascular diseases. Academic Press; 2018. p. 493-512.
9. Marques FK, Campos FM, Filho OA, Carvalho AT, Dusse LM, Gomes KB. Circulating microparticles in severe preeclampsia. Clin Chim Acta. 2012 Dec 24;414:253-8. doi: 10.1016/j.cca.2012.09.023.
10. Carvalho LML, Ferreira CN, Sóter MO, Sales MF, Rodrigues KF, Martins SR, et al. Microparticles: Inflammatory and haemostatic biomarkers in Polycystic Ovary Syndrome. Mol Cell Endocrinol. 2017 Mar 5;443:155-162. doi: 10.1016/j.mce.2017.01.017.
11. Nomura S, Shouzu A, Omoto S, Nishikawa M, Iwasaka T. Effects of losartan and simvastatin on monocyte-derived microparticles in hypertensive patients with and without type 2 diabetes mellitus. Clin Appl Thromb Hemost. 2004 Apr;10(2):133-41. doi: 10.1177/107602960401000203.
12. Jannes CE, Silvino JPP, Silva PRS, Lima IR, Tada MT, Oliveira TGM, et al. Screening for Familial Hypercholesterolemia in Small Towns: Experience from 11 Brazilian Towns in the Hipercolbrasil Program. Arq Bras Cardiol. 2022 Apr;118(4):669-677. English, Portuguese. doi: 10.36660/abc.20201371.
13. Williams RR, Hunt SC, Schumacher MC, Hegele RA, Leppert MF, Ludwig EH, et al. Diagnosing heterozygous familial hypercholesterolemia using new practical criteria validated by molecular genetics. Am J Cardiol. 1993 Jul 15;72(2):171-6. doi: 10.1016/0002-9149(93)90155-6.
14. de Paiva Silvino JP, Jannes CE, Tada MT, Lima IR, Silva IFO, Pereira AC, et al. Cascade screening and genetic diagnosis of familial hypercholesterolemia in clusters of the Southeastern region from Brazil. Mol Biol Rep. 2020 Dec;47(12):9279-9288. doi: 10.1007/s11033-020-06014-0.
15. Campos FM, Franklin BS, Carvalho AT, Filho AL, Paula SC, Fontes CJ, et al. Augmented plasma microparticles during acute Plasmodium vivax infection. Malar J. 2010;9:1-8. doi: 10.1186/1475-2875-9-327.
16. Foody JM, Toth PP, Tomassini JE, Sajjan S, Ramey DR, Neff D, et al. Changes in LDL-C levels and goal attainment associated with addition of ezetimibe to simvastatin, atorvastatin, or rosuvastatin compared with titrating statin monotherapy. Vasc Health Risk Manag. 2013;9:719-27. doi: 10.2147/VHRM.S49840.
17. Ballantyne CM, Hoogeveen RC, Raya JL, Cain VA, Palmer MK, Karlson BW; GRAVITY Study Investigators. Efficacy, safety and effect on biomarkers related to cholesterol and lipoprotein metabolism of rosuvastatin 10 or 20 mg plus ezetimibe 10 mg vs. simvastatin 40 or 80 mg plus ezetimibe 10 mg in high-risk patients: Results of the GRAVITY randomized study. Atherosclerosis. 2014 Jan;232(1):86-93. doi: 10.1016/j.atherosclerosis.2013.10.022.
18. Izar MCO, Giraldez VZR, Bertolami A, Santos Filho RDD, Lottenberg AM, Assad MHV, et al. Update of the Brazilian Guideline for Familial Hypercholesterolemia - 2021. Arq Bras Cardiol. 2021 Oct;117(4):782-844. English, Portuguese. doi: 10.36660/abc.20210788.
19. Hjuler Nielsen M, Irvine H, Vedel S, Raungaard B, Beck-Nielsen H, Handberg A. Elevated atherosclerosis-related gene expression, monocyte activation and microparticle-release are related to increased lipoprotein-associated oxidative stress in familial hypercholesterolemia. PLoS One. 2015 Apr 13;10(4):e0121516. doi: 10.1371/journal.pone.0121516.
20. Nielsen MH, Irvine H, Vedel S, Raungaard B, Beck-Nielsen H, Handberg A. The Impact of Lipoprotein-Associated Oxidative Stress on Cell-Specific Microvesicle Release in Patients with Familial Hypercholesterolemia. Oxid Med Cell Longev. 2016;2016:2492858. doi: 10.1155/2016/2492858.
21. Chen YT, Yuan HX, Ou ZJ, Ou JS. Microparticles (Exosomes) and Atherosclerosis. Curr Atheroscler Rep. 2020 May 28;22(6):23. doi: 10.1007/s11883-020-00841-z.
22. de Gonzalo-Calvo D, Cenarro A, Garlaschelli K, Pellegatta F, Vilades D, Nasarre L, et al. Translating the microRNA signature of microvesicles derived from human coronary artery smooth muscle cells in patients with familial hypercholesterolemia and coronary artery disease. J Mol Cell Cardiol. 2017 May;106:55-67. doi: 10.1016/j.yjmcc.2017.03.005.
23. Chistiakov DA, Orekhov AN, Bobryshev YV. Cardiac Extracellular Vesicles in Normal and Infarcted Heart. Int J Mol Sci. 2016 Jan 5;17(1):63. doi: 10.3390/ijms17010063.
24. Wagner KT, Radisic M. A New Role for Extracellular Vesicles in Cardiac Tissue Engineering and Regenerative Medicine. Adv Nanobiomed Res. 2021 Nov;1(11):2100047. doi: 10.1002/anbr.202100047.
25. Pestana RMC, Teixeira-Carvalho A, Dos Santos LI, de Oliveira AN, Soares CE, Sabino AP, et al. Microparticles and cardiotoxicity secondary to doxorubicin-based chemotherapy in breast cancer patients. Int J Cardiol. 2024 Jan 15;395:131435. doi: 10.1016/j.ijcard.2023.131435.
26. Curtis AM, Edelberg J, Jonas R, Rogers WT, Moore JS, Syed W, et al. Endothelial microparticles: sophisticated vesicles modulating vascular function. Vasc Med. 2013 Aug;18(4):204-14. doi: 10.1177/1358863X13499773.
27. Finn NA, Eapen D, Manocha P, Al Kassem H, Lassegue B, Ghasemzadeh N, et al. Coronary heart disease alters intercellular communication by modifying microparticle-mediated microRNA transport. FEBS Lett. 2013 Nov 1;587(21):3456-63. doi: 10.1016/j.febslet.2013.08.034.
28. Schiro A, Wilkinson FL, Weston R, Smyth JV, Serracino-Inglott F, Alexander MY. Endothelial microparticles as conveyors of information in atherosclerotic disease. Atherosclerosis. 2014 Jun;234(2):295-302. doi: 10.1016/j.atherosclerosis.2014.03.019.
29. Dignat-George F, Boulanger CM. The many faces of endothelial microparticles. Arterioscler Thromb Vasc Biol. 2011 Jan;31(1):27-33. doi: 10.1161/ATVBAHA.110.218123. .
30. Suades R, Padró T, Alonso R, Mata P, Badimon L. Lipid-lowering therapy with statins reduces microparticle shedding from endothelium, platelets and inflammatory cells. Thromb Haemost. 2013 Aug;110(2):366-77. doi: 10.1160/TH13-03-0238.
31. Huang B, Cheng Y, Xie Q, Lin G, Wu Y, Feng Y, et al. Effect of 40 mg versus 10 mg of atorvastatin on oxidized low-density lipoprotein, high-sensitivity C-reactive protein, circulating endothelial-derived microparticles, and endothelial progenitor cells in patients with ischemic cardiomyopathy. Clin Cardiol. 2012 Feb;35(2):125-30. doi: 10.1002/clc.21017.
32. Otomo K, Amengual O, Fujieda Y, Nakagawa H, Kato M, Oku K, et al. Role of apolipoprotein B100 and oxidized low-density lipoprotein in the monocyte tissue factor induction mediated by anti-β2 glycoprotein I antibodies. Lupus. 2016 Oct;25(12):1288-98. doi: 10.1177/0961203316638165.
33. Owens AP 3rd, Passam FH, Antoniak S, Marshall SM, McDaniel AL, Rudel L, et al. Monocyte tissue factor-dependent activation of

Copyright© AE&M all rights reserved.

coagulation in hypercholesterolemic mice and monkeys is inhibited by simvastatin. J Clin Invest. 2012 Feb;122(2):558-68. doi: 10.1172/JCI58969.

34. Rauch U. Tissue factor and cardiomyocytes. Thromb Res. 2012 May;129 Suppl 2:S41-3. doi: 10.1016/j.thromres.2012.02.029.
35. Varon D, Shai E. Platelets and their microparticles as key players in pathophysiological responses. J Thromb Haemost. 2015 Jun;13 Suppl 1:S40-6. doi: 10.1111/jth.12976.
36. Mobarrez F, He S, Bröijersen A, Wiklund B, Antovic A, Antovic J, et al. Atorvastatin reduces thrombin generation and expression of tissue factor, P-selectin and GPIIIa on platelet-derived microparticles in patients with peripheral arterial occlusive disease. Thromb Haemost. 2011 Aug;106(2):344-52. doi: 10.1160/TH10-12-0810.
37. Tehrani S, Mobarrez F, Antovic A, Santesson P, Lins PE, Adamson U, et al. Atorvastatin has antithrombotic effects in patients with type 1 diabetes and dyslipidemia. Thromb Res. 2010 Sep;126(3):e225-31. doi: 10.1016/j.thromres.2010.05.023.
38. Almquist T, Mobarrez F, Jacobson SH, Wallén H, Hjemdahl P. Effects of lipid-lowering treatment on circulating microparticles in patients with diabetes mellitus and chronic kidney disease. Nephrol Dial Transplant. 2016 Jun;31(6):944-52. doi: 10.1093/ndt/gfv337.

SUPPLEMENTARY MATERIAL

Table S1. Extracellular vesicle phenotyping panel

Filter	530/30	575/26	780/60	670/14	450/50
Antibody	anti-CD51/61	anti-CD142	anti-CD41a	anti-caveolin-3	Annexin V
Fluorochrome	FITC	PE	PE-Cy7	Alexa Fluor 647	eFluor 450
Specificity	endothelium	tissue factor	platelets	cardiomyocyte	phosphatidylserine
Concentration	1.0 µg/100 µL	0.125 µg/100 µL	0.125 µg/100 µL	1.8 µg/100 µL	5.0 µL/test
Clone	monoclonal (clone 23C6)	monoclonal (clone HTF-1)	monoclonal (clone HIP8)	polyclonal	monoclonal
Catalog number#	11-0519-42 (ThermoFisher)	12-1429-42 (ThermoFisher)	25-0419-42 (ThermoFisher)	sc-5310 (Santa Cruz)	88-8006-72 (eBioscience)

Copyright© AE&M all rights reserved.

Archives of Endocrinology and Metabolism
ISSN 2359-4292
OFFICIAL JOURNAL OF THE BRAZILIAN SOCIETY OF ENDOCRINOLOGY AND METABOLISM

original

Intact and bioactive PTH values are strongly correlated in kidney transplant recipients

Tábata Carolina Faria Nascimento de Assis[1]
https://orcid.org/0000-0002-0467-9255

Humberto Campos Clemente[2]
https://orcid.org/0009-0000-2049-6304

Daniel Borges Drumond[1]
https://orcid.org/0009-0009-8575-1455

Leandro Junior Lucca[1]
https://orcid.org/0000-0001-8236-637X

Miguel Moyses-Neto[1]
https://orcid.org/0000-0003-1351-4775

Francisco José Albuquerque de Paula[3]
https://orcid.org/0000-0003-1262-3486

Elen Almeida Romão[1]
https://orcid.org/0000-0002-9302-3089

[1] Divisão de Nefrologia, Departamento de Clínica Médica, Faculdade de Medicina de Ribeirão Preto, Universidade de São Paulo, São Paulo, SP, Brasil
[2] Faculdade de Medicina de Ribeirão Preto, Universidade de São Paulo, Ribeirão Preto, SP, Brasil
[3] Divisão de Endocrinologia e Metabologia, Departamento de Clínica Médica, Faculdade de Medicina de Ribeirão Preto, Universidade de São Paulo, Ribeirão Preto, SP, Brasil

ABSTRACT

Objective: This study aims to evaluate the correlation between parathyroid hormone measured by a second-generation assay (PTHG2) and by a third-generation assay (PTHG3), and their association with mineral and bone disorder (MBD) biochemical parameters and radiographic vascular calcification score in kidney transplant recipients (KTRs). **Materials and methods:** We evaluated 87 KTRs and measured PTHG2, PTHG3, biochemical profile, urinary fractional excretion of calcium (FE Ca) and phosphate, 25(OH)D_3, and Kauppila score for vascular calcification. Statistical analysis: Non-parametric tests and logistic regression analysis were performed. The significance level was set to 5%. **Results:** In our population, the mean age was 54 years, the mean time after transplantation was 9.4 years (± 7.6), and the mean estimated glomerular filtration rate (GFR, calculated using the Chronic Kidney Disease Epidemiology Collaboration equation — CKD-EPI) was 59.1 mL/min/1.73 m^2. The correlation between PTHG2 and PTHG3 was almost perfect (r = 0.99; 95% CI = 0.98-0.99) and there was no significant difference between the PTHG2/PTHG3 ratio from different KTR-CKD stages. Investigating the association among PTH and the MBD biochemical profile, there was only correlation between PTH and FE Ca (p-value 0.01). **Conclusion:** We concluded that there is no advantage in PTHG3 dosage over PTHG2 measurement in this population.

Keywords: Kidney transplantation; parathyroid hormone; vascular calcification; chronic kidney disease-mineral and bone disorder

INTRODUCTION

Chronic kidney disease (CKD) is a condition of high morbidity and mortality. Its prevalence reached about 9.1% of the world population and more than 2.5 million people were on renal replacement therapy in 2017 (1). In this context, mineral and bone disorders (MBD) stand out among the factors that increase CKD morbidity (2).

Kidney transplant is the best choice for treatment of end-stage CKD, as it promotes higher quality and life expectancy (3). However, mineral and bone disease may remain after renal transplantation, either due to persistent hyperparathyroidism, chronic use of corticosteroids, or progressive renal graft dysfunction (4).

From the earliest stages of CKD, there is a reduction in urinary phosphorus excretion. As compensation, there is an increase in phosphaturic mechanisms, represented by FGF-23 and parathyroid hormone

Received on May/13/2025
Accepted on Oct/17/2025
DOI: 10.20945/2359-4292-2026-0021

Correspondence to:
Elen Almeida Romão
Divisão de Nefrologia,
Departamento de Clínica Médica,
Faculdade de Medicina de Ribeirão Preto,
Universidade de São Paulo
Avenida Bandeirantes, 3900
14048-900 – Ribeirão Preto, SP, Brasil
earomao@fmrp.usp.br

Associated editor:
Marise Lazaretti-Castro
https://orcid.org/0000-0001-9186-2834

This is an open-access article distributed under the terms of the Creative Commons Attribution License

Copyright© AE&M all rights reserved.

(PTH). PTH 1-84 is an 84 amino acid polypeptide secreted by parathyroid principal cells under hypocalcemia stimulus – the initial sequence of amino acids being the amino-terminal fragment and the last sequence, the carboxy-terminal fragment (5).

The first 34 amino acids of the amino-terminal portion are involved in the activation of the PTH1R receptor. Therefore, PTH 1-34 corresponds to the biologically active fragment, responsible for its hormonal action in bones and kidneys (5).

Under hypercalcemia, PTH is cleaved into several parts in the parathyroid (before its secretion) and in the liver (in peripheral metabolism): the amino-terminal fragments are rapidly degraded and the carboxy-terminal fragments remain in the bloodstream, from where it is slowly filtered by the kidneys (6). These carboxy-terminal fragments usually accumulate in renal failure. Furthermore, the inflammatory state of CKD increases oxidative stress and, consequently, post-translational modifications of the PTH molecule, such as the oxidation of methionine residues at positions 8 and 18 (7). Thus, one may conclude that PTH measurement can be extremely challenging.

Non-bioactive presentations often mentioned in previous studies are the PTH 7-84 fragment and the oxidized PTH (7,8), which curiously were not detected by high-resolution mass spectrometry. This fact, apart from possible methodological disparities, raises doubts about the real role of these presentations *in vivo* (6).

Over the past few decades, increasingly sensitive tests have been developed to measure PTH levels. The most commercially available is the second-generation test (PTHG2), which has the inconvenience of also measuring non-bioactive fragments of PTH. Newer third-generation methods (PTHG3) have emerged to address these technical problems, with final values approximately reduced to half of the PTHG2 measurements (9).

Despite the variety of studies about PTH measurement methods in patients with CKD, few studies have been conducted to evaluate these different methodologies in kidney transplant recipients (KTRs). Our study aims to evaluate the correlation between PTHG2 and PTHG3 to clarify whether there would be an advantage in PTHG3 dosing in this population. Furthermore, we intend to investigate whether PTHG2 and PTHG3 have a stronger association with vascular calcification (Kauppila score) and some BMD parameters after kidney transplantation. We hypothesized that intact and bioactive PTH values are also correlated in KTRs.

MATERIALS AND METHODS

Study population

This is a cross-sectional, convenience sampling, single center study. We included adults who had received at least 90 days previously, a single renal transplant between November 2016 and October 2018. We excluded patients with inadequate biological samples or with clinical complications at the time of recruitment, such as rejection, infectious diseases, and neoplasms. All patients were classified into 5 stages of CKD, according to KDIGO guidelines (3). The clinical data were collected from medical records and interviews.

All patients gave written informed consent. This study was approved by the Research Ethics Committee of the Clinical Hospital of Ribeirão Preto, University of São Paulo in Ribeirão Preto, Brazil (*Hospital das Clínicas da Faculdade de Medicina da USP de Ribeirão Preto* – HCFMRP-USP), No. 1.746.953, in 2016.

Laboratory parameters

Fasting blood samples were collected for measurement of total calcium, albumin, phosphorus, and alkaline phosphatase. In urine samples, we measured creatinine, calcium, and phosphorus. The tests were performed using the enzymatic method (WIENER®), according to standard laboratory protocols. The urinary fractional excretion of calcium (FE Ca) and phosphate were calculated with the usual equations.

The 25-hydroxyvitamin D [25(OH)D_3] was evaluated by chemiluminescence using the LIAISON® test. PTHG2 measurements were performed with the LIAISON® N-TACT® kit (reference value range: 14.5-87.1 pg/mL), while PTHG3 was evaluated by the LIAISON® 1-84 PTH assay (reference value range: 6.7-38.8 pg/mL), both from DiaSorin (Saluggia, Italy). Samples for PTHG2 and PTHG3 determinations were centrifugated and subsequently frozen at -70 °C for later duplicate analysis.

Copyright© AE&M all rights reserved.

Radiographic parameters

The assessment of vascular calcification was performed using the Kauppila score. This score indicates a greater cardiovascular risk (a positive index) in the presence of seven or more points of calcification in the abdominal aorta parallel to the L1-L4 vertebrae on a lateral abdominal x-ray, on a scale that ranges from 0 to 24 (10).

Two experienced radiologists classified the radiographs according to the Kauppila score. Agreement between evaluators regarding the presence of vascular calcification was analyzed, with a Kappa coefficient of 0.91.

Statistical analysis

Epidemiological and clinical data are presented as mean (standard deviation), median (minimal – maximal values), or percentage. We used LibreOffice Writer version 7.1.6.2, LibreOffice Calc version 7.1.6.2, and R for Windows version 4.0.2. The significance level was set to 5%.

To investigate whether there is PTHG2 retention with CKD progression, the Kruskal-Wallis test was performed to analyze the PTHG2/PTHG3 ratio for each CKD stage. Correlation studies were performed using Spearman's rank correlation coefficient.

Finally, a logistic regression model was adjusted for the Kauppila calcification score and each PTH method.

RESULTS

Patient characteristics

A total of 87 patients were evaluated. Demographic, clinical, and laboratory data are presented in **Tables 1** and **2**. The mean time after transplantation was 9.4 years (± 7.6). Induction of immunosuppression was performed with thymoglobulin and basiliximab in 49.43% and 48.28% of cases, respectively. Current immunosuppression consisted mainly of prednisone, tacrolimus, and mycophenolate sodium. Regarding specific medications for CKD-MBD, 21.84% used cholecalciferol or ergocalciferol, 12.6% used cinacalcet, and 3.45% used calcitriol. Finally, **Table 3** describes PTHG2 and PTHG3 values according to CKD stage.

Primary endpoints

In all CKD stages, PTHG2 values were higher than PTHG3 values. PTHG2 was approximately 2.6 times greater than PTHG3 **(Table 3)**. At the 5% significance level, there is no evidence that the PTHG2/PTHG3 ratio changes between CKD stages (Kruskal-Wallis test p-value 0.37). These data are best visualized in the box plot of **Figure 1**.

Table 3 presents the Spearman correlation coefficients between PTHG2 and PTHG3 for the complete sample and for each CKD stage. As seen in this table and in the scatterplots shown in **Figure 2**, these two variables are highly correlated. The minimum value was 0.93 for CKD stage 1, 0.94 for stage 3B, and 0.96 for stage 4, which means that the correlation remains high even at the most severe levels of the renal disease.

Secondary endpoints

Considering the interference of drugs and parathyroidectomy in bone metabolism, we excluded patients who were using calcitriol, cholecalciferol, ergocalciferol, and cinacalcet from the analysis of the secondary endpoints, as well as patients who had undergone parathyroidectomy. Thus, 58 patients were studied.

Table 1. Demographic and clinical data

Variables	All patients
Age (years), mean (standard deviation)	54 (13.0)
Male, No. (%)	53 (60.92)
Parathyroidectomy, No. (%)	4 (4.5)
Modality of Dialysis	
Haemodialysis, No. (%)	69 (79.3)
Peritoneal dialysis, No. (%)	3 (3.4)
Both, no. (%)	14 (16.1)
None, no. (%)	1 (1.2)
Chronic kidney disease aetiology	
Hypertension, No. (%)	22 (25.29)
Diabetes mellitus, No. (%)	14 (16.09)
Polycystic kidney disease, No. (%)	3 (3.45)
Glomerulopathy, No. (%)	21 (24.14)
Urinary obstruction, No. (%)	3 (3.45)
Unknown aetiology, No. (%)	24 (27.7)
Donor	
Living, No. (%)	19 (21.84)
Deceased, No. (%)	68 (78.2)
Retransplant, No. (%)	4 (4.6)

Copyright© AE&M all rights reserved.

Table 2. Laboratory data

Variable	No.	Minimum	Median	Maximum
CKD-EPI (mL/min/1,73 m^2)	87	14.0	59.0	125.0
PTHG2 (pg/mL)	87	10.6	119.0	739.0
PTHG3 (pg/mL)	87	5.9	46.2	246.0
25(OH)D_3 (ng/mL)	85	5.0	23.8	61.0
ALP (U/L)	87	84.5	175.0	554.6
Phosphorus (mg/dL)	87	1.8	3.4	6.1
Total Calcium (mg/dL)	87	7.3	9.8	12.6
Albumin (g/dL)	87	3.6	4.3	4.8
FE Ca (%)	87	0.0	0.6	7.8
FE P (%)	85	2.0	17.7	41.8

ALP: alkaline phosphatase; FE Ca: fractional excretion of calcium; FE P: fractional excretion of phosphate; CV: coefficient of variation.

Table 3. Descriptive data of PTHG2 and PTHG3 according to CKD stage. Correlation between PTHG2 and PTHG3 for the total sample and for each CKD stage

CKD	*n*	PTH	Median	Minimum-Maximum	p-Value*	Spearman (rho)#	95% CI
Total	87	G2	119.0	10.6-739	<0.001	0.99	0.98-0.99
		G3	46.2	5.9-246			
1	9	G2	119	38.3-252	0.004	0.93	
		G3	46.2	14-82			
2	34	G2	102.6	10.6-739	<0.001	0.99	
		G3	40.6	5.9-246			
3A	19	G2	143.0	36.3-493	<0.001	0.99	
		G3	52.3	16.1-161			
3B	15	G2	78.9	41.3-168	<0.001	0.94	
		G3	30.9	16.6-65			
4	10	G2	192.5	123-694	0.002	0.96	
		G3	70.4	51.1-229			

CV: coefficient of variation; CI: confidence interval.
*Wilcoxon test p-Values to verify the difference between PTHG2 and PTHG3 for the total sample and for each CKD stage.
#Spearman correlation coefficient (rho) between PTHG2 and PTHG3 for total sample and for each CKD stage.

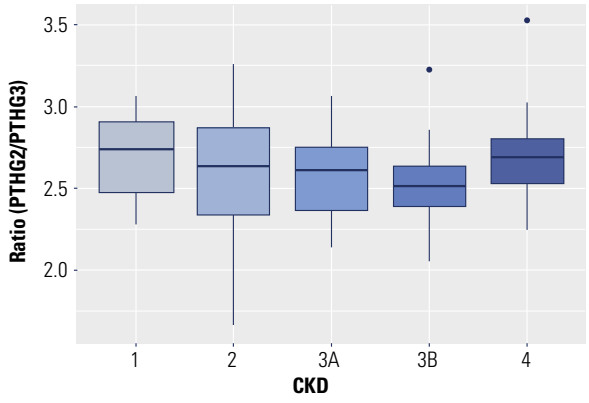


Figure 1. PTHG2/PTHG3 ratio according to CKD stage *box plot*.

Table 4 shows Spearman correlation coefficient values between some laboratory variables and PTHG2 and PTHG3, as well as the corresponding p-values. At the 5% significance level, there is evidence of a negative association between PTH (regardless of the method) and glomerular filtration rate (GFR) and a positive association between PTH (regardless of the method) and FE Ca. There was no correlation between PTH values (regardless of the method).

To verify whether there is an effect of PTHG2 and PTHG3 on the Kauppila calcification score (Table A.1), a logistic regression model was adjusted for each PTH method. Table 5 shows that at 5% significance level, all

Copyright© AE&M all rights reserved.

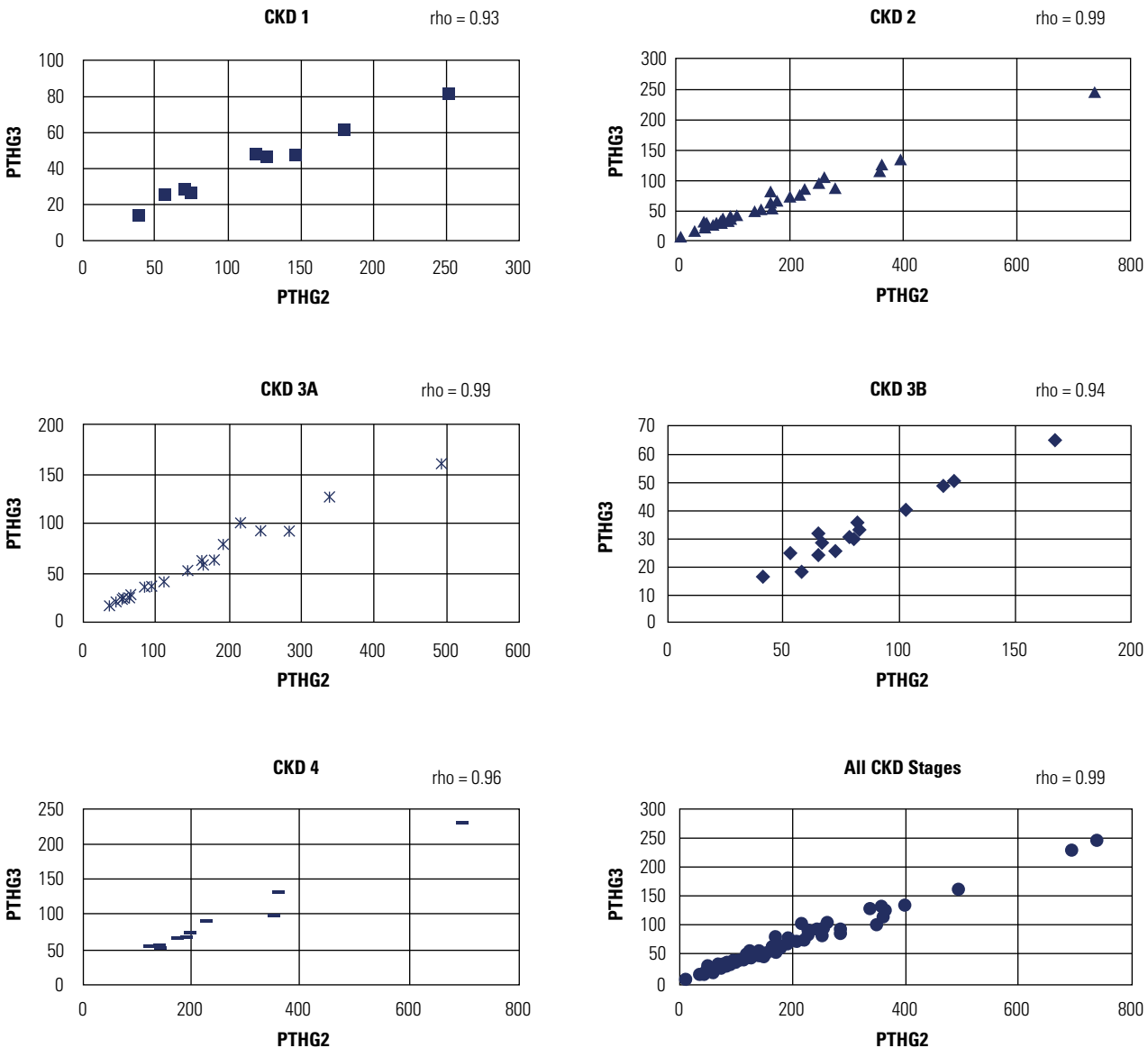


Figure 2. Dispersion diagram. Spearman correlation (rho) between PTHG2 and PTHG3 according to stage of kidney disease.

Table 4. Spearman correlation coefficients (rho) between some laboratory variables and PTHG2 and PTHG3 – 58 patients

	PTHG2		PTHG3	
Variable	**rho**	**p-Value**	**rho**	**p-Value**
CKD-EPI	**-0.27**	**0.037**	**-0.30**	**0.024**
25(OH)D_3	-0.15	0.275	-0.15	0.263
ALP	0.02	0.888	0.03	0.834
Phosphorus	-0.02	0.913	-0.02	0.912
Total Calcium	0.06	0.633	0.05	0.703
FE Ca	**0.33**	**0.011**	**0.33**	**0.011**
FE P	0.15	0.282	0.18	0.176

ALP: alkaline phosphatase; FE Ca: fractional excretion of calcium; FE P: fractional excretion of phosphate.

Copyright© AE&M all rights reserved.

Table 5. Estimates and p-values related to the logistic regression and the Hosmer and Lemeshow test (HL)

Calcification Score	PTHG2			PTHG3		
	Estimate	p-value	p-value HL test	Estimate	p-value	p-value HL test
Kauppila	0.0006	0.818	0.567	0.0033	0.677	0.764

models are well adjusted (p-values for the Hosmer and Lemeshow test ≥ 0.57) and that there is no evidence of an effect of PTHG2 and PTHG3 on calcification scores (p-values ≥ 0.68).

DISCUSSION

The determination of PTH by both PTHG2 and PTHG3 includes the use of two antibodies in "sandwich": the first antibody captures the carboxy-terminal fragment of PTH (usually amino acids 39-84), while the second antibody selects and quantifies, among the captured molecules, those with the amino-terminal fragment – being an intermediate amino acid sequence in PTHG2 tests (e.g., 12-24, 26-32, 12-18, 13-34, etc.) and an initial sequence in PTHG3 tests (e.g., 1-4) (6,8,11).

As expected, PTHG2 does not identify the beginning of the amino-terminal sequence and may quantify undesirable PTH fragments which lost the first amino acids. As stated previously, PTH 1-34 is the biologically active fragment (5).

In contrast, PTHG3 detects the first and the last amino acids of the molecule, identifying the "whole" PTH. However, PTHG3 cross-reacts with forms of PTH 1-84 that have undergone post-translational changes, such as such as the oxidation of methionine residues at positions 8 and 18 and the phosphorylation of serine 17. The latter represents a molecule hyper-secreted in parathyroid neoplasms, corresponding to 15% of the final PTHG3 measurement in patients with CKD (6,7,12,13).

As a primary endpoint, our study evaluated the correlation between PTHG2 (intact PTH) and PTHG3 (bioactive PTH) levels in KTRs. A very strong correlation (r = 0.99; 95% CI = 0.98 – 0.99) was found between PTHG2 and PTHG3 levels, with the value of PTHG2 being about 2.6 times the PTHG3 measurement, a higher ratio than found in previous studies (9,13).

Our study agrees with data previously found in chronic renal volunteers. Einbinder and cols., in a study that evaluated 98 patients with non-dialytic CKD in stages 3, 4, and 5, found a strong correlation (r = 0.963, p-value < 0.01) between PTHG2 and PTHG3 values (14). O'Flaherty and cols., in a study comprising 140 pre-dialysis volunteers, found a correlation in patients with end-stage CKD (r = 0.98, p-value < 0.01) and in patients with better CKD stages (r = 0.96, p-value < 0.01) (15). Gannagé-Yared and cols., in a study comprising 92 patients on hemodialysis, found a significant correlation between PTHG2 and PTHG3 (r = 0.923, p-value < 0.01) (13). Melamed and cols., in a study that evaluated 515 patients on hemodialysis and peritoneal dialysis, found a very strong correlation between PTHG2 and PTHG3 (r = 0.99, p-value < 0.01) (9).

The PTHG2/PTHG3 ratio did not vary significantly between CKD stages (p-value 0.37). These data suggest that, despite the retention of unwanted PTH fragments, a proportional increase in PTHG2 relative to PTHG3 was not found as the GFR was reduced. Different results were found by O'Flaherty and cols., who observed 18% lower PTHG3 values in stages 1-4 and 40% lower PTHG3 values in stage 5 when compared to PTHG2 (15).

In the present study, the negative correlation between PTH and GFR was expected since this variable determines the severity of the renal disease. Except for the FE Ca, there were no correlations between PTHG2 or PTHG3 levels and other MBD parameters and Kauppila calcification score. Probably the serum calcium levels remained stable because of a greater urinary calcium excretion as PTH increases. It is noteworthy that, although significant, the correlation between PTH and FE Ca can be considered weak in both cases (the highest absolute value was 0.33).

In the pre-dialysis population, Einbinder and cols. found significant correlations between both PTH measurement methods and calcium, phosphorus, and 25(OH)D3 values, while O'Flaherty and cols. found

Copyright© AE&M all rights reseved.

only correlation between PTHG3 (bioactive PTH; 1-84) and calcium and phosphorus levels (14,15).

In the dialysis population, Gannagé-Yared and cols. found a correlation only between PTH (regardless of the method) and alkaline phosphatase and type I collagen degradation products (13). In contrast, the CHOICE study found a negative correlation with calcium and a positive correlation with phosphorus between PTHG3 (bioactive PTH; 1-84) and unwanted PTH fragments (represented by the PTHG2-PTHG3 difference). In the latter study, mortality was associated only with PTHG3 (9).

To our knowledge, the only study that evaluated the correlation between PTHG2 and PTHG3 in transplanted patients was carried out by Tan and cols. These authors evaluated 83 patients: 44 pre-dialysis, 15 on hemodialysis, 15 on peritoneal dialysis, and 9 after renal transplantation. PTHG2 and PTHG3 had a good correlation, and PTHG3 (PTH 1–84) showed a positive association with phosphate and alkaline phosphatase (16). However, unlike our study, all KTRs included were already in end-stage CKD.

Our study has several limitations, such as the small number of patients, the single-center and convenience sampling, the cross-sectional design, and the absence of multivariate analyses. These limitations must be acknowledged, as they may restrict the generalizability of the findings.

In summary, based on our data, it is possible to establish a very strong correlation between levels of PTHG2 and PTHG3 in KTRs. Therefore, our study suggests that there is no advantage in PTHG3 dosage over PTHG2 measurement. However, apart from the FE Ca, no correlations have been established between PTH, several MBD parameters, and Kauppila calcification score. Further longitudinal studies are needed.

Funding: this study was financed in part by the *Coordenação de Aperfeiçoamento de Pessoal de Nível Superior – Brasil* (CAPES) – Finance Code 001. One author received CNPq scholarships.

Acknowledgements: National Council for Scientific and Technological Development (CNPq) provided scholarship; Prof. Denise Aparecida Botter, Prof. Mônica Carneiro Sandoval, and Maurício Vieira da Cunha (Centre for Applied Statistics – Department of Statistics, University of São Paulo, São Paulo, Brazil) performed the statistical analysis; Foundation to Support Teaching, Research and Assistance of the Hospital das Clínicas of the Ribeirão Preto Medical School – University of São Paulo (FAEPA) provided financial support.

Authors' contributions: study conception and design: EAR, MMN, LLJ, FJAP; data acquisition: HCC, DBD; statistical analysis: DBD, HCC; data analysis and interpretation: TCFNA, EAR; writing, revision, and editing: TCFNA, MMN, FJAP, EAR. Each author contributed intellectually during the writing or review of the manuscript and accepted responsibility for the overall work ensuring that questions regarding the accuracy or completeness of any part of the study were adequately investigated and resolved.

Disclosure: no potential conflict of interest relevant to this article was reported.

Data availability: datasets related to this article will be available upon request to the corresponding author.

REFERENCES

1. GBD Chronic Kidney Disease Collaboration. Global, regional, and national burden of chronic kidney disease, 1990-2017: a systematic analysis for the Global Burden of Disease Study 2017. Lancet. 2020 Feb 29;395(10225):709-733. doi: 10.1016/S0140-6736(20)30045-3.
2. Sharma AK, Toussaint ND, Elder GJ, Rajapakse CS, Holt SG, Baldock P, et al. Changes in bone microarchitecture following kidney transplantation-Beyond bone mineral density. Clin Transplant. 2018 Sep;32(9):e13347. doi: 10.1111/ctr.13347.
3. Chapman JR. The KDIGO clinical practice guidelines for the care of kidney transplant recipients. Transplantation. 2010 Mar 27;89(6):644-5. doi: 10.1097/TP.0b013e3181d62f1b.
4. Vangala C, Pan J, Cotton RT, Ramanathan V. Mineral and Bone Disorders After Kidney Transplantation. Front Med (Lausanne). 2018 Jul 31;5:211. doi: 10.3389/fmed.2018.00211.
5. Gardella TJ, Nissenson RA, Jüppner H. Parathyroid hormone. In: Bilezikian JP, editor. Primer on the Metabolic Bone Diseases and Disorders of Mineral Metabolism. 9th ed. Hoboken: John Wiley & Sons; 2019. p. 205-11.
6. Ulmer CZ, Kritmetapak K, Singh RJ, Vesper HW, Kumar R. High-Resolution Mass Spectrometry for the Measurement of PTH and PTH Fragments: Insights into PTH Physiology and Bioactivity. J Am Soc Nephrol. 2022 Aug;33(8):1448-1458. doi: 10.1681/ASN.2022010036.
7. Hocher B, Yin L. Why Current PTH Assays Mislead Clinical Decision Making in Patients with Secondary Hyperparathyroidism. Nephron. 2017;136(2):137-142. doi: 10.1159/000455289.
8. Komaba H, Takeda Y, Shin J, Tanaka R, Kakuta T, Tominaga Y, Fukagawa M. Reversed whole PTH/intact PTH ratio as an indicator of marked parathyroid enlargement: five case studies and a literature review. NDT Plus. 2008 Aug;1(Suppl 3):iii54-iii58. doi: 10.1093/ndtplus/sfn088.
9. Melamed ML, Eustace JA, Plantinga LC, Jaar BG, Fink NE, Parekh RS, et al. Third-generation parathyroid hormone assays and all-cause mortality in incident dialysis patients: the CHOICE study. Nephrol Dial Transplant. 2008 May;23(5):1650-8. doi: 10.1093/ndt/gfm849.
10. Kauppila LI, Polak JF, Cupples LA, Hannan MT, Kiel DP, Wilson PW. New indices to classify location, severity and progression of calcific lesions in the abdominal aorta: a 25-year follow-up study. Atherosclerosis. 1997 Jul 25;132(2):245-50. doi: 10.1016/s0021-9150(97)00106-8.
11. Komaba H, Goto S, Fukagawa M. Critical issues of PTH assays in CKD. Bone. 2009 Apr;44(4):666-70. doi: 10.1016/j.bone.2008.12.016.
12. Rubin MR, Silverberg SJ, D'Amour P, Brossard JH, Rousseau L, Sliney J Jr, et al. An N-terminal molecular form of parathyroid hormone (PTH) distinct from hPTH(1-84) is overproduced in parathyroid carcinoma. Clin Chem. 2007 Aug;53(8):1470-6. doi: 10.1373/clinchem.2007.085506.
13. Gannagé-Yared MH, Farès C, Ibrahim T, Rahal ZA, Elias M, Chelala D. Comparison between a second and a third generation parathyroid

Copyright© AE&M all rights reserved.

hormone assay in hemodialysis patients. Metabolism. 2013 Oct;62(10):1416-22. doi: 10.1016/j.metabol.2013.05.007.

14. Einbinder Y, Benchetrit S, Golan E, Zitman-Gal T. Comparison of Intact PTH and Bio-Intact PTH Assays Among Non-Dialysis Dependent Chronic Kidney Disease Patients. Ann Lab Med. 2017 Sep;37(5):381-387. doi: 10.3343/alm.2017.37.5.381.
15. O'Flaherty D, Sankaralingam A, Scully P, Manghat P, Goldsmith D, Hampson G. The relationship between intact PTH and biointact PTH (1-84) with bone and mineral metabolism in pre-dialysis chronic kidney disease (CKD). Clin Biochem. 2013 Oct;46(15):1405-9. doi: 10.1016/j.clinbiochem.2013.06.023.
16. Tan K, Ong L, Sethi SK, Saw S. Comparison of the Elecsys PTH(1-84) assay with four contemporary second generation intact PTH assays and association with other biomarkers in chronic kidney disease patients. Clin Biochem. 2013 Jun;46(9):781-6. doi: 10.1016/j.clinbiochem.2013.01.016.

APPENDICE

Table A.1. Descriptive measures of PTHG2 and PTHG3 by Kauppila Score – 58 patients

Index	n	PTH	Mean	Standard deviation	Minimum	Median	Maximum
Negative	35	G2	143.1	134.8	10.6	85.1	739
		G3	53.1	45.3	5.9	35.7	246
Positive	11	G2	153.2	95.2	36.3	123.0	360
		G3	59.2	32.3	16.1	50.5	114
NA	12	G2	148.3	86.9	34.1	154.0	283
		G3	56.7	30.4	15.0	56.5	93

Copyright© AE&M all rights reserved.

Archives of Endocrinology and Metabolism
ISSN 2359-4292
OFFICIAL JOURNAL OF THE BRAZILIAN SOCIETY OF ENDOCRINOLOGY AND METABOLISM

original

Accuracy of clinical risk factor-based models as a screening test for detecting gestational diabetes mellitus in a low-resource setting

Olayinka Comfort Senbanjo[1]
https://orcid.org/0000-0002-6365-2247

Fatimat Motunrayo Akinlusi[1,2]
https://orcid.org/0000-0003-0999-5879

Kabiru Afolarin Rabiu[1,2]
https://orcid.org/0000-0003-2640-6562

[1] Department of Obstetrics and Gynaecology, Lagos State University Teaching Hospital, No 1-5 Oba Akinjobi Way, GRA, Ikeja, Lagos State, Nigeria
[2] Department of Obstetrics and Gynaecology, Lagos State University College of Medicine, Ikeja, Lagos State, Nigeria

ABSTRACT

Objective: Screening and diagnosing gestational diabetes mellitus (GDM) usually requires a 2-hour, 75 g oral glucose tolerance test (OGTT), which can be challenging for both patients and healthcare systems. Alternative clinical risk factor-based models have been suggested but have not been extensively tested, particularly in low-resource countries. This study aimed to evaluate the accuracy of these risk factor-based models as screening tools. **Subject and methods**: This prospective cohort study involved 400 consenting pregnant women receiving antenatal care in Lagos, Nigeria. Participants were evaluated for GDM risk using three clinical models and underwent universal screening and diagnosis at 24 to 28 weeks with a single-step, 2-hour 75g OGTT, using IADPSG/WHO criteria. The Receiver Operating Characteristic (ROC) curve was used to assess the accuracy of the risk factor-based models. **Results**: The mean age of the subjects was 31.0 ± 5.3 years. The prevalence of GDM, according to the IADPSG/WHO 2013 criteria, was 19.0%. Using the clinical risk score models developed by Naylor and cols., Caliskan and cols., and Phaloprakarn and cols., positive risk scores for GDM were found in 85%, 67.3%, and 93.8% of subjects, respectively. The sensitivity, specificity, and accuracy of these models ranged from 71.1% to 96.1%, 6.7% to 33.6%, and 23.8% to 40.8%, respectively. However, the negative predictive values were relatively high, ranging from 83.2% to 88%. **Conclusion**: The clinical risk factor-based prediction models evaluated in this study may effectively identify women at low risk for GDM who can be exempted from the 2-hour OGTT.

Keywords: Accuracy; gestational diabetes mellitus; clinical risk factor-based models; screening; low resource setting

INTRODUCTION

Globally, the prevalence of gestational diabetes mellitus (GDM) ranges from 1% to 28%, depending on the location, characteristics of the studied population, and the diagnostic criteria used (1). More than 80% of the burden of GDM is found in low- and middle-income countries, and it is speculated to contribute significantly to the high maternal and infant mortality rates in these countries (2). In the United States (3), recent estimates show that GDM complicates up to 9% of all pregnancies, while the mean prevalence of GDM for countries in Europe is 5.4% (4). In Africa, a systematic review of studies on GDM reported a pooled prevalence of about 14%, contributing significantly to the total global burden of gestational diabetes (5). In Nigeria, the prevalence of GDM ranges between 0.3% and 35.9% (6,7). It is reported that Nigeria has the highest prevalence in Africa, and GDM is one of the five most common medical conditions complicating pregnancy in women attending maternal and child health care facilities in Nigeria (7-9).

Every pregnant woman needs to be screened for gestational diabetes mellitus (GDM) because pregnancy provides a crucial opportunity to identify and treat this condition, ensuring favorable pregnancy outcomes and preventing the progression to type 2 diabetes mellitus and other serious complications.

Received on June/1/2025
Accepted on Nov/5/2025
DOI: 10.20945/2359-4292-2026-0020

Correspondence to:
Olayinka Comfort Senbanjo
Department of Obstetrics and Gynaecology,
Lagos State University Teaching Hospital,
No 1-5 Oba Akinjobi Way, GRA, Ikeja,
Lagos State, Nigeria
olayinkasenbanjo@yahoo.com

Associated editor:
João Roberto de Sá
https://orcid.org/0000-0003-3115-5606

This is an open-access article distributed under the terms of the Creative Commons Attribution License

Copyright© AE&M all rights reserved.

Currently, the oral glucose tolerance test (OGTT) is considered the gold standard for confirming GDM diagnosis. (10). While this method enables healthcare providers to identify nearly all pregnant women with GDM, it has some limitations, such as poor reproducibility, long waiting times, and patient discomfort, including nausea and vomiting in some cases (11). Additionally, this method may be impractical in low- and middle-income countries due to cost constraints, resulting in lower acceptance of the test (2,11,12). As a result, several professional organizations have suggested using alternative tests, including clinically based risk factors, as screening tools for GDM (2,11,13). However, it is important to note that while screening based on risk factors has been proposed by several professional organizations, many other international organizations, such as the American Diabetes Association (14) and the Brazilian Society of Diabetes (15), advocate for universal biochemical screening for all pregnant women. This is because using only risk-factor-based approaches tends to miss a significant number of cases.

In sub-Saharan African countries, many health facilities relied on a checklist of GDM-associated risk factors to select pregnant women who should undergo the diagnostic test using the OGTT (8,16,17). However, GDM in this high-risk population remained underdiagnosed (8,17). The use of risk factors as a screening test and the diagnostic accuracy of the risk factors are unclear either when used separately or collectively as a checklist. It is also unknown whether the use of the risk factor assessment is preferable to plasma glucose measurement as a general screening strategy for GDM at the first contact. There are established clinical risk factor-based models that have been developed and advocated for use in some countries, such as Naylor and cols. in Canada (18), Caliskan in Turkey (19), and Phaloprakarn in Bangladesh (20). The widespread applicability of these models has not been tested, especially in low- and middle-income countries.

The aim of this study was to determine the prevalence of GDM and to evaluate the diagnostic accuracy of these established clinical risk factor-based models for the detection of GDM in Lagos, Nigeria.

SUBJECTS AND METHODS

Study setting

The study was conducted at the antenatal clinic of the Institute of Maternal and Child Health, Ayinke House, Lagos State University Teaching Hospital (LASUTH), Ikeja, Lagos State, Southwestern Nigeria. LASUTH is one of two teaching hospitals in Lagos State. It is located in Ikeja Local Government Area and is owned by the Lagos State Government. The hospital functions as a training center for resident doctors and provides healthcare for residents of Lagos State and surrounding areas. The Institute of Maternal and Child Health, Ayinke House, is managed by the Department of Obstetrics and Gynecology. The obstetrics services are provided through the antenatal clinic (ANC) and the emergency room. These services care for both booked and unbooked pregnant women. The ANC accepts and cares for all pregnant women who choose to register at LASUTH. The ANC operates every day except weekends, serving an average of 30 patients daily. It is staffed by approximately four Consultant Obstetricians and Gynecologists, five resident doctors, and four nurses.

Study design

This study was a prospective, hospital-based, cohort study of all consecutive consenting pregnant women at the gestational age of 24 weeks to 28 weeks.

Ethical approval and consent to participate

The study was conducted in full accordance with current relevant laws and international agreements. Approval to carry out this research was granted by the Health Research and Ethics Committee of Lagos State University Teaching Hospital, Ikeja, Lagos State, with approval number LREC/06/10/1403. Written informed consent was obtained from all participants who agreed to take part in the study.

Inclusion criteria

These are pregnant women who booked for antenatal care and had their booking weight and height measured and recorded at gestational age less than or equal to 24 weeks and with singleton pregnancy.

Copyright© AE&M all rights reserved.

Exclusion criteria

Pregnant women with a history of pre-gestational diabetes mellitus, on drugs that can affect glycaemic profile, such as steroids and beta-agonists, multiple pregnancies, and unwilling to participate in the study were excluded from the study.

Sample size

The minimum number of subjects' 'n' required for the study was estimated from the formula:

$$n = z^2p\,(1\text{-}p) \div d^2$$

Where 'n' is the desired sample size,

'z' is the critical value and in a two-tailed test, it is equal to 1.96.

'p' is the prevalence of gestational diabetes from previous studies in Nigeria. Previous studies in Nigeria gave the prevalence of gestational diabetes within ranges of 0.5% - 35.9%. For this study, a prevalence of 35.9% by Onyenekwe and cols. was used (7).

'd' is the absolute sampling error that can be tolerated. In this study, it was fixed at 5 percent

Therefore, the minimum sample size 'n' = 1.96^2 x 0.359 x (1 – 0.359) ÷ 0.05^2 = 353.8 which is approximately 354. Taking into consideration a possible attrition rate of 10% among pregnant women, the minimum sample size for this study was 389.4. This sample size was rounded up to 400.

Selection of study participants and test procedures

Prior to the commencement of the study, the researcher informed the doctors and nurses in the Department of Obstetrics and Gynaecology about the research and the recruitment protocol. The researcher also trained three research assistants on the use of the study proforma and the different measurements to be taken with hands-on demonstration to ensure standardization.

Data were obtained from all consented pregnant women using a purposely designed interviewer-administered questionnaire and from the information in Naylor and cols. (18), Caliskan and cols. (19), and Phaloprakarn and cols. risk scoring models (20). Information collected includes socio-demographic characteristics, obstetric history (such as parity, previous miscarriage, history of GDM, and history of perinatal death), and family history of diabetes mellitus. The families were assigned a socio-economic class using the method recommended by Ogunlesi and cols. (21). Those with mean scores of 1 and 2 were further classified as upper class, those with mean scores of 3 as middle class, and those with mean scores of 4 and 5 as falling into the lower social class. Dating of the pregnancy and gestational age estimation was based on the first day of the last menstrual period in women with a 28-day menstrual cycle, compared with the woman's fundal height. The researcher used the earliest ultrasound (i.e., a scan done at less than or equal to 20 weeks of gestation) if the woman was unsure of her date. The weight and height of all subjects measured at gestational ages less than or equal to 24 weeks were recorded. Random blood glucose measurements were performed in all selected subjects at their first contact. Afterward, all participants were requested to return to the antenatal clinic fasting after a week for an Oral Glucose Tolerance Test (OGTT) to confirm the presence of GDM. The test was conducted between the 24th and 28th week of gestation.

A venous blood sample was taken from the participants to perform random blood glucose tests using an analyzer based on the enzymatic oxidase-peroxidase method of glucose measurement. After ensuring aseptic technique, about three milliliters of venous blood were drawn from a vein in the antecubital fossa with a 21G needle butterfly device equipped with a safety system. The blood was collected into a vacutainer tube containing sodium fluoride, a glycolytic inhibitor, and kept on ice from the time of phlebotomy until it was delivered to the laboratory. Each blood sample was centrifuged within two to four hours of collection to obtain plasma. The plasma samples were stored at -20°C and pooled together to determine plasma glucose concentration. The resulting value was recorded in the participant's study proforma.

All study participants were required to arrive early in the morning for an oral glucose tolerance test after fasting for approximately 8 to 12 hours overnight. Each patient was called the day before the test to remind her to fast. A 75-gram glucose load was prepared by dissolving 75 grams of anhydrous glucose in 250 to 300 ml of clean water. Participants were advised

Copyright© AE&M all rights reserved.

to drink the liquid as quickly as comfortable and to remain relaxed, avoiding vigorous activity during the test. Venous blood for glucose measurement was collected as described above, and samples were analyzed using the enzymatic reaction of the oxidase-peroxidase method for glucose estimation.

The first sample collected prior to the glucose load is the fasting plasma glucose, while the second and third blood samples shall be taken at 1 hour and 2 hours, respectively, after the glucose load.

Diagnostic cut-offs

Gestational diabetes mellitus in the participants was diagnosed using the criteria from clinical risk factor-based models and plasma glucose levels according to the International Association of Diabetes and Pregnancy Study Groups/World Health Organization (IADPSG/WHO 2013) guidelines (10,12). GDM prevalence as determined by the IADPSG/WHO 2013 criteria was used as the reference standard.

Naylor and cols. clinical risk score (18)

The screening score is based on clinical variables such as age, body mass index (BMI), and ethnicity. Using these variables, women were assigned a clinical risk score, with a maximum possible score of 10 points. Women with scores of 0-1 were categorized as low risk, while those with scores of 2-3 and scores higher than 3 were categorized as intermediate and high risk, respectively. For this study, women with a score of 0-1 were considered negative for GDM, while those with scores of 2-10 were considered positive for GDM.

Caliskan and cols. clinical risk score (19)

The screening score was based on clinical variables such as age, BMI, family history of diabetes mellitus, a prior pregnancy with a baby weighing more than 4000g, and previous adverse pregnancy outcomes (defined as any of the following: recurrent spontaneous abortions, fetal anomalies despite a normal karyotype, or prior unexplained in utero fetal death at a gestational age over 20 weeks). A score of one was assigned for each of these five variables, with a maximum possible score of five. A risk score greater than 2 is considered sufficient to diagnose GDM.

Phaloprakarn and cols. clinical risk score (20)

This risk factor-based model relies on clinical risk variables such as age over 35 years, BMI above 27 kg/m², a first-degree relative with type 2 diabetes mellitus or a personal history of GDM, prior delivery of a macrosomic infant, or previous adverse pregnancy outcomes (more than 2 miscarriages, congenital malformations, or stillbirth). The risk score is calculated using the equation: 6 times the woman's age plus 11 times her BMI plus 109 if there is a family history of diabetes in a first-degree relative, plus 42 if she previously delivered a baby weighing more than 4000 g, plus 49 if there has been an adverse pregnancy outcome such as two or more abortions, congenital malformations, or stillbirth. A score greater than 380 indicates a positive screen for GDM.

Data analysis

Data entry and analysis were conducted using SPSS version 24 software. Descriptive statistics such as frequency, percentages, means, standard deviations, and the corresponding 95% CI were used to summarize the variables. The sensitivity, specificity, positive predictive value, and negative predictive value of the clinical risk factor-based models were calculated by identifying the total number of women with true positive, true negative, false positive, and false negative results relative to the gold standard 2-hour 75g OGTT. A receiver-operating characteristic (ROC) curve was plotted, and the area under the curve (AUC) was calculated to assess the overall performance of the clinical risk factor-based models. A p-value of less than 0.05 was considered statistically significant for all tests.

RESULTS

Socio-demographic characteristics of the study participants

The socio-demographic characteristics of the participants are shown in **Table 1**. Their age ranges from 18-51 years with a mean age of 31.0 ± 5.3 years. Most (93.8%) of the participants were in the age group 21-40 years. They are predominantly of the Yoruba tribe (70%) and the modal parity was nullipara (53%). Three hundred and forty-five (86.3%) participants belonged to the high socio-economic class (social class 1).

Copyright© AE&M all rights reserved.

Table 1. Socio-demographic and anthropometric characteristics of the study population

Parameters	Frequency	Percentages
Age (years)		
≤ 20	5	1.2
21-30	196	49.0
31-40	179	44.8
> 40	20	5.0
Tribe		
Yoruba	280	70.0
Hausa	1	0.2
Ibo	61	15.3
Others	58	14.5
Parity		
0	212	53.0
1	98	24.5
2-4	81	20.3
≥ 5	9	2.2
Occupation		
Professional/technical/managerial	145	36.2
Clerical, sales and services, skilled manual	232	58.0
Unskilled manual, farmer, and other	23	5.8
Highest level of education		
No formal education	0	0.0
Primary	6	1.5
Secondary	57	14.2
Tertiary	337	84.3
Husband's Occupation		
Professional/technical/managerial	258	64.5
Clerical, sales and services, skilled manual	136	34.0
Unskilled manual, farmer, and other	6	1.5
Husband's highest level of education		
No formal education	1	0.2
Primary	4	1.0
Secondary	49	12.3
Tertiary	346	86.5
Social class		
1	345	86.25
2	50	12.5
3	5	1.25
*Weight (kg)	72.9 ± 16.1	
*Height (Meter)	1.62 ± 0.065	
Body mass index		
<18.5	10	2.5
18.5 -24.9	137	34.3
25-29.9	126	31.5
≥ 30	127	31.8

*Values are means (SD).

Obstetric characteristics of the study participants

Table 2 shows the obstetric history of the study participants. Thirty (7.5%) participants gave a history of previous delivery of a macrosomic baby, 22 (5.5%) had a previous history of stillbirth, 58 (14.5%) had a previous history of miscarriage, 23 (5.8%) had a previous history of GDM, 10 (2.5%) had a previous history of congenital anomaly and only one (0.25%) had a previous history of polyhydramnios. Fifteen (3.8%) of the participants had the conception of the index pregnancy by artificial reproductive technology.

Table 2. Obstetric characteristics of the study population

Parameters	Frequency	Percentages
Previous macrosomic infant ≥ 4000g		
No	370	92.5
Yes	30	7.5
Previous unexplained stillbirth		
No	378	94.5
Yes	22	5.5
Previous abortion or miscarriage		
No	338	84.5
Yes	58	14.5
Previous history of GDM		
No	377	94.3
Yes	23	5.7
Index pregnancy by artificial reproductive technology		
No	385	96.2
Yes	15	3.8
Fetal gender of index pregnancy		
Male	89	22.3
Female	51	12.8
Don't know	260	65.0
Previous history of congenital anomaly		
No	390	97.5
Yes	10	2.5
Unexplained polyhydramnios		
No	399	99.25
Yes	1	0.25

Prevalence of GDM using the various diagnostic criteria

Table 3 shows the prevalence of GDM based on various diagnostic and screening criteria. According to the IADPSG/WHO 2013 guideline, the prevalence of GDM based on the "gold standard" 2-hour OGTT was 19.0%. The prevalence based on FPG was 10.5%, whereas none of the participants met the criteria for GDM based on 1-hour OGTT. A total of 76 participants met the criteria of either 2-hour OGTT and or FPG giving a prevalence of 19.0%.

Copyright© AE&M all rights reserved.

Table 3. Prevalence of GDM using various diagnostic criteria

Test and reference cut-off values	Mean (SD)	95% CI	No (%)
IADPSG/WHO 2013 guideline			
Fasting plasma glucose > 92 mg/dL (5.1 mmol/L)	79.1 (10.7)	78.1-80.2	42 (10.5)
1-hour OGTT > 180 mg/dL (10 mmol/L)	112.6 (14.5)	111.2-114.1	0 (0.0)
2-hour OGTT > 153 mg/dL (8.5 mmol/L)	110.4 (31.6)	107.3-113.5	52 (13.0)
FBS and or 2-hour OGTT	-	-	76 (19.0)
Naylor and cols. clinical risk score			
0-1 (Low risk)	-	-	60 (15.0)
2-3 (Intermediate risk)	-	-	182 (45.5)
>3 (High risk)	-	-	158 (39.5)
Caliskan and cols. clinical risk score			
0-1 (Negative screen)	-	-	131 (32.8)
≥ 2 (Positive screen)	-	-	269 (67.2)
Phaloprakarn clinical risk score			
< 380 (Negative screen)	-	-	25 (6.2)
≥ 380 (Positive screen)	-	-	375 (93.8)

According to the clinical risk score by Naylor and cols., 340 (85%) participants had a risk score that was significant enough to consider diagnostic screening for GDM while the risk score by Caliskan and cols. shows that 269 (67.3%) participants can be considered to have GDM. However, the clinical risk score by Phaloprakarn and cols. shows that 375 (93.8%) participants can be considered to have GDM.

Accuracy of selected published clinical risk-based scores and fasting plasma glucose for the diagnosis of GDM

Table 4 shows the diagnostic accuracy of selected published clinical risk scores for diagnosing GDM, using the IADPSG/WHO 2013 diagnostic criteria as the gold standard. All tested clinical risk scores exhibited low specificity, ranging from 6.7% to 33.6%, and a positive predictive value (PPV) between 19.5% and 20.1%. However, the sensitivity and negative predictive value (NPV) were comparatively higher, with sensitivity ranging from 71.1% to 96.1% and NPV from 83.2% to 88%. The highest accuracy was observed with the Caliskan clinical risk score screening test, which achieved an accuracy of 40.8%. In contrast, the fasting plasma glucose (FPG) test demonstrated low sensitivity (53.9%) but exhibited high specificity (98.8%), PPV (91.1%), NPV (90.1%, and accuracy (90.3%).

Figures 1-3 illustrate the ROC curves for the clinical risk factor-based models in our population, which had an AUC ranging from 51.6% to 52.9%, indicating unsatisfactory discriminatory capacity. The ROC curve for FPG showed an AUC of 84.1%, reflecting a good performance for screening of GDM (Figure 4).

DISCUSSION

The prevalence of gestational diabetes mellitus (GDM) among women in Lagos, based on the IADPSG/WHO 2013 criteria, was found to be 19%. This figure is significantly higher than the range of 1.5% to 11.5% reported in earlier studies conducted in Lagos

Table 4. Accuracy of selected published clinical risk scores and fasting plasma glucose in the diagnosis of GDM using IADPG/WHO 2013 diagnostic criteria as reference standard

Parameter	TP	FN	FP	TN	Sensitivity (95% CI)	Specificity (95% CI)	PPV (95% CI)	NPV (95% CI)	Accuracy (95% CI)
Naylor and cols.	67	9	273	51	88.2 (80.9-95.5)	15.7 (11.7-19.7)	19.7 (15.5-23.9)	85.0 (76.0-94.0)	29.5 (25.0-34.0)
Caliskan and cols.	54	22	215	109	71.1 (60.9-81.3)	33.6 (28.5-38.7)	20.1 (15.3-24.9)	83.2 (76.8-89.6)	40.8 (36.0-46.0)
Phaloprakarn and cols.	73	3	302	22	96.1 (91.8-100.0)	6.7 (4.1-9.5)	19.5 (15.5-23.5)	88.0 (75.3-100.0)	23.8 (19.6-28.0)
FPG (> 5.1 mmol/L)	41	35	4	320	53.9 42.3-65.2	98.9 96.5-99.6	91.9 78.6-96.8	90.1 86.4-93.0	90.3 86.7-93.0

Copyright© AE&M all rights reserved.

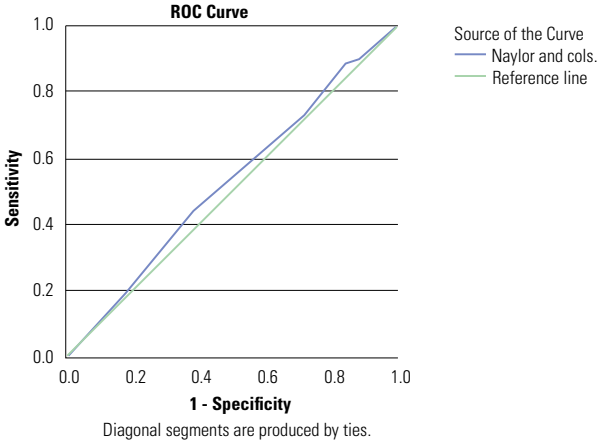


Figure 1. Receiver operating characteristic curves showing performance of Naylor and cols. clinical risk score in predicting GDM.

Figure 1 shows the ROC curves for the Naylor and cols. clinical risk score indicating the performance of the test with reference to IADPSG diagnostic criteria. The Area Under the Curve (AUC) was 0.526 (95% CI 0.453-0.598) suggesting that the clinical risk score is non-discriminatory.

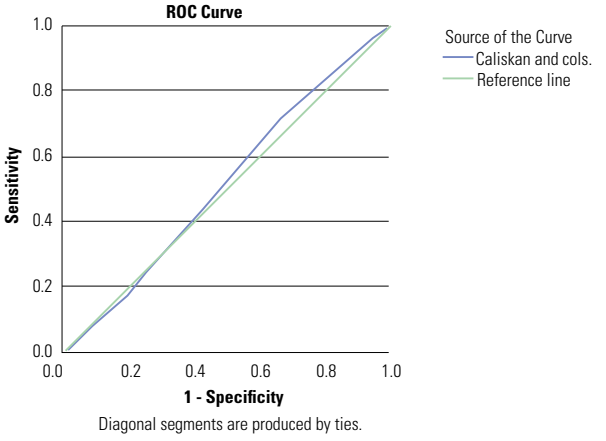


Figure 2. Receiver operating characteristic curves showing performance of Caliskan and cols. clinical risk score in predicting GDM.

Figure 2 shows the ROC curves for the Caliskan and cols. clinical risk score indicating the performance of the test with reference to IADPSG diagnostic criteria. The Area Under the Curve (AUC) was 0.516 (95% CI 0.446-0.586), suggesting that the clinical risk score is non-discriminatory.

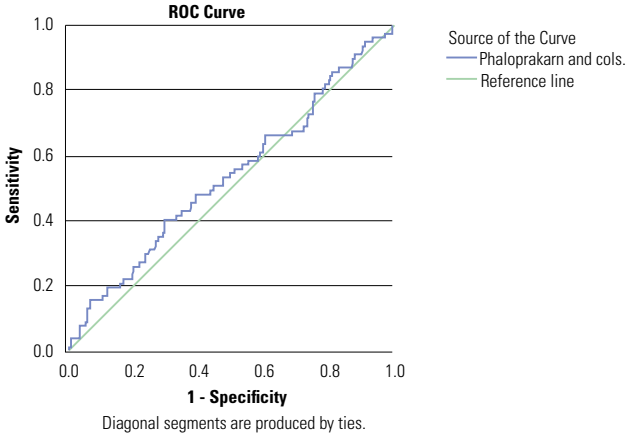


Figure 3. Receiver operating characteristic curves showing performance of Phaloprakarn and cols. clinical risk score in predicting GDM.

Figure 3 shows the ROC curves for the Phaloprakarn and cols. clinical risk score indicating the performance of the test with reference to IADPSG diagnostic criteria. The Area Under the Curve (AUC) was 0.529 (95% CI 0.455-0.603), suggesting that the clinical risk score is non-discriminatory.

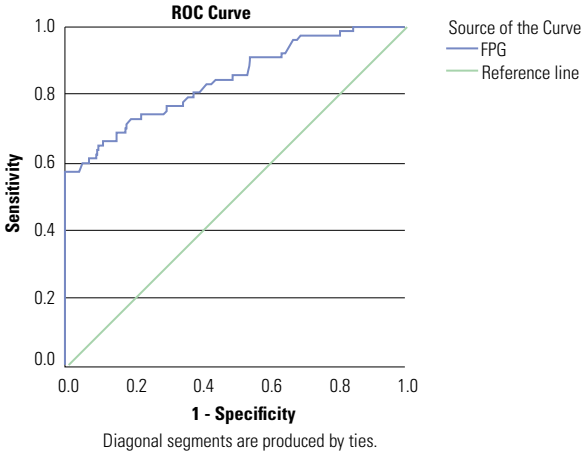


Figure 4. Receiver operating characteristic curves showing the performance of FPG in predicting GDM.

Figure 4 shows the ROC curves for FPG, indicating the test's performance relative to IADPSG diagnostic criteria. The Area Under the Curve (AUC) was 0.841 (95% CI 0.786-0.897), suggesting that the test has a good performance for screening of GDM.

between 1987 and 2004 (22-24). These earlier studies employed different diagnostic criteria, which may account for the observed different prevalence rates. This finding is in keeping with the study by Goyal and cols., which reveals a marked variation in the prevalence of GDM, accompanied by a significant degree of disagreement among different diagnostic criteria (25).

Additionally, the prevalence of GDM in this study surpasses the 4.9% reported in Ibadan by Fawole and cols. about 10 years ago, despite their study only including women at high risk for GDM (17). The observed increase in GDM rates may be attributed to the global rise in obesity and overweight conditions over the years.

Copyright© AE&M all rights reserved.

Interestingly, the prevalence of GDM in this study aligns closely with the 24% found in a recent study at the Lagos University Teaching Hospital, although the methods used for glucose assays in that study were not specified (26). Conversely, a study by Onyenekwe and cols. (7), conducted in southeastern Nigeria, reported a GDM prevalence of 35.9%. This may have been an overestimation due to the reliance on glucometers, which could compromise the accuracy of plasma glucose measurements, as well as the fact that the oral glucose tolerance test (OGTT) was only conducted on those with risk factors for GDM (7).

While there is a substantial body of literature on GDM prevalence in Nigeria, the varying results can largely be attributed to different diagnostic criteria and glucose assay methods used by researchers. When compared to studies outside Nigeria that utilized the IADPSG diagnostic criteria, the prevalence of GDM in Lagos was notably higher than figures from the United States (7.6%), Ireland (7.2%), and Turkey (14.5%), yet lower than the 34.9% reported in Punjab, India, and 38.6% in Kuala Lumpur, Malaysia (27-31).

This aligns with previous findings that indicate lower GDM prevalence rates in North America and Europe compared to those in sub-Saharan African countries. In contrast, countries in the Middle East, North Africa, and Southeast Asia demonstrate the highest global prevalence of GDM. Notably, the prevalence in this study was similar to the 18.3% reported in the Marrakech and Safi districts of Morocco (32). This trend may signify a growing burden of GDM in Nigeria. It is crucial, therefore, to ensure that all pregnant women are screened for GDM and receive timely diagnoses to facilitate appropriate treatment for those affected.

There are indications that combining clinical risk factors to develop a clinical prediction model may be more effective in accurately detecting women with GDM than using each risk factor individually for screening (33). In this study, all the evaluated models based on clinical risk factors showed high sensitivity, low specificity, and poor overall accuracy in identifying GDM. This suggests that while these models are good at detecting many cases of GDM, they could also be useful for screening to identify women who are unlikely to have GDM.

Instructively, the methodology for the risk factor-based scoring models used a two-step GDM screening strategy, which differs from the IADPSG/WHO guidelines and the practice in the index study. The goal of each model is not to replace challenge-based glucose tolerance testing but to exclude low-risk women from further testing. If our study participants had been selectively screened based on Naylor, Caliskan, and Phaloprakarn risk scores, 15%, 32.8%, and 6.3%, respectively, would not have undergone diagnostic testing. Of this total, 85%, 83.2%, and 88%, respectively, would be negative if universal screening with a diagnostic test was performed. The high negative predictive values highlight that risk factor-based models could be useful tools for excluding GDM and reducing the need for OGTT screening. However, due to low PPV, any woman testing positive on these models should undergo a formal 75 g 2-hour OGTT to confirm the diagnosis. This approach can lower costs for patients and improve healthcare system efficiency, especially in low-resource settings.

The models demonstrated high sensitivity but low specificity and poor accuracy, which is consistent with the study by Adam and Reeder (34). They evaluated eight clinical prediction models in the South African population, including the three models analyzed in this study, and found all eight models performed poorly in detecting GDM. The area under the ROC curve for the three models tested in this study ranged from 51.6% to 52.9%, similar to the 51.8% to 59.4% range found in South Africa. These findings suggest that these models are ineffective in differentiating between individuals with GDM and those without it, which makes them non-discriminatory. This limitation is significant, particularly in a country like Nigeria, where resources may be scarce and accurate screening for GDM is essential. With this limitation, there is clear evidence that these specific models are not suitable for the Nigerian population without significant modification. A recent study from Southern India that assessed the utility of clinical parameters as a screening tool for GDM reported a high sensitivity of 90.4% and a specificity of 32.1% (35). This model incorporated several clinical parameters along with biochemical factors such as triglycerides, which may help explain

Copyright© ACE&M all rights reserved.

the slightly higher sensitivity and specificity observed. However, the area under the ROC curve was only 68%, indicating marginal discriminative power. These findings indicate that clinical risk factor-based prediction models serve primarily as effective rule-out tests for screening women for GDM.

The diagnostic accuracy of the models tested in this study is lower than the 73.3% to 83.2% reported for the derivation populations of these models. Among the three clinical prediction models evaluated, the Caliskan model demonstrated the highest accuracy. The Caliskan risk score successfully identified or predicted approximately 41% of cases with GDM, while the Naylor and cols. and Phaloprakarn and cols. risk scores identified about 30% and 24%, respectively. The low discriminatory power of these tests may be attributed to their derivation from a different population, as well as the use of a selective screening approach and diagnostic criteria that differ from the IADPSG guidelines in developing these scoring systems. Beyond the influence of ethnicity and the use of different diagnostic criteria in the derivation of the models, the risk factors for GDM and their respective weights can vary significantly across Caucasian, Asian, and African populations. The models that were tested were not specifically developed or validated for a West African population, which may explain their low accuracy in this context. Additionally, the current study used early-pregnancy BMI instead of pre-pregnancy BMI. Early pregnancy weight is often slightly higher than pre-pregnancy weight, which would systematically raise the BMI. This may inflate the models' sensitivity while further reducing their specificity, especially for those that depend heavily on this metric.

In Nigeria, the guidelines for the management of GDM were developed by a team of endocrinologists only (36). The recommendations include risk assessment at booking, a one-step (75-g OGTT), or a two-step method (50-g GCT with 100-g OGTT) using Carpenter and Coustan criteria for diagnosis. The Carpenter and Coustan criteria define specific fasting and postprandial plasma glucose levels after a 100-gram oral glucose tolerance test, which, if exceeded, indicate GDM (37). Despite the availability of this guideline on GDM, the practice varies across obstetric units in Nigeria. This may be because the guideline is not precise in its documentation and appears impractical. It is suggested that the risk models may be considered by obstetricians to screen out patients going for the diagnostic test. However, aside from saving cost and time, we must bear in mind the false negative cases and the known benefits of treatment. It is important to highlight that the review of guidelines for managing GDM in Nigeria, based on established, practical, and accepted international standards, is long overdue. Moreover, with the findings in this study showing that the FPG test has good performance for screening of GDM. In Brazil, the Society of Diabetes 2025 guideline, explicitly recommend an alternative diagnostic pathway starting with an FPG at the first prenatal visit, followed by a repeat FPG between 24-28 weeks if the initial test is normal (17). Therefore, further research into the accuracy of biochemical screening parameters, such as the FPG test or the 50g glucose challenge, as second-line screening tests to identify false-negative cases detected by risk models, warrants further consideration.

This study has some limitations. First, the study used weight and height measured in early pregnancy for the calculation of body mass index, unlike the risk factor-based models assessed in this study which used pregravid BMI of participants for computing their risk score. This may have affected the sensitivity and specificity of these clinical risk-based scoring models. In low- and middle-income countries, it is difficult to get a record of pre-pregnancy weight as most women do not go for preconception consultations in health facilities. Nonetheless, the influence of pregnancy on weight status at the early stage is considered minimal, and as such, measurement of weight and height and their association to compute BMI remains a valuable tool for the assessment of nutritional status in pregnancy. Second, most of the study subjects were of the high socio-economic class, and this may have an influence on the prevalence of GDM. Lastly, this study was carried out in a tertiary health facility that receives high-risk referrals. Therefore, the reported GDM prevalence of 19.0% and the performance of the screening models may not be generalizable to primary care or rural settings, where such a screening tool is most needed.

Copyright© AE&M all rights reserved.

In conclusion, the burden of GDM is high in Lagos, Nigeria. This is similar to other resource-poor nations where available health facilities are grossly inadequate to take care of the existing problem of infectious diseases and the rising epidemics of non-communicable diseases. The clinical risk factor-based predictive models examined in this study could be utilized to identify a low-risk population of women who should be exempted from the cumbersome OGTT. Furthermore, efforts should focus on developing a cost-effective screening tool with an optimal cut-off value that is both highly sensitive and more specific for detecting GDM, particularly in low-resource settings.

Acknowledgment: we appreciate and thank all the women who volunteered to participate in this study.

Funding: the authors received no financial support for this study.

Authors' contribution: OCS conceived the study, designed the study, collected data, interpreted the data and wrote the first draft. FMA participated in the design of the study, supervised data collection, interpretation of data and writing of the first draft. KAR supervised study design, data collection, data analysis, data interpretation and writing of the first draft. All the authors have read and approved the final submitted version.

Disclosure: no potential conflict of interest relevant to this article was reported.

Data availability: datasets related to this article will be available upon request to the corresponding author.

REFERENCES

1. Jiwani A, Marseille E, Lohse N, Damm P, Hod M, Kahn JG. Gestational diabetes mellitus: results from a survey of country prevalence and practices. J Matern Fetal Neonatal Med. 2012 Jun;25(6):600-10. doi: 10.3109/14767058.2011.587921.
2. Hod M, Kapur A, Sacks DA, Hadar E, Agarwal M, Di Renzo GC, et al. The International Federation of Gynecology and Obstetrics (FIGO) Initiative on gestational diabetes mellitus: A pragmatic guide for diagnosis, management, and care. Int J Gynaecol Obstet. 2015 Oct;131 Suppl 3:S173-211. doi: 10.1016/S0020-7292(15)30033-3.
3. DeSisto CL, Kim SY, Sharma AJ. Prevalence estimates of gestational diabetes mellitus in the United States, Pregnancy Risk Assessment Monitoring System (PRAMS), 2007-2010. Prev Chronic Dis. 2014 Jun 19;11:E104. doi: 10.5888/pcd11.130415.
4. Eades CE, Cameron DM, Evans JMM. Prevalence of gestational diabetes mellitus in Europe: A meta-analysis. Diabetes Res Clin Pract. 2017 Jul;129:173-181. doi: 10.1016/j.diabres.2017.03.030.
5. Muche AA, Olayemi OO, Gete YK. Prevalence and determinants of gestational diabetes mellitus in Africa based on the updated international diagnostic criteria: a systematic review and meta-analysis. Arch Public Health. 2019 Aug 6;77:36. doi: 10.1186/s13690-019-0362-0.
6. Wokoma FS, Celestine T, John C, Enyindah E. Gestational diabetes mellitus in a Nigerian antenatal population. Trop J Obstet Gynaecol. 2001;18(2):56-60. doi: 10.4314/tjog.v18i2.14430.
7. Onyenekwe BM, Young EE, Nwatu CB, Okafor CI, Ugwueze CV, Chukwu SN. Prevalence of gestational diabetes in South East Nigeria using the updated diagnostic guidelines. Int J Diabetes Metab. 2019; 25(1-2): 26-32. doi: 10.1159/000500089.
8. Macaulay S, Dunger DB, Norris SA. Gestational diabetes mellitus in Africa: a systematic review. PLoS One. 2014 Jun 3;9(6):e97871. doi: 10.1371/journal.pone.0097871.
9. Babah OA, Owie E, Ohazurike EO, Akinajo OR. Prevalence and pattern of medical disorders in pregnancy at the time of delivery at Lagos University Teaching Hospital, Lagos, Nigeria. Sub-Saharan Afr J Med. 2018; 5(3):93-98. doi: 10.4103/ssajm.ssajm_32_18.
10. Agarwal MM. Gestational diabetes mellitus: An update on the current international diagnostic criteria. World J Diabetes. 2015 Jun 25;6(6):782-91. doi: 10.4239/wjd.v6.i6.782.
11. Goyal A, Gupta Y, Kubihal S, Kalaivani M, Bhatla N, Tandon N. Utility of Screening Fasting Plasma Glucose and Glycated Hemoglobin to Circumvent the Need for Oral Glucose Tolerance Test in Women with Prior Gestational Diabetes. Adv Ther. 2021 Feb;38(2):1342-1351. doi: 10.1007/s12325-020-01618-1.
12. Bhavadharini B, Uma R, Saravanan P, Mohan V. Screening and diagnosis of gestational diabetes mellitus - relevance to low and middle income countries. Clin Diabetes Endocrinol. 2016 Jun 1;2:13. doi: 10.1186/s40842-016-0031-y.
13. Metzger BE, Coustan DR. Summary and recommendations of the Fourth International Workshop-Conference on Gestational Diabetes Mellitus. The Organizing Committee. Diabetes Care. 1998 Aug;21 Suppl 2:B161-7. PMID: 9704245.
14. American Diabetes Association Professional Practice Committee. 2. Diagnosis and Classification of Diabetes: Standards of Care in Diabetes-2024. Diabetes Care. 2024 Jan 1;47(Suppl 1):S20-S42. doi: 10.2337/dc24-S002.
15. Zajdenverg L, Façanha CFS, Dualib PM, Golbert A, Moisés ECD, Calderon I de MP, et al. Screening and diagnosis of hyperglycemia in pregnancy [Internet]. In: Guidelines of the Brazilian Diabetes Society. [place unknown]: Brazilian Diabetes Society; 2022. [cited 2025 Oct 31]. Available from: https://doi.org/10.29327/557753.2022-11.
16. Mwanri AW, Kinabo J, Ramaiya K, Feskens EJ. Gestational diabetes mellitus in sub-Saharan Africa: systematic review and metaregression on prevalence and risk factors. Trop Med Int Health. 2015 Aug;20(8):983-1002. doi: 10.1111/tmi.12521.
17. Fawole AO, Ezeasor C, Bello FA, Roberts A, Awoyinka BS, Tongo O, et al. Effectiveness of a structured checklist of risk factors in identifying pregnant women at risk of gestational diabetes mellitus: a cross-sectional study. Niger J Clin Pract. 2014 Jul-Aug;17(4):495-501. doi: 10.4103/1119-3077.134051.
18. Naylor CD, Sermer M, Chen E, Farine D. Selective screening for gestational diabetes mellitus. Toronto Trihospital Gestational Diabetes Project Investigators. N Engl J Med. 1997 Nov 27;337(22):1591-6. doi: 10.1056/NEJM199711273372204.
19. Caliskan E, Kayikcioglu F, Oztürk N, Koc S, Haberal A. A population-based risk factor scoring will decrease unnecessary testing for the diagnosis of gestational diabetes mellitus. Acta Obstet Gynecol Scand. 2004 Jun;83(6):524-30. doi: 10.1111/j.0001-6349.2004.00389.x.
20. Phaloprakarn C, Tangjitgamol S, Manusirivithaya S. A risk score for selective screening for gestational diabetes mellitus. Eur J Obstet Gynecol Reprod Biol. 2009 Jul;145(1):71-5. doi: 10.1016/j.ejogrb.2009.04.016.
21. Ogunlesi TA, Dedeke IOF, Kuponiyi OT. Socio-economic classification of children attending specialist paediatric centres in Ogun state, Nigeria. Niger Med Pract. 2008;54(1):21-25. doi: 10.4314/nmp.v54i1.28943.
22. Abudu OO, Kuti JA. Screening for diabetes in pregnancy in a Nigerian population with a high perinatal mortality rate. Asia Oceania J Obstet Gynaecol. 1987 Sep;13(3):305-9. doi: 10.1111/j.1447-0756.1987.tb00270.x.

Copyright© AE&M all rights reserved.

23. Olarinoye JK, Ohwovoriole AE, Ajayi GO. Diagnosis of gestational diabetes mellitus in Nigerian pregnant women--comparison between 75G and 100G oral glucose tolerance tests. West Afr J Med. 2004 Jul-Sep;23(3):198-201. doi: 10.4314/wajm.v23i3.28120.
24. Adegbola O, Ajayi GO. Screening for gestational diabetes mellitus in Nigerian pregnant women using fifty-gram oral glucose challenge test. West Afr J Med. 2008 Jul;27(3):139-43. Erratum in: West Afr J Med. 2009 Jan;28(1):66. PMID: 19256316.
25. Goyal A, Gupta R, Gupta A, Yadav A, Jadhav A, Singh R. Agreement and disagreement between diagnostic criteria for gestational diabetes and implications for clinical practice: A retrospective observational study. Diabetes Metab Syndr. 2025 Feb; 19(2): 103207. doi: 10.1016/j.dsx.2025.103207.
26. Okunowo BO, Fasanmade OA, Odeniyi IA, Olopade O, Ohwovoriole AE. Role of risk factors for gestational diabetes mellitus in determining newborn outcomes in a Nigerian teaching hospital [Internet]. 2019 [cited 2023 Jun 29]. Available from: https://ir.unilag.edu.ng/handle/123456789/7623.
27. Casagrande SS, Linder B, Cowie CC. Prevalence of gestational diabetes and subsequent Type 2 diabetes among U.S. women. Diabetes Res Clin Pract. 2018 Jul;141:200-208. doi: 10.1016/j.diabres.2018.05.010.
28. O'Dea A, Tierney M, Danyliv A, Glynn LG, McGuire BE, Carmody LA, et al. Screening for gestational diabetes mellitus in primary versus secondary care: The clinical outcomes of a randomised controlled trial. Diabetes Res Clin Pract. 2016 Jul;117:55-63. doi: 10.1016/j.diabres.2016.04.023.
29. Sevket O, Ates S, Uysal O, Molla T, Dansuk R, Kelekci S. To evaluate the prevalence and clinical outcomes using a one-step method versus a two-step method to screen gestational diabetes mellitus. J Matern Fetal Neonatal Med. 2014 Jan;27(1):36-41. doi: 10.3109/14767058.2013.799656.
30. Arora GP, Thaman RG, Prasad RB, Almgren P, Brøns C, Groop LC, et al. Prevalence and risk factors of gestational diabetes in Punjab, North India: results from a population screening program. Eur J Endocrinol. 2015 Aug;173(2):257-67. doi: 10.1530/EJE-14-0428.
31. Basri NI, Mahdy ZA, Ahmad S, Abdul Karim AK, Shan LP, Abdul Manaf MR, et al. The World Health Organization (WHO) versus The International Association of Diabetes and Pregnancy Study Group (IADPSG) diagnostic criteria of gestational diabetes mellitus (GDM) and their associated maternal and neonatal outcomes. Horm Mol Biol Clin Investig. 2018 Feb 17;34(1). doi: 10.1515/hmbci-2017-0077.
32. Utz B, Assarag B, Smekens T, Ennassiri H, Lekhal T, El Ansari N, et al. Detection and initial management of gestational diabetes through primary health care services in Morocco: An effectiveness-implementation trial. PLoS One. 2018 Dec 28;13(12):e0209322. doi: 10.1371/journal.pone.0209322.
33. Niu ZR, Bai LW, Lu Q. Establishment of gestational diabetes risk prediction model and clinical verification. J Endocrinol Invest. 2024 May;47(5):1281-1287. doi: 10.1007/s40618-023-02249-3.
34. Adam S, Rheeder P. Selective Screening Strategies for Gestational Diabetes: A Prospective Cohort Observational Study. J Diabetes Res. 2017;2017:2849346. doi: 10.1155/2017/2849346.
35. Dinakaran A, Thiruvengadam R, Srinivasan AR, Manikandan, Nanda SK, Daniel M, et al. Prediction Models for Gestational Diabetes Mellitus: Diagnostic Utility of Clinical and Biochemical Markers. Indian J Endocrinol Metab. 2025 May-Jun;29(3):295-302. doi: 10.4103/ijem.ijem_497_24.
36. Diabetes Association of Nigeria. Clinical practice guidelines for diabetes management in Nigeria. 1st ed. Port Harcourt: Diabetes Association of Nigeria; 2011 [cited 2023 Jun 29]. Available from: https://gracelanddiabetesfoundation.org/wp-content/uploads/2018/03/Guideline-For-Diabetes-Management-In-Nigeria-2nd-Edition.pdf.
37. Oriot P, Radikov J, Gilleman U, Loumaye R, Ryckoort V, Debue E, et al. Gestational diabetes mellitus screening according to Carpenter-Coustan and IADPSG criteria: A 7-year follow-up of prevalence, treatment and neonatal complications at a Belgian general hospital. Diabetes Metab. 2018 Jun;44(3):309-312. doi: 10.1016/j.diabet.2017.09.003.

Copyright© AE&M all rights reserved.

Archives of Endocrinology and Metabolism
ISSN 2359-4292
OFFICIAL JOURNAL OF THE BRAZILIAN SOCIETY OF ENDOCRINOLOGY AND METABOLISM

original

MicroRNAs miR-29a-3p and miR-192-5p: promising urinary biomarkers for kidney function loss

Cristine Dieter[1,2,3,*]
https://orcid.org/0000-0003-2765-930X

Eliandra Girardi[1,*]
https://orcid.org/0000-0003-4485-0202

Marcia Puñales[4]
https://orcid.org/0000-0002-9598-0405

Daisy Crispim[1,2]
https://orcid.org/0000-0001-5095-9269

[1] Serviço de Endocrinologia, Hospital de Clínicas de Porto Alegre, Porto Alegre, RG, Brasil
[2] Programa de Pós-graduação em Ciências Médicas: Endocrinologia, Faculdade de Medicina, Departamento de Clínica Médica, Universidade Federal do Rio Grande do Sul, Porto Alegre, RS, Brasil.
[3] Programa de Pós-graduação em Saúde e Desenvolvimento Humano, Universidade La Salle, Canoas, RS, Brasil
[4] Instituto da Criança com Diabetes, Hospital Nossa Senhora da Conceição, Porto Alegre, RS, Brasil

*The authors contributed equally to this work.

ABSTRACT

Objective: This study aimed to evaluate the expression of miR-29a-3p and miR-192-5p in patients with type 1 diabetes mellitus (T1DM) with diabetic kidney disease (DKD) compared to those without DKD. **Subjects and methods**: This study included 29 patients with T1DM, comprising 13 without DKD (non-DKD group) and 16 with DKD, who were further subdivided into nine patients with moderate DKD and seven with severe DKD. MiR-29a-3p and miR-192-5p expression levels were measured in urine samples using qPCR and are presented as medians (25–75th percentiles). **Results**: miR-29a-3p levels were higher in patients with DKD compared to the non-DKD group [1.24 (0.97–1.74) versus 0.83 (0.72–0.99); P = 0.008]. Its expression showed a negative correlation with estimated glomerular filtration rate (eGFR) (P = 0.007) and a positive correlation with creatinine levels (P = 0.004). MiR-192-5p levels were higher in patients with moderate DKD compared to the non-DKD group [2.15 (1.45–4.21) versus vs. 1.42 (0.98–2.45); P = 0.015], showing a negative correlation with eGFR (P = 0.003) and a positive correlation with creatinine (P = 0.006). **Conclusion**: The differential expression of miR-29a-3p and miR-192-5p in DKD highlights their potential as promising biomarkers for this complication.

Keywords: Diabetic kidney disease; microRNAs; miR-192-5p; miR-29a-3p

INTRODUCTION

Diabetic kidney disease (DKD) is a major chronic complication of diabetes mellitus (DM), affecting approximately 40% of individuals with DM and often progressing to end-stage renal disease (1). Key pathological features of DKD include glomerular mesangial expansion (hypertrophy), tubulointerstitial fibrosis, thickening of the glomerular basement membrane due to extracellular matrix (ECM) protein accumulation, and podocyte dysfunction, all of which collectively contribute to the development of proteinuria (1).

Early DKD detection is essential to prevent its progression to renal failure. Emerging research highlights the potential of novel biomarkers to identify the onset and progression of renal disease. Among these, microRNAs (miRNAs) stand out as a promising class of biomarkers. MiRNAs are small non-coding RNAs that regulate gene expression and are detectable in various human body fluids, including blood, saliva, and urine (2). They are critical in maintaining tissue homeostasis and driving disease processes, impacting nearly all fundamental cellular functions (3). Their stability in fluids and tissues is enhanced by protection from endogenous RNase activity, making them highly reliable for diagnostic purposes (2). Consequently, circulating miRNAs are increasingly recognized as

Received on Jun/4/2025
Accepted on Oct/12/2025
DOI: 10.20945/2359-4292-2026-0019

Correspondence to:
Daisy Crispim
Rua Ramiro Barcelos, 2350,
prédio 12, 4° andar
90035-003 – Porto Alegre, RS, Brasil
dcmoreira@hcpa.edu.br

Associated editor:
Melanie Rodacki
https://orcid.org/0000-0002-9007-1325

This is an open-access article distributed under the terms of the Creative Commons Attribution License

Copyright© AE&M all rights reserved.

valuable biomarkers for monitoring pathophysiological changes and predicting disease outcomes (2).

In this context, several studies have proposed different miRNAs as potential biomarkers for DKD (4,5). A systematic review by Assmann and cols. (6) highlighted that miR-21-5p, miR-29a-3p, miR-126-3p, miR-192-5p, miR-214-3p, and miR-342-3p are dysregulated in patients with DKD compared to the non-DKD group. Additionally, Lv and cols. (7) identified multiple miRNAs in plasma, urine, and exosomes as potential biomarkers for DKD. Among these, miR-29a-3p and miR-192-5p have garnered particular attention due to their involvement in DKD pathogenesis. Both miRNAs have been reported as dysregulated in DKD patients compared to controls; however, findings regarding their expression levels are inconsistent, with some studies reporting upregulation and others reporting downregulation [reviewed in (8)]. For instance, Liu and cols. (9) reported an upregulation of miR-29a-3p in the serum of patients with type 2 DM (T2DM) compared to healthy controls. Interestingly, increased miR-29a-3p expression was associated with both the onset and progression of DKD (9). Conversely, miR-192-5p has been linked to a protective role in DKD, as its overexpression was shown to attenuate high-glucose-induced apoptosis and cell hypertrophy while improving the viability of proximal tubular cells (10).

Given the inconclusive findings on the roles of miR-29a-3p and miR-192-5p in DKD, this study aimed to investigate their expression levels in urine samples from patients with type 1 DM (T1DM) with and without DKD.

SUBJECTS AND METHODS

Study design and population

This study was conducted in accordance with the Strengthening the Reporting of Observational Studies in Epidemiology (STROBE) guidelines for association studies (11). It included an independent cohort of patients with T1DM stratified by estimated glomerular filtration rate (eGFR) values. All patients were recruited from outpatient clinics of Instituto da Criança com Diabetes – Grupo Hospitalar Conceição (Rio Grande do Sul State, Brazil), between November 2019 and December 2022. T1DM diagnosis was based on the American Diabetes Association criteria (12).

Patients were categorized into two groups based on their eGFR values: the normal eGFR group (≥ 90 mL/min/1.73 m^2; non-DKD group) and the altered eGFR group (< 60 mL/min/1.73 m^2; DKD group), in accordance with the Kidney Disease Improving Global Outcomes (KDIGO) guidelines (13). The DKD group was further subdivided according to the degree of kidney function loss: moderate DKD (moderate to severe loss, eGFR 30–60 mL/min/1.73 m^2) and severe DKD (severe loss leading to kidney failure, eGFR < 30 mL/min/1.73 m^2). The eGFR was calculated using serum creatinine levels and the Chronic Kidney Disease Epidemiology Collaboration (CKD-EPI) creatinine equation (13).

Exclusion criteria included any febrile illness within the previous three months, chronic inflammatory or rheumatic diseases, hepatitis, HIV positivity, glucocorticoid treatment, liver or cardiac failure, kidney transplantation, hereditary dyslipidemia, and inborn or acquired metabolic disorders, except for DM. This extensive list was carefully selected to minimize potential biases, as these conditions can affect miRNA expression. Moreover, all samples were collected in the morning to control for diurnal variations, which may also influence miRNA expression.

The study protocol was approved by the Research Ethics Committees of Hospital de Clínicas de Porto Alegre and Grupo Hospitalar Conceição/Instituto da Criança com Diabetes (HCPA No. 2019-0336, CAAE No. 13955019.0.0000.5327). All participants provided written informed consent prior to inclusion in the study.

Clinical and biochemical parameters

A standardized questionnaire was used to collect information on age, age at diagnosis, T1DM duration, medication use, and ethnicity, which was determined by self-classification. All patients underwent physical and laboratory evaluations, as previously described (14). Serum creatinine was measured using the Jaffé reaction (15). The eGFR was calculated using the Chronic Kidney Disease Epidemiology Collaboration (CKD-EPI) equation: eGFR = 141 x min (SCR/κ, 1)$^{\alpha}$

Copyright© AE&M all rights reserved.

x max (SCR/κ, 1)$^{-1,209}$ x 0,993^{age} x 1,018 [if female] x 1,159 [if Black] (16).

MiRNA extraction and quantification by qPCR

Midstream 20 mL voided urine samples were collected from all patients. Immediately after collection, samples were centrifuged at 3,500 x g for 5 min at 4 ℃, and the supernatants were stored at -80 ℃ until miRNA expression analysis. Total RNA was extracted from 200 µL of urine using the miRNeasy Serum/Plasma kit (Qiagen; Hilden, Germany) following the manufacturer's protocol. Quality control was performed using synthetic spike-in RNAs (RNA Spike-In Kit, Qiagen) to ensure the robustness of RNA isolation and the quality of extracted miRNAs. RNA isolation controls (UniSp2, UniSp4, and UniSp5; Qiagen) were included in thawed plasma samples before isolation to monitor extraction efficiency. Purity and concentration of RNA samples were assessed using the NanoDrop ND-1000 Spectrophotometer (Thermo Fisher Scientific, DE, USA).

After RNA isolation, 4 µL of total RNA was reverse transcribed into cDNA using the miRCURY LNA RT Kit (Qiagen), following the manufacturer's instructions. The cDNA synthesis controls (UniSp6, Qiagen) and cel-miR-39-3p, provided in the RNA Spike-In Kit (Qiagen), were included in the reverse transcription reaction to assess the efficiency of the process.

Quantitative PCR (qPCR) was performed using a ViiA™ 7 Fast Real-Time PCR System (Thermo Fisher Scientific) under the following cycling conditions: 95 ℃ for 2 min, followed by 40 cycles at 95 ℃ for 10 s and 56 ℃ for 1 min. Each sample was analyzed in triplicate, with a negative control included in every experiment. Relative quantification of hsa-miR-29a-3p (GeneGlobe assay ID: YP00204698) and hsa-miR-192-5p (GeneGlobe assay ID: YP00204099) was performed using the $2^{-\Delta\Delta Cq}$ method, with results expressed as fold change (FC) relative to a calibrator sample (17). MiR-93-5p (GeneGlobe assay ID: YP00204715) was used as the reference gene.

Statistical analyses

The normality of variable distribution was assessed using the Kolmogorov–Smirnov and Shapiro–Wilk tests. Variables with a normal distribution are presented as mean ± standard deviation (SD), while those with a skewed distribution were log-transformed prior to analysis and are reported as median (25–75th percentiles). Categorical data are expressed as percentages. Clinical and laboratory characteristics were compared between groups using one-way ANOVA for continuous variables or χ^2 tests for categorical variables. Relative miRNA expression (qPCR data) was compared between groups using one-way ANOVA followed by post-hoc analysis. Correlations between quantitative variables were analyzed using Spearman's correlation test. To investigate the discriminatory power of miRNAs in distinguishing DKD patients from T1DM controls, receiver-operating characteristic (ROC) curves were generated, and areas under the curves (AUCs) were calculated. All statistical analyses were conducted using SPSS software (version 18.0, SPSS Inc., Chicago, IL, USA), and P-values < 0.05 were considered statistically significant.

Using the OpenEpi web tool (https://www.openepi.com), we calculated that at least nine patients per group were required to achieve adequate statistical power (β = 80% and α = 0.05) to detect two fold change (± 1.5 SD) differences in miRNA expressions between groups. This sample size is consistent with previous studies analyzing miRNA expression (18-22).

RESULTS

Clinical and laboratory characteristics of individuals included in the study

Table 1 summarizes clinical and laboratory characteristics of patients in the non-DKD and DKD groups. No significant differences were observed between groups regarding mean age, BMI, HbA1c, triglycerides, or cholesterol levels. Similarly, proportions of male and white participants did not differ significantly between patients with and without DKD (P > 0.500). As expected, the DKD group exhibited a higher prevalence of hypertension, elevated creatinine levels, and lower eGFR values compared to the non-DKD group (P < 0.050). Moreover, the prevalence of diabetic retinopathy (DR) was significantly higher among participants with DKD than in those without DKD (72.2% versus 16.7%; P = 0.003).

Copyright© AE&M all rights reserved.

Table 1. Clinical and laboratory characteristics of patients included in this study

Characteristic	Non-DKD group (n = 13)	DKD group (n = 16)	P
Age (years)	32.3 ± 5.6	32.8 ± 5.2	0.784
Gender (% male)	50.0	44.4	1.000
BMI (kg/m^2)	27.5 ± 4.2	26.4 ± 4.8	0.464
HbA1c (%)	7.8 ± 1.0	8.9 ± 2.4	0.110
Ethnicity (% of white)	83.3	72.2	0.688
Hypertension (%)	0.0	94.4	<0.001
Duration of T1DM (years)	21.7 ± 8.3	23.1 ± 7.3	0.598
Triglycerides (mg/dL)	85.0 (70.0 – 92.0)	109.0 (83.0 – 292.0)	0.121
Total cholesterol (mg/dL)	169.5 (141.0 – 182.3)	186.0 (157.0 – 203.0)	0.764
HDL cholesterol (mg/dL)	52.0 (47.0 – 71.7)	49.5 (36.2 – 61.7)	0.337
Creatinine (ug/dL)	0.8 (0.7 – 0.9)	2.4 (1.8 – 3.7)	<0.001
eGFR (mL/min per 1.73 m^2)	114.3 ± 12.8	31.0 ± 13.6	<0.001
Diabetic retinopathy	16.7	72.2	0.003

Variables are shown as mean ± SD, median (25th-75th percentiles) or %. BMI: body mass index; HbA1c: glycated hemoglobin; T1DM: type 1 diabetes mellitus.

Expressions of hsa-miR-29a-3p and hsa-miR-192-5p in the urine of T1DM patients with and without DKD

Expression levels of miR-29a-3p and miR-192-5p were evaluated in urine samples from T1DM patients, categorized according to the presence of DKD. As shown in **Figure 1A**, miR-29a-3p expression was significantly upregulated in patients with DKD compared to those in the non-DKD group [1.24 (0.97–1.74) versus 0.83 (0.72–0.99); P = 0.008]. When the DKD group was further stratified by the degree of kidney function loss, the highest miR-29a-3p levels were observed in patients with severe DKD compared to non-DKD patients [severe DKD: 1.42 (1.25–1.84); moderate DKD: 1.00 (0.78–1.59); non-DKD: 0.83 (0.72–0.99); P = 0.014; **Figure 1B**]. Similarly, miR-192-5p expression tended to be higher in DKD patients compared to the non-DKD group, although this difference did not reach statistical significance [2.14 (1.45–4.20) versus 1.42 (0.97–2.45); P = 0.084; **Figure 1C**]. Notably, this upregulation was more pronounced among patients with moderate DKD compared to non-DKD group [severe DKD: 1.77 (0.83–2.45); moderate DKD: 3.72 (1.66–4.61); non-DKD group: 1.42 (0.97–2.45); P = 0.043]; **Figure 1D**).

Next, we performed a correlation analysis between urinary mir-29a-3p and miR-192-5p expression levels and eGFR and creatinine values in all T1DM patients. Mir-29a-3p expression showed a negative correlation with eGFR (r = -0.490, P = 0.007) and a positive correlation with creatinine levels (r = -0.524, P = 0.004). In contrast, miR-192-5p expression did not show any significant correlation with DKD-related parameters (P > 0.050).

Moreover, we calculated the sensitivity and specificity of both miRNAs for detecting DKD using ROC curve analyses. For miR-29a-3p, the AUC was 0.945, with a sensitivity of 1.00 and a specificity of 0.923 in patients with severe DKD. The cut-off value for this miRNA was 1.144 to distinguish severe DKD patients from T1DM controls. Regarding miR-192-5p, the AUC was 0.812, with a sensitivity of 0.667 and a specificity of 0.846. The cut-off value was 2.955 to differentiate moderate DKD patients from T1DM controls.

DISCUSSION

The identification of novel biomarkers for DKD is essential for detecting DM patients at risk of progressing to DKD or end-stage renal disease (ESRD). Among emerging candidates, miRNAs have been widely proposed as potential biomarkers for several diseases, including DKD. In this study, two miRNAs were highlighted as potential biomarkers for DKD: miR-29a-3p, which was associated with severe kidney function loss, and miR-192-5p, which demonstrated a significant association with moderate kidney function loss.

Copyright© AE&M all rights reserved.

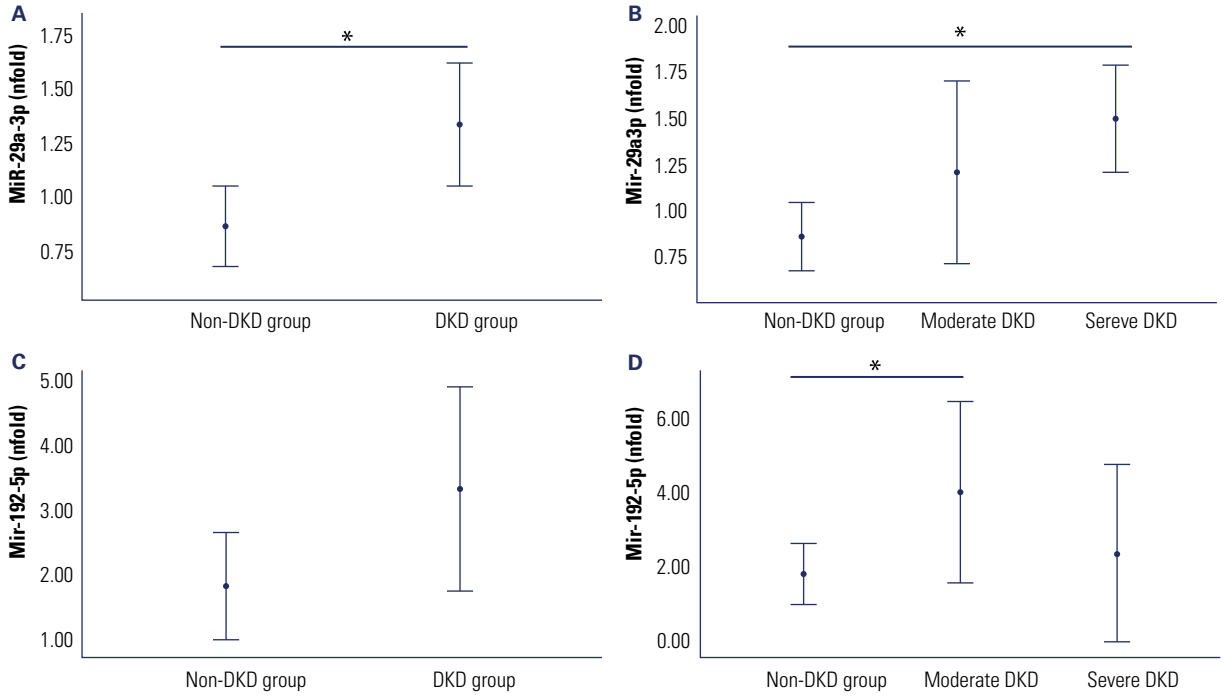


Figure 1. Mir-29a-3p and miR-192-5p expression levels in urine from T1DM patients with and without DKD. (**A**) Mir-29a-3p expression in the non-DKD and DKD groups. (**B**) Mir-29a-3p expression in patients classified as non-DKD, moderate DKD, and severe DKD groups. (**C**) MiR-192-5p expression in the non-DKD and DKD groups. (**D**) miR-192-5p expression in patients classified as non-DKD, moderate DKD, and severe DKD groups. Relative expression was quantified by qPCR. Data are shown as fold changes relative to the calibrator (ΔΔCq method) and are presented as median (25-75th percentiles). P-values were obtained using ANOVA or Student's *t*-tests, as applicable. *P < 0.050.

Here, miR-29a-3p expression was significantly upregulated in urine samples from T1DM patients with severe DKD compared to those without this complication. This finding aligns with Peng and cols. (23), who reported elevated urinary miR-29a-3p levels in patients with T2DM with albuminuria compared to those with normal urinary albumin excretion (UAE) levels. Additionally, miR-29a-3p levels were also positively correlated with UAE. Chien and cols. (24) similarly observed increased miR-29a-3p expression in plasma samples from patients with more advanced DKD compared to T2DM patients with normal UAE levels. Notably, higher plasma miR-29a-3p levels were associated with a rapid rise in creatinine, suggesting its potential as a prognostic marker for renal function decline in T2DM patients (24). A cross-sectional study performed by Liu and cols. (9) further demonstrated upregulation of miR-29a-3p in T2DM patients with DKD compared to controls. Consistent with our findings, miR-29a-3p expression was higher in the clinical proteinuria group (severe DKD) compared to the microalbuminuria group (moderate DKD) (9). The authors proposed serum miR-29a-3p as a potential diagnostic biomarker for DKD (9). Supporting these observations, miR-29a-3p was found to be upregulated in glomerular tissue from patients with DKD compared to those without this complication (25). Moreover, in patients with acute kidney injury (AKI), serum miR-29a-3p expression was significantly elevated compared to healthy controls, suggesting a potential association with AKI severity (26).

In contrast to our findings, Assmann and cols. (27) reported a downregulation of miR-29a-3p in plasma samples from T1DM patients with severe DKD compared to those with moderate DKD or without this complication. Similarly, Pezzolesi and cols. (28) found that miR-29a-3p was downregulated in the plasma of fast progressors to ESRD compared to non-progressors. These discrepancies may be explained by differences in sample types and methodological approaches. Our study analyzed urine samples, whereas Assmann and cols. (27) and Pezzolesi and cols. (28) focused on plasma samples. Additionally, DKD classification criteria varied across studies. In our analysis, DKD was

Copyright© AE&M all rights reserved.

defined solely on eGFR values, while Assmann and cols. (27) used a combination of eGFR and UAE levels, and Pezzolesi and cols. (28) used the urinary albumin-to-creatinine ratio along with eGFR.

The present study found that miR-192-5p expression was significantly upregulated in T1DM patients with moderate DKD compared to both those with severe DKD and the non-DKD group. Consistent with our findings, Jia and cols. (29) reported higher levels of miR-192-5p in urinary extracellular vesicles from T2DM patients with microalbuminuria compared to normoalbuminuric patients and healthy controls. They also observed a downregulation of miR-192-5p in patients with macroalbuminuria compared to those with microalbuminuria. Thus, their results also indicate that miR-192-5p is particularly elevated in patients with microalbuminuria. Additionally, Assmann and cols. (27) demonstrated an upregulation of miR-192-5p in plasma samples from T1DM patients with moderate DKD compared to both patients without DKD and those with severe DKD, further supporting its role as a biomarker for early renal impairment.

In contrast with these results, Akpinar and cols. (30) reported a downregulation of miR-192-5p in patients with DKD compared to controls. Their study included 50 healthy controls and 100 patients with T2DM, who were categorized into three subgroups based on UAE levels: normal to mildly increased (A1, n = 51), moderately increased (A2, n = 25), and severely increased (A3, n = 24) (30). Notably, the downregulation of miR-192-5p was most pronounced in patients in the A3 group. Similarly, Ma and cols. (31) observed significantly lower serum levels of miR-192-5p in T2DM patients with microalbuminuria compared to normoalbuminuric patients, with an additional decrease observed in those with macroalbuminuria relative to those with microalbuminuria.

In addition to their established roles in kidney injury, miR-29a and miR-192 are involved in systemic processes such as inflammation, oxidative stress, and extracellular matrix remodeling, contributing to cardiac fibrosis. These processes are key drivers of atherosclerosis development and progression, as well as left ventricular diastolic dysfunction, which are frequent comorbidities in patients with DKD (32). Additionally, other microRNAs, such as miR-423-5p, have been associated with glucose metabolism dysregulation and plaque progression in atherosclerosis (33). Given that many cases of chronic kidney disease result from diabetic nephropathy, these findings highlight multidirectional systemic consequences of altered microRNA expression. Future research could explore integrated biomarker panels that include miR-29a, miR-192, and other cardiovascular-related miRNAs to improve prediction of the interplay between renal and cardiovascular outcomes in diabetes.

Although most studies on DKD have been conducted in patients with T2DM, our analysis focused on individuals with T1DM, providing novel insights into the epigenetic mechanisms of DKD in this population. Since DKD development differs between diabetes types (34) — despite sharing some pathways — and factors such as obesity and dyslipidemia, more frequent in T2DM, can influence epigenetic profiles, studies targeting T1DM are particularly relevant. Another strength of this study is the use of urinary samples, which may better reflect kidney-specific processes compared to serum or plasma. A limitation of this study is the relatively small sample size; however, it is comparable to that used in most similar studies (20,21,35-40) and provided sufficient statistical power. Future studies with larger and longitudinal cohorts are warranted to validate and expand these findings.

The identification of novel biomarkers for DKD is essential for facilitating early detection and improving the management of patients at risk of disease progression. Our study demonstrates that miR-29a-3p and miR-192-5p are differentially expressed in patients with DKD, underscoring their potential as biomarkers for distinct stages of the disease. Their differential expression may serve as a valuable indicator of disease severity and progression, providing critical insights into the underlying pathophysiological mechanisms of DKD. These findings not only enhance our understanding of molecular pathways associated with DKD but also suggest promising avenues for incorporating these biomarkers into diagnostic and therapeutic strategies. However, further studies are required to validate these findings and explore their clinical applicability in larger and more diverse cohorts.

Copyright© AE&M all rights reserved.

Funding: this study was partially supported by grants from *Conselho Nacional de Desenvolvimento Científico e Tecnológico* (CNPq – Process 402655/2021-4 – CNPq/MCTI/FNDCT No. 18/2021), *Financiamento e Incentivo à Pesquisa* (FIPE) at *Hospital de Clínicas de Porto Alegre* (grant No. 2019-0336), *Fundação de Amparo à Pesquisa do Estado do Rio Grande do Sul* (Fapergs; Edital FAPERGS/CNPq 07/2022 – *Programa de Apoio à Fixação de Jovens Doutores no Brasil* e EDITAL FAPERGS 09/2023 – *Programa Pesquisador Gaúcho* – PqG), *Coordenação de Aperfeiçoamento de Pessoal de Nível Superior* (CAPES), and the Graduate Program in Medical Sciences: Endocrinology – *Universidade Federal do Rio Grande do Sul*. C.D. received scholarships from CAPES, D.C. received a scholarship from CNPq, and E.G. received scholarships from FAPERGS.

Ethical approval: the study protocol was approved by the Research Ethics Committee at *Hospital de Clínicas de Porto Alegre* and *Grupo Hospitalar Conceição/Instituto da Criança com Diabetes* (HCPA No. 2019-0336, CAAE No. 13955019.0.0000.5327).

Informed consent to participate: informed consent was obtained from all individual participants included in the study.

Disclosure: no potential conflict of interest relevant to this article was reported.

Data availability: all data generated or analyzed during this study are included in this published article.

REFERENCES

1. Jha R, Lopez-Trevino S, Kankanamalage HR, Jha JC. Diabetes and Renal Complications: An Overview on Pathophysiology, Biomarkers and Therapeutic Interventions. Biomedicines. 2024 May 15;12(5):1098. doi: 10.3390/biomedicines12051098.
2. Shang R, Lee S, Senavirathne G, Lai EC. microRNAs in action: biogenesis, function and regulation. Nat Rev Genet. 2023 Dec;24(12):816-833. doi: 10.1038/s41576-023-00611-y.
3. Stefani G, Slack FJ. Small non-coding RNAs in animal development. Nat Rev Mol Cell Biol. 2008 Mar;9(3):219-30. doi: 10.1038/nrm2347.
4. Kato M, Natarajan R. MicroRNAs in diabetic nephropathy: functions, biomarkers, and therapeutic targets. Ann N Y Acad Sci. 2015 Sep;1353(1):72-88. doi: 10.1111/nyas.12758.
5. Soltani-Fard E, Taghvimi S, Karimi F, Vahedi F, Khatami SH, Behrooj H, et al. Urinary biomarkers in diabetic nephropathy. Clin Chim Acta. 2024 Jul 15;561:119762. doi: 10.1016/j.cca.2024.119762.
6. Assmann TS, Recamonde-Mendoza M, de Souza BM, Bauer AC, Crispim D. MicroRNAs and diabetic kidney disease: Systematic review and bioinformatic analysis. Mol Cell Endocrinol. 2018 Dec 5;477:90-102. doi: 10.1016/j.mce.2018.06.005.
7. Lv J, Wu Y, Mai Y, Bu S. Noncoding RNAs in Diabetic Nephropathy: Pathogenesis, Biomarkers, and Therapy. J Diabetes Res. 2020 Jun 19;2020:3960857. doi: 10.1155/2020/3960857.
8. Motshwari DD, Matshazi DM, Erasmus RT, Kengne AP, Matsha TE, George C. MicroRNAs Associated with Chronic Kidney Disease in the General Population and High-Risk Subgroups-A Systematic Review. Int J Mol Sci. 2023 Jan 16;24(2):1792. doi: 10.3390/ijms24021792.
9. Liu Q, Wang M, Xu T, Liang W, Yang F. Significance of serum miR-29a in the occurrence and progression of diabetic nephropathy: A cross-sectional study. J Clin Lab Anal. 2022 Feb;36(2):e24210. doi: 10.1002/jcla.24210.
10. Sahoo B, Mishra DD, Tiwari S. MiR-192-5p targets cell cycle regulation in diabetic kidney disease via cyclin-dependent kinase inhibitor 3. Noncoding RNA Res. 2024 Nov 19;11:60-72. doi: 10.1016/j.ncrna.2024.11.003.
11. von Elm E, Altman DG, Egger M, Pocock SJ, Gøtzsche PC, Vandenbroucke JP; STROBE Initiative. The Strengthening the Reporting of Observational Studies in Epidemiology (STROBE) Statement: guidelines for reporting observational studies. Int J Surg. 2014 Dec;12(12):1495-9. doi: 10.1016/j.ijsu.2014.07.013.
12. American Diabetes Association Professional Practice Committee. 2. Classification and Diagnosis of Diabetes: Standards of Medical Care in Diabetes-2022. Diabetes Care. 2022 Jan 1;45(Suppl 1):S17-S38. doi: 10.2337/dc22-S002.
13. Group KDIGOKCW. KDIGO 2012 Clinical Practice Guideline for the Evaluation and Management of Chronic Kidney Disease. Kidney Int. 2013;Suppl. 3:1-150.P. doi: 10.1038/kisup.2012.77.
14. Assmann TS, Brondani Lde A, Bauer AC, Canani LH, Crispim D. Polymorphisms in the TLR3 gene are associated with risk for type 1 diabetes mellitus. Eur J Endocrinol. 2014 Mar 8;170(4):519-27. doi: 10.1530/EJE-13-0963.
15. Zelmanovitz T, Gross JL, Oliveira JR, Paggi A, Tatsch M, Azevedo MJ. The receiver operating characteristics curve in the evaluation of a random urine specimen as a screening test for diabetic nephropathy. Diabetes Care. 1997 Apr;20(4):516-9. doi: 10.2337/diacare.20.4.516.
16. Levey AS, Stevens LA, Schmid CH, Zhang YL, Castro AF 3rd, Feldman HI, et al.; CKD-EPI (Chronic Kidney Disease Epidemiology Collaboration). A new equation to estimate glomerular filtration rate. Ann Intern Med. 2009 May 5;150(9):604-12. doi: 10.7326/0003-4819-150-9-200905050-00006. Erratum in: Ann Intern Med. 2011 Sep 20;155(6):408.
17. Bustin SA, Benes V, Garson JA, Hellemans J, Huggett J, Kubista M, et al. The MIQE guidelines: minimum information for publication of quantitative real-time PCR experiments. Clin Chem. 2009 Apr;55(4):611-22. doi: 10.1373/clinchem.2008.112797.
18. Wang G, Kwan BC, Lai FM, Chow KM, Li PK, Szeto CC. Urinary sediment miRNA levels in adult nephrotic syndrome. Clin Chim Acta. 2013 Mar 15;418:5-11. doi: 10.1016/j.cca.2012.12.011.
19. Fiorentino L, Cavalera M, Mavilio M, Conserva F, Menghini R, Gesualdo L, et al. Regulation of TIMP3 in diabetic nephropathy: a role for microRNAs. Acta Diabetol. 2013 Dec;50(6):965-9. doi: 10.1007/s00592-013-0492-8.
20. Delić D, Eisele C, Schmid R, Baum P, Wiech F, Gerl M, et al. Urinary Exosomal miRNA Signature in Type II Diabetic Nephropathy Patients. PLoS One. 2016 Mar 1;11(3):e0150154. doi: 10.1371/journal.pone.0150154.
21. Barutta F, Tricarico M, Corbelli A, Annaratone L, Pinach S, Grimaldi S, et al. Urinary exosomal microRNAs in incipient diabetic nephropathy. PLoS One. 2013 Nov 4;8(11):e73798. doi: 10.1371/journal.pone.0073798.
22. Argyropoulos C, Wang K, Bernardo J, Ellis D, Orchard T, Galas D, et al. Urinary MicroRNA Profiling Predicts the Development of Microalbuminuria in Patients with Type 1 Diabetes. J Clin Med. 2015 Jul 17;4(7):1498-517. doi: 10.3390/jcm4071498.
23. Peng H, Zhong M, Zhao W, Wang C, Zhang J, Liu X, et al. Urinary miR-29 correlates with albuminuria and carotid intima-media thickness in type 2 diabetes patients. PLoS One. 2013 Dec 9;8(12):e82607. doi: 10.1371/journal.pone.0082607.
24. Chien HY, Chen CY, Chiu YH, Lin YC, Li WC. Differential microRNA Profiles Predict Diabetic Nephropathy Progression in Taiwan. Int J Med Sci. 2016 Jun 1;13(6):457-65. doi: 10.7150/ijms.15548.
25. Baker MA, Davis SJ, Liu P, Pan X, Williams AM, Iczkowski KA, et al. Tissue-Specific MicroRNA Expression Patterns in Four Types of Kidney Disease. J Am Soc Nephrol. 2017 Oct;28(10):2985-2992. doi: 10.1681/ASN.2016121280.
26. Aguado-Fraile E, Ramos E, Conde E, Rodríguez M, Martín-Gómez L, Lietor A, Candela Á, Ponte B, Liaño F, García-Bermejo ML. A Pilot Study Identifying a Set of microRNAs As Precise Diagnostic Biomarkers of Acute Kidney Injury. PLoS One. 2015 Jun 16;10(6):e0127175. doi: 10.1371/journal.pone.0127175.

Copyright© AE&M all rights reserved.

27. Assmann TS, Recamonde-Mendoza M, Costa AR, Puñales M, Tschiedel B, Canani LH, et al. Circulating miRNAs in diabetic kidney disease: case-control study and in silico analyses. Acta Diabetol. 2019 Jan;56(1):55-65. doi: 10.1007/s00592-018-1216-x.
28. Pezzolesi MG, Satake E, McDonnell KP, Major M, Smiles AM, Krolewski AS. Circulating TGF-β1-Regulated miRNAs and the Risk of Rapid Progression to ESRD in Type 1 Diabetes. Diabetes. 2015 Sep;64(9):3285-93. doi: 10.2337/db15-0116.
29. Jia JJ, Zhang X, Ge CR, Jois M. The polymorphisms of UCP2 and UCP3 genes associated with fat metabolism, obesity and diabetes. Obes Rev. 2009 Sep;10(5):519-26. doi: 10.1111/j.1467-789X.2009.00569.x.
30. Akpınar K, Aslan D, Fenkçi SM, Caner V. miR-21-3p and miR-192-5p in patients with type 2 diabetic nephropathy. Diagnosis (Berl). 2022 Aug 18;9(4):499-507. doi: 10.1515/dx-2022-0036.
31. Ma X, Lu C, Lv C, Wu C, Wang Q. The Expression of miR-192 and Its Significance in Diabetic Nephropathy Patients with Different Urine Albumin Creatinine Ratio. J Diabetes Res. 2016;2016:6789402. doi: 10.1155/2016/6789402.
32. Badacz R, Przewłocki T, Legutko J, Żmudka K, Kabłak-Ziembicka A. microRNAs Associated with Carotid Plaque Development and Vulnerability: The Clinician's Perspective. Int J Mol Sci. 2022 Dec 9;23(24):15645. doi: 10.3390/ijms232415645.
33. Huang Y, Feng X, Fan H, Luo J, Wang Z, Yang Y, et al. Circulating miR-423-5p levels are associated with carotid atherosclerosis in patients with chronic kidney disease. Nutr Metab Cardiovasc Dis. 2024 May;34(5):1146-1156. doi: 10.1016/j.numecd.2023.12.018.
34. Dieter C, Assmann TS, Lemos NE, Massignam ET, Souza BM, Bauer AC, et al. -866G/A and Ins/Del polymorphisms in the UCP2 gene and diabetic kidney disease: case-control study and meta-analysis. Genet Mol Biol. 2020 Mar 27;43(2):e20180374. doi: 10.1590/1678-4685-GMB-2018-0374.
35. Argyropoulos C, Wang K, Bernardo J, Ellis D, Orchard T, Galas D, Johnson JP. Urinary MicroRNA Profiling Predicts the Development of Microalbuminuria in Patients with Type 1 Diabetes. J Clin Med. 2015 Jul 17;4(7):1498-517. doi: 10.3390/jcm4071498.
36. Argyropoulos C, Wang K, McClarty S, Huang D, Bernardo J, Ellis D, et al. Urinary microRNA profiling in the nephropathy of type 1 diabetes. PLoS One. 2013;8(1):e54662. doi: 10.1371/journal.pone.0054662. Epub 2013 Jan 24. Erratum in: PLoS One. 2013;8(8). doi:10.1371/annotation/37e647d5-1781-4edf-86a8-e3b533c32ad9.
37. Conserva F, Barozzino M, Pesce F, Divella C, Oranger A, Papale M, et al. Urinary miRNA-27b-3p and miRNA-1228-3p correlate with the progression of Kidney Fibrosis in Diabetic Nephropathy. Sci Rep. 2019 Aug 6;9(1):11357. doi: 10.1038/s41598-019-47778-1.
38. Dimuccio V, Bellucci L, Genta M, Grange C, Brizzi MF, Gili M, et al. Upregulation of miR145 and miR126 in EVs from Renal Cells Undergoing EMT and Urine of Diabetic Nephropathy Patients. Int J Mol Sci. 2022 Oct 11;23(20):12098. doi: 10.3390/ijms232012098.
39. Zang J, Maxwell AP, Simpson DA, McKay GJ. Differential Expression of Urinary Exosomal MicroRNAs miR-21-5p and miR-30b-5p in Individuals with Diabetic Kidney Disease. Sci Rep. 2019 Jul 29;9(1):10900. doi: 10.1038/s41598-019-47504-x.
40. Li X, Xu R, Liu X, Xu L, Xue M, Cheng Y, et al. Urinary miR-3137 and miR-4270 as potential biomarkers for diabetic kidney disease. J Clin Lab Anal. 2020 Dec;34(12):e23549. doi: 10.1002/jcla.23549.

Copyright© AE&M all rights reserved.

Archives of Endocrinology and Metabolism
ISSN 2359-4292
OFFICIAL JOURNAL OF THE BRAZILIAN SOCIETY OF ENDOCRINOLOGY AND METABOLISM

original

Differences in the aggressiveness of familial versus sporadic non-medullary thyroid cancer: An unresolved controversy

Fabíola Yukiko Miasaki[1]
https://orcid.org/0000-0001-6852-4300

Teresa Cristina Santos Cavalcanti[2]
https://orcid.org/0000-0002-8555-6547

Hans Graf[1]
https://orcid.org/0000-0001-8671-1556

Edna Teruko Kimura[3]
https://orcid.org/0000-0001-8403-4459

Peter Andreas Kopp[4]
https://orcid.org/0000-0001-5980-0529

Gisah Amaral de Carvalho[1]
https://orcid.org/0000-0002-2387-665X

[1] Divisão de Endocrinologia (Serviço de Endocrinologia e Metabologia do Paraná), Departamento de Clínica Médica, Universidade Federal do Paraná, Curitiba, PR, Brasil
[2] Departamento de Patologia, Universidade Federal do Paraná, Curitiba, PR, Brasil
[3] Departamento de Biologia Celular e do Desenvolvimento, Instituto de Ciências Biomédicas, Universidade de São Paulo, São Paulo, SP, Brasil
[4] Division of Endocrinology, Diabetology and Metabolism, Centre Hospitalier Universitaire Vaudois, University of Lausanne, Lausanne, Switzerland

ABSTRACT

Objective: Familial non-medullary thyroid cancer (FNMTC) is defined as non-medullary thyroid cancer occurring in two or more first-degree relatives, without features of known hereditary syndromes. Although familial predisposition is well established, its clinical behavior remains debated. This study aimed at characterizing familial cases compared to sporadic non-medullary thyroid cancer (SNMTC). **Subjects and methods:** FNMTC and SNMTC patients were recruited from the Endocrine Division (SEMPR) of the Federal University of Paraná, Brazil, and private endocrine clinics in Curitiba, Paraná, Brazil (2000-2019). Baseline, histopathological, and clinical data were analyzed using SPSS Statistics 26.0. Statistical comparisons employed chi-square, Student's t test, and Mann-Whitney U test, as appropriate. Post hoc power analysis was performed using G*Power 3.1.9.7, and R 2025.05.0. **Results:** We analyzed 39 FNMTC and 119 SNMTC patients. Papillary thyroid carcinoma was the predominant histological type in both groups. FNMTC patients were diagnosed at a younger age (38.5 ± 14.2 vs. 46.6 ± 13.8 years, p = 0.003) and more frequently presented with lymph node metastases at diagnosis (46.2% vs. 21.8%, p = 0.007), with a 4.57-fold increased risk. Despite these differences, long-term outcomes did not differ significantly between groups. An earlier disease onset in subsequent generation suggests a possible anticipation phenomenon. **Conclusion:** These findings suggest that FNMTC patients may present with earlier onset and higher rates of lymph node involvement, underscoring the need for thorough preoperative lateral neck evaluation. In view of a possible anticipation phenomenon, cervical ultrasound screening might be considered starting in adolescence.

Keywords: Thyroid neoplasms; thyroid cancer, papillary; genetic predisposition to disease; neoplastic syndromes, hereditary

INTRODUCTION

The occurrence of thyroid cancer in twins was first reported in 1953 by Firminger and Skelton (1). Soon afterwards, in 1955, Robinson and Orr also reported 24-year-old monozygotic twins affected by isolated papillary thyroid cancer (2). However, the concept of Familial Non-Medullary Thyroid Carcinoma (FNMTC) has only been firmly established in the last decades (3). FNMTC is defined by two or more first-degree relatives affected by non-medullary thyroid carcinoma (papillary, follicular, oncocytic, anaplastic) without syndromic signs (Cowden syndrome, Gardner syndrome/Familial Adenomatous Polyposis, Carney complex, Werner syndrome) (4,5).

Patients with FNMTC account for 1.5%-10% of thyroid cancer cases (6-12), and many controversies still surround this entity. Multicentricity and lymph node metastases were observed more commonly in FNMTC by some (10,11,13,14) but not all authors (7,8,15). Similarly, some but not all have reported

Received on Apr/16/2025
Accepted on Oct/8/2025

DOI: 10.20945/2359-4292-2026-0018

Correspondence to:
Fabíola Yukiko Miasaki
fabiola.miasaki@ufpr.br

Associated editor:
Celia Regina Nogueira
https://orcid.org/0000-0002-4014-0660

This is an open-access article distributed under the terms of the Creative Commons Attribution License

Copyright© AE&M all rights reserved.

a higher incidence of recurrences, as well as a compromised disease-specific survival in FNMTC compared to sporadic non-medullary thyroid cancer (SNMTC) (16).

Syndromic forms of FNMTC have well-documented genetic etiologies. Mutations in *PTEN*, *APC*, *WRN*, and *PRKAR1A* are associated with Cowden syndrome, Gardner syndrome/Familial Adenomatous Polyposis, Werner syndrome, and Carney complex, respectively. In contrast, non-syndromic FNMTC has no single well-defined genetic predisposition, although an autosomal dominant inheritance pattern with incomplete penetrance is likely (17). Although multiple loci and variants have been described in FNMTC, most of these alterations appear to be restricted to a limited number of families or are private to specific kindreds. FNMTC has been linked to several loci, including *TCO*, *NMTC1*, *PRN1*, *4q32*, *6q22*, *8p23.1-22*, and *8q24*, as well as variants in *NKX2-1*, *FOXE-1/PTCSC2*, *SRGAP1*, *SRRM2*, *NOP53*, *HAPB2*, and *PDPR*. Additionally, genes associated with the shelterin complex, such as *TINF2*, *POT1*, and *ACD* are thought to be implicated in its pathogenesis (18,19). Moreover, multigenic mechanisms have also been postulated as a mechanism to confer PTC predisposition (20). However, the extent of their contribution to FNMTC susceptibility remains mostly uncertain and requires additional investigation.

Given the ongoing controversies concerning the clinical behavior of FNTMC, the absence of high penetrance mutations outside of the syndromic forms, and the observed heterogeneity in FNMTC families in terms of age-dependent penetrance and expressivity, it remains of interest and importance to thoroughly characterize such families. This may ultimately provide novel insights into mechanisms of carcinogenesis, impact clinical management, and permit to establish structured recommendations for screening, and, in some cases, refine treatment strategies.

With the goal of contributing to a better understanding of FNMTC as a clinical entity, this study aimed at characterizing the clinical presentation at diagnosis and treatment response of familial cases, in comparison to sporadic thyroid cancer.

SUBJECTS AND METHODS

Patients with FNMTC and SNMTC diagnosed between 2000 and 2019 were included in this study. FNMTC was defined as the presence of non-medullary thyroid cancer (papillary, follicular, oncocytic, or anaplastic) in two or more first-degree relatives. Furthermore, patients with signs indicative or suggestive of syndromes associated with thyroid cancer such as Cowden syndrome, Gardner syndrome/Familial Adenomatous Polyposis, Carney complex, Werner syndrome, or ataxia-telangiectasia were excluded. A specific questionnaire and clinical examination were performed to exclude syndromes associated with thyroid carcinomas in the Endocrine Division (SEMPR), Department of Internal Medicine, Federal University of Parana. SNMTC was defined as the absence of a history of thyroid cancer in the family and cases were selected from our institutional database.

FNMTC patients were identified through the SEMPR's dedicated database and were also recruited from private endocrine clinics in Curitiba between 2015 and 2019. The thyroid cancer database of SEMPR has been established in 2007 and has formal approval by the Hospital's Ethics Committee (CAAE: 48391715.8.0000.0096). In 2007, all information was collected retrospectively and, since then, prospectively. Some affected relatives of the index cases of these FNMTC kindreds have received treatment outside of Curitiba (Rio de Janeiro (Brazil), Londrina (Brazil), Bogota (Colombia)). In these instances, the medical records were obtained from the treating physicians and/or clinical institutions for chart review.

The control cohort comprising SNMTC is formed by patients followed at the Federal University of Parana, Curitiba, a tertiary hospital, and consists of patients that have been diagnosed and followed exclusively at this institution. Patients referred because of advanced metastatic disease were excluded from the control cohort to avoid potential bias. No children or adolescents under the age of 14 were included in this study.

Data about the type of surgery, patient characteristics (sex, age at diagnosis), histological characteristics (type, size, presence/absence of

Copyright© AE&M all rights reserved.

capsule, capsular invasion, angio-lymphatic invasion, perineural invasion, gross extrathyroidal extension, presence of lymph node involvement, extra nodal extension, and distant metastases) were collected. These data were compiled, and each case was classified according to the American Joint Committee on Cancer (AJCC) TNM classification, 8th edition (21), and the 2009 American Thyroid Association (ATA) risk stratification system (22), rather than the version from 2015 (23), because detailed data on lymph node size and/or the number of lymphovascular invasions was missing.

An expert thyroid pathologist revised all cases with unclear pathology reports and excluded one case of non-invasive follicular neoplasm with papillary-like features (NIFTP). Response to therapy was determined with parameters including biochemical markers (thyroglobulin (Tg) and antithyroglobulin antibodies), as well as imaging studies (ultrasound, scintigraphy, computerized tomography), and classified according to the 2015 ATA guidelines (excellent response, biochemical incomplete response, structural incomplete response, and indeterminate response) (23).

To study the possibility of an anticipation phenomenon – an earlier onset of disease manifestations in subsequent generations – we only included FNMTC kindreds with documented DTC in a parent and some of their offspring.

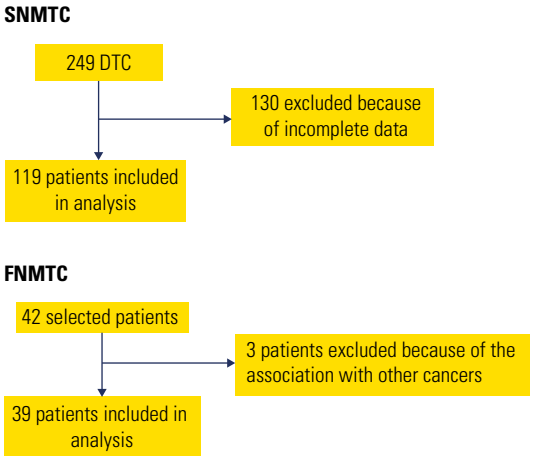
The statistical analyses were performed using SPSS Statistics for Windows (Version 26.0, IBM Corporation, Armonk, New York). For qualitative variables, we used the Chi-square/Fisher's test; and for quantitative analyses, the T-student test or the Mann-Whitney U test as indicated. Post hoc power analyses were performed using G*Power 3.1.9.7 and R 2025.05.0.

This project was approved by the Ethics Committee of the Clinical Hospital at the Federal University of Parana (CAAE: 40511015.5.0000.0096).

RESULTS

In total, we recruited 42 familial cases, of which three were excluded. Because the focus of this study was on FNMTC without any tumors in other organs, one kindred with two cases was excluded due to concurrent breast cancer and heterozygosity for a pathogenic *ATM* variant (*ATM* c.3848T>C; p.L1283P) (24). Another family was excluded due to a strong familial history of lung cancer.

For SNMTC cases, we evaluated 249 patients for enrollment. However, 130 had insufficient data leaving a final SNMTC cohort of 119 subjects (**Figure 1**).



SNMTC: sporadic non-medullary thyroid cancer; FNMTC: familial non-medullary thyroid cancer.

Figure 1. Flow diagram of patient exclusion criteria for SNMTC and FNMTC groups.

Baseline characteristics

There were no sex differences between the FNMTC and SNMTC groups, with the majority being female (79.5% *vs.* 88.2%, $p = 0.187$). Management strategies were also similar: all FNMTC patients (100%) and most SNMTC patients (96.6%) underwent total thyroidectomy. Central neck dissection was only performed in patients with clinical evidence of lymph node metastases but not in a prophylactic manner.

FNMTC patients were diagnosed at a younger age than SNMTC patients (38.5 ± 14.2 *vs.* 46.6 ± 13.8, $p = 0.003$). Furthermore, when analyzing the age of diagnosis between the first and second generations of FNMTC, a significant difference was found, with diagnosis at a younger age in the second generation (49.7 ± 11.6 *vs.* 32.5 ± 13.1 years, $p = 0.002$). The third generation was not included in this analysis, as it comprised only a single patient.

The mean available follow-up period was shorter for FNMTC patients compared to SNMTC subjects (7.0 ± 3.6 *vs.* 10.4 ± 5.3 years, $p < 0.001$). In addition,

Copyright© AE&M all rights reserved.

all SNMTC patients were treated within the Public Health System. However, as patients with oncologic conditions receive treatment priority, this did not appear to affect the timing of surgery or subsequent treatments.

A summary of patient characteristics is provided in **Table 1**.

Histopathological characteristics

In both groups, papillary thyroid cancer was the predominant histological type: (104/119, 87.4% in SNMTC *vs.* 38/39, 97.4% in FNMTC, p = 0.178). Interestingly, the mean tumor size was smaller in the FNMTC group (18.28 ± 13.56 mm *vs.* 25.27 ± 20.39 mm, p = 0.084), although not statistically significant. For other histopathological characteristics (capsular invasion, angiolymphatic invasion, extrathyroidal extension, multicentricity), there were no statistically significant differences between the two groups.

Lymph node and distant metastatic disease

Despite similar primary tumor characteristics, FNMTC patients had a significantly higher rate of lymph node metastasis at initial surgery compared to SNMTC patients (46.2% *versus* 21.8%, p = 0.007). Univariate and multivariate analyses were performed to assess for potential confounding factors. Univariate analysis showed that the main factors for lymph node involvement were family history, age at diagnosis, angiolymphatic invasion and minimal extrathyroidal extension. Multivariate analysis revealed that FNMTC patients had a 4.57-fold higher risk of lymph node metastasis (**Table 2**). Additionally, younger age was associated with a higher risk of lymph node involvement (p = < 0.001; OR = 0.94). Minimal extrathyroidal extension was also correlated with an increased risk of lymph node metastasis.

The prevalence of distant metastatic disease at initial diagnosis did not differ between the SNMTC and FNMTC groups (9.2% *versus* 0%, p = 0.067).

The TNM stages of both groups (FNMTC and SNMTC) is shown in **Table 3** (American Joint Committee on Cancer Staging System 8th edition) (21).

Radioiodine therapy

The frequency of radioiodine therapy was comparable between the FNMTC and SNMTC groups (p = 0.799). The administered activities were lower on average in the FNMTC group (3.49 ± 3.06 GBq *vs.* 5.5 ± 6.03), although the difference did not reach statistical significance (p = 0.054). The administered activities ranged from zero to 38.48 GBq in the SNMTC group, and from zero to 14.8 GBq in FMNTC patients.

Response to therapy and recurrences

There were no significant differences in response to therapy between the two groups (p = 0.230), nor in the incidence of recurrences (p = 0.187).

DISCUSSION

Although it has been known for decades that thyroid cancer can be highly heritable (25,26), leading to the concept of FNMTC, its clinical behavior and outcomes compared to SNMTC remain a subject of debate. While some studies suggest that FNMTC exhibits a more aggressive presentation, others report no significant differences in disease manifestation and progression (10,15,27,28).

The findings presented here suggest that FNMTC is associated with a higher prevalence of lymph node

Table 1. Baseline characteristics of patients with SNMTC versus FNMTC

	SNMTC	FNMTC	p-value
Age (years old)	46.65 ± 13.77	38.74 ± 14.48	0.003 (power 93.8%)
Sex (female)	105 (88.2%)	31 (79.5%)	0.187 (power 24.8%)
Follow-up (years)	10.40 ± 5.32	7.05 ± 3.58	<0.001
Public Health System patients	119 (100%)	9 (23.1%)	<0.001 (power 100%)
Total thyroidectomy	115 (96.6%)	39 (100%)	0.573 (power 0.1%)

Student's t-test for independent samples (age), Fisher's exact test for categorical variables; p < 0.05.
SNMTC: sporadic non-medullary thyroid cancer; FNMTC: familial non-medullary thyroid cancer.

Copyright© AE&M all rights reserved.

Table 2. Multivariate analysis for risk of lymph node metastasis

Predictor[a]	Classification	Total	N		P[b]	OR (IC95%)[b]
			No Mean ± dp or n (%)	Yes Mean ± dp or n (%)		
Age	Mean ± dp	158	47.2 ± 13.3	38.2 ± 14.9	<0.001	0.94 (0.91-0.98)
Familiarity	SNMTC		93 (78.2%)	26 (21.8%)		
	FNMTC		21 (53.8%)	18 (46.2%)	0.003	4.57 (1.67-12.5)
Angiolymphatic invasion	0 (ref)	70	55 (78.6%)	15 (21.4%)		
	1	68	43 (63.2%)	25 (36.8%)	0.091	2.23 (0.88-5.68)
Extrathyroidal invasion	0 (ref)	123	99 (80.5%)	24 (19.5%)		
	1	27	11 (40.7%)	16 (59.3%)	<0.001	10.15 (3.33-30.93)

[a] Predictors were selected according to the statistical significance in the univariate analysis. Perineural invasion was excluded due to the small number of cases exhibiting this feature (only 7).
[b] Multivariate Logistic Regression Model and Wald Test, $p < 0.05$.

Table 3. Characteristics of SNMTC versus FNMTC

		SNMTC	FNMTC	p-value
Histological characteristics				
Size (mm)		25.27 ± 20.39 (1.6-95)	18.28 ± 13.56 (5-60)	0.084 (power: 68.4%)
Histology	Papillary	104 (87.4%)	38 (97.4%)	0.178
	Follicular	9 (7.6%)	1 (2.6%)	(power: 36.1%)
	Oncocytic	6 (5%)	-	
Multicentric disease		39/112 (34.8%)	18/39 (46.2%)	0.251 (power: 20.2%)
No capsular invasion		21/108 (19.4%)	6/37 (16.2%)	0.365 (power: 22.4%)
Angiolymphatic invasion		50/102 (49%)	18/36 (50%)	1.000 (power: 3.6%)
Minimal extrathyroidal extension		22/113 (19.5%)	5/37 (13.5%)	0.471 (power: 8.2%)
Gross extrathyroidal extension		7/113 (6.2%)	0/39 (0%)	0.191 (power: 4.5%)
Initial clinical presentation				
Cervical lymph node involvement		26 (21.8%)	18 (46.2%)	0.007 (power: 79.3%)
Distant metastases		11 (9.2%)	0 (0%)	0.067 (power: 41.6%)
AJCC/TNM according to 8th edition				
I		101 (84.9%)	39 (100%)	
II		13 (10.9%)	0 (0%)	
IVa		1 (0.8%)	0 (0%)	
IVb		4 (3.4%)	0 (0%)	

SNMTC: sporadic non-medullary thyroid cancer; FNMTC: familial non-medullary thyroid cancer; AJCC/TNM: American Joint Committee on Cancer/Tumor, Node, Metastasis system.

metastasis at initial diagnosis (46.2% *vs.* 21.8%, p = 0.007). Similar results have been reported in several studies (9,10,12); although others did not make this observation (8,11,13,15,29,30). One might argue that the surgeons involved were more inclined to perform central lymph node dissection, potentially influencing the results, as lymph node micrometastases are highly prevalent in PTC. Yet, as outlined above and consistent with current guidelines (23,31), prophylactic central lymph node dissection was not performed in this cohort. Nonetheless, the involvement of multiple surgeons makes it impossible to rule out performance bias.

Although the follow-up period is relatively short, we observed a higher recurrence rate in the FNMTC group compared to SNMTC patients (20.5% *vs.* 11.8%). However, this difference did not reach statistical significance (p = 0.187). This finding is consistent with previous reports, which suggested that while FNMTC may exhibit more lymph node metastasis.

Copyright© AE&M all rights reserved.

But the long-term oncologic outcomes do not differ significantly from those of SNMTC patients (7,12).

In the cohort presented here, the mean age at diagnosis was significantly lower in the FNMTC group than in the SNMTC group (38.5 ± 14.2 *vs.* 46.6 ± 13.8, $p = 0.003$). Previous studies have consistently reported younger age at diagnosis in FNMTC patients (3,6,10,13,15,27,29), though this trend was not observed in families with only two affected members (32). One potential confounder in our analysis might be ascertainment bias. Many of the FNMTC patients had better access to healthcare, facilitating earlier detection and diagnosis of thyroid abnormalities. Furthermore, the diagnosis of thyroid cancer in one individual may prompt screening of family members, leading to earlier detection, even for small carcinomas.

The possibility of anticipation, in which disease onset occurs earlier in successive generations, has been suggested for FNMTC (30). To explore this, we analyzed the age difference between generations within FNMTC families and observed a significant trend toward earlier diagnosis in subsequent generations ($p = 0.002$), with some cases diagnosed more than a decade earlier. Although intriguing, this finding should be interpreted with caution and requires further confirmation. As discussed, early case identification and screening in families with known thyroid cancer may contribute to detection and ascertainment bias. This, in turn, increases the risk of a Type I error in assessing age-of-onset anticipation, and no statistical analysis can eliminate this potential limitation (33).

Several factors may explain the discrepancies in the literature regarding initial presentation and clinical course of FNMTC. One major challenge is the classification of familial cases. Charkes postulated that using a criterion of only two affected individuals per family poses a high risk (62%-69%) of misclassifying sporadic cases as familial due to the high incidence of DTC (34). However, other studies have suggested that even families with only two affected members may exhibit more aggressive disease (32). The inclusion of both two-member and larger families in most studies, including ours, further complicates comparisons. In our cohort, 56% of FNMTC cases originated from families with at least three affected members. Comparing patients from families with at least three affected members to those from families with only two affected individuals, we found no significant differences in sex, age, or histological characteristics (data not shown).

FNMTC studies encompass families from diverse genetic backgrounds. In the absence of a known high penetrance gene, it is likely that FNMTC exhibits genetic heterogeneity, with multiple low-penetrance genetic variants at multiple loci contributing to disease susceptibility (18,32). Environmental factors may also play a role in disease manifestation and progression, further complicating efforts to delineate the underlying mechanisms of FNTMC.

Regarding treatment outcomes, no significant differences were observed between the SNMTC and FNMTC groups in terms of the ATA response-to-therapy reclassification. This suggests that the therapeutic interventions were equally effective in both groups. However, we acknowledge the limitations of our study, including a relatively short follow-up period (mean: 7.1 ± 3.6 years) and a limited sample size. Nevertheless, our findings align with previous studies reporting comparable treatment responses between FNMTC and SNMTC patients (7,12).

In conclusion, according to the data obtained from this cohort, FNMTC appears to be associated with a higher prevalence of lymph node metastases compared to SNMTC. Therefore, a thorough preoperative evaluation of the lateral neck remains essential.

Furthermore, our findings suggest that there may be an anticipation phenomenon in FNMTC, although detection and ascertainment bias remain a possible alternative explanation. Yet, based on these findings, structured ultrasound evaluation beginning at approximately 15 years of age may be recommended for individuals in subsequent generations.

Funding: The work has been supported by a grant from the *Coordenação de Aperfeiçoamento de Pessoal de Nível Superior* (CAPES; PDSE—88881.362254/2019-01) to F.Y.M., the *Conselho Nacional de Desenvolvimento Científico e Tecnológico* (CNPq, Brazilian National Council for Scientific and Technological Development) #311210/2021-0, and #409443/2021-2 to E.T.K.

Disclosure: no potential conflict of interest relevant to this article was reported.

Copyright© AE&M all rights reserved.

Data availability: datasets related to this article will be available upon request to the corresponding author.

REFERENCES

1. Firminger HI, Skelton FR. Carcinoma of the thyroid: papillary adenocarcinoma occurring in twins and a case of Hürthle cell carcinoma; tumor conference. J Kans Med Soc. 1953;54(9):427-32.
2. Robinson DW, Orr TG. Carcinoma of the thyroid and other diseases of the thyroid in identical twins. AMA Arch Surg. 1955;70(6):923-8. doi: 10.1001/archsurg.1955.01270120131015.
3. Grossman RF. Familial Nonmedullary Thyroid Cancer: An Emerging Entity That Warrants Aggressive Treatment. Arch Surg. 1995;130(8):892. doi: 10.1001/archsurg.1995.01430080094015.
4. Mazeh H, Sippel RS. Familial Nonmedullary Thyroid Carcinoma. Thyroid. 2013;23(9):1049-56. doi: 10.1089/thy.2013.0079.
5. Guilmette J, Nosé V. Hereditary and familial thyroid tumours. Histopathology. 2018;72(1):70-81. doi: 10.1111/his.13373.
6. Loh KC. Familial Nonmedullary Thyroid Carcinoma: A Meta-Review of Case Series. Thyroid. 1997;7(1):107-13. doi: 10.1089/thy.1997.7.107.
7. Maxwell EL, Hall FT, Freeman JL. Familial Non-Medullary Thyroid Cancer: A Matched-Case Control Study. Laryngoscope. 2004;114(12):2182-6. doi: 10.1097/01.mlg.0000149454.91005.65.
8. Ito Y, Kakudo K, Hirokawa M, Fukushima M, Yabuta T, Tomoda C, et al. Biological behavior and prognosis of familial papillary thyroid carcinoma. Surgery. 2009;145(1):100-5. doi: 10.1016/j.surg.2008.08.004.
9. Pitoia F, Cross G, Salvai ME, Abelleira E, Niepomniszcze H. Patients with familial non-medullary thyroid cancer have an outcome similar to that of patients with sporadic papillary thyroid tumors. Arq Bras Endocrinol Metabol. 2011;55(3):219-23. doi: 10.1590/S0004-27302011000300007.
10. Mazeh H, Benavidez J, Poehls JL, Youngwirth L, Chen H, Sippel RS. In Patients with Thyroid Cancer of Follicular Cell Origin, a Family History of Nonmedullary Thyroid Cancer in One First-Degree Relative Is Associated with More Aggressive Disease. Thyroid. 2012;22(1):3-8. doi: 10.1089/thy.2011.0192.
11. Park YJ, Ahn HY, Choi HS, Kim KW, Park DJ, Cho BY. The Long-Term Outcomes of the Second Generation of Familial Nonmedullary Thyroid Carcinoma Are More Aggressive than Sporadic Cases. Thyroid. 2012;22(4):356-62. doi: 10.1089/thy.2011.0163.
12. Jiwang L, Zhendong L, Shuchun L. Clinicopathologic characteristics of familial versus sporadic papillary thyroid carcinoma. Acta Otorhinolaryngol Ital. 2015;35(4):234–42.
13. Alsanea O, Wada N, Ain K, Wong M, Taylor K, Ituarte PHG, et al. Is familial non-medullary thyroid carcinoma more aggressive than sporadic thyroid cancer? A multicenter series. Surgery. 2000;128(6):1043-51. doi: 10.1067/msy.2000.110848.
14. Uchino S, Noguchi S, Kawamoto H, Yamashita H, Watanabe S, Yamashita H, et al. Familial Nonmedullary Thyroid Carcinoma Characterized by Multifocality and a High Recurrence Rate in a Large Study Population. World J Surg. 2002;26(8):897-902. doi: 10.1007/s00268-002-6615-y.
15. Robenshtok E, Tzvetov G, Grozinsky-Glasberg S, Shraga-Slutzky I, Weinstein R, Lazar L, et al. Clinical Characteristics and Outcome of Familial Nonmedullary Thyroid Cancer: A Retrospective Controlled Study. Thyroid. 2011;21(1):43-8. doi: 10.1089/thy.2009.0406.
16. Triponez F, Wong M, Sturgeon C, Caron N, Ginzinger DG, Segal MR, et al. Does Familial Non-Medullary Thyroid Cancer Adversely Affect Survival? World J Surg. 2006;30(5):787-93. doi: 10.1007/s00268-005-0398-x.
17. Stoffer SS, Van Dyke DL, Bach JV, Szpunar W, Weiss L, Opitz JM, et al. Familial papillary carcinoma of the thyroid. Am J Med Genet. 1986;25(4):775-82. doi: 10.1002/ajmg.1320250415.
18. Miasaki FY, Fuziwara CS, Carvalho GAD, Kimura ET. Genetic Mutations and Variants in the Susceptibility of Familial Non-Medullary Thyroid Cancer. Genes. 2020;11(11):1364. doi: 10.3390/genes11111364.
19. Brock P, Sevigny M, Liyanarachchi S, Comiskey DF, Li W, Saarinen S, et al. *PDPR* Gene Variants Predisposing to Papillary Thyroid Cancer. Thyroid. 2024;34(5):575-82. doi: 10.1089/thy.2023.0560.
20. Liyanarachchi S, Gudmundsson J, Ferkingstad E, He H, Jonasson JG, Tragante V, et al. Assessing thyroid cancer risk using polygenic risk scores. Proc Natl Acad Sci. 2020;117(11):5997-6002. doi: 10.1073/pnas.1919976117.
21. Tuttle RM, Haugen B, Perrier ND. Updated American Joint Committee on Cancer/Tumor-Node-Metastasis Staging System for Differentiated and Anaplastic Thyroid Cancer (Eighth Edition): What Changed and Why? Thyroid. 2017;27(6):751-6. doi: 10.1089/thy.2017.0102.
22. Cooper DS, Doherty GM, Haugen BR, Kloos RT, Lee SL, Mandel SJ, et al. Revised American Thyroid Association Management Guidelines for Patients with Thyroid Nodules and Differentiated Thyroid Cancer: The American Thyroid Association (ATA) Guidelines Taskforce on Thyroid Nodules and Differentiated Thyroid Cancer. Thyroid. 2009;19(11):1167-214. doi: 10.1089/thy.2009.0110.
23. Haugen BR, Alexander EK, Bible KC, Doherty GM, Mandel SJ, Nikiforov YE, et al. 2015 American Thyroid Association Management Guidelines for Adult Patients with Thyroid Nodules and Differentiated Thyroid Cancer: The American Thyroid Association Guidelines Task Force on Thyroid Nodules and Differentiated Thyroid Cancer. Thyroid. 2016;26(1):1-133. doi: 10.1089/thy.2015.0020.
24. Miasaki FY, Saito KC, Yamamoto GL, Boguszewski CL, De Carvalho GA, Kimura ET, et al. Thyroid and Breast Cancer in 2 Sisters with Monoallelic Mutations in the Ataxia Telangiectasia Mutated (*ATM*) Gene. J Endocr Soc. 2022;6(4):bvac026. doi: 10.1210/jendso/bvac026.
25. Hemminki K, Eng C, Chen B. Familial Risks for Nonmedullary Thyroid Cancer. J Clin Endocrinol Metab. 2005;90(10):5747-53. doi: 10.1210/jc.2005-0935.
26. Goldgar DE, Easton DF, Cannon-Albright LA, Skolnick MH. Systematic Population-Based Assessment of Cancer Risk in First-Degree Relatives of Cancer Probands. J Natl Cancer Inst. 1994;86(21):1600-8. doi: 10.1093/jnci/86.21.1600.
27. Wang X, Cheng W, Li J, Su A, Wei T, Liu F, et al. Endocrine Tumours: Familial nonmedullary thyroid carcinoma is a more aggressive disease: a systematic review and meta-analysis. Eur J Endocrinol. 2015;172(6):R253-62. doi: 10.1530/EJE-14-0960.
28. McDonald TJ, Driedger AA, Garcia BM, Van Uum SHM, Rachinsky I, Chevendra V, et al. Familial Papillary Thyroid Carcinoma: A Retrospective Analysis. J Oncol. 2011;2011:1-8. doi: 10.1155/2011/948786.
29. Moses W, Weng J, Kebebew E. Prevalence, Clinicopathologic Features, and Somatic Genetic Mutation Profile in Familial Versus Sporadic Nonmedullary Thyroid Cancer. Thyroid. 2011;21(4):367-71. doi: 10.1089/thy.2010.0256.
30. Capezzone M, Robenshtok E, Cantara S, Castagna MG. Familial non-medullary thyroid cancer: a critical review. J Endocrinol Invest. 2021;44(5):943-50. doi: 10.1007/s40618-020-01435-x.
31. Rosário PW, Ward LS, Carvalho GA, Graf H, Maciel RMB, Maciel LMZ, et al. Thyroid nodules and differentiated thyroid cancer: update on the Brazilian consensus. Arq Bras Endocrinol Metabol. 2013;57(4):240-64. doi: 10.1590/S0004-27302013000400002.
32. Capezzone M, Sagnella A, Pilli T, Maino F, Forleo R, Cantara S, et al. Role of Age at Diagnosis in Defining Potential Familial Nonmedullary Thyroid Cancer in Kindreds with Two Affected Members. J Clin Endocrinol Metab. 2021;106(2):e855-65. doi: 10.1210/clinem/dgaa798.
33. Vieland VJ, Huang J. Statistical Evaluation of Age-at-Onset Anticipation: A New Test and Evaluation of Its Behavior in Realistic Applications. Am J Hum Genet. 1998;62(5):1212-27. doi: 10.1086/301823.
34. Charkes ND. On the Prevalence of Familial Nonmedullary Thyroid Cancer in Multiply Affected Kindreds. Thyroid. 2006;16(2):181-6. doi: 10.1089/thy.2006.16.181.

Copyright© AE&M all rights reserved.

Archives of Endocrinology and Metabolism
ISSN 2359-4292
OFFICIAL JOURNAL OF THE BRAZILIAN SOCIETY OF ENDOCRINOLOGY AND METABOLISM

original

Non-invasive detection of metastatic papillary thyroid carcinoma after radical surgery using salivary metabolomic biomarkers

Fei Yu[1*] https://orcid.org/0000-0002-7269-2056
Jingya Pan[2*] https://orcid.org/0000-0003-1978-8523
Liuting Zhang[3*] https://orcid.org/0000-0002-0273-2630
Shaohua Li[1] https://orcid.org/0009-0006-3159-5846
Chuan Zhang[1] https://orcid.org/0000-0002-5584-0715
Jingjing Fu[1] https://orcid.org/0000-0003-0348-8577
Peng Zhou[1] https://orcid.org/0009-0000-5947-1569
Jun Wang[1] https://orcid.org/0009-0000-4072-073X
Xiaochen Yao[1] https://orcid.org/0000-0001-7161-2870
Yudan Ni[1] https://orcid.org/0009-0009-6589-8126
Ailing Zhang[1] https://orcid.org/0009-0003-1495-856X
Qingle Meng[1] https://orcid.org/0009-0007-2729-4802
Rui Yang[1] https://orcid.org/0009-0008-0557-1044
Lei Xu[1] https://orcid.org/0009-0002-8002-4696
Feng Wang[1] https://orcid.org/0000-0003-1089-3095
Jianhua Wang[2] https://orcid.org/0009-0006-9308-7003
Liang Shi[1] https://orcid.org/0000-0001-9551-0641

[1] Department of Nuclear Medicine, Nanjing First Hospital, Nanjing Medical University, Nanjing, China
[2] Department of Thyroid and Breast Surgery, Affiliated Hospital of Integrated Traditional Chinese and Western Medicine of Nanjing University of Chinese Medicine, Nanjing, China
[3] Department of Functional Examination, Nanjing First Hospital, Nanjing Medical University, Nanjing, China

* These authors contributed equally to this work and share first authorship.

ABSTRACT

Objective: Accurate assessment of metastatic status is crucial for determining radioactive iodine (RAI) dosing in postoperative papillary thyroid carcinoma (PTC) patients. This study aimed to identify unbiased biomarkers in metastatic PTC patients after surgery by applying a metabolomics workflow in saliva samples. **Materials and methods:** Saliva samples from 70 postoperative PTC patients (35 metastatic PTC patients in metastasis group and 35 non-metastatic PTC patients in control group) were analyzed using liquid chromatography – mass spectrometry. Orthogonal partial least-squares-discriminant analysis was applied to identify differential metabolites and significant pathways were examined within these metabolites. Receiver operating characteristic curve (ROC) analysis was utilized to further evaluate the diagnostic performance of candidate metabolites. **Results:** A total of 119 differential metabolites were identified, with 108 upregulated and 11 downregulated. Pathway analysis revealed 13 significantly dysregulated metabolic pathways in metastatic PTC, including necroptosis, choline metabolism in cancer, sphingolipid signaling, valine, leucine and isoleucine biosynthesis, linoleic acid metabolism and pantothenate and CoA biosynthesis. ROC analysis demonstrated six discriminating biomarkers (5 lipids, 1 amine) that effectively distinguished metastatic from non-metastatic PTC, with all area under the curve values exceeding 0.8. Notably, these metabolites maintained diagnostic performance even in the thyroglobulin antibody-positive subgroup (≥ 4.11 IU/mL) for metastatic screening. **Conclusion:** This study demonstrates the potential of salivary biomarkers as a non-invasive diagnostic approach for metastatic PTC to aid the appropriate dosing for RAI therapy. It also offers new insights into the mechanisms of PTC metastasis and potential targets for adjuvant therapy.

Keywords: Metabolomics; metabolite; saliva; metastasis; papillary thyroid carcinoma

Received on Apr/23/2025
Accepted on Oct/6/2025
DOI: 10.20945/2359-4292-2026-0017

Correspondence to:
Feng Wang
fengwang@njmu.edu.cn

Jianhua Wang
jianhuawang@njucm.edu.cn

Liang Shi
liangshi@njmu.edu.cn

Associated editor:
Madson Queiroz de Almeida
https://orcid.org/0000-0002-2957-6148

This is an open-access article distributed under the terms of the Creative Commons Attribution License

INTRODUCTION

Thyroid cancer (TC) is the most common endocrine malignancy, with its incidence rising steadily annually (1,2). Among the various types of TC, papillary thyroid carcinoma (PTC) is the most predominant subtype, accounting for approximately 85%-90% of all cases (3). At the time of diagnosis, around 20%-50% of PTC patients present with lymph node metastases, while 5% have distant metastases (4-6). Additionally,

Copyright© AE&M all rights reserved.

approximately 10%-30% of patients with PTC develop recurrence or disease progression after initial treatment (6). Evidently, metastatic PTC patients face substantially elevated risks of disease recurrence and poor clinical outcomes.

The standard treatment for PTC begins with surgical resection, followed by radioactive iodine (RAI) therapy and thyroid-stimulating hormone (TSH) suppression. Patients with persistent lymph node metastasis after initial surgery are typically administered ^{131}I at doses of 100-150 mCi, whereas those with distant metastases receive 150-200 mCi (6). A precise pre-RAI assessment of metastatic status is crucial for determining a patient-specific ^{131}I dose, which significantly influences treatment outcomes.

Ultrasonography (US), which is the standard imaging modality for evaluating lymph node metastasis in TC (7), has been reported to have a diagnostic accuracy of only 72% (8). Moreover, the computed tomography (CT) manifestations of lung metastases are highly variable, posing significant challenges in distinguishing metastatic nodules from benign lesions (9). These limitations highlight the insufficiency of relying solely on imaging features for definitive metastasis detection, underscoring the need for integrated diagnostic approaches. Thyroglobulin (Tg) is a widely used biomarker for monitoring PTC, but the prevalence of thyroglobulin antibody (TgAb) can significantly interfere with its accurate measurement (10). Therefore, there is an urgent need to identify novel biomarkers that can accurately assess metastatic status after radical thyroidectomy.

Metabolomics, a high-throughput technique, quantifies small-molecule metabolites using various specimens like blood, urine, saliva, faeces, tissue, and cell cultures. Cararo Lopes and cols. profiled normal and tumour thyroid tissues from differentiated thyroid carcinoma (DTC) patients, revealing metabolic alterations implicated in energy maintenance and anabolic metabolism in DTC. Furthermore, they identified a panel of six key metabolites – adenosine, ascorbic acid, betaine, guanidoacetic acid, phenylacetic acid, and pyruvate – significantly associated with metastatic PTC (11). Multiple plasma-based or serum-based metabolomic studies have also revealed distinct metabolite profiles linked to PTC development (12-14) or metastasis (15,16). Recently, the use of saliva has attracted much attention in the field of biomedical research because of its advantages of non-invasiveness, ease of collection and storage, and a lack of need for professional operation. Accumulating evidence supports the use of saliva as a promising non-invasive medium for tumour biomarker discovery, with clinical validation in breast cancer (17,18), oral squamous cell carcinoma (19), and other malignancies. To date, only one saliva-based metabolomics study has demonstrated that a panel consisting of alanine, valine, proline, and phenylalanine improves the accuracy of early PTC diagnosis (20). However, existing studies have focused predominantly on preoperative PTC patients, and there remains a lack of research on postoperative patients prior to RAI therapy – particularly regarding the use of salivary metabolic biomarkers to guide RAI dose.

Therefore, to characterize salivary metabolic alterations in postoperative PTC patients scheduled for RAI treatment, we conducted a comprehensive untargeted metabolomic analysis using liquid chromatography-mass spectrometry (LC-MS) to identify potential salivary biomarkers.

MATERIALS AND METHODS

Patients

Following total thyroidectomy, patients with PTC were referred to our department for RAI therapy. Approximately 1-2 days before radioiodine administration, we measured serum thyroid hormone, thyroid-stimulating hormone (TSH), stimulated thyroglobulin (s-Tg), and anti-thyroglobulin antibody (TgAb) levels, and conducted neck ultrasonography, chest computed tomography (CT), and whole-body bone scans. The empirical treatment doses of ^{131}I were administered under the condition of a serum TSH level of at least 30 mIU/L. Four days after treatment, post-therapeutic ^{131}I SPECT/CT was performed for all patients and independently reviewed by two experienced nuclear medicine physicians.

A case-control study was conducted using age-, sex-, and serum TgAb level-matched cohorts. Only patients aged ≥ 18 years with histologically

Copyright© ACE&M all rights reserved.

confirmed PTC were included. Postoperative PTC patients presenting with lymph node or distant metastasis were assigned to the metastasis group. Metastatic status was confirmed if at least one of the following criteria was met: (1) Pathological confirmation of metastasis via surgical specimens or fine-needle aspiration biopsy; (2) Imaging evidence (ultrasonography, chest CT scan, whole-body bone scintigraphy, or PET/CT) along with elevated serum Tg and/or TgAb levels; (3) Metastatic lesions identified on post-therapeutic radioiodine whole-body scan after exclusion of physiological uptake. The non-metastasis group included postoperative PTC patients who met all of the following criteria: (1) No evidence of lymph node/distant metastases before and after initial RAI therapy; (2) No biochemical recurrence (defined as suppressed Tg < 0.2 ng/mL or stimulated Tg < 1 ng/mL) or structural disease progression during at least 12 months of follow-up after ablation. All radiographic findings were independently evaluated by two board-certified radiologists with ≥ 10 years of thyroid imaging experience. The study protocol was reviewed and approved by the ethics committee of Nanjing First Hospital (No. KY20240924-10). Informed consent was obtained from all subjects involved in the study.

Saliva sample collection

All unstimulated saliva samples were collected within a fixed time window (8:30-10:30 a.m.) prior to RAI therapy. Participants were required to avoid eating, drinking, smoking, and oral hygiene procedures for at least 1 hour prior to collection. Additionally, they rinsed their mouths thoroughly with water at least 10 minutes beforehand. During the collection procedure, participants were directed to accumulate saliva in their oral cavities for a minimum of one minute and then expectorate directly into a sterile tube, avoiding inclusion of coughed-up mucus. If the initial attempt did not yield enough saliva, the process was repeated until a minimum volume of 1 mL was obtained. The saliva samples were then centrifuged at 3000 revolutions per minute (rpm) for 10 min at 4 °C. The supernatants were aliquoted and stored at -80 °C until subsequent analysis.

Untargeted metabolomics analysis of saliva samples

The saliva samples were thawed at 4 °C and 100 μL aliquots were mixed with 400 μL of cold methanol/acetonitrile (1:1, v/v) to remove the protein. The mixture was centrifuged for 20 min (14000 g, 4 °C). The supernatant was dried under vacuum centrifuge. For liquid chromatograph-mass spectrometer (LC-MS) analysis, the samples were reconstituted in 100 μL acetonitrile/water (1:1, v/v) and centrifuged at 14,000 g at 4 °C for 15 min, then the supernatant was injected. Equal volumes of each study sample were combined to create a pooled quality control (QC) sample. All samples were analyzed in the same batch by technicians to avoid batch effects. Continuous sample analysis was conducted in random order, with QC samples inserted into the queue to monitor and evaluate system stability.

Analysis was performed using an UHPLC (Vanquish UHPLC, Thermo) coupled to a Orbitrap Exploris™ 480 in Shanghai Applied Protein Technology Co., Ltd. For Hydrophilic Interaction Liquid Chromatography (HILIC) separation, samples were analyzed using a 2.1 mm × 100 mm ACQUIY UPLC BEH Amide 1.7 μm column (waters, Ireland). In both electrospray ionization (ESI) positive and negative modes, the mobile phase contained A = 25 mM ammonium acetate and 25 mM ammonium hydroxide in water and B = acetonitrile. The gradient was 95% B for 0.5 min and was linearly reduced to 65% in 6.5 min, then reduced to 40% in 1 min and kept for 1min, then increased to 95% in 0.1 min and kept for 2.9 min.

The ESI source conditions were set as follows: Ion Source Gas1 (Gas1) as 50, Ion Source Gas2 (Gas2) as 2, source temperature: 350 ℃, IonSpray Voltage Floating (ISVF): +3,500 V/-2,800V. In MS only acquisition, the instrument was set to acquire over the m/z range 70-1200 Da, the resolution was set at 60,000 and the accumulation time was set at 100 ms. In auto MS/MS acquisition, the instrument was set to acquire over the m/z range 70-1,200 Da, the resolution was set at 60,000 and the accumulation time was set at 100 ms, exclude time within 4 s.

Data processing

The raw MS data were converted to MzXML files using ProteoWizard MSConvert before importing into

Copyright© AE&M all rights reserved.

freely available XCMS software. For peak picking, the following parameters were used: centWave m/z = 10 ppm, peakwidth = c (10, 60), prefilter = c (10, 100). For peak grouping, bw = 5, mzwid = 0.025, minfrac = 0.5 were used. CAMERA (Collection of Algorithms of MEtabolite pRofile Annotation) was used for annotation of isotopes and adducts. In the extracted ion features, only the variables having more than 50% of the nonzero measurement values in at least one group were kept. Compound identification of metabolites was performed by comparing of accuracy m/z value (<10 ppm), and MS/MS spectra with an in-house database established with available authentic standards. Putative metabolite identification was also required to meet level 2 or higher criteria as specified in the Metabolomics Standards Initiative (MSI) guidelines (21).

Statistical analysis

For clinical data analysis, continuous variables were compared between two groups using either Student's t-test (for normally distributed data) or the Wilcoxon rank-sum test (for non-normal distributions). Categorical variables were analyzed using the chi-square test. Statistical significance was defined as $P < 0.05$. All statistical analyses were conducted using R software (version 4.4.0).

In the metabolomic analysis, internal standards were not used for normalization due to the non-targeted nature of the metabolic profiling. Nevertheless, the detected peak areas were log2 normal transformed and then subjected to multivariate analysis using the R package *ropls*. Multivariate analysis included unit variance-scaled principal component analysis (PCA) and orthogonal partial least-squares discriminant analysis (OPLS-DA). Model robustness was evaluated via 7-fold cross-validation and response permutation testing. The contribution of each variable to the classification was assessed based on its variable importance in the projection (VIP) value from the OPLS-DA model. Student's t test was applied to determine the significance of differences between two groups of independent samples. VIP > 1 and $P < 0.05$ were used to screen significant changed metabolites. KEGG pathway enrichment analysis was performed based on differentially expressed metabolites. The diagnostic performance of metabolites and serum Tg in distinguishing metastatic status in PTC patients was evaluated using receiver operating characteristic (ROC) curve analysis. Correlations between variables were assessed using Pearson correlation analysis.

RESULTS

Demographic and clinical data

A total of 70 PTC patients were enrolled and stratified into two groups based on their metastatic status: the metastasis group (35 patients; mean age 41.54 ± 14.39 years, sixteen males and nineteen females) and the non-metastasis group (35 patients; mean age 43.71 ± 13.26 years, sixteen males and nineteen females). No significant differences were observed in age or sex between these two groups ($P = 0.51$ and 1.000, respectively). Serum TgAb levels were comparable between the groups ($P = 0.87$), whereas s-Tg levels were significantly elevated in the metastasis group ($P < 0.001$). Further subgroup analysis based on TgAb status demonstrated comparable age, sex, and metastatic site distributions between the TgAb-negative subgroup and the TgAb-positive subgroup. However, the TgAb-positive subgroup had significantly higher TgAb levels and significantly lower Tg levels compared to the TgAb-negative subgroup. More details of these subjects were shown in **Table 1**.

Results of sample quality control (QC)

As shown in **Figures 1A** and **1B,** the chromatograms exhibit strong overlap in both positive and negative ion modes. Minimal fluctuations were observed in both retention time and peak response intensity, reflecting that the instrument maintained optimal performance throughout the entire detection process, thereby ensuring stable and reliable signal acquisition. In the PCA of QC samples, the samples were clustered closely together (**Figures 1C** and **1D**, green circles). As indicated in **Figure 1E** and 1F, over 80% of the QC samples exhibited a relative peak area with a relative standard deviation (RSD) ≤ 30%. Overall, the QC results confirmed the high reproducibility and stability of the data in this study.

Copyright© AE&M all rights reserved.

Table 1. Characteristics of participants in this study

Variables	Metastasis group (n=35)	Non-metastasis group (n=35)	*P*	TgAb-negative group (n=42)	TgAb-positive group (n=28)	*P*
Age (years)	41.54±14.39	43.71±13.26	0.514	44.29±12.64	40.14±15.23	0.239
Sex						
Male	16 (45.71%)	16 (45.71%)		18 (42.86%)	14 (50.00%)	
Female	19 (54.29%)	19 (54.29%)	1.000	24 (57.14%)	14 (50.00%)	0.732
Tg (ug/l)	84.26 (23.19-292.00)	3.90 (0.36-9.60)	**<0.001**	34.97 (7.09-190.5)	0.85 (0.09-14.48)	**<0.001**
TgAb (IU/ml)	1.94 (0.95-28.05)	2.63 (0.99-8.04)	0.874	1.12 (0.79-1.64)	44.58 (7.51-243.5)	**<0.001**
Metastatic site						
Only cervical lymph node metastasis	22 (62.86%)	/	/	12 (28.57%)	10 (35.71%)	0.713
Distant metastasis	13 (37.14%)	/	/	10 (23.81%)	3 (10.71%)	0.286

Tg: thyroglobulin; TgAb: anti-thyroglobulin antibody.

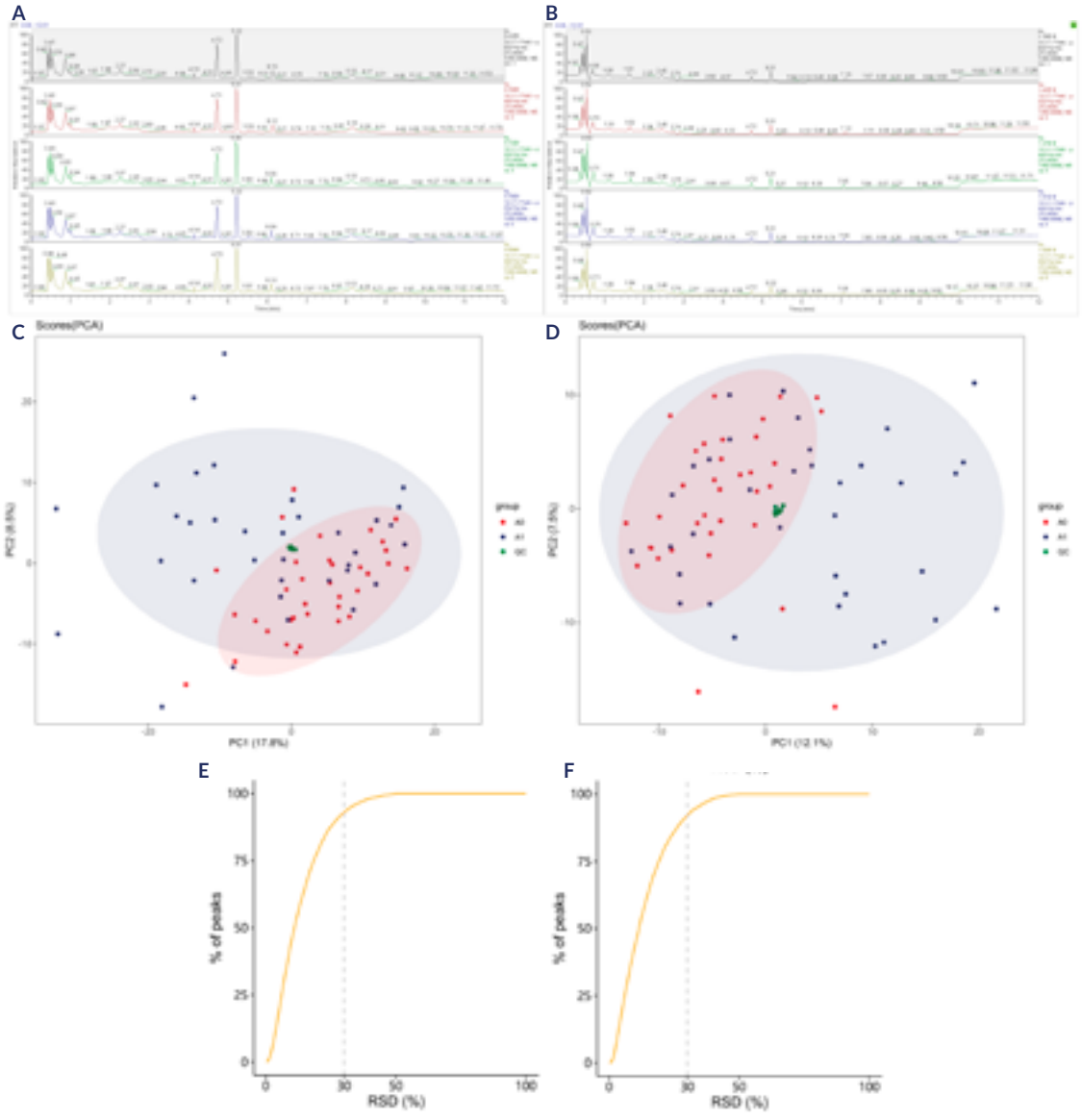


Figure 1. Information of sample quality control. (**A**) Base peak ion chromatograms of samples from each group in positive ion mode. (**B**) Base peak ion chromatograms of samples from each group in negative ion mode. (**C**) PCA analysis of all samples in positive ion mode. metastasis group (A1, blue circles); non-metastasis group (A0, red circle); QC samples (green circles). (**D**) PCA analysis of all samples in negative ion mode. metastasis group (A1, blue circles); non-metastasis group (A0, red circle); QC samples (green circles). (**E**) and distribution of the relative peak area RSD in the QC samples in positive ion mode. (**F**) and distribution of the relative peak area RSD in the QC samples in negative ion mode.

Copyright© AE&M all rights reserved.

Results of metabolites identification and classification

After data processing, saliva metabolomic analysis detected 8,810 metabolic features in positive ion mode and 5,371 in negative ion mode across all study samples. Among these, 432 (positive mode) and 250 (negative mode) met level 2 or higher identification criteria according to MSI guidelines. In total, 682 metabolites were definitively identified, with 513 (75.2%) categorized into four major classes: lipids and lipid-like molecules (n = 192, 28.15%), organic acids and derivatives (n = 160, 23.46%), organoheterocyclic compounds (n = 98, 14.37%) and benzenoids (n = 63, 9.24%) (Figure 2).

Identification of differential metabolites

To identify differential metabolites between the metastasis and non-metastasis group (fold-change ≥ 1.5 or ≤ 0.67 and $P < 0.05$), univariate statistical analysis was performed on all 8810 metabolic features. In positive ion mode, 1109 differential features were identified (1,040 up-regulated, 69 down-regulated); in negative ion mode, 786 were identified (719 up-regulated, 67 down-regulated) (Figure 3).

Multivariate statistical analysis was subsequently conducted to obtain a deeper and more comprehensive understanding of the data. PCA was used to obtain an overview of the salivary metabolomic data. As shown

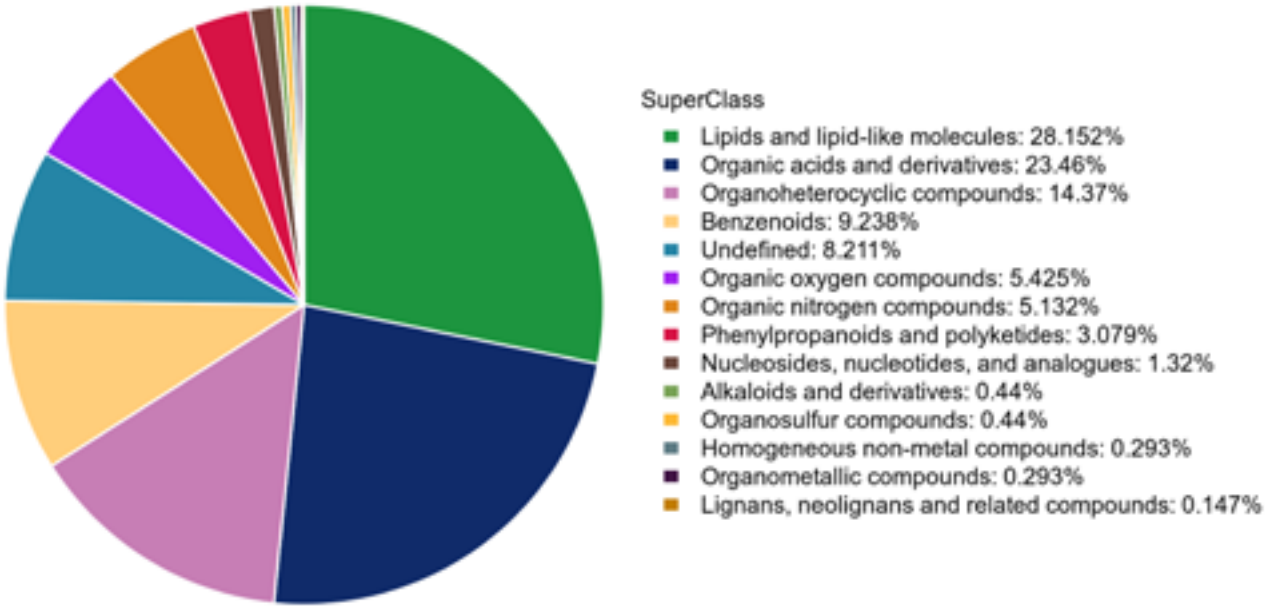


Figure 2. Pie chart of metabolite classification.

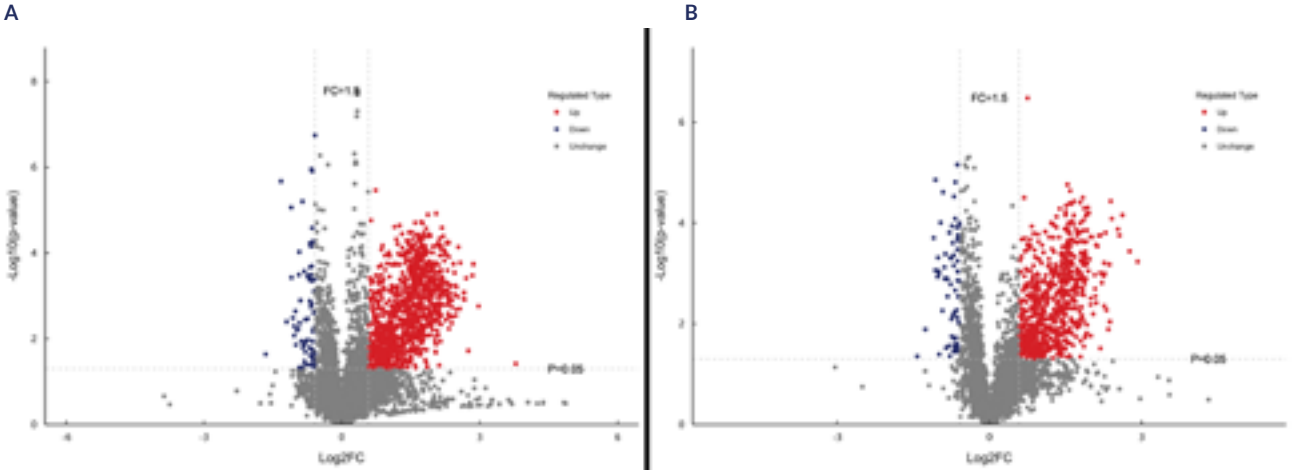


Figure 3. Volcano plot of differential metabolites between the metastasis and non-metastasis group in positive (A) and negative (B) ion modes.

Copyright© AE&M all rights reserved.

in Figure 1C and 1D, the PCA score plot displays a partial but not very obvious separation among the metastasis and non-metastasis groups. We then applied OPLS-DA to examine the metabolomic differences, and the score plot demonstrated a definite separation of samples between the two groups with no overlap (Figure 4A, 4B). Moreover, 200 permutation tests were carried out to verify whether the OPLS-DA model is overfitting, where R2 > 0 and Q2 < 0 indicate a reliable and non-overfit model. The resulting models were considered robust and reliable, with R^2 and Q^2 intercepts of 0.935 and -0.339 in positive ion mode, and 0.684 and -0.314 in negative ion mode, confirming the absence of overfitting (Figures 4C and 4D). These results also indicated that the OPLS-DA models exhibit high separating capacity, effectively distinguishing metastatic from non-metastatic PTC patients.

Differential metabolites between the metastatic group and the metastasis-free group were identified based on the following conditions: 1) VIP ≥ 1 in the OPLS-DA model; 2) $P < 0.05$. A comprehensive analysis revealed a total of 119 differential metabolites, segregated into two ion modes. In positive ion mode, 64 metabolites were upregulated and 9 metabolites were downregulated. In negative ion mode, 44 metabolites were upregulated and 2 metabolites were downregulated (Figure 5).

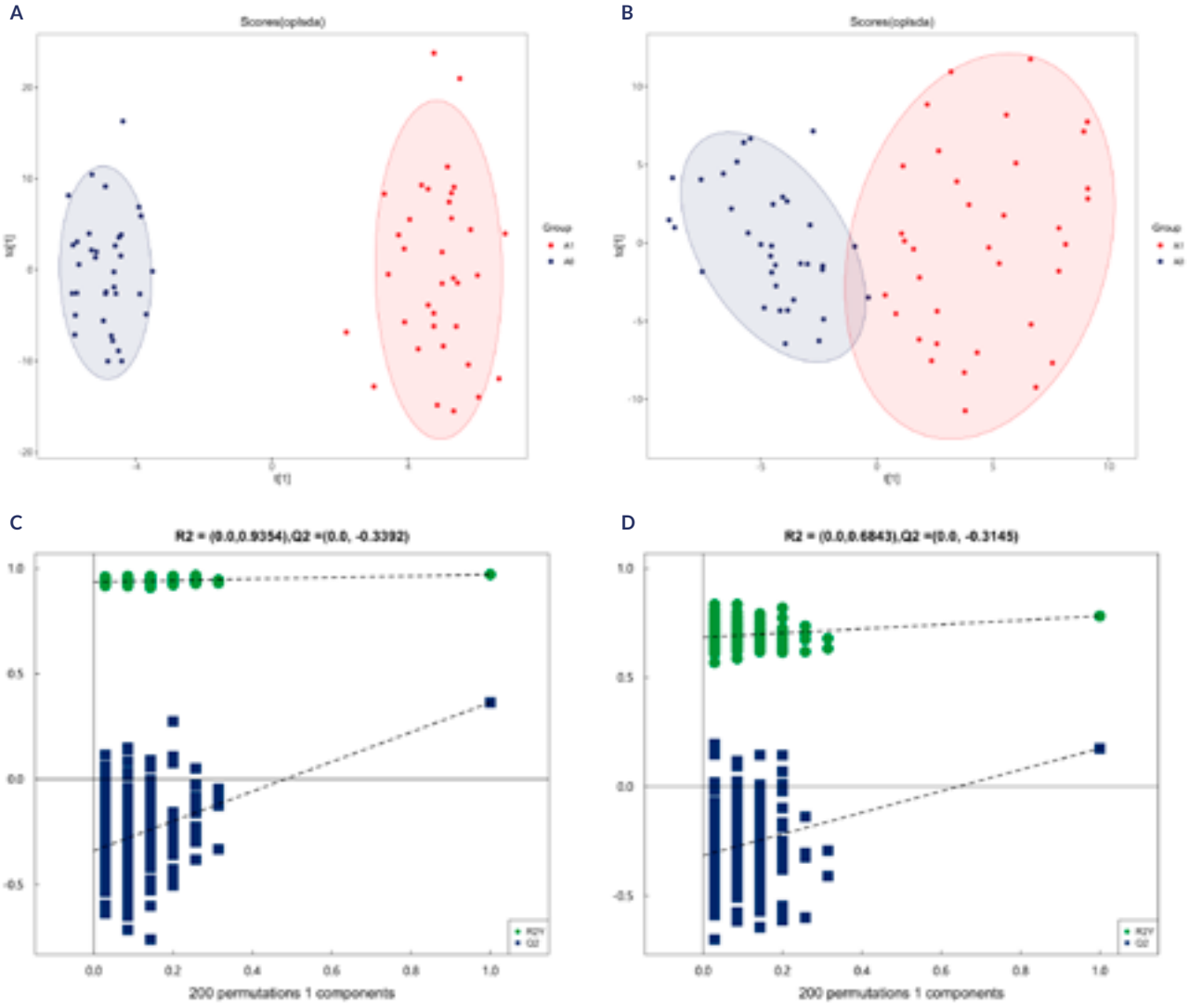


Figure 4. OPLS-DA score plots between the metastasis and non-metastasis group in positive (A) and negative (B) ion modes. The two rightmost points in the figure are the actual R2Y and Q2 values of the OPLS-DA model, and the remaining points are the R2Y and Q2 values obtained by randomly arranging the samples used (positive (C) and negative (D) ion modes.

Copyright© AE&M all rights reserved.

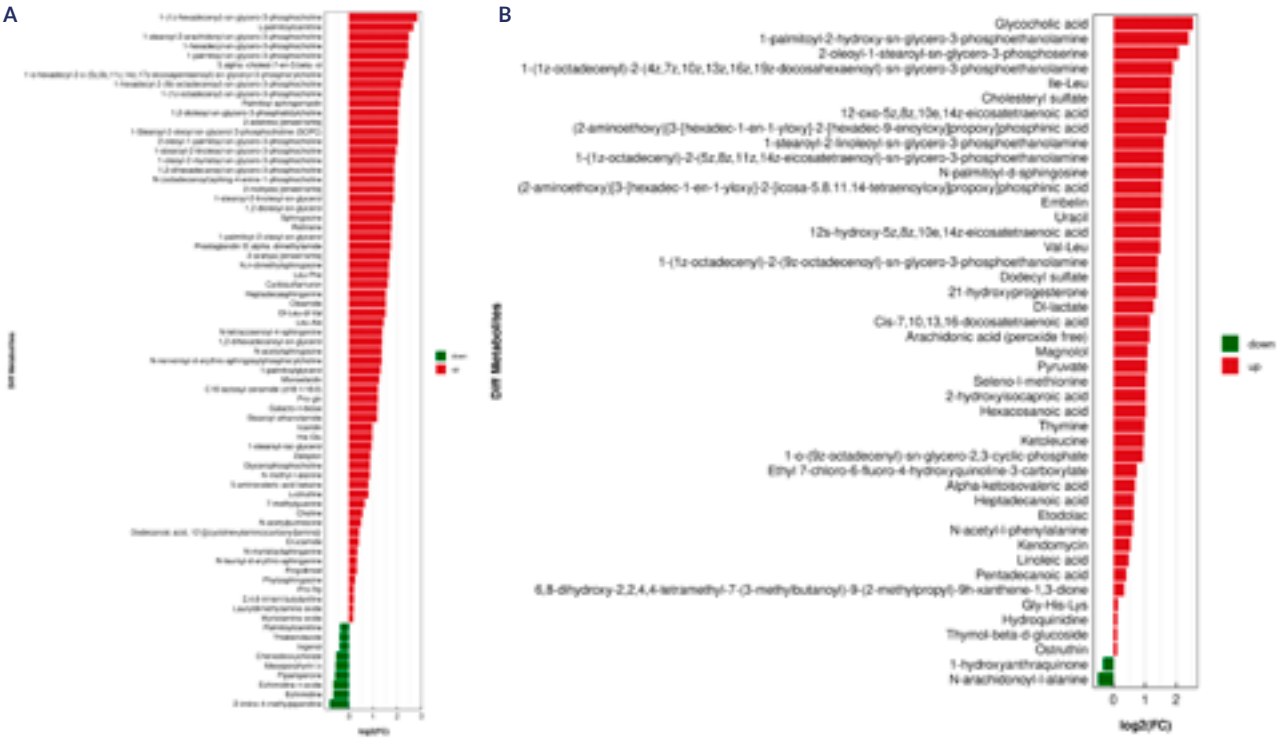


Figure 5. Differential metabolites identified in the positive and negative ion modes in the metastatic group compared to the non-metastatic group.

Metabolic pathway enrichment analysis of differential metabolites

Enrichment analysis of metabolic pathways was performed using the KEGG database. Pathways with a significance threshold of $P < 0.05$ were considered significantly enriched in differential metabolites. In the current study, metabolic pathway enrichment analysis (depicted in **Figure 6**) was conducted on all 119 differential metabolites, and 13 metabolic pathways that exhibited significant differences between the two groups were identified. These pathways included: necroptosis; choline metabolism in cancer; sphingolipid signaling pathway; sphingolipid metabolism; aldosterone synthesis and secretion; valine, leucine and isoleucine biosynthesis; linoleic acid metabolism; pantothenate and CoA biosynthesis; lipoic acid metabolism; arachidonic acid metabolism; retrograde endocannabinoid signaling; glycerophospholipid metabolism and ovarian steroidogenesis.

Analysis of the discriminating ability of candidate metabolites

Among the 119 differentially expressed metabolites identified through comprehensive metabolomic profiling, we conducted ROC curve analysis to screen for salivary biomarkers with the potential to discriminate metastatic status in PTC. As shown in **Tables 2-3**, six metabolites, N-lauroyl-d-erythro-sphinganine, N-myristoylsphinganine, heptadecasphinganine, chenodeoxycholate (CDCA), 1-palmitoyl-sn-glycero-3-phosphocholine (PGPC) and 1-palmitoyl-2-hydroxy-sn-glycero-3-phosphoethanolamine (PHGPE) had areas under the curve (AUCs) exceeding 0.8. Quantitative analysis revealed a significantly lower level of CDCA in the metastatic group, in contrast to higher levels of the other five metabolites (**Figure 7**). Furthermore, correlation matrix plots revealed correlations among the six discovered metabolites (**Figure 8**). Of particular interest, CDCA exhibited significant negative correlations with several other metabolites in the network.

Serum Tg is the primary clinical tumour biomarker for TC, but its measurement can be interfered by the presence of TgAb. We evaluated the diagnostic performance of serum Tg for metastasis prediction. ROC analysis yielded AUC values of 0.827 across all patients, 0.932 in TgAb-negative samples (TgAb < 4.11 IU/mL), and 0.697 in TgAb-positive samples (TgAb ≥ 4.11 IU/mL) (**Tables 3-4**). We then performed

Copyright© AE&M all rights reserved.

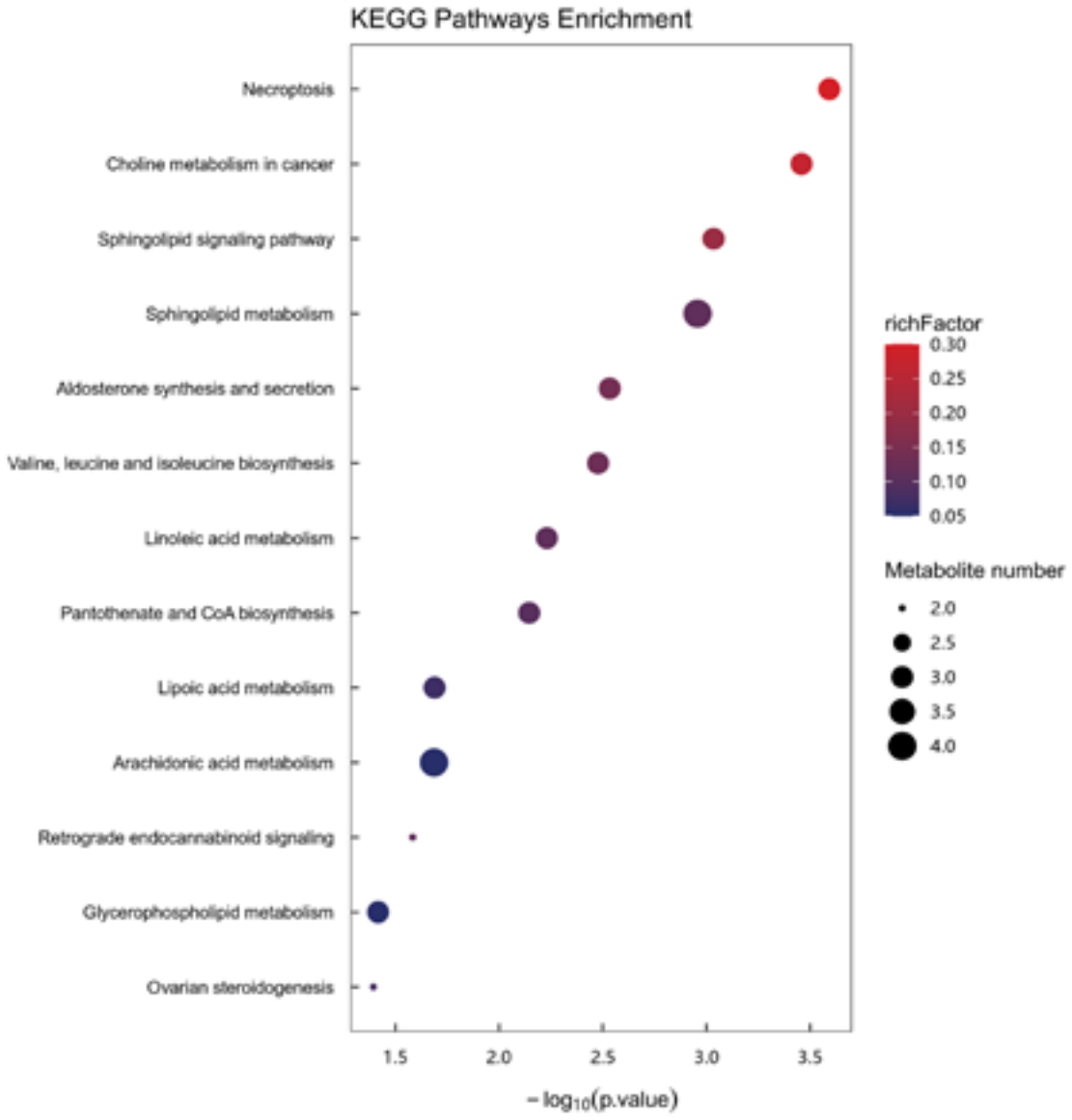


Figure 6. Results of metabolic pathway enrichment analysis of differential metabolites. The color of the dot represents the rich factor and the dot size represents the number of differential metabolites annotated to this pathway.

Table 2. Details of differentially metabolites with AUC > 0.8 in saliva

Name	SuperClass	Level	VIP	Fold change	*P*	AUC[a]	AUC[b]	AUC[c]
N-lauroyl-d-erythro-sphinganine	Lipids and lipid-like molecules	2	1.07	1.25	**<0.001**	0.869	0.873	0.851
N-myristoylsphinganine	Lipids and lipid-like molecules	2	2.61	1.27	**<0.001**	0.862	0.834	0.913
Heptadecasphinganine	Organic nitrogen compounds	2	2.04	2.91	**0.001**	0.859	0.823	0.908
Chenodeoxycholate	Lipids and lipid-like molecules	1	5.17	0.69	**<0.001**	0.834	0.802	0.892
1-palmitoyl-sn-glycero-3-phosphocholine	Lipids and lipid-like molecules	1	3.72	5.47	**<0.001**	0.812	0.782	0.862
1-palmitoyl-2-hydroxy-sn-glycero-3-phosphoethanolamine	Lipids and lipid-like molecules	1	1.45	5.23	**<0.001**	0.802	0.805	0.836

VIP: the variable importance in the projection, obtained from OPLS-DA with a threshold of 1.0; AUC: Area under the curve; [a]: AUC calculated in total samples; [b]: AUC calculated in samples with negtive TgAb; [c]: AUC calculated in samples with postive TgAb.
Level: the confidence level of the identified biomarkers according to the Metabolomics Standards Initiative (MSI) guidelines.
P: P-value calculated by *t*-test.

Copyright© AE&M all rights reserved.

Table 3. Quantitative indexes of Tg and six identified biomarkers in all samples

Variables	Class	Cut-off	AUC	Sensitivity	Specificity	PPV	NPV
Tg (ug/l)		21.39	0.827	0.771	0.857	0.844	0.790
N-lauroyl-d-erythro-sphinganine	Sphingolipids	24.85	0.869	0.771	0.829	0.818	0.784
N-myristoylsphinganine	Sphingolipids	27.29	0.862	0.686	0.914	0.889	0.744
Heptadecasphinganine	Amines	23.28	0.859	0.943	0.686	0.750	0.923
Chenodeoxycholate	Steroids and steroid derivatives	26.96	0.834	0.686	0.971	0.960	0.756
1-palmitoyl-sn-glycero-3-phosphocholine	Glycerophospholipids	22.97	0.812	0.886	0.657	0.721	0.852
1-palmitoyl-2-hydroxy-sn-glycero-3-phosphoethanolamine	Glycerophospholipids	22.64	0.802	0.600	0.943	0.913	0.702

AUC: Area under the curve; PPV: Positive Predictive Value; NPV: Negative Predictive Value; Tg: Thyroglobulin.
The cut-off values for the six identified metabolites were determined based on their log2-transformed peak areas.

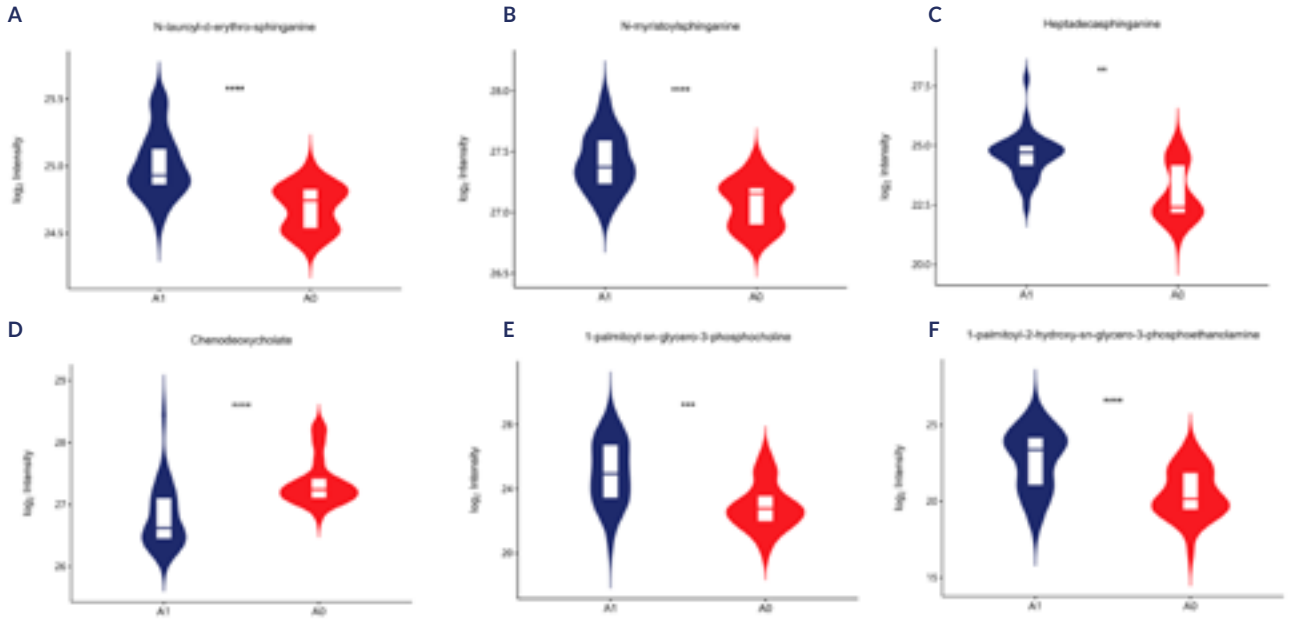


Figure 7. Expression of six discovered metabolites in both groups. Metastasis group (A1, blue); non-metastasis group (A0, red).

a stratified subgroup analysis based on TgAb levels to systematically evaluate the diagnostic performance of the six candidate metabolites according to TgAb status. Our findings demonstrated that in the TgAb-negative subgroup, all six metabolites maintained robust discriminatory capacity for detecting metastasis. Though these metabolites alone were slightly inferior to Tg, combining Tg with any metabolite improved AUC (notably, the combination of Tg and N-lauroyl-d-erythro-sphinganine achieved an AUC of 0.994). Importantly, in the TgAb-positive subgroup, these metabolites also retained their diagnostic utility for metastatic screening and surpassed serum Tg in performance (Tables 3-5).

DISCUSSION

Radioactive iodine (RAI) therapy is a cornerstone treatment for patients with DTC following total thyroidectomy and is critical for ablating residual thyroid tissue as well as for treating metastatic disease (6). Administering an appropriate ^{131}I dose optimizes therapeutic efficacy, reduces recurrence, and improves prognosis. Patients with metastatic PTC often require escalated ^{131}I activities (150-200 mCi) to achieve effective treatment. Conventional diagnostics (ultrasonography, Tg, CT) may fail to detect occult metastases because of: (1) anatomically complex locations, (2) TgAb interference compromising Tg interpretation, or (3) limited spatial resolution in detecting small

Copyright© AE&M all rights reserved.

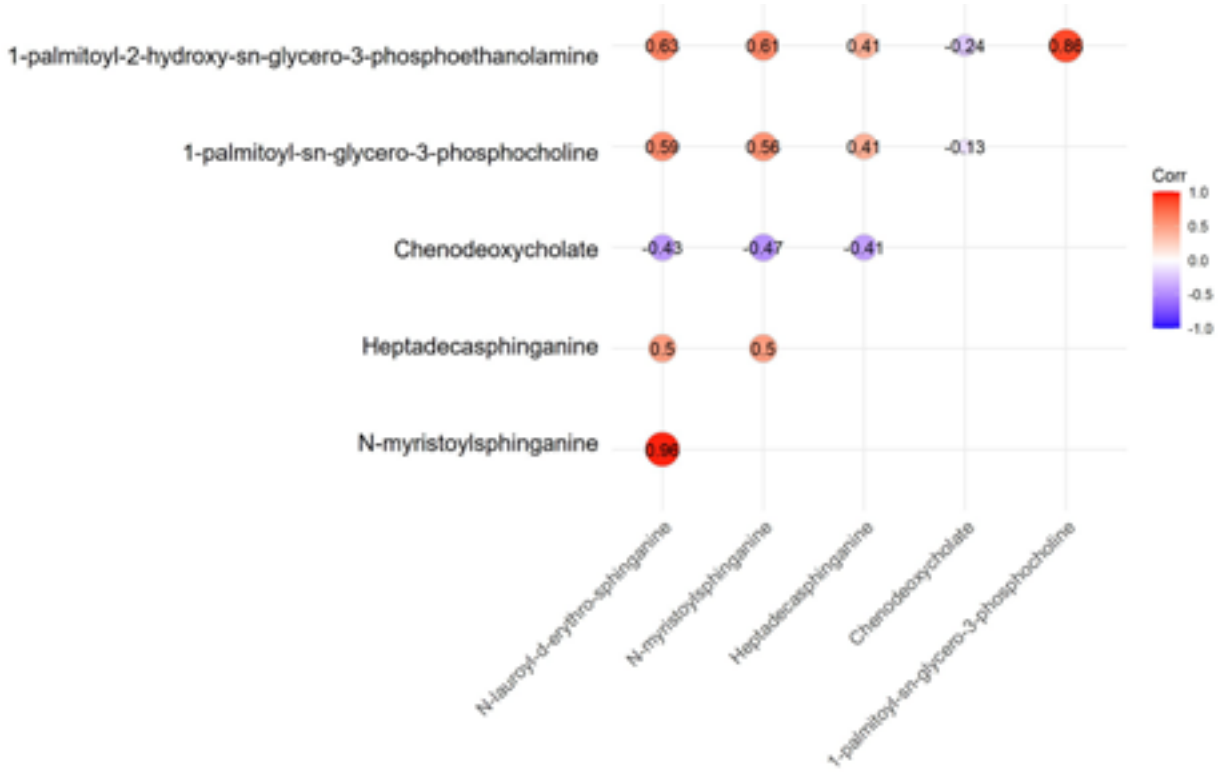


Figure 8. Correlation matrix plots displaying the spearman's correlation among the six discovered metabolites.

Table 4. Quantitative indexes of Tg and six identified biomarkers across different TgAb status

Variables	TgAb-negtative subgroup						TgAb-positive subgroup					
	Cut-off	AUC	Sensitivity	Specificity	PPV	NPV	Cut-off	AUC	Sensitivity	Specificity	PPV	NPV
Tg (ug/l)	50.50	0.932	0.773	1.000	1.000	0.800	10.70	0.697	0.539	0.933	0.875	0.700
N-lauroyl-d-erythro-sphinganine	24.85	0.873	0.773	0.950	0.944	0.792	24.92	0.851	0.615	1.000	1.000	0.750
N-myristoylsphinganine	27.32	0.834	0.591	0.950	0.929	0.679	27.23	0.913	0.923	0.867	0.857	0.929
Heptadecasphinganine	23.28	0.823	0.909	0.650	0.741	0.867	23.28	0.908	1.000	0.733	0.765	1.000
Chenodeoxycholate	26.97	0.802	0.636	0.950	0.933	0.704	26.96	0.892	0.769	1.000	1.000	0.833
1-palmitoyl-sn-glycero-3-phosphocholine	23.62	0.782	0.773	0.750	0.773	0.750	22.99	0.862	0.923	0.733	0.750	0.917
1-palmitoyl-2-hydroxy-sn-glycero-3-phosphoethanolamine	20.34	0.805	0.864	0.650	0.731	0.813	23.01	0.836	0.769	0.933	0.909	0.824

AUC: Area under the curve; PPV: Positive Predictive Value; NPV: Negative Predictive Value; Tg: Thyroglobulin.
The cut-off values for the six identified metabolites were determined based on their log2-transformed peak areas.

Table 5. The diagnostic efficacy of Tg combined with other identified biomarkers in TgAb-negative subgroup

Combined variables	AUC	Sensitivity	Specificity	PPV	NPV
Tg + N-lauroyl-d-erythro-sphinganine	0.994	1.000	0.950	0.957	1.000
Tg + N-myristoylsphinganine	0.949	0.909	0.950	0.952	0.905
Tg + Heptadecasphinganine	0.960	0.773	1.000	1.000	0.800
Tg + Chenodeoxycholate	0.972	0.955	0.950	0.955	0.950
Tg + 1-palmitoyl-sn-glycero-3-phosphocholine	0.972	0.773	1.000	1.000	0.800
Tg + 1-palmitoyl-2-hydroxy-sn-glycero-3-phosphoethanolamine	0.960	0.773	1.000	1.000	0.800

AUC: Area under the curve; PPV: Positive Predictive Value; NPV: Negative Predictive Value; Tg: Thyroglobulin.

Copyright© AE&M all rights reserved.

pulmonary metastatic lesions. These limitations potentially lead to suboptimal dosing of ^{131}I. Therefore, this study employs non-invasive saliva metabolomic profiling in postoperative PTC patients to identify novel predictive biomarkers, thereby enabling personalized ^{131}I dosing based on metastatic risk stratification.

Using ROC curve analysis, we identified six salivary biomarkers that demonstrated high diagnostic accuracy in discriminating metastatic from non-metastatic PTC. Among these novel candidates, N-lauroyl-D-erythro-sphinganine, N-myristoylsphinganine, and heptadecasphinganine are sphinganine derivatives that function as components of sphingolipids, which play crucial roles in cell signaling and membrane structure (22). Notably, bioactive sphingolipids are known to mediate oncogenic processes such as proliferation, migration, and invasion (23,24), directly supporting their association with metastasis. Similarly, PGPC and PHGPE belong to the phospholipid class, which constitutes fundamental components of cellular membranes and mediate critical biological processes including chemical-energy storage, cellular signaling, and cell-cell interactions. All these processes are pertinent to cellular transformation, cancer progression, and metastasis (25). In addition to the five identified upregulated lipids in the metastatic group, we also observed significantly downregulated levels of CDCA, a primary bile acid implicated in lipid metabolism. CDCA functions as a high-affinity endogenous ligand for the farnesoid X receptor (FXR) and plays critical regulatory roles through FXR activation to modulate key metabolic pathways (26). Specifically, CDCA has been shown to suppress gluconeogenesis and de novo lipogenesis, attenuates inflammatory responses, while concomitantly enhancing fatty acid β-oxidation in hepatic and adipose tissues (27). The regulatory effect of CDCA on lipid metabolism is consistent with the inverse correlation we observed between the CDCA levels and the levels of the five lipids, suggesting that downregulation of CDCA may promote pathogenic lipid accumulation to facilitate metastatic progression. Recent studies have highlighted that CDCA plays a complex role in cancer development and progression, exerting both oncogenic and tumour suppressive effects (28-31). Our data suggest that perturbations in bile acid-related metabolism occur in metastatic disease. Whether these changes are tumour-suppressive or actionable cannot be inferred from these observational analyses and will require mechanistic and interventional studies.

TgAb compromises the utility of Tg in PTC surveillance by interfering with its assay accuracy. Our TgAb-based subgroup analysis confirmed that Tg effectively predicts metastasis in TgAb-negative PTC patients but has limited predictive value in the TgAb-positive cohort. Notably, the six identified salivary metabolites demonstrated persistent diagnostic robustness for post-operative metastatic surveillance in TgAb-positive PTC patients. This finding may address a critical unmet need in TgAb-interfered clinical monitoring scenarios. Furthermore, the identified novel biomarkers could complement serum Tg levels to enhance the accuracy of metastasis detection in TgAb-negative PTC patients.

Our metabolomic profiling revealed significant disruptions in 13 key metabolic pathways. Necroptosis, a programmed form of necrosis, was identified as the most significantly enriched pathway in our analysis. This pathway has been widely implicated in tumour progression and metastasis across multiple cancer types (32,33). Equally noteworthy is the aberrant activation of choline metabolism, which is a well-characterized metabolic hallmark of carcinogenesis (34). This observation is consistent with our previous finding of decreased plasma choline levels in PTC patients compared with both healthy individuals and those with benign nodules (35). Furthermore, lipid metabolism (36) and amino acid metabolism (37) play vital roles in cancer progression and metastasis. In line with these established mechanisms, our results also identified an association between PTC metastasis and alterations in both lipid and amino acid metabolism. Collectively, these findings are biologically plausible and offer novel insights into the molecular mechanisms underlying PTC metastasis.

We also compared our results with those of Cararo Lopes and cols. (11). Comprehensive analysis revealed that the vast majority of metabolites were upregulated both in DTC versus normal tissue (as reported by Cararo Lopes and cols.) and in metastatic

Copyright© AE&M all rights reserved.

versus non-metastatic samples in saliva (as identified in our study). Notably, metabolites such as choline, pyruvate, and several amino acids, which were reported by Cararo Lopes and cols. to be elevated in DTC tissue, were also consistently upregulated in metastatic PTC in our cohort. Additionally, our results support the importance of anabolic metabolism in PTC progression, corroborating and extending the prior observations of Cararo Lopes and cols. in DTC versus normal tissue. Therefore, our findings suggest that there may be a continuum of metabolic modifications extending from normal thyroid tissue to primary PTC and, further, to metastatic disease.

This study represents the first application of salivary metabolomics in the surveillance of PTC metastasis. Nevertheless, several limitations must be acknowledged. As a single-centre preliminary investigation, this study was limited by a relatively small sample size, the lack of an independent validation cohort, and insufficient mechanistic exploration. Moving forwards, additional work is needed to substantiate the mechanistic insights, such as employing isotope tracing and flux analyses to characterize metabolic rewiring, performing genetic or pharmacological perturbation of candidate metabolic enzymes, and obtaining orthogonal validation in independent clinical cohorts. Future directions should primarily emphasize the application of these metabolite markers in prospective, multi-centre studies to evaluate their clinical utility for monitoring PTC metastasis.

In conclusion, this research provides new insights into the metabolic alterations associated with postoperative PTC metastasis. Six potential salivary biomarkers for the detection of PTC metastasis were successfully identified. This metabolomics investigation further revealed 13 pathways (primarily involved in necroptosis, choline, sphingolipid, and valine, leucine and isoleucine biosynthesis pathways) that are involved in the metastatic progression of PTC, potentially revealing new therapeutic opportunities. These biomarkers and metabolic pathways elucidated in this study open up promising directions for the development of innovative diagnostic methods and therapeutic strategies for PTC patients.

Funding: this work was supported by National Natural Science Foundation of China (No. 82272038), The China Postdoctoral Science Foundation (No. 2023M741765), Nanjing Health Science and Technology Development Project (No. YKK22114), Jiangsu Provincial Medical Key Discipline Cultivation Unit (No. JSDW202247), Jiangsu Province Research Hospital Cultivation Unit (No. YJXYYJSDW1).

Author contributions: FW, JW and LS conceived and designed the study. JP, LZ, SL, CZ, JF, PZ, JW and XY collected the samples and clinical data. FY and LS performed the experiment. FY conducted all statistical analyses. FY, JP and LZ drafted the manuscript; YN, AZ, QM, RY and LX played an important role in interpreting the results. All authors revised and approved the final version of the manuscript.

Disclosure: no potential conflict of interest relevant to this article was reported.

Data availability: datasets related to this article will be available upon request to the corresponding author.

REFERENCES

1. Sung H, Ferlay J, Siegel RL, Laversanne M, Soerjomataram I, Jemal A, et al. Global Cancer Statistics 2020: GLOBOCAN Estimates of Incidence and Mortality Worldwide for 36 Cancers in 185 Countries. CA Cancer J Clin. 2021;71(3):209-49. doi: 10.3322/caac.21660
2. Zheng RS, Chen R, Han BF, Wang SM, Li L, Sun KX, et al. [Cancer incidence and mortality in China, 2022]. Zhonghua Zhong Liu Za Zhi. 2024;46(3):221-31. doi: 10.3760/cma.j.cn112152-20240119-00035
3. Cabanillas ME, McFadden DG, Durante C. Thyroid cancer. Lancet. 2016;388(10061):2783-95. doi: 10.1016/S0140-6736(16)30172-6
4. Mao J, Zhang Q, Zhang H, Zheng K, Wang R, Wang G. Risk Factors for Lymph Node Metastasis in Papillary Thyroid Carcinoma: A Systematic Review and Meta-Analysis. Front Endocrinol (Lausanne). 2020;11:265. doi: 10.3389/fendo.2020.00265
5. Fallahi P, Ferrari SM, Galdiero MR, Varricchi G, Elia G, Ragusa F, et al. Molecular targets of tyrosine kinase inhibitors in thyroid cancer. Semin Cancer Biol. 2022;79:180-96. doi: 10.1016/j.semcancer.2020.11.013
6. Haugen BR, Alexander EK, Bible KC, Doherty GM, Mandel SJ, Nikiforov YE, et al. 2015 American Thyroid Association Management Guidelines for Adult Patients with Thyroid Nodules and Differentiated Thyroid Cancer: The American Thyroid Association Guidelines Task Force on Thyroid Nodules and Differentiated Thyroid Cancer. Thyroid. 2016;26(1):1-133. doi: 10.1089/thy.2015.0020
7. Lee JY, Yoo RE, Rhim JH, Lee KH, Choi KS, Hwang I, et al. Validation of Ultrasound Risk Stratification Systems for Cervical Lymph Node Metastasis in Patients with Thyroid Cancer. Cancers (Basel). 2022;14(9):2106. doi: 10.3390/cancers14092106
8. Zhang A, Wu S, You Z, Liu W. Application of Preoperative Ultrasonography in the Diagnosis of Cervical Lymph Node Metastasis in Thyroid Papillary Carcinoma. Front Surg. 2022;9:851657. doi: 10.3389/fsurg.2022.851657
9. Acquisto A, Duran Derijckere I, De Angelis R. An Atypical Behavior of Metastatic Lung Disease in a Young Woman with Osteosarcoma: A Case Report. Cureus. 2022;14(1):e21589. doi: 10.7759/cureus.21589
10. Nixon AM, Provatopoulou X, Kalogera E, Zografos GN, Gounaris A. Circulating thyroid cancer biomarkers: Current limitations and future prospects. Clin Endocrinol (Oxf). 2017;87(2):117-26. doi: 10.1111/cen.13369
11. Cararo Lopes E, Sawant A, Moore D, Ke H, Shi F, Laddha S, et al. Integrated metabolic and genetic analysis reveals distinct features of human differentiated thyroid cancer. Clin Transl Med. 2023;13(6):e1298. doi: 10.1002/ctm2.1298

Copyright© AE&M all rights reserved.

12. Huang FQ, Li J, Jiang L, Wang FX, Alolga RN, Wang MJ, et al. Serum-plasma matched metabolomics for comprehensive characterization of benign thyroid nodule and papillary thyroid carcinoma. Int J Cancer. 2019;144(4):868-76. doi: 10.1002/ijc.31925
13. Razavi SA, Mahmanzar M, Nobakht MGBF, Zamani Z, Nasiri S, Hedayati M. Plasma metabolites analysis of patients with papillary thyroid cancer: A preliminary untargeted (1)H NMR-based metabolomics. J Pharm Biomed Anal. 2024;241:115946. doi: 10.1016/j.jpba.2023.115946
14. Yu S, Liu C, Hou Y, Li J, Guo Z, Chen X, et al. Integrative metabolomic characterization identifies plasma metabolomic signature in the diagnosis of papillary thyroid cancer. Oncogene. 2022;41(17):2422-30. doi: 10.1038/s41388-022-02254-5
15. Xu B, Gao W, Xu T, Liu C, Wu D, Tang W. A UPLC Q-Exactive Orbitrap Mass Spectrometry-Based Metabolomic Study of Serum and Tumor Tissue in Patients with Papillary Thyroid Cancer. Toxics. 2022;11(1). doi: 10.3390/toxics11010044
16. Shen CT, Zhang Y, Liu YM, Yin S, Zhang XY, Wei WJ, et al. A distinct serum metabolic signature of distant metastatic papillary thyroid carcinoma. Clin Endocrinol (Oxf). 2017;87(6):844-52. doi: 10.1111/cen.13437
17. Murata T, Yanagisawa T, Kurihara T, Kaneko M, Ota S, Enomoto A, et al. Salivary metabolomics with alternative decision tree-based machine learning methods for breast cancer discrimination. Breast Cancer Res Treat. 2019;177(3):591-601. doi: 10.1007/s10549-019-05330-9
18. Zhong L, Cheng F, Lu X, Duan Y, Wang X. Untargeted saliva metabonomics study of breast cancer based on ultra performance liquid chromatography coupled to mass spectrometry with HILIC and RPLC separations. Talanta. 2016;158:351-60. doi: 10.1016/j.talanta.2016.04.049
19. Wang Q, Gao P, Cheng F, Wang X, Duan Y. Measurement of salivary metabolite biomarkers for early monitoring of oral cancer with ultra performance liquid chromatography-mass spectrometry. Talanta. 2014;119:299-305. doi: 10.1016/j.talanta.2013.11.008
20. Zhang J, Wen X, Li Y, Zhang J, Li X, Qian C, et al. Diagnostic approach to thyroid cancer based on amino acid metabolomics in saliva by ultra-performance liquid chromatography with high resolution mass spectrometry. Talanta. 2021;235:122729. doi: 10.1016/j.talanta.2021.122729
21. Sumner LW, Amberg A, Barrett D, Beale MH, Beger R, Daykin CA, et al. Proposed minimum reporting standards for chemical analysis Chemical Analysis Working Group (CAWG) Metabolomics Standards Initiative (MSI). Metabolomics. 2007;3(3):211-21. doi: 10.1007/s11306-007-0082-2
22. Hannun YA, Obeid LM. Sphingolipids and their metabolism in physiology and disease. Nat Rev Mol Cell Biol. 2018;19(3):175-91. doi: 10.1038/nrm.2017.107
23. Adada MM, Canals D, Jeong N, Kelkar AD, Hernandez-Corbacho M, Pulkoski-Gross MJ, et al. Intracellular sphingosine kinase 2-derived sphingosine-1-phosphate mediates epidermal growth factor-induced ezrin-radixin-moesin phosphorylation and cancer cell invasion. FASEB J. 2015;29(11):4654-69. doi: 10.1096/fj.15-274340
24. van der Weyden L, Arends MJ, Campbell AD, Bald T, Wardle-Jones H, Griggs N, et al. Genome-wide in vivo screen identifies novel host regulators of metastatic colonization. Nature. 2017;541(7636):233-6. doi: 10.1038/nature20792
25. Bandu R, Mok HJ, Kim KP. Phospholipids as cancer biomarkers: Mass spectrometry-based analysis. Mass Spectrom Rev. 2018;37(2):107-38. doi: 10.1002/mas.21510
26. Li C, Zhang S, Chen X, Ji J, Yang W, Gui T, et al. Farnesoid X receptor activation inhibits TGFBR1/TAK1-mediated vascular inflammation and calcification via miR-135a-5p. Commun Biol. 2020;3(1):327. doi: 10.1038/s42003-020-1058-2
27. Fiamoncini J, Rist MJ, Frommherz L, Giesbertz P, Pfrang B, Kremer W, et al. Dynamics and determinants of human plasma bile acid profiles during dietary challenges. Front Nutr. 2022;9:932937. doi: 10.3389/fnut.2022.932937
28. Casaburi I, Avena P, Lanzino M, Sisci D, Giordano F, Maris P, et al. Chenodeoxycholic acid through a TGR5-dependent CREB signaling activation enhances cyclin D1 expression and promotes human endometrial cancer cell proliferation. Cell Cycle. 2012;11(14):2699-710. doi: 10.4161/cc.21029
29. Soma T, Kaganoi J, Kawabe A, Kondo K, Tsunoda S, Imamura M, et al. Chenodeoxycholic acid stimulates the progression of human esophageal cancer cells: A possible mechanism of angiogenesis in patients with esophageal cancer. Int J Cancer. 2006;119(4):771-82. doi: 10.1002/ijc.21917
30. Liu J, Wei Y, Jia W, Can C, Wang R, Yang X, et al. Corrigendum to "Chenodeoxycholic acid suppresses AML progression through promoting lipid peroxidation via ROS/p38 MAPK/DGAT1 pathway and inhibiting M2 macrophage polarization" [Redox Biol. 56 (2022) 102452]. Redox Biol. 2023;59:102566. doi: 10.1016/j.redox.2022.102566
31. Rezen T, Rozman D, Kovacs T, Kovacs P, Sipos A, Bai P, et al. The role of bile acids in carcinogenesis. Cell Mol Life Sci. 2022;79(5):243. doi: 10.1007/s00018-022-04278-2
32. Yan J, Wan P, Choksi S, Liu ZG. Necroptosis and tumor progression. Trends Cancer. 2022;8(1):21-7. doi: 10.1016/j.trecan.2021.09.003
33. Su Z, Yang Z, Xu Y, Chen Y, Yu Q. Apoptosis, autophagy, necroptosis, and cancer metastasis. Mol Cancer. 2015;14:48. doi: 10.1186/s12943-015-0321-5
34. Sonkar K, Ayyappan V, Tressler CM, Adelaja O, Cai R, Cheng M, et al. Focus on the glycerophosphocholine pathway in choline phospholipid metabolism of cancer. NMR Biomed. 2019;32(10):e4112. doi: 10.1002/nbm.4112
35. Shi L, Guo M, Shi C, Gao G, Xu X, Zhang C, et al. Distinguishing benign and malignant thyroid nodules using plasma trimethylamine N-oxide, carnitine, choline and betaine. J Cancer Res Clin Oncol. 2024;150(3):142. doi: 10.1007/s00432-024-05666-w
36. Martin-Perez M, Urdiroz-Urricelqui U, Bigas C, Benitah SA. The role of lipids in cancer progression and metastasis. Cell Metab. 2022;34(11):1675-99. doi: 10.1016/j.cmet.2022.09.023
37. Li Z, Zhang H. Reprogramming of glucose, fatty acid and amino acid metabolism for cancer progression. Cell Mol Life Sci. 2016;73(2):377-92. doi: 10.1007/s00018-015-2070-4

Copyright© AE&M all rights reserved.

Archives of Endocrinology and Metabolism
ISSN 2359-4292
OFFICIAL JOURNAL OF THE BRAZILIAN SOCIETY OF ENDOCRINOLOGY AND METABOLISM

original

Comparative diagnostic accuracy of the triglyceride/HDL-c ratio and lipid accumulation product index for the early detection of metabolic syndrome among adults with obesity in Indonesia: findings from the 2023 Health Survey

Alya Ayu Alvitananda[1]
https://orcid.org/0009-0001-7342-1805

Etika Ratna Noer[1]
https://orcid.org/0000-0002-1555-5944

Ahmad Syauqy[1]
https://orcid.org/0000-0002-9552-2834

Edward Kurnia Setiawan Limijadi[2]
https://orcid.org/0000-0002-8476-2971

Adriyan Pramono[1]
https://orcid.org/0000-0003-2159-4576

[1] Department of Nutrition, Faculty of Medicine, Diponegoro University, Semarang, Indonesia
[2] Department of Clinical Pathology, Faculty of Medicine, Diponegoro University, Semarang, Indonesia

ABSTRACT

Objective: To evaluate the diagnostic performance and determine the optimal cutoff values of the triglyceride-to-high-density lipoprotein cholesterol ratio and lipid accumulation product index as predictors of metabolic syndrome among adults with obesity in Indonesia. **Materials and methods:** This cross-sectional study analyzed secondary data from the 2023 Indonesia Health Survey, which included 3,988 samples (2,958 women). Descriptive statistics were used to characterize the sample. Receiver Operating Characteristic curve analysis and the Youden index were employed to assess diagnostic performance and determine the optimal cutoff values of the triglyceride-to-high-density lipoprotein cholesterol ratio and lipid accumulation product index. The associations between both predictors and the presence of metabolic syndrome were examined using multivariable logistic regression. **Results**: The lipid accumulation product index exhibited greater predictive accuracy than the triglyceride-to-high-density lipoprotein cholesterol ratio, particularly among men. This result indicated the superior utility of the lipid accumulation product index as a clinical screening tool for metabolic syndrome, with area under the curve values of 0.842 (95% CI 0.817-0.866) for men and 0.737 (95% CI 0.720-0.755) for women, compared to that of the triglyceride-to-high-density lipoprotein cholesterol ratio, with area under the curve values of 0.810 (95% CI 0.784–0.837) for men and 0.728 (95% CI 0.710-0.746) for women. The optimal cutoff values of the triglyceride-to-high-density lipoprotein cholesterol ratio and lipid accumulation product index were 4.456 (sensitivity 64.8%, specificity 81.4%) and 45.752 (sensitivity 75.5%, specificity 81.2%) for men and 2.792 (sensitivity 59.2%, specificity 76.8%) and 41.285 (sensitivity 58.6%, specificity 75.8%) for women, respectively. **Conclusion**: The lipid accumulation product index demonstrated superior accuracy in predicting metabolic syndrome among adults with obesity, particularly among men. Sex-specific cutoff values enhance its reliability and practicality for early screening and intervention to prevent metabolic complications.

Keywords: Metabolic syndrome; obesity; predictor

Received on Feb/5/2025
Accepted on Sep/23/2025

DOI: 10.20945/2359-4292-2026-0016

Correspondence to:
Adriyan Pramono
adriyanpramono@fk.undip.ac.id

Associated editor:
Marcio C. Mancini
https://orcid.org/0000-0003-1278-0406

This is an open-access article distributed under the terms of the Creative Commons Attribution License

INTRODUCTION

Metabolic syndrome (MetS) is a complex condition characterized by a cluster of metabolic disorders, including central obesity, dyslipidemia, hypertension, and insulin resistance (IR) (1,2). Metabolic syndrome is associated with increased risks of cardiovascular disease (CVD), stroke, and type 2 diabetes mellitus (T2DM) and contributes significantly to global morbidity and mortality (3,4). The global prevalence

Copyright© AE&M all rights reserved.

of MetS is increasing, particularly in developing countries, primarily because of increasing obesity rates among adults (5). In the Asia-Pacific region, nearly one-fifth or more of the adult population in many countries has been diagnosed with MetS, exhibiting an increasing trend (6).

In Indonesia, the prevalence of MetS is estimated at 21.66%, with a disproportionately higher rate among women (46%), which is nearly twice that among men (28%) (7). This high prevalence is accompanied by an 8.6% increase in obesity over the past decade (8-10). Obesity, a major public health concern, is a key contributor to MetS through mechanisms such as ectopic fat accumulation and systemic inflammation, which promote IR, a central pathway in the development of metabolic and physiological disturbances associated with MetS (11,12). As a result, this condition significantly increases the risk of cardiometabolic complications and contributes to national morbidity and mortality (13).

Although several international organizations have proposed diagnostic criteria for MetS (14-17), including the widely recognized Harmonizing the Metabolic Syndrome: A Joint Interim Statement 2009 (18), their implementation in large-scale population screenings remains challenging in Indonesia. These challenges are particularly evident in primary health care settings, where limited resources and uneven health care infrastructure pose significant barriers. In addition, comprehensive and up-to-date data on the prevalence of MetS at national, regional, and population-specific levels remain scarce (19). Therefore, there is a need for simpler and more accessible screening tools to support the early detection and prevention of MetS.

Given that fat mass and its distribution are significant metabolic factors, various cost-effective and simple alternative biomarkers have been explored to improve the accuracy of MetS diagnosis. Among them are the triglyceride-to-high-density lipoprotein cholesterol ratio (TG/HDL-c) and the lipid accumulation product (LAP) index (20-22). TG/HDL-c, which integrates key lipid components, has shown potential as a surrogate marker for MetS, IR, and atherosclerosis severity (23,24). Similarly, the LAP index combines waist circumference (WC) and triglyceride (TG) levels, providing a practical measure of visceral fat accumulation (25).

The LAP index and TG/HDL-c, which incorporate WC and lipid parameters, not only reflect underlying metabolic dysfunction but also offer more accurate assessment of visceral adiposity and metabolic risk. In this study, both markers demonstrated superior diagnostic performance for MetS, as indicated by their higher AUC values. In contrast, conventional anthropometric indicators such as body mass index (BMI), WC, waist-to-hip ratio (WHR), and waist-to-height ratio (WHtR), while easy to measure, present notable limitations. Body mass index is widely used to assess general obesity, but it does not differentiate between muscle mass and body fat. Similarly, waist-based indicators such as WC, WHR, and WHtR can reflect central obesity but are unable to distinguish between visceral and subcutaneous fat (22,26).

Although useful, the diagnostic performance and optimal cutoff values of the TG/HDL-c and LAP index are influenced by several factors, including population characteristics, ethnicity, sex, geographic region, and lifestyle habits such as diet, physical activity, and medication use (27). These variations underscore the importance of context-specific validation, particularly in diverse populations such as those inhabiting Indonesia. Nonetheless, their accessibility and ease of use make these markers appealing for early MetS screening and risk stratification (28).

To date, no study has systematically compared the diagnostic performance and determined the optimal cutoff values of the TG/HDL-c ratio and LAP index among adults with obesity in the Indonesian population. Therefore, this study aims to evaluate and compare the effectiveness of the TG/HDL-c ratio and LAP index as predictors of MetS and to determine their optimal cutoff values for this specific population.

MATERIALS AND METHODS

This study received ethical approval from Pusat Data dan Teknologi Informasi (PUSDATIN) Kementerian Kesehatan Republik Indonesia (Approval Number: FRM/SMKI-PUSDATIN/70/0226/2024) and the Ethics Committee of Diponegoro University Faculty of Medicine (Approval Number: No. 469/EC/KEPK/FK-UNDIP/IX/2024).

Copyright© AE&M all rights reserved.

Study population

This study employed a cross-sectional design using secondary data from the 2023 Indonesian Health Survey (IHS), which encompassed 345,000 households across 34,500 census blocks in 514 districts or cities from 38 provinces in Indonesia. To ensure data quality, the IHS incorporated interagency cooperation, pilot studies, enumerator training, technical supervision, external validation, quality control, and tool calibration. Stratification was performed both explicitly at the census block level (based on area classification and access to health care) and implicitly at the household level (based on the education of the head of household). Census blocks were selected using the probability proportional to size (PPS) method to ensure proportional regional representation, and households were selected systematically. National biomedical estimates were derived from 2,500 census blocks with individual selection to ensure population representativeness (10).

From this subsample, subjects were selected via total sampling, including those who met the inclusion criteria: age 19 to 64 years; having obesity, defined as a BMI of ≥ 25 kg/m^2; and complete data on demographic characteristics, lifestyle (i.e., smoking and physical activity), lipid profile, fasting blood glucose (FBG), BMI, blood pressure, and WC are available. Subjects with incomplete (missing) data were excluded using the listwise deletion method. Individuals with extreme values were also excluded based on predefined criteria. Extreme data were defined as those with skewness or kurtosis values outside the range of -1 to +1 and identified as outliers on the basis of stem-and-leaf plots (29). The final sample size analyzed in this study was 3,988 individuals.

Basic characteristics

All the data in this study were secondary data previously collected by the IHS Team in 2023. The demographic and lifestyle characteristics included age, sex, place of residence, education, physical activity, and smoking behavior. This data was gathered through interviews by using a validated, structured questionnaire. The physical activity and smoking questionnaires were tested and validated by the IHS Team to ensure the accuracy of question flow, content, and implementation in the Indonesian population.

Physical activity levels were assessed using the Global Physical Activity Questionnaire (GPAQ), which is part of the WHO STEPwise approach to NCD risk factor surveillance (STEPS) program. Research conducted in nine countries, including Indonesia, has highlighted the good reliability and validity of the GPAQ, confirming its suitability for monitoring physical activity in the Indonesian population (10,30,31).

Physical activity behaviors were categorized into two groups: sufficient (≥ 150 minutes per week of combined vigorous and moderate activity) and insufficient (< 150 minutes per week of combined activity). Smoking status was classified as follows: ever smokers (those who smoked daily or occasionally in the past month or those with a history of smoking) and nonsmokers (those who had never smoked up to the time of data collection). Education level was categorized into two groups: high (≥ high school) and low (< high school) (10,30).

Anthropometric measurements

The anthropometric data collected in this study included weight, height, and WC. All measurements were conducted by trained health care personnel following standardized procedures. Instruments were calibrated to ensure accuracy and consistency. Weight was measured using a digital scale (0.1 kg accuracy), while height was measured using a stadiometer (1 mm accuracy). Body mass index was calculated using the formula weight (kg)/height (m^2), and a BMI of ≥ 25 kg/m^2 was classified as obesity. Waist circumference was measured at the midpoint between the lowest rib and the top of the pelvic bone, with the tape wrapped around the body passing through the umbilicus. This measurement was used to assess central obesity. Blood pressure was measured twice on the left upper arm using a digital sphygmomanometer (10).

Biochemical data

The biochemical data analyzed in this study included FBG, TG, and high-density lipoprotein (HDL) levels. Blood samples were collected by trained medical personnel who had undergone standardized training.

Copyright© AE&M all rights reserved.

Samples were collected after the subjects had fasted for 8 to 12 hours. Fasting blood glucose was measured using capillary blood samples analyzed with the Accu-Chek Performa device. TG and HDL levels were measured using venous blood samples analyzed by a chemical autoanalyzer with enzymatic methods (10).

A 7 mL-venous blood sample was drawn and placed in a yellow tube for biochemical analysis. After centrifugation at 3,000 rpm for 10 minutes, the serum was transferred to 5 mL microtubes and stored at -20 ℃. The samples were transported to the National Health Laboratory within 48 hours using standardized packaging and shipping protocols. Potential confounders, such as chronic illnesses, bleeding disorders, anticoagulant use, and other physician-identified conditions, were considered during collection (10).

Definition of metabolic syndrome

Metabolic syndrome was the dependent variable in this study and was diagnosed using the Harmonizing the Metabolic Syndrome: A Joint Interim Statement 2009 criteria, which had previously been applied in prevalence studies of MetS across various provinces and ethnic groups in Indonesia. The WC cutoff was adjusted explicitly for the Indonesian population (32). Subjects were classified as having MetS if they exhibited at least three of the following five risk factors: (1) central obesity: WC > 80 cm in women and > 90 cm in men; (2) high TG: ≥ 150 mg/dL (1.7 mmol/L); (3) low HDL: HDL < 40 mg/dL (1.03 mmol/L) in men or < 50 mg/dL (1.29 mmol/L) in women; (4) high blood pressure: systolic blood pressure ≥ 130 mmHg or diastolic ≥ 85 mmHg; and (5) high FBG: blood glucose ≥ 100 mg/dL (5.6 mmol/L) (18).

Triglyceride/HDL-c and lipid accumulation product index

The TG/HDL-c and LAP index were calculated using the following formulas:

TG/HDL-c formula: TG (mg/dL)/HDL (mg/dL) (4)

LAP index formula:

Men = WC (cm) – 65 x TG (mmol/L) (33)

Women = WC (cm) – 58 x TG (mmol/L) (33)

Since the original LAP index formula utilizes TG values in mmol/L, TG concentrations initially recorded in mg/dL were converted to mmol/L by dividing by 88.57 prior to calculation.

Statistical analysis

Data was analyzed using Statistical Package for the Social Sciences (SPSS) version 26.0 for Windows and Microsoft Excel and MedCalc, with statistical significance set at $p < 0.05$. Numerical variables are presented as the means and standard deviations, whereas categorical variables are presented as counts and percentages.

Data normality, skewness, and kurtosis values were evaluated using stem-and-leaf plots. Data were considered normally distributed if the skewness and kurtosis values fell within the range of -1 to +1 and if no extreme outliers were identified (29).

Independent *t* tests were used to compare numerical variables, whereas Chi-squared tests were used to compare categorical variables between men and women. Diagnostic accuracy was assessed using the area under the curve (AUC) analysis of the Receiver Operating Characteristic (ROC) curve, stratified by sex. The indicator with the highest AUC was considered the best predictor, with values closer to 1 indicating better accuracy. The AUC values were classified as follows: very weak (0.5 to 0.6), weak (0.6 to 0.7), moderate (0.7 to 0.8), good (0.8 to 0.9), and excellent (> 0.9) (34).

To statistically compare the AUCs of the TG/HDL-c ratio and the LAP index, DeLong's test for two correlated ROC curves was employed. This method allowed assessment of whether the discriminative ability of one marker was significantly superior to that of the other, with analyses performed separately for men and women.

The optimal cutoff values of the TG/HDL-c and LAP index were determined using the following Youden index equation: Youden index = sensitivity + specificity -1 (35).

Finally, a logistic regression model using the full model approach was employed to assess the associations between the TG/HDL-c, the LAP index, and the presence of MetS. The analysis adjusted for potential confounders, including age, sex, BMI, education level, place of residence, smoking status, and physical activity, to ensure more accurate and reliable results.

Copyright© ACE&M all rights reserved.

RESULTS

This study analyzed 3,988 samples, comprising 1,030 men and 2,958 women aged 19 to 64. The prevalence of MetS significantly increased with age, as illustrated in Figure 1. The overall prevalence of MetS in this study population was 56%, with a slightly higher prevalence observed in men (56.6%) than in women (55.7%), although this difference was not statistically significant ($p > 0.05$) (Table 1).

The characteristics of the participants stratified by sex are presented in Table 1. Significant differences were observed between men and women in terms of

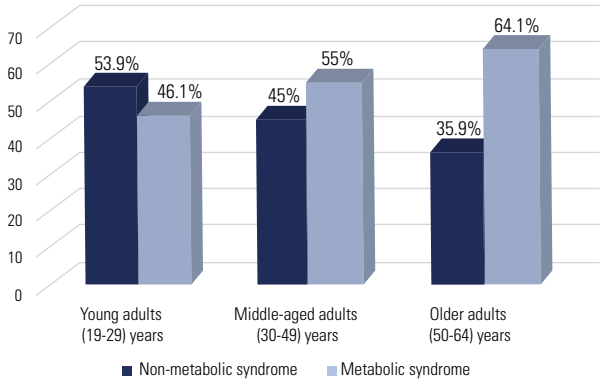


Figure 1. Prevalence of metabolic syndrome across adult age groups.

Table 1. Characteristics of participants stratified by sex

Variables	Men (1,030) N%	Women (2,958) N%	Total (3,988) N%	p-value
Prevalence of metabolic syndrome				
Non-metabolic syndrome	447 (43.4)	1,309 (44.3)	1,756 (44)	0.634
Metabolic syndrome	583 (56.6)	1,649 (55.7)	2,232 (56)	
Age, years	43.49 ± 11.35	40.90 ± 10.25	41.57 ± 10.61	< 0.001*
Body mass index, kg/m^2	27.74 ± 2.42	28.85 ± 3.25	28.56 ± 3.09	< 0.001*
Education level				
Low	431 (41.8)	1,695 (42.7)	2126 (53.3)	< 0.001*
High	599 (58.2)	1,263 (57.3)	1,862 (46.7)	
Place of residence				
Rural	351 (34.1)	1,134 (38.3)	1,485 (37.2)	0.015*
Urban	679 (65.9)	1,824 (61.7)	2,503 (62.8)	
Smoking status				
Nonsmoker	422 (41.0)	2,909 (98.3)	3,331 (83.5)	< 0.001*
Ever smoker	608 (59.0)	49 (1.7)	657 (16.5)	
Physical activity				
Low	365 (35.4)	682 (23.1)	1,047 (26.3)	< 0.001*
Moderate	665 (64.6)	2,274 (76.9)	2,939 (73.7)	
Components of metabolic syndrome				
Waist circumference, cm	91.60 ± 7.83	89.35 ± 8.06	89.93 ± 8.06	< 0.001*
Triglyceride level, mg/dL	168.42 ± 66.94	116.09 ± 39.79	129.61 ± 53.44	< 0.001*
HDL level, mg/dL	37.49 ± 6.65	43.85 ± 8.14	42.1 ± 8.27	< 0.001*
Systolic blood pressure, mmHg	128.95 ± 13.32	125.67 ± 15.79	126.52 ± 15.26	< 0.001*
Diastolic blood pressure, mmHg	84.24 ± 8.63	84.71 ± 8.81	84.59 ± 8.76	0.144
Fasting blood glucose level, mg/dL	98.18 ± 8.71	94.96 ± 7.79	95.79 ± 8.16	< 0.001*
Predictors of metabolic syndrome				
TG/HDL-c	4.70 ± 2.16	2.76 ± 1.11	3.26 ± 1.68	< 0.001*
LAP index	51.00 ± 25.59	41.41 ± 18.39	43.89 ± 20.91	< 0.001*

Results expressed as n (%) or mean ± standard deviation.
The p-values were calculated using the Chi-squared test for categorical variables and the independent *t* test for numerical variables.
*Statistical significance was set at $p < 0.05$.
HDL: high-density lipoprotein; TG/HDL-c: triglyceride-to-high-density lipoprotein cholesterol ratio; LAP: lipid accumulation product.

Copyright© AE&M all rights reserved.

age, BMI, educational level, place of residence, smoking status, physical activity, WC, triglyceride levels, HDL levels, systolic blood pressure, fasting blood glucose levels, the TG/HDL-c, and the LAP index ($p < 0.05$). However, no significant difference in diastolic blood pressure was detected ($p > 0.05$). Additionally, the average age of men (43.49 ± 11.35) was slightly greater than that of women (40.90 ± 10.25).

Table 2 displays the baseline characteristics of participants with and without MetS, stratified by sex. For men, significant differences ($p < 0.05$) were found in all the variables except for education, place of residence, smoking status, and physical activity. In women, almost all the variables were significantly different, except place of residence, smoking status, and physical activity ($p > 0.05$). As expected, most components of MetS, including WC, TG, blood pressure, FBG, the TG/HDL-c, and the LAP index, exhibited worse values in the MetS group, while HDL levels were lower.

Table 3 and **Figure 2** present the ROC analysis results for the TG/HDL-c and LAP index as predictors of MetS stratified by sex. Both indicators showed good predictive ability for MetS in men (AUC = 0.8-0.9; $p < 0.001$), with the LAP index demonstrating superior performance (AUC = 0.842; 95% CI 0.817-0.866) compared to the TG/HDL-c (AUC = 0.810; 95% CI 0.784-0.837), and this difference was statistically significant, as determined by DeLong's test ($p < 0.05$).

In women, both indicators showed moderate predictive ability (AUC = 0.7–0.8; $p < 0.001$). Although the LAP index had a slightly greater AUC (0.737; 95% CI 0.720–0.755) than the TG/HDL-c did (AUC = 0.728; 95% CI 0.710-0.746), the difference was not

Table 2. Baseline characteristics of study participants with and without metabolic syndrome, stratified by sex

Variables N%	Men		p-value	Women		p-value
	Without MetS N%	With MetS N%		Without MetS N%	With MetS N%	
Age, years	42.40 ± 11.35	44.32 ± 11.29	0.007*	39.07 ± 10.13	42.35 ± 10.12	< 0.001*
Body mass index, kg/m^2	27.04 ± 2.00	28.27 ± 2.58	< 0.001*	28.28 ± 3.16	29.30 ± 3.24	< 0.001*
Education level						
Low	181 (40.5)	250 (42.9)	0.441	698 (53.3)	997 (39.5)	< 0.001*
High	266 (59.5)	333 (57.1)		611 (46.7)	652 (60.5)	
Place of residence						
Rural	157 (35.1)	194 (33.3)	0.535	484 (37.0)	650 (39.4)	0.175
Urban	290 (64.9)	389 (66.7)		825 (63.0)	999 (60.6)	
Smoking status						
Nonsmoker	182 (40.7)	240 (41.2)	0.884	1287 (98.3)	1622 (98.4)	0.927
Ever smoker	265 (59.3)	343 (58.8)		22 (1.7)	27 (1.6)	
Physical activity						
Low	149 (33.3)	216 (37.0)	0.217	306 (23.4)	376 (22.8)	0.695
Moderate	298 (66.7)	367 (63.0)		1001 (76.6)	1273 (77.2)	
Components of metabolic syndrome						
Waist circumference, cm	88.03 ± 7.30	94.33 ± 7.08	< 0.001*	86.86 ± 8.41	91.34 ± 7.18	< 0.001*
Triglyceride level, mg/dL	135.05 ± 56.44	194.02 ± 63.02	< 0.001*	100.85 ± 30.78	128.19 ± 41.93	< 0.001*
HDL level, mg/dL	40.38 ± 6.89	35.27 ± 5.51	< 0.001*	46.40 ± 8.69	41.84 ± 7.06	< 0.001*
Systolic blood pressure (mmHg)	124.60 ± 11.79	132.29 ± 13.47	< 0.001*	118.62 ± 13.41	131.26 ± 15.29	< 0.001*
Diastolic blood pressure (mmHg)	81.23 ± 8.00	86.56 ± 8.38	< 0.001*	80.37 ± 7.62	88.15 ± 8.14	< 0.001*
Fasting blood glucose level, mg/dL	94.87 ± 7.35	100.73 ± 8.82	< 0.001*	92.06 ± 6.27	97.26 ± 8.10	< 0.001*
Predictors of metabolic syndrome						
TG/HDL-c	3.46 ± 1.62	5.6 ± 2.05	< 0.001*	2.27 ± 0.85	3.15 ± 1.13	< 0.001*
LAP index	34.69 ± 17.20	63.50 ± 23.87	< 0.001*	32.96 ± 14.23	48.12 ± 18.55	< 0.001*

Results expressed as mean ± standard deviation or n (%).

The p-values were calculated using the Chi-squared test for categorical variables and the independent *t* test for numerical variables.

*Statistical significance was set at $p < 0.05$.

MetS: matabolic syndrome; HDL: high-density lipoprotein; TG/HDL-c: triglyceride-to-high-density lipoprotein cholesterol ratio; LAP: lipid accumulation product.

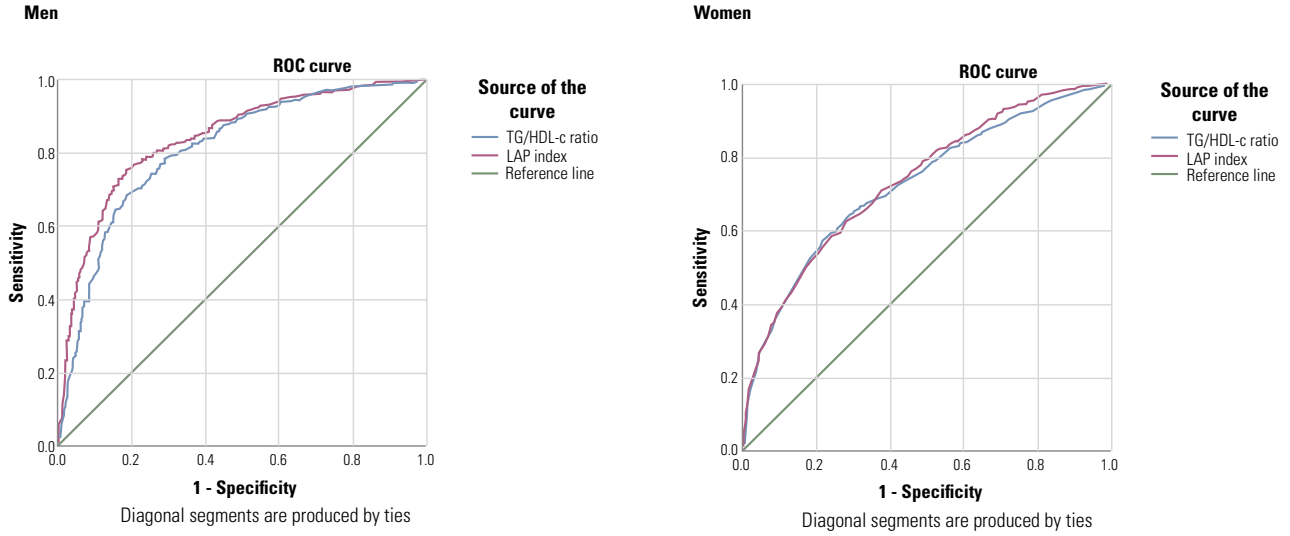
Copyright© AE&M all rights reserved.

Table 3. Outcomes of the Receiver Operating Characteristic curve for men and women

Predictors of metabolic syndrome	AUC	95% CI	Standard error	p-value	Sensitivity (%)	Specificity (%)	Youden index	Optimal cutoff	LR+	LR-
Men										
TG/HDL-c	0.810	0.784-0.837	0.14	< 0.001*	64.8	81.4	0.499	4.456	3.686	0.388
LAP	0.842	0.817-0.866	0.12	< 0.001*	75.5	81.2	0.567	45.752	4.016	0.302
Women										
TG/HDL-c	0.728	0.710-0.746	0.009	< 0.001*	59.2	76.8	0.360	2.793	2.549	0.532
LAP	0.737	0.720-0.755	0.009	< 0.001*	58.6	75.8	0.344	41.285	2.419	0.547

* Statistically significant (p-value < 0.05).

AUC: area under the curve; 95% CI 95% of confidence interval; LR+: likelihood ratio +; LR-: likelihood ratio-; TG/HDL-c: triglyceride-to-high-density lipoprotein cholesterol ratio; LAP: lipid accumulation product.



ROC: Receiver Operating Characteristic; TG/HDL-c: triglyceride-to-high-density lipoprotein cholesterol ratio; LAP: lipid accumulation product.

Figure 2. Receiver Operating Characteristic curves of each indicator in the prediction of metabolic syndrome risk based on sex.

statistically significant (p > 0.05). Detailed results of the AUC comparisons using DeLong's test are presented in **Supplementary Table 1**.

Furthermore, in this study, the optimal cutoff values were determined using the Youden index. For men, the TG/HDL-c had a Youden index of 0.499, with an optimal cutoff value of 4.456 (Sn = 64.8%, Sp = 81.4%), while the LAP index had a Youden index of 0.567, with an optimal cutoff value of 45.752 (Sn = 75.5%, Sp = 81.2%). In women, the TG/HDL-c had a Youden index of 0.360, with an optimal cutoff value of 2.793 (Sn = 59.2%, Sp = 76.8%), whereas the LAP index had a Youden index of 0.344, with an optimal cutoff value of 41.285 (Sn = 58.6%, Sp = 75.8%).

As shown in **Table 4**, both the TG/HDL-c and the LAP index were independently and significantly associated with the incidence of MetS across all the models (p < 0.001), including the fully adjusted Model 6, which controlled for age, sex, BMI, education level, place of residence, smoking status, and physical activity.

In the male subgroup, the LAP index demonstrated a significantly greater AUC than the TG/HDL-c did (p < 0.05). In contrast, among women, the LAP index had a slightly greater AUC than the TG/HDL-c did; however, the difference was not statistically significant (p > 0.05) (**Supplementary Table 2**).

Consistent with the primary findings, external validation using data from the 2018 Indonesian Basic Health Survey (IHS) in a population of adults with obesity (age: 19 to 50 years; BMI ≥ 25 kg/m^2; *n* = 4,727, comprising 999 men and 3,728 women) confirmed moderate to good discriminative ability of both the TG/HDL-c and LAP index in predicting MetS. The LAP

Copyright© AE&M all rights reserved.

Table 4. Associations of the triglyceride-to-high-density lipoprotein cholesterol ratio and lipid accumulation product index with metabolic syndrome: analysis with adjustment for confounding variables

	Model unadjusted			Model adjusted for age and sex			Mode adjusted body mass index		
	OR	95% CI	p-value	OR	95% CI	p-value	OR	95% CI	p-value
TG/HDL-c	1.207	1.129-1.290	< 0.001*	1.479	1.365-1.603	< 0.001*	1.270	1.184-1.364	< 0.001*
LAP	1.049	1.043-1.055	< 0.001*	1.040	1.034-1.046	< 0.001*	1.043	1.037-1.050	< 0.001*

	Model adjusted for education level and place of residence			Model adjusted for smoking status and physical activity			Model adjusted for age, sex, body mass index, education level, place of residence, smoking status, and physical activity		
	OR	95% CI	p-value	OR	95% CI	p-value	OR	95% CI	p-value
TG/HDL-c	1.211	1.133-1.296	< 0.001*	1.332	1.237-1.435	< 0.001*	1.574	1.445-1.714	< 0.001*
LAP	1.049	1.043-1.055	< 0.001*	1.045	1.040-1.051	< 0.001*	1.033	1.027-1.040	< 0.001*

*Significant, $p < 0.05$.
OR: odds ratio; 95% CI 95% of confidence interval; TG/HDL-c: triglyceride-to-high-density lipoprotein cholesterol ratio; LAP: lipid accumulation product.

index consistently demonstrated better performance than the TG/HDL-c in men, although the difference was not statistically significant.

DISCUSSION

In this study, both the TG/HDL-c and LAP index were found to be useful for predicting MetS, with the LAP index showing better performance, especially in adult men with obesity. The analysis employed an obesity cutoff of BMI ≥ 25 kg/m², which is more appropriate for Asian populations, including the Indonesian population, and aligns with current recommendations to enhance the clinical evaluation and prevention of metabolic complications (36). The LAP index is a key obesity indicator that reflects visceral fat accumulation on the basis of the WC component and atherogenic dyslipidemia on the basis of triglyceride levels (12,22).

Visceral fat has higher metabolic and proinflammatory activity than subcutaneous fat does (37). This fat produces free fatty acids (FFA) and proinflammatory cytokines and decreases adiponectin, which triggers IR, dyslipidemia, renin-angiotensin-aldosterone system (RAAS) activation, and hyperglycemia (25,38,39). Moreover, atherogenic dyslipidemia occurs when the liver increases the production of very low-density lipoprotein (VLDL) in response to excessive lipolysis of FFAs due to IR. This lipid accumulation exacerbates IR through lipotoxicity, resulting in the formation of a negative feedback loop. Therefore, the LAP index provides a comprehensive overview of cardiometabolic risk in MetS (40).

A study from China evaluating obesity-related parameters and lipids to predict MetS revealed that the LAP index was superior to other measures, such as the Visceral Adiposity Index (VAI), TG/HDL-c, WHtR, and BMI. In line with our research, the LAP index performed better than the TG/HDL-c (41).

In this study, the LAP index demonstrated a strong ability to predict MetS, particularly in men with adequate Sn values and high Sp-values. In women, the performance of this index was moderately effective, but still clinically relevant. These findings are consistent with those of previous cohort studies in China that evaluated 13 indices related to obesity and lipids and revealed that the LAP index has excellent predictive ability in men (AUC = 0.912; 95% CI 0.903-0.921), with a cutoff of 27.895 (Sn = 83.5%, Sp = 83.6%), whereas in women, the LAP index has a slightly lower AUC of 0.876 (95% CI 0.867–0.885), with a cutoff of 35.867 (Sn = 73.2%, Sp = 83.4%) (42).

The high consistency of the AUC values of the LAP index in various international studies supports its reliability as a tool for identifying MetS risk (43,44). The superior performance of the LAP index in men in this study was also assessed, with a Sp-value above 80%, supporting its use in early screening to minimize overdiagnosis and improve targeted interventions (45).

Moreover, the TG/HDL-c may better reflect atherogenic dyslipidemia, but this ratio does not give sufficient importance to body fat distribution, which makes it less specific for assessing MetS risk, especially in populations with obesity. This ratio component,

Copyright© ACE&M all rights reserved.

especially the HDL, is influenced by external factors and fluctuates. HDL-c dysfunction can also cause high HDL levels despite increased metabolic risk, thereby reducing Sn levels and the AUC (46). Therefore, the TG/HDL-c is more appropriately considered a systemic biomarker (47).

However, the TG/HDL-c also has good predictive ability, although slightly less than the LAP index, particularly in women. As further support, a study in Iran revealed that the TG/HDL-c is a potential indicator of MetS (AUC = 0.85 in both men and women), which is consistent with our findings, although the AUC values in that study were slightly greater (48). Similarly, a study of elderly individuals in China revealed that the TG/HDL-c demonstrated good predictive ability (AUC = 0.813; 95% CI 0.784-0.842), with slightly lower cutoff values: 1.437 for men (Sn = 74.8% and Sp = 78.4%) and 1.196 for women (Sn = 86.4% and Sp = 67.4%) (49).

Notably, the differences in the AUC and cutoff values between our study and others may be attributed to variations in genetic background, lifestyle factors, body composition, dietary habits, and the use of different MetS criteria across populations.

This study also highlights significant differences in LAP index values and TG/HDL-c between sexes, with men having higher average values. These findings are consistent with the characteristics of the components of both indicators, such as WC and lipid levels. Men have higher WC and TG levels and lower HDL levels, whereas women generally have normal TG levels and higher HDL levels. This combination results in higher final values for both predictors, indicating a higher risk for men.

These observations are closely related to body fat distribution, which is influenced by hormonal and physiological factors. Men tend to store fat in the visceral area, leading to a higher WC, even though the BMI was higher in women in this study. This visceral fat distribution is influenced by testosterone. Women store more fat in the subcutaneous area, particularly in the thighs and hips, because of the influence of estrogen. Subcutaneous fat does not significantly increase WC, despite having a higher total fat mass (50).

Visceral fat increases the release of FFA and TG synthesis in the liver, whereas estrogen increases lipoprotein lipase (LPL) activity, which accelerates TG metabolism (51). These findings indicate that men are more likely to experience metabolic disorders (52). Moreover, lower HDL levels in men are also associated with higher liver lipase activity (53).

In addition, men tend to have higher systolic blood pressure and FBG levels because of the influence of testosterone, which increases RAAS activity. Conversely, estrogen in women protects blood vessels by lowering RAAS, acting as an anti-inflammatory agent, and maintaining HDL levels. (54). Moreover, there were no significant differences in diastolic blood pressure, possibly because vascular compensation maintains its stability (55).

The aforementioned explanation elucidates the rationale behind the superior predictive ability of the LAP index compared to the TG/HDL-c in men, with both indices demonstrating greater predictive power than those in the female cohort. This disparity is likely attributable to the influence of testosterone, a more pronounced accumulation of visceral fat, and more significant dyslipidemia in men. Conversely, in women, the predominance of subcutaneous fat distribution, more stable triglyceride levels, and elevated HDL levels may contribute to the lower predictive performance values relative to men. The corresponding predictive abilities of the LAP index and the TG/HDL-c were comparable, with no significant differences observed between the two. Furthermore, the larger sample size of women, coupled with narrower variability in lipid and anthropometric profiles, may also account for the absence of statistically significant differences identified.

Moreover, lifestyle factors such as smoking and a lack of physical activity also play a role. Our results revealed that compared with women, men ever smoked more and were less active, which increased the risk of MetS. Physical activity increases insulin sensitivity and reduces inflammation, whereas smoking exacerbates metabolic disorders (56,57). In addition, the older average age of the men in this study was also associated with increased risk of MetS components (58).

In line with findings that men have more MetS components and riskier lifestyles, the prevalence of MetS in this study was slightly higher in men (56.6%)

Copyright© AE&M all rights reserved.

than in women (55.7%), differing from previous findings that showed a higher prevalence in women (59). This difference may also be influenced by the larger number of women (n = 2,958) than men (n = 1,030). Although MetS is generally more common in women, men tend to have more severe metabolic disorders (60).

The prevalence of MetS was 56% higher in this study than in previous studies in Indonesia (32). This increase, along with high obesity rates, highlights the importance of deploying more effective screening tools for diverse populations so that interventions such as diet management, pharmacological therapy, and lifestyle modifications can be targeted appropriately to prevent MetS complications.

In conclusion, the findings of this study suggest that both the lipid accumulation product index and triglycerides/HDL-c serve as sex-specific predictors of metabolic syndrome in adults with obesity, each with distinct optimal cutoff values. The lipid accumulation product index exhibited superior performance in men and is recommended as a practical screening tool in primary health care and public health contexts in Indonesia, particularly where resources are constrained. In women, both indices demonstrated comparable predictive capabilities; however, the lipid accumulation product index is preferable because of its ease of calculation, practicality, and cost-effectiveness, rendering it more suitable for screening within the general population.

This study contributes to the national literature by using 2023 Indonesian Basic Health Survey data, which are representative of the broader population, and involved trained enumerators to minimize bias. However, this study has several limitations, including its cross-sectional design, which precludes causal inferences. Additionally, the potential for residual confounding remains due to unmeasured variables such as dietary intake, medication use, comorbidities, psychological stress, and genetic predispositions, all of which may influence metabolic outcomes and their interaction with the two predictors, as well as the overall prevalence of metabolic syndrome.

Further research is needed, including longitudinal studies controlling for these factors and more comprehensive clinical and genetic profiles, both in Indonesia and globally. Direct measurement of body fat or visceral fat would also strengthen the findings and provide a more accurate understanding of the role of obesity in metabolic syndrome.

Funding: this study received no external funding.

Authors' contributions: AAA fully accessed the research data, designed the study, analyzed the data, and drafted the manuscript. AP, ERN, AS, and EKSL contributed to the study design. AP supervised the analysis and made suggestions, corrections, and revisions during manuscript preparation. All the authors reviewed and approved the final manuscript.

Acknowledgments: the authors express their sincere gratitude to the participants of this study and the 2023 Indonesia Health Survey team for providing valuable data. AP gratefully acknowledges the support from the LPPM Undip RAP Scheme (No. 222-234/UN7.D2/PP/IV/2025).

Disclosure: no potential conflict of interest relevant to this article was reported.

Data availability: the data used in this study were obtained from Pusat Data dan Teknologi Informasi (PUSDATIN) of the Kementerian Kesehatan Republik Indonesia through a structured data request and ethical approval.

REFERENCES

1. Hayden MR. Overview and New Insights into the Metabolic Syndrome: Risk Factors and Emerging Variables in the Development of Type 2 Diabetes and Cerebrocardiovascular Disease. Medicina (B Aires). 2023;59(3):561. doi: 10.3390/medicina59030561
2. Fahed G, Aoun L, Bou Zerdan M, Allam S, Bou Zerdan M, Bouferraa Y, et al. Metabolic Syndrome: Updates on Pathophysiology and Management in 2021. Int J Mol Sci. 2022;23(2):786. doi: 10.3390/ijms23020786
3. Lee M-K, Han K, Kim MK, Koh ES, Kim ES, Nam GE, et al. Changes in metabolic syndrome and its components and the risk of type 2 diabetes: a nationwide cohort study. Sci Rep. 2020;10(1):2313. doi: 10.1038/s41598-020-59203-z
4. Liu X, Ma C, Yin F, Wang R, Lu Q, Lu N, et al. Performance of Two Novel Obesity Indicators for the Management of Metabolic Syndrome in Young Adults. Front Endocrinol (Lausanne). 2021;12. doi: 10.3389/fendo.2021.719416
5. Chew NW, Ng CH, Tan DJ, Kong G, Lin C, Chin YH, et al. The global burden of metabolic disease: Data from 2000 to 2019. Cell Metab. 2023;35(3):414-428.e3. doi: 10.1016/j.cmet.2023.02.003
6. Ranasinghe P, Mathangasinghe Y, Jayawardena R, Hills AP, Misra A. Prevalence and trends of metabolic syndrome among adults in the asia-pacific region: a systematic review. BMC Public Health. 2017;17(1):101. doi: 10.1186/s12889-017-4041-1
7. Sigit FS, Tahapary DL, Trompet S, Sartono E, Willems van Dijk K, Rosendaal FR, et al. The prevalence of metabolic syndrome and its association with body fat distribution in middle-aged individuals from Indonesia and the Netherlands: a cross-sectional analysis of two population-based studies. Diabetol Metab Syndr. 2020;12:2. doi: 10.1186/s13098-019-0503-1
8. Kementerian Kesehatan Republik Indonesia. Laporan Nasional Riskesdas. Jakarta: Kemenkes RI; 2013.
9. Kementerian Kesehatan Republik Indonesia. Laporan Nasional Riskesdas 2018. Jakarta: Kemenkes RI; 2018.

Copyright© AE&M all rights reserved.

10. Tim Penyusun SKI dalam Angka 2023. Survey Kesehatan Indonesia (SKI) dalam Angka 2023. Jakarta: Kementerian Kesehatan Republik Indonesia dan Badan Kebijakan Pembangunan Kesehatan; 2023.
11. Jiang J, Cai X, Pan Y, Du X, Zhu H, Yang X, et al. Relationship of obesity to adipose tissue insulin resistance. BMJ Open Diabetes Res Care. 2020;8(8):e000741. doi: 10.1136/bmjdrc-2019-000741
12. Tamini S, Bondesan A, Caroli D, Sartorio A. The Lipid Accumulation Product Index (LAP) and the Cardiometabolic Index (CMI) Are Useful for Predicting the Presence and Severity of Metabolic Syndrome in Adult Patients with Obesity. J Clin Med. 2024;13:2843. doi: 10.3390/jcm13102843
13. Rahajeng E, Sulistiowati E, Kusumawardhani N. Diabetes Risk Obese Among Indonesian Adults with Metabolic Syndrome by 6-Years Prospective Cohort Study. Proc 4th Int Symp Heal Res (ISHR 2019). Paris, France: Atlantis Press; 2020. Available from: https://www.atlantis-press.com/article/125934968
14. Zhu L, Spence C, Yang WJ, Ma GX. The IDF Definition Is Better Suited for Screening Metabolic Syndrome and Estimating Risks of Diabetes in Asian American Adults: Evidence from NHANES 2011–2016. J Clin Med. 2020;9(12):3871. doi: 10.3390/jcm9123871
15. Huang PL. A comprehensive definition for metabolic syndrome. Dis Model Mech. 2009;2(5-6):231-7. doi: 10.1242/dmm.001180
16. De Luis DA, Lopez Mongil R, Gonzalez Sagrado M, Lopez Trigo JA, Mora PF, Castrodeza Sanz J. Prevalence of metabolic syndrome with international diabetes federation criteria and ATP III program in patients 65 years of age or older. J Nutr Heal aging. 2010;14(5):400-4. doi: 10.1007/s12603-010-0087-9
17. Ramachandran A, Snehalatha C, Satyavani K, Sivasankari S, Vijay V. Metabolic syndrome in urban Asian Indian adults-a population study using modified ATP III criteria. Diabetes Res Clin Pract. 2003;60(3):199-204. doi: 10.1016/S0168-8227(03)00060-3
18. Alberti KG, Eckel RH, Grundy SM, Zimmet PZ, Cleeman JI, Donato KA, et al. Harmonizing the Metabolic Syndrome. Circulation. 2009;120(16):1640-5. doi: 10.1161/CIRCULATIONAHA.109.192644
19. Suastika K. The challenges of metabolic disorders in Indonesia: focus on metabolic syndrome, prediabetes, and diabetes. Med J Indones. 2020;29:350-3. doi: 10.13181/mji.com.205108
20. Xu H, Jin C, Guan Q. Causal Effects of Overall and Abdominal Obesity on Insulin Resistance and the Risk of Type 2 Diabetes Mellitus: A Two-Sample Mendelian Randomization Study. Front Genet. 2020;11:603. doi: 10.3389/fgene.2020.00603
21. Radetti G, Grugni G, Lupi F, Fanolla A, Caroli D, Bondesan A, et al. High Tg/HDL-cholesterol Ratio Highlights a Higher Risk of Metabolic Syndrome in Children and Adolescents with Severe Obesity. J Clin Med. 2022;11(15):4488. doi: 10.3390/jcm11154488
22. Shao Q, Li J, Wu Y, Liu X, Wang N, Jiang Y, et al. Enhanced Predictive Value of Lipid Accumulation Product for Identifying Metabolic Syndrome in the General Population of China. Nutrients. 2023;15(14):3168. doi: 10.3390/nu15143168
23. Ghani ZA, Qaddori H, Al-Mayah Q. Triglyceride/high-density lipoprotein ratio as a predictor for insulin resistance in a sample of healthy Iraqi adults. J Med Life. 2023;16(5):668-74. doi: 10.25122/jml-2022-0239
24. Krawczyk M, Rumińska M, Witkowska-Sędek E, Majcher A, Pyrżak B. Usefulness of the Triglycerides to High-Density Lipoprotein Cholesterol ratio (TG/HDL-c) in prediction of metabolic syndrome in Polish obese children and adolescents. Acta Biochim Pol. 2018;65(4):605-11. doi: 10.18388/abp.2018_2649
25. Alves LF, Cruz JO, da Costa Souza AL, de Oliveira CC. Performance of adiposity indicators in predicting metabolic syndrome in older adults. Arch Endocrinol Metab. 2021;65(5):588-95; doi: 10.20945/2359-3997000000372
26. Solorzano M, Granfeldt G, Ulloa N, Molina-Recio G, Molina-Luque R, Aguayo C, et al. Comparison of Diagnostic Models to Estimate the Risk of Metabolic Syndrome in a Chilean Pediatric Population: A Cross-Sectional Study. Metabolites. 2023;13(2):293. doi: 10.3390/metabo13020293
27. Ramos-Lopez O, Riezu-Boj JI, Milagro FI, Cuervo M, Goni L, Martinez JA. Prediction of Blood Lipid Phenotypes Using Obesity-Related Genetic Polymorphisms and Lifestyle Data in Subjects with Excessive Body Weight. Int J Genomics. 2018;2018:1-10. doi: 10.1155/2018/4283078
28. Tamini S, Bondesan A, Caroli D, Sartorio A. The Lipid Accumulation Product Index (LAP) and the Cardiometabolic Index (CMI) Are Useful for Predicting the Presence and Severity of Metabolic Syndrome in Adult Patients with Obesity. J Clin Med. 2024;13(10):2843. doi: 10.3390/jcm13102843
29. Mishra P, Pandey C, Singh U, Gupta A, Sahu C, Keshri A. Descriptive statistics and normality tests for statistical data. Ann Card Anaesth. 2019;22(1):67. doi: 10.4103/aca.ACA_157_18
30. Syauqy A, Wiragapa LR, Soekatri MY, Ernawati F, Nissa C, Dieny FF. Hubungan antara Pola Makan dan Kondisi Penyerta dengan Prevalensi Strok pada Usia Dewasa di Indonesia: Analisis Data RISKESDAS 2018. GIZI Indones. 2023;46:121-32. doi: 10.36457/gizindo.v46i1.785
31. Bull FC, Maslin TS, Armstrong T. Global Physical Activity Questionnaire (GPAQ): Nine Country Reliability and Validity Study. J Phys Act Heal. 2009;6(6):790-804. doi: 10.1123/jpah.6.6.790
32. Herningtyas EH, Ng TS. Prevalence and distribution of metabolic syndrome and its components among provinces and ethnic groups in Indonesia. BMC Public Health. 2019;19(1):377. doi: 10.1186/s12889-019-6711-7
33. Jeong SH, Jang BN, Kim SH, Jang S-I, Park E-C. Investigation of the Association between Smoking Behavior and Metabolic Syndrome Using Lipid Accumulation Product Index among South Korean Adults. Int J Environ Res Public Health. 2021;18(8):4151. doi: 10.3390/ijerph18084151
34. Çorbacıoğlu ŞK, Aksel G. Receiver operating characteristic curve analysis in diagnostic accuracy studies. Turkish J Emerg Med. 2023;23:195–198. doi: 10.4103/tjem.tjem_182_23
35. Yuan M, Li P, Wu C. Semiparametric inference of the Youden index and the optimal cut-off point under density ratio models. Can J Stat. 2021;49:965-86. doi: 10.1002/cjs.11600
36. Nugraha GI, Tahapary DL, Hidayat RW, Manikam NR, Syamsunarno MR, Kurniawan F, et al. The urgency in proposing the optimal obesity cutoff value in Indonesian population: A narrative review. Medicine (Baltimore). 2022;101(49):e32256. doi: 10.1097/MD.0000000000032256
37. Roriz AK, Passos LC, de Oliveira CC, Eickemberg M, Moreira P de A, Sampaio LR. Evaluation of the Accuracy of Anthropometric Clinical Indicators of Visceral Fat in Adults and Elderly. Atkin SL, editor. PLoS One. 2014;9(7):e103499. doi: 10.1371/journal.pone.0103499
38. Chen X, Zhao Y, Sun J, Jiang Y, Tang Y. Identification of metabolic syndrome using lipid accumulation product and cardiometabolic index based on NHANES data from 2005 to 2018. Nutr Metab (Lond). 2024;21(1):96. doi: 10.1186/s12986-024-00864-2
39. Crujeiras AB, Cordero P, Garcia-Diaz DF, Stachowska E, González-Muniesa P. Molecular Basis of the Inflammation Related to Obesity. Oxid Med Cell Longev. 2019;2019:1-2. doi: 10.1155/2019/5250816
40. Wasilewska N, Lebensztejn D. Non-alcoholic fatty liver disease and lipotoxicity. Clin Exp Hepatol. 2021;7(1):1-6. doi: 10.5114/ceh.2021.104441
41. Gu Z, Zhu P, Wang Q, He H, Xu J, Zhang L, et al. Obesity and lipid-related parameters for predicting metabolic syndrome in Chinese elderly population. Lipids Health Dis. 2018;17(1):289. doi: 10.1186/s12944-018-0927-x
42. De Paoli M, Zakharia A, Werstuck GH. The Role of Estrogen in Insulin Resistance. Am J Pathol. 2021;191(9):1490-8. doi: 10.1016/j.ajpath.2021.05.011
43. Motamed N, Razmjou S, Hemmasi G, Maadi M, Zamani F. Lipid accumulation product and metabolic syndrome: a population-based study in northern Iran, Amol. J Endocrinol Invest. 2016;39(4):375-82. doi: 10.1007/s40618-015-0369-5

Copyright© AE&M all rights reserved.

44. Taverna MJ, Martínez-Larrad MT, Frechtel GD, Serrano-Ríos M. Lipid accumulation product: a powerful marker of metabolic syndrome in healthy population. Eur J Endocrinol. 2011;164(4):559-67. doi: 10.1530/EJE-10-1039
45. Parikh R, Mathai A, Parikh S, Chandra Sekhar G, Thomas R. Understanding and using sensitivity, specificity and predictive values. Indian J Ophthalmol. 2008;56(1):45. doi: 10.4103/0301-4738.37595
46. von Eckardstein A, Nordestgaard BG, Remaley AT, Catapano AL. High-density lipoprotein revisited: biological functions and clinical relevance. Eur Heart J. 2023;44(16):1394-407. doi: 10.1093/eurheartj/ehac605
47. Park B, Jung DH, Lee HS, Lee YJ. Triglyceride to HDL-cholesterol Ratio and the Incident Risk of Ischemic Heart Disease Among Koreans Without Diabetes: A Longitudinal Study Using National Health Insurance Data. Front Cardiovasc Med. 2021;8. doi: 10.3389/fcvm.2021.716698
48. Rezapour M, Shahesmaeili A, Hossinzadeh A, Zahedi R, Najafipour H, Gozashti MH. Comparison of Lipid Ratios to Identify Metabolic Syndrome. Arch Iran Med. 2018;21(12):572-7.
49. Nie G, Hou S, Zhang M, Peng W. High TG/HDL ratio suggests a higher risk of metabolic syndrome among an elderly Chinese population: a cross-sectional study. BMJ Open. 2021;11:e041519. doi: 10.1136/bmjopen-2020-041519
50. Tchernof A, Brochu D, Maltais-Payette I, Mansour MF, Marchand GB, Carreau A, et al. Androgens and the Regulation of Adiposity and Body Fat Distribution in Humans. Compr Physiol. Wiley; 2018. p. 1253–1290. Available from: https://onlinelibrary.wiley.com/doi/10.1002/cphy.c170009.
51. Wat LW, Chao C, Bartlett R, Buchanan JL, Millington JW, Chih HJ, et al. A role for triglyceride lipase brummer in the regulation of sex differences in Drosophila fat storage and breakdown. Hassan BA, editor. PLOS Biol. 2020;18:e3000595. doi: 10.1371/journal.pbio.3000595
52. Ciarambino T, Crispino P, Guarisco G, Giordano M. Gender Differences in Insulin Resistance: New Knowledge and Perspectives. Curr Issues Mol Biol. 2023;45:7845-7861. doi: 10.3390/cimb45100496
53. Cohen E, Margalit I, Goldberg E, Krause I. Gender as an Independent Risk Factor for the Components of Metabolic Syndrome Among Individuals Within the Normal Range of Body Mass Index. Metab Syndr Relat Disord. 2018;16:537-42. doi: 10.1089/met.2018.0071
54. Nwia SM, Leite AP, Li XC, Zhuo JL. Sex differences in the renin-angiotensin-aldosterone system and its roles in hypertension, cardiovascular, and kidney diseases. Front Cardiovasc Med. 2023;10. doi: 10.3389/fcvm.2023.1198090
55. Drury ER, Wu J, Gigliotti JC, Le TH. Sex differences in blood pressure regulation and hypertension: renal, hemodynamic, and hormonal mechanisms. Physiol Rev. 2024;104:199-251. doi: 10.1152/physrev.00041.2022
56. Sterpi V, Ricci E, Chiaffarino F, Fedele F, Esposito G, Parazzini F, et al. The sitting men: A systematic review of spare and working time exposure to sedentariness in relation to semen parameters. Andrology. 2024; doi: 10.1111/andr.13816
57. Bae C-Y, Piao M, Kim M, Im Y, Kim S, Kim D, et al. Biological age and lifestyle in the diagnosis of metabolic syndrome: the NHIS health screening data, 2014-2015. Sci Rep. 2021;11:444. doi: 10.1038/s41598-020-79256-4
58. Kytikova OY, Antonyuk MV, Kantur TA, Novgorodtseva TP, Denisenko YK. Prevalence and biomarkers in metabolic syndrome. Obe Metab. 2021;18:302-12. doi: 10.14341/omet12704
59. Sigit FS, Tahapary DL, Trompet S, Sartono E, Willems van Dijk K, Rosendaal FR, et al. The prevalence of metabolic syndrome and its association with body fat distribution in middle-aged individuals from Indonesia and the Netherlands: a cross-sectional analysis of two population-based studies. Diabetol Metab Syndr. 2020;12:2. doi: 10.1186/s13098-019-0503-1
60. Henstridge DC, Abildgaard J, Lindegaard B, Febbraio MA. Metabolic control and sex: A focus on inflammatory-linked mediators. Br J Pharmacol. 2019;176(21):4193-207. doi: 10.1111/bph.14642

Copyright© AE&M all rights reserved.

Supplementary Table 1. Area under the curve comparison between the lipid accumulation product index and the triglyceride-to-high-density lipoprotein cholesterol ratio using DeLong's test stratified by sex

Group	AUC LAP (95% CI)	AUC TG/HDL-c (95% CI)	AUC Difference	95% CI of Difference	p-value (DeLong)
Men	0.842 (0.818-0.863)	0.810 (0.785-0.834)	0.0313	0.00987-0.0527	0.0042*
Women	0.737 (0.721-0.753)	0.728 (0.711-0.744)	0.0095	-0.00531-0.0242	0.2092

* Statistically significant (p-value < 0.05).

AUC: area under the curve; LAP: lipid accumulation product; 95% CI 95% of confidence interval; TG/HDL-c: triglycerides to high-density lipoprotein cholesterol ratio.

Supplementary Table 2. External validation of the predictive accuracy of the triglycerides to high-density lipoprotein cholesterol ratio and lipid accumulation product index for MetS in adults with obesity (Indonesian Basic Health Survey 2018 Data)

Predictors of metabolic syndrome	AUC	95% CI	Standard error	p-value	Sensitivity (%)	Specificity (%)	Youden index	Optimal cutoff	LR+	LR-	p-value DeLong Test
Men (n: 999)											
TG/HDL-c	0.825	0.799-0.851	0.13	< 0.001*	81.5	71.5	0.530	3.225	2.862	0.258	0.176
LAP	0.838	0.814-0.863	0.12	< 0.001*	77.6	76.1	0.537	42.150	3.247	0.295	
Women (n: 3728)											
TG/HDL-c	0.766	0.751-0.782	0.008	< 0.001*	59.2	81.0	0.402	2.374	3.119	0.504	0.168
LAP	0.759	0.744-0.774	0.008	< 0.001*	66.2	73.1	0.070	33.737	2.460	0.463	

*Statistically significant (p-value < 0.05),

AUC: area under the curve; 95% CI 95% of confidence interval; LR+: likelihood ratio +; LR-: likelihood ratio -; TG/HDL-c: triglycerides to high-density lipoprotein cholesterol ratiol; LAP: lipid accumulation product.

Copyright© AE&M all rights reserved.

Archives of Endocrinology and Metabolism
ISSN 2359-4292
OFFICIAL JOURNAL OF THE BRAZILIAN SOCIETY OF ENDOCRINOLOGY AND METABOLISM

original

Evaluation of breast calcification, calcification characteristics, and BI-RADS categories in patients with primary hyperparathyroidism

Fatma Dilek Dellal Kahramanca[1]
https://orcid.org/0000-0003-0755-4543

Sevgul Faki[2]
https://orcid.org/0000-0003-1856-1263

Ekin Yigit Koroglu[2]
https://orcid.org/0000-0003-3895-5817

Arzu Ozsoy[3]
https://orcid.org/0000-0001-9524-5593

Ahmet Dirikoc[4]
https://orcid.org/0000-0002-1315-8208

Oya Topaloglu[4]
https://orcid.org/0000-0003-2501-935X

Reyhan Ersoy[4]
https://orcid.org/0000-0002-7437-1176

Bekir Cakir[4]
https://orcid.org/0000-0001-7526-8827

[1] University of Health Sciences, Ankara Bilkent City Hospital, Endocrinology Department, Ankara, Turkey
[2] Ankara Bilkent City Hospital, Endocrinology Department, Ankara, Turkey
[3] Ankara Bilkent City Hospital, Radiology Department, Ankara, Turkey
[4] Ankara Yildirim Beyazit University, Endocrinology Department, Ankara, Turkey

ABSTRACT

Objective: To determine the frequency and types of breast calcification, the distribution of breast imaging-reporting and data system (BI-RADS) scores, and the association between calcification and biochemical/clinical findings in patients with primary hyperparathyroidism (PHPT). **Subjects and methods**: We recruited ≥ 40-year-old female patients with PHPT (n = 104) and age-matched healthy women (n = 107) as controls. Mammography was performed on all participants. Calcification, calcification type, and BI-RADS scores were recorded, and patients were divided into two groups based on PHPT duration and presence/absence of calcification. **Results**: BI-RADS score distribution was indifferent between groups. The frequency of calcification and distribution of calcification types showed no difference between groups. Likewise, mammography findings were consistent among PHPT patients regardless of disease duration. There was no cutoff for disease duration that could predict the presence of calcification. Breast calcification was negatively correlated with parathyroid hormone (r = -0.220, p = 0.025) and 24-hour urine calcium levels (r = -0.195, p = 0.048), and positively correlated with age (r = 0.219, p = 0.025) in PHPT patients. Of the six patients who underwent cytological examination, one was found to be malignant (PHPT group). **Conclusion**: Female patients with PHPT do not have an increased incidence of breast calcification or higher BI-RADS scores compared to healthy women, and the calcification rates were unaffected by the duration of the disease. The presence of calcification does not appear to be associated with an increased risk of breast cancer in PHPT patients. Nonetheless, given the frequency of breast cancer and that the only patient with breast cancer was part of the PHPT group, it would be appropriate to screen these patients for breast cancer carefully.

Keywords: Primary hyperparathyroidism; hypercalcemia; breast calcification; BI-RADS; breast cancer

INTRODUCTION

Primary hyperparathyroidism (PHPT) is a disease characterized by the autonomous secretion of parathyroid hormone (PTH) from the parathyroid glands due to adenoma, hyperplasia, or carcinoma, despite normal or elevated serum calcium levels. The clinical manifestations of this disease primarily include nephrolithiasis-nephrocalcinosis, and osteoporosis. Additionally, disrupted calcium metabolism in PHPT (1) can lead to ectopic calcification in several organs, such as the skin (2), gallbladder (3), sclerochoroid (4-7), eyes (8), heart valves (9,10), myocardium (11), abdominal aorta (12), brain (13-15), cerebral gyrus (16), joint (11,17), lungs (18-20), pancreas (21), and stomach (22). The precise mechanism of this type of calcification is not fully understood; however, potential causes include increased levels of the calcium-phosphate product and the local secretion of free

Received on Mar/22/2025
Accepted on Oct/27/2025
DOI: 10.20945/2359-4292-2026-0015

Correspondence to:
Fatma Dilek Dellal Kahramanca
Üniversiteler Mahallesi Bilkent
Cad. No: 1 Çankaya
06800 – Ankara, Turkey
drdellal@yahoo.com

Associated editor:
Marise Lazaretti-Castro
https://orcid.org/0000-0001-9186-2834

This is an open-access article distributed under the terms of the Creative Commons Attribution License

Copyright© ACE&M all rights reserved.

hydrogen ions, which result in an alkaline environment (18,22).

Breast calcification, commonly observed in mammography, can be present in both breast cancer and benign lesions. The morphology and distribution of calcifications are instrumental in evaluating whether breast lesions are benign or suspicious. Although studies (23-26), case series (27), and case reports (28-31) have documented breast calcification in patients with secondary hyperparathyroidism (SHPT), to our knowledge, there is no study examining its prevalence and characteristics in patients with PHPT. The incidence of breast cancer has been reported to be higher in patients with PHPT compared to those without PHPT. Hypothetically, this finding could be attributed to increased calcium deposition in the breasts and more frequent breast examinations in these patients (32). Given the above, we aimed to determine the frequency and characteristics of breast calcification, analyze the distribution of Breast Imaging-Reporting and Data System (BI-RADS) scores, and explore the relationship between calcification and biochemical or clinical features in patients with PHPT.

SUBJECTS AND METHODS

Female patients aged ≥ 40 years old with PHPT and age- and body mass index (BMI)-matched healthy women were recruited. The healthy participants were selected from women referred to the radiology clinic for routine mammographic screening by physicians in family medicine, general surgery, and obstetrics and gynecology. These participants were matched for age, BMI, smoking status, menopausal status, and breast disease history. According to the American Cancer Society's 2015 guideline update, women aged ≥ 40 years are recommended to undergo mammography (33).

PHPT was diagnosed based on either the presence of hypercalcemia along with elevated or inappropriately normal serum PTH levels, indicating overt PHPT, or normal serum calcium and 25-hydroxyvitamin (OH) D levels with elevated serum PTH and increased 24-hour urinary calcium/fractional excretion of calcium levels, indicating normocalcemic PHPT (9). Exclusion criteria included a PHPT duration of < 6 months, chronic kidney or liver disease, malignancy, pregnancy, lactation, history of breast surgery, history of chest radiotherapy, and use of medications affecting blood calcium levels (e.g., calcium supplements, thiazide diuretics, lithium, vitamin A, teriparatide, bisphosphonates, corticosteroids, rifampin, phenobarbital, phenytoin, calcitonin, chloroquine, plicamycin, etc.). Smoking habits, alcohol consumption, breast disease history, and family history of breast cancer were also recorded. Weight (kilograms) was divided by the square of height (meters) to determine the BMI.

Serum levels of calcium (normal: 8.5–10.4 mg/dL), albumin (normal: 3.2–4.8 g/dL), phosphate (normal: 2.4–5.1 mg/dL), magnesium (normal: 1.3–2.7 mg/dL), intact PTH (normal: 18.4–80.4 ng/L), 25 (OH) D (normal: 30–150 ng/mL), and alkaline phosphatase (normal: 42–98 U/L) were measured in the morning after an 8-hour fast and recorded. The 24-hour urinary calcium and fractional excretion of calcium were similarly documented. Corrected serum calcium was calculated using the formula: Corrected calcium (mg/dL) = [0.8 × (4 - serum albumin (g/dL))] + measured calcium (mg/dL). The highest recorded calcium and PTH levels were noted from the Ankara Bilkent City Hospital database or the national patient health database. Calcium × phosphate product levels and the highest such levels in the databases were also recorded. Hypercalcemia was classified as mild (10.5–11.9 mg/dL), moderate (12–13.9 mg/dL), or severe (≥ 14 mg/dL). PHPT duration was defined as the time between the first diagnosis and the date of mammography. The earliest available high serum calcium value in the hospital or national database was recorded as the time of initial diagnosis.

All participants underwent mammography using the Senographe Pristina Mammography system (GE Healthcare, Fairfield, Buc, France). Mammographic features were analyzed and reported according to the American College of Radiology's BI-RADS by our radiologist (A.O.), who was blinded to the patients' diagnoses. Calcification morphology was classified as benign or suspicious. Benign calcifications included skin, vascular, popcorn-like, large rod-like, round, rim, dystrophic, milk-of-calcium, and suture calcifications. Suspicious calcifications were described as amorphous, coarse heterogeneous, fine pleomorphic, or fine linear/linear branching. Additionally, the

Copyright© AE&M all rights reserved.

distribution of calcifications was classified as benign if diffuse, and as suspicious if linear or segmental (34).

Calcifications were recorded as unilateral or bilateral, indicating presence in one breast or both, respectively. Breast density was classified as A, B, C, or D, reflecting breast composition from almost entirely fatty to extremely dense, according to BI-RADS. Scores ranged from 0 to 6, where 0 required further imaging, 1 was negative, 2 was benign, 3 was probably benign, 4 was suspicious (with subcategories 4A, 4B, and 4C for low, intermediate, and high suspicion of malignancy, respectively), 5 was highly suggestive of malignancy, and 6 was a biopsy-proven malignancy (34). Participants were asked to return for further diagnostic evaluation when findings such as suspicious breast calcifications, asymmetric densities, or a mass were identified. If malignancy was suspected, a biopsy followed by surgery, if necessary, was suggested.

Dual energy X-ray absorptiometry was used to measure bone mineral density (BMD) in the femur, radius, and lumbar spine (L1–L4) with an anterior-posterior projection in both the patient and control groups (Lunar iDXA, GE Healthcare, USA). Postmenopausal subjects with a BMD T score of ≤ -2.5 were classified as having osteoporosis, those with a T score between -2.5 and -1 were classified as having osteopenia, and those with a T score ≥ -1 were categorized as normal. In premenopausal women, a BMD Z score of ≤ -2 indicated a bone density below the expected range for age, and > -2 was within the expected range. Premenopausal subjects with scores below the expected range were included in the osteoporosis group, whereas those within the expected range were considered to have normal BMD. Nephrolithiasis was defined as either a history of the condition or diagnosis by imaging modalities. If any, histopathological findings of parathyroidectomy with/without thyroidectomy as well as breast cytopathology were noted.

Patients and controls were compared with regard to demographic and laboratory data, as well as mammographic results, including calcification presence and types and BI-RADS scores, were compared between patients and controls. PHPT patients were further divided into groups based on disease duration of less than or more than 48 months and analyzed with respect to the same parameters. Additionally, patients with and without breast calcifications were compared.

This study was approved by the institution's ethical committee (Date: January 18, 2021, no: 26379996/21, Chairman: Kara H.), in compliance with the Declaration of Helsinki. Informed consent was obtained from all patients and controls.

SPSS 24 package (IBM Corp., Armonk, NY, USA) was used for the statistical analysis. Descriptive statistics were given as mean ± standard deviation when normally distributed, and median (interquartile range 25%-75%) when not normally distributed. Nominal variables were given as percentage and number of cases. Chi-squared or Fisher exact test was used when categorical variables were compared. Student *t* test was used for parametric variables and Kruskal-Wallis test was used for nonparametric variables. Spearman's or Pearson's tests were used to assess correlation of breast calcification and laboratory or clinical variables. A p value < 0.05 was considered significant.

The sample size was determined for a comparison between two independent groups with PHPT and healthy controls. The calculation assumed a significance level (α) of 0.05, a statistical power ($1-\beta$) of 0.80, and an expected effect size (Cohen's d) of 0.35, defined as the smallest clinically meaningful difference anticipated in the study. Under the assumptions of equal group sizes, approximate normal distribution, and homogeneous variances, the required sample size was 102 participants per group (204 in total). The Student's *t*-test will be used for the primary comparison, while the Mann–Whitney U test will be applied if distributional assumptions are not met. All calculations were performed using G*Power version 3.1.

RESULTS

Overall, 104 patients and 107 controls were included. Demographic and clinical findings, laboratory results, and imaging results are summarized in **Tables 1–3**. Age distribution and BMI were similar between both groups (p = 0.920 and p = 0.391, respectively). The median duration of PHPT was 48 months (min-max: 6–180 months). The frequency of current smoking was comparable between the patient and control groups. Regular alcohol consumption was observed

Copyright© ACEM All rights reserved.

Table 1. Demographic and clinical data in patients with primary hyperparathyroidism and healthy control subjects; comparisons include primary hyperparathyroidism patients within and beyond 48 months, as well as primary hyperparathyroidism patients with and without breast calcification

Variables	PHPT (n = 104)	Control (n = 107)	*p*	PHPT duration within 48 months (n = 54)	PHPT duration more than 48 months (n = 50)	*p*	PHPT patients with calcification (n = 63)	PHPT patients without calcification (n = 41)	*p*
Age (years)	56 (50–62.8)	56 (50–63)	0.920	57.5 (50.75–63.25)	56 (50–62.3)	0.593	58.0 (53.0–63.0)	53 (49–60.5)	0.026
Height (cm)	157.8 ± 6.4	159.2 ± 6.6	0.122	157.0 ± 5.7	158.7 ± 7.1	0.171	157.32 ± 6.048	158.54 ± 6.92	0.363
Weight (kg)	75 (65–85)	74.5 (66.0–82.25)	0.945	75 (65–83.1)	72.2 (65.5–88.1)	0.699	72.1 (64.075–86.875)	76.0 (66.5–83.9)	0.754
BMI (kg/m^2)	29.8 (25.7–34.1)	29.1 (26.2–32.5)	0.391	29.95 (26.88–33.48)	29.4 (25.3–34.7)	0.840	29.15 (25.575–34.875)	30.2 (26.75–32.65)	0.973
PHPT duration (months)	48 (24.3–69.5)						49.78 (26.00–74.00)	48 (17–67)	0.508
Current smoking (n = 206)	29 (27.9)	18 (17.6)	0.08	14 (25.9)	15 (30.0)	0.643	8 (12.7)	7 (17.1)	0.535
Breast disease history (n = 207)	15 (14.4)	11 (10.7)	0.416	10 (18.5)	5 (10.0)	0.217	10 (18.5)	5 (10.0)	0.217
Family breast cancer history (n = 206)	9 (8.7)	13 (12.6)	0.367	5 (9.3)	4 (8.2)	0.844	5 (9.3)	4 (8.2)	0.844
Menopausal status			0.066			0.491			0.113
Premenopause	20 (19.2)	11 (10.3)		9 (16.7)	11 (22.0)		9 (14.3)	11 (26.8)	
Peri- and postmenopause	84 (80.8)	96 (89.7)		45 (83.3)	39 (78.0)		54 (85.7)	30 (73.2)	

PHPT: primary hyperparathyroidism; BMI: body mass index.

Copyright© AE&M all rights reserved.

Table 2. Laboratory results in patients with primary hyperparathyroidism compared to healthy control subjects. Comparison includes primary hyperparathyroidism patients assessed within 48 months and those assessed more than 48 months after diagnosis, as well as primary hyperparathyroidism patients with and without breast calcification

Variables	PHPT (n = 104)	Control (n = 107)	*p*	PHPT duration within 48 months (n = 54)	PHPT duration more than 48 months (n = 50)	*p*	PHPT patients with calcification (n = 63)	PHPT patients without calcification (n = 41)	*p*
Calcium (mg/dL)	11.1 (10.7–11.5)	9.6 (9.4–9.9)	<0.001	11.0 (10.7–11.3)	11.1 (10.8–11.9)	0.260	11.1 (10.7–11.5)	11.1 (10.75–11.4)	0.931
Highest calcium	11.6 (11.3–11.9)	9.9 (9.7–10.2)	<0.001	11.4 (11.1–11.7)	11.9 (11.5–12.3)	< 0.001	11.6 (11.29–11.90)	11.6 (11.24–12.01)	0.907
Calcium higher than 12 mg/dL	10 (9.6%)	0	0.001	0 (0.0%)	10 (20.0%)	0.001	5 (7.9%)	5 (12.2%)	0.472
Albumin (g/dL)	45 (43–47)	49.0 (45.0–45.4)	<0.001	45 (43.8–46.3)	45.0 (43.0–47.0)	0.832	45 (43.0–47.0)	40.04 (44.0–48.0)	0.267
Corrected calcium	10.65 (10.31–10.98)	9.21 (8.96–9.46)	<0.001	10.59 (10.30–10.93)	10.75 (10.32–11.14)	0.145	10.76 (10.32–11.02)	10.56 (10.30–10.97)	0.519
Highest corrected calcium	11.17 (10.87–11.52)	9.49 (9.23–9.79)	<0.001	10.98 (10.80–11.29)	11.42 (11.03–11.81)	<0.001	11.17 (10.88–11.50)	11.09 (10.77–11.65)	0.944
Phosphate (mg/dL)	2.8 ± 0.5	3.8 ± 0.5	<0.001	2.8 ± 0.5	2.7 ± 0.5	0.237	2.8 ± 0.5	2.7 ± 0.5	0.104
Calcium x phosphate (mg^2/dL^2)	29.43 (26.18–33.95)	35.35 (30.99–37.77)	<0.001	29.42 (26.24–33.97)	29.43 (25.43–33.56)	0.694	29.65 (26.71–33.98)	28.30 (24.70–32.90)	0.142
Highest calcium x phosphate (mg^2/dL^2)	30.69 (26.73–34.98)	35.96 (33.21–38.58)	<0.001	30.60 (26.92–34.86)	31.13 (26.56–36.01)	0.920	31.38 (28.65–36.00)	30.41 (25.71–34.69)	0.133
Magnesium (mg/dL)	2.1 (2.0–2.2)	2.0 (1.8–2.1)	<0.001	2.1 (2.0–2.2)	2.0 (2.0–2.2)	0.225	2.0 (1.9–2.2)	2.1 (2.0–2.3)	0.153
Alkaline phosphatase (U/L)	107 (87–131)	77 (67–93)	<0.001	105 (81.8–132)	107 (87.5–123.5)	0.868	107 (888.25–123.50)	107 (82.5–133.5)	0.745
Parathyroid hormone (ng/L)	156 (113.5–224.5)	52 (40–69)	<0.001	148.5 (111.8–208)	156 (120–261.3)	0.313	140.0 (112.0–204.0)	187 (131.5–258.5)	0.026
Highest parathyroid hormone	207.5 (155–285.1)	60 (43–75)	<0.001	193.5 (153.5–263)	225 (154.3–300)	0.416	187.0 (146.0–273.0)	235 (176–300)	0.104
25(OH) vitamin D (ng/mL)	39 (23–55.7)	48 (32–71.7)	0.001	37 (24.5–54.2)	39.5 (20.0–57.5)	735	40.0 (23.0–57.0)	37 (24.0–49.5)	0.630
Fractionated urinary calcium	0.021 (0.017–0.029)			0.0225 (0.0160–0.0290)	0.0200 (0.01775–0.02825)	0.545	0.0210 (0.0160–0.0280)	0.0220 (0.0180–0.02950)	0.196
Urinary calcium (mg/24h)	314.1 (230.0–428.1)			345 (203.7–491.3)	295.5 (233.8–411.5)	0.478	293 (202.72–411.0)	354 (271–470.5)	0.048
Urinary creatinine (mg/24h)	932.5 (737.0–1168.5)			985 (735.8–1177.5)	906 (731.8–1157.5)	0.569	917 (746.0–1151.0)	978 (704.5–1174.0)	0.793
Volume (mL)	2500.0 (1562.5–3475.0)			2600 (2000–3500)	2450 (1500–3425)	0.515	2600 (1500–3500)	2500 (1650–3325)	0.907

PHPT: primary hyperparathyroidism.

Copyright© AE&M all rights reserved.

Table 3. Results of mammography and bone mineral densitometry in patients with primary hyperparathyroidism and healthy control subjects. Comparison includes primary hyperparathyroidism patients within 48 months and beyond 48 months since diagnosis, as well as primary hyperparathyroidism patients with and without breast calcification

Variables	PHPT (n = 104)	Control (n = 107)	*p*	PHPT duration within 48 months (n = 54)	PHPT duration more than 48 months (n = 50)	*p*	PHPT patients with calcification (n = 63)	PHPT patients without calcification (n = 41)	*p*
Breast density			0.625			0.256			0.422
A	8 (7.7)	14 (13.1)		3 (5.6)	5 (10.0)		4 (6.3)	4 (9.8)	
B	41 (39.4)	40 (37.4)		18 (33.3)	23 (46.0)		23 (36.5)	18 (43.9)	
C	44 (42.3)	41 (38.3)		25 (46.3)	19 (38.0)		27 (42.9)	17 (41.5)	
D	11 (10.6)	12 (11.2)		8 (14.8)	3 (6.0)		9 (14.3)	2 (4.9)	
BI-RADS			0.508			0.678			0.267
BI-RADS 0	78 (75.0)	74 (69.2)		39 (72.2)	39 (78.0)		48 (76.2)	30 (73.2)	
BI-RADS 1	5 (4.8)	8 (7.5)		2 (3.7)	3 (6.0)		1 (1.6)	4 (9.8)	
BI-RADS 2	17 (16.3)	23 (21.5)		11 (20.4)	6 (12.0)		11 (17.5)	6 (14.6)	
BI-RADS 3 and 4	4 (3.8)	2 (1.9)		2 (3.7)	2 (4.0)		3 (4.8)	1 (2.4)	
Presence of calcification	63 (60.6)	72 (67.3)	0.310	33 (61.1%)	30 (60.0)				
Localization of calcifications			0.392			0.599			
Unilateral	10 (15.9)	16 (21.6)		6 (18.2)	4 (13.3)				
Bilateral	53 (84.1)	58 (78.4)		27 (81.8)	26 (86.7)				
Nephrolithiasis	29 (27.9)	3 (2.8)	<0.001	9 (16.7)	20 (40.0)	0.908	20 (31.7)	9 (22.0)	0.276
Bone mineral density (n = 193)			<0.001			0.599			0.280
Normal	11 (10.7)	27 (30.0)	0.001	8 (14.8)	3 (6.1)		5 (7.9)	6 (15.0)	
Osteopenia	47 (45.6)	51 (56.7)	0.126	24 (44.4)	23 (46.9)		27 (42.9)	20 (50.0)	
Osteoporosis	45 (43.7)	12 (13.3)	<0.001	22 (40.7)	23 (46.9)	0.908	20 (31.7)	9 (22.0)	0.276

PHPT: Primary hyperparathyroidism, BI-RADS: Breast imaging-reporting and data system

Copyright© AE&M all rights reserved.

in 3 patients and 1 control. The rates of previous benign breast disease and family breast cancer history were similar in both groups ($p = 0.416$ and $p = 0.367$, respectively). Menopausal status was also comparable ($p = 0.066$).

Serum levels of calcium, corrected calcium, highest calcium, magnesium, alkaline phosphatase, and PTH were higher, while phosphate, albumin, calcium x phosphate, and highest calcium x phosphate levels were lower in the PHPT group than the control group ($p < 0.001$ for all). Similarly, the 25 (OH) vitamin D level was lower in the patient group ($p = 0.001$). The majority of PHPT patients (63.5%) had mild hypercalcemia, 9.6% had moderate hypercalcemia, and the remaining 26.9% had normocalcemic PHPT. The rates of nephrolithiasis and osteoporosis were higher in the PHPT group than in the control group ($p < 0.001$ for both).

The BI-RADS score did not differ, with BI-RADS 0 being the most prevalent score in both groups. Calcifications were observed in 63 (60.6%) patients with PHPT and 72 (67.3%) individuals in the control group. In the PHPT group, 1 patient had suspicious calcifications, 1 patient had both benign and suspicious calcifications (**Figure 1**), and the rest had benign calcifications on mammography. All breast calcifications were benign in the control group. Calcifications were mostly bilateral in both groups ($p = 0.392$).

Parathyroidectomy was performed on 63 patients (60.6%). Except for one patient with atypical parathyroid adenoma, all patients had histopathologically confirmed parathyroid adenoma. Concomitant thyroidectomy was performed on 19 (18.3%) patients, revealing papillary thyroid carcinoma in 12 patients, noninvasive follicular thyroid neoplasm with papillary-like nuclear features (NIFT-P) in 1 patient, concurrent papillary thyroid carcinoma and NIFT-P in 2 patients, and benign findings in 4 patients.

PHPT patients were categorized based on the presence (n = 63, 60.6%) or absence (n = 41, 39.4%) of breast calcification. PTH and urinary calcium levels were lower, and age was higher in PHPT patients with breast calcification than those without calcification ($p = 0.026$, $p = 0.048$, and $p = 0.026$, respectively). Other clinical and laboratory variables were similar in both groups. A weak correlation was found between breast calcification and age ($r = 0.219$, $p = 0.025$), PTH ($r = -0.220$, $p = 0.025$), and 24-hour urinary calcium levels ($r = -0.195$, $p = 0.048$) in PHPT patients. There was no cut-off for disease duration that could predict the presence of calcification. The area under the ROC curve was 0.534 (95% CI: 0.456–0.612, $p = 0.400$), indicating no significance.

PHPT patients were divided based on a disease duration of less than or greater than 48 months, the median duration. Both groups were similar regarding the frequency and localization of calcification, BI-RADS score, breast density, history of benign breast disease, and family breast cancer history ($p > 0.05$ for all). Similarly, age, BMI, current smoking status, menopausal status, and BMD,=, along with laboratory parameters except for the highest calcium level, were comparable between the two groups ($p > 0.05$ for all). The highest calcium level and nephrolithiasis frequency were more prominent in the longer duration group than the shorter duration one ($p < 0.001$ and $p = 0.008$, respectively). All patients with calcium levels of > 12 mg/dL were in the longer duration group. One patient with suspicious calcification was in the shorter duration group, and one with both suspicious and benign calcification was in the longer duration group; others had benign calcifications.

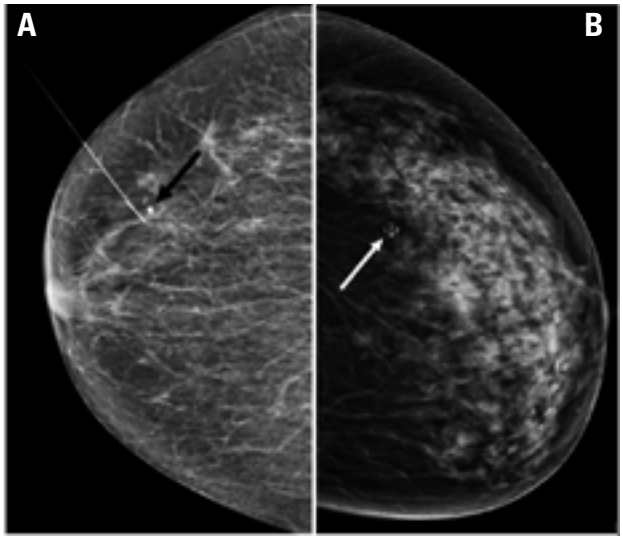


Figure 1. Mammographic findings in two patients with primary hyperparathyroidism showing suspicious breast calcifications. (**A**) Punctate calcifications are clustered in the upper outer quadrant of the right breast, identified as suspicious (at the tip of the localization wire's hook). The punctate calcification indicated by the black arrow is benign. (**B**) Pleomorphic microcalcifications formed in clusters in the central section of the outer quadrant of the left breast are indicated as suspicious (white arrow).

Copyright© AE&M all rights reserved.

Biopsy referral rates were 1.9% (2/104) in PHPT patients and 3.7% (4/107) in the control group. Two PHPT patients with suspicious calcifications underwent excisional breast biopsy, resulting in one invasive breast cancer and one atypical ductal hyperplasia diagnosis. Three controls underwent tru-cut biopsy, and one underwent excisional biopsy, with all 4 controls having benign cytology.

DISCUSSION

The rate and type of breast calcification, as well as the distribution of BI-RADS scores, were similar in female patients with and without PHPT. Patients with disease durations both shorter and longer than 48 months also exhibited similar mammographic findings. These results may suggest that the presence of calcification is not associated with an increased incidence of breast cancer in PHPT patients. In the patient group, breast calcification was positively correlated with age and negatively correlated with PTH and 24-hour urine calcium levels.

Several studies have explored the relationship between PHPT and breast cancer. Both conditions exhibit similar sex and age associations (35) and have shown a steadily increased incidence over the past 40 years (32). Breast cancer is the most frequent cancer in women and is more common in women than in men, similarly to PHPT (36,37). The frequency of the association between breast cancer and PHPT was found to be similar to that of the general population in one study (38). Conversely, in a large-scale cohort study comparing the incidence of subsequent malignancy in patients who underwent surgery for PHPT with those who did not, PHPT was associated with an increased risk of developing cancer (e.g., kidney, colon, and squamous cell skin cancer), particularly breast cancer. This risk remains consistent over time and does not diminish even 15 years post-operation. Therefore, the increased risk of malignancy is not due to the biochemical changes in PHPT, but likely results from shared genetic and environmental etiological factors (39). These common factors are considered to be ionizing radiation and hypercalcemia. Another reported risk factor associated with a higher incidence of both diseases is being overweight (40).

Although there is no literature examining hypercalcemia-specific breast tissue, it is hypothesized that calcium accumulation in the breast may be more pronounced in PHPT, leading to an increased diagnosis of breast cancer due to more frequent breast-focused examinations (32). To determine whether calcium accumulation in breast tissue increases in PHPT, we designed this study. We observed similar frequencies and morphologies of breast calcification, as well as BI-RADS scores in PHPT patients and controls. Therefore, we conclude that the higher prevalence of breast cancer among PHPT patients, as suggested in the literature, may not be attributed to calcification presence. On the other hand, we identified one malignant and one atypical ductal hyperplasia case, both in the PHPT group, while all four cases in the control group were benign. Although there is no statistically significant difference between patient and control groups, we believe that PHPT patients should be carefully examined for breast cancer as both malignant and atypical cytological findings were present in this group.

Examining the inverse relationship, the frequency of PHPT in breast cancer patients was higher than its incidence in the healthy female population (35,41). In non-aggressive breast cancer patients without evidence of PHPT, significantly higher calcium and PTH levels were noted, regardless of clinical stage and antitumor treatment, compared to the healthy controls (41). The prognosis of breast cancer patients, irrespective of previous PHPT operations, was found to be similar (40).

Although no study exists in the literature examining breast tissue calcification in PHPT patients, there are three studies concerning patients with SHPT due to chronic kidney disease or end-stage renal disease (23-25). An increase of up to 94% in breast calcification rates has been noted in patients with SHPT associated with chronic renal failure, specifically among those on long-term hemodialysis (25). The increased calcification in SHPT compared to the general population is thought to relate to decreased phosphate excretion and rising levels of serum calcium-phosphate product, though it likely results from multiple factors, including the duration of renal failure, dialysate calcium concentration, tissue pH, calcium, magnesium and fluoride levels, metabolic acidosis, hyperoxalemia, hyperlipidemia,

Copyright© AE&M all rights reserved.

and corticosteroid treatment. Calcifications occurred in both breasts in 98% of SHPT patients (23).

Correlation between calcification and either serum PTH levels or the calcium-phosphate product SHPT has been inconsistent across studies. Breast calcifications associated with SHPT are benign, not linked with breast masses, and should not be confused with suspicious calcifications indicative of breast cancer, according to earlier studies (23,25). These studies, however, did not include data on BI-RADS, callback rates for additional diagnostic workups, biopsy recommendation rates, clinical outcomes related to increasing calcifications, or the incidence of suspicious calcifications. A more recent study by Castellanos and cols. (24) found that while increased breast calcification is generally benign, the incidence of malignancy-associated calcifications is slightly higher in SHPT patients compared to a control group. Consequently, these patients have a higher likelihood of being referred for a biopsy if recalled for further diagnostic evaluation (24). None of the three studies reported breast cytology results, leaving a gap in the literature on whether women with SHPT have a higher incidence of breast cancer.

Contrary to these findings in SHPT patients, our study did not detect an increased rate of breast calcification in PHPT patients. Similar to findings in SHPT studies, most calcifications in PHPT were benign and bilateral. Only two participants, both with PHPT, had suspicious calcifications. One potential explanation for the differing calcification rates between PHPT and SHPT could be the comparatively lower phosphate and calcium-phosphate product levels in PHPT patients, as opposed to SHPT patients. Despite a reduction in phosphate levels, the calcium-phosphate product may still be high in PHPT due to elevated calcium levels from increased bone resorption, particularly in severe hypercalcemia. The role of the calcium-phosphate product in PHPT remains unclear, despite its widespread application in chronic renal disease management. Few studies have explored its level in PHPT patients, with some linking it to renal dysfunction but not to aortic valve calcification (9,42). Lower product level may be related to the reduced phosphate levels and the modestly elevated or even normal calcium levels observed in most of our patients. Another possibility regarding the differences in PHPT and SHPT calcification rates is that the microenvironment of breast tissue in PHPT patients differs from systemic levels in a manner that promotes calcification.

In our study, we found a negative correlation between calcification in PHPT patients and PTH levels, in contrast to the study of Sommer and cols. (23) involving patients with renal hyperparathyroidism, which showed a positive correlation. We additionally observed positive correlations of breast calcification with age and a negative correlation with urinary calcium levels. The frequency of breast calcification is known to increase with age, and microcalcification is more common in older patients (43). However, our evaluation of PHPT patients concerning breast calcification and its related factors is the first in the literature. Further research is needed to elucidate whether renal dysfunction, more severe hypercalcemia/hypophosphatemia, higher PTH levels, or other factors might affect calcification rates in PHPT patients.

Several studies have compared laboratory and demographic characteristics in PHPT patients with and without calcifications in various tissues or organs. The severity of abdominal aortic calcification in PHPT and breast calcification frequencies in SHPT correlate with PTH levels (12,23). Patients with mild PHPT have shown increased calcification area in the aortic valve, positively and independently associated with PTH levels (9). Pepe and cols. (12) reported that older age, years since menopause, and time since diagnosis as distinguishing factors between PHPT patients with and without abdominal aortic calcification. In another study, age was the sole predictor of gallstone development in PHPT patients (3). Normocalcemic PHPT patients with renal calcifications had increased serum PTH, $1.25(OH)_2$ vitamin D, and urinary calcium compared to those without calcifications (44). Contrary to this study, Perez and cols. (45) reported that PHPT patients with nephrolithiasis had similar serum calcium and PTH levels compared to patients without nephrolithiasis, although urinary calcium levels were increased. Ejlsmark-Svensson (46) found that renal calcification correlated with the severity of PHPT as measured by PTH levels, 24-hour urine calcium, and the degree of hypercalcemia (46).

Copyright© AE&M all rights reserved.

It is suggested that increased serum calcium levels due to the oversecretion of PTH may lead to calcium deposits in breast ducts (47). In our study, we did not find an increased rate of calcification in PHPT patients compared to the control group. Nevertheless, PHPT patients with breast calcification had lower PTH and urinary calcium levels but were older compared to those without calcification. Additionally, as noted earlier, calcification in PHPT patients correlated positively with age and negatively with PTH levels and 24-hour urinary calcium levels. Differences in the physiological characteristics of various tissues, the variable effects of PTH on these organs or tissues, the selection of different patient groups (e.g., normocalcemic PHPT, mild PHPT, asymptomatic PHPT), and diagnostic criteria (e.g., imaging methods, serum calcium range) may explain the diversity of results in the literature (35).

The duration of PHPT can affect the course of some clinical and laboratory parameters. PHPT patients managed nonoperatively showed an increased annual rate of renal stone events in the year before and after diagnosis, with the rate decreasing after five years (48). Some studies have shown that a proportion of patients with normocalcemic PHPT progressed to hypercalcemia over time, while other studies did not find this progression (49). In our study, nephrolithiasis was more frequent, and the highest calcium levels were more prominent in the group with longer disease duration compared to the group with shorter duration.

Despite our promising findings, this study has some limitations. Due to the increasing access to laboratory and imaging modalities, patients are diagnosed at earlier stages in recent years. Consequently, most of the patients in the study had mild hypercalcemia. This may have contributed to possibly lower rates of calcium-phosphate product levels and, therefore, a lower rate of breast calcification. Additionally, the cross-sectional design might have resulted in a low number of breast cancer patients. Given the often asymptomatic or subclinical nature of PHPT, underestimation of the disease duration is possible in the current study. Consequently, the disease duration may be inaccurately short in some cases, possibly because the disease started earlier than the first record available in the hospital database. This may affect some analyses performed based on disease duration, particularly its effect on the frequency of breast calcification. The lack of data on ionized calcium measurements, calcification subtypes, and the physical examination findings of the breast were other limitations of the study.

In conclusion, it can be inferred from this study that breast calcification may not be considered a target organ involvement, and the presence of calcification is not related to an increased incidence of breast cancer in PHPT patients. Although not statistically significant, the fact that all patients with non-benign cytology results were in the PHPT group may suggest that PHPT patients should be carefully screened for breast cancer. Nonetheless, these results should be confirmed in patients with different levels of hypercalcemia, in different age groups, and among patients with longer follow-up periods and a larger cohort.

Acknowledgments: none.

Disclosure: no potential conflict of interest relevant to this article was reported.

Data availability: datasets related to this article will be available upon request to the corresponding author.

REFERENCES

1. Walker MD, Silverberg SJ. Primary hyperparathyroidism. Nat Rev Endocrinol. 2018;14(2):115-125. doi: 10.1038/nrendo.2017.104.
2. Sepriano AR, Pereira Pombo de Araújo FC, Mourão de Almeida Lourenço Dias PM, da Cunha Branco, J. Normocalcemic primary hyperparathyroidism presenting as calcinosis cutis. J Clin Rheumatol. 2014;20(6):330-331. doi: 10.1097/RHU.0000000000000142.
3. Bhadada SK, Bhansali A, Shah VN, Behera A, Ravikiran M, Santosh R. High prevalence of cholelithiasis in primary hyperparathyroidism: a retrospective analysis of 120 cases. Indian J. Gastroenterol. 2011;30(2):100-101. doi: 10.1007/s12664-011-0101-0.
4. Atas F, Saatci A. Bilateral sclerochoroidal calcification in a case with asymptomatic primary hyperparathyroidism. Europ Eye Res. 2022;2(2),84-87. doi: 10.14744/eer.2022.35744.
5. Suzuki J, Takeda M, Sekine N, Kanno M, Kii T, Kofune M, et al. Bilateral metastatic sclerochoroidal calcification in a patient with hyperparathyroidism. Ophthalmologica. 1992;205(1):10-14. doi: 10.1159/000310304.
6. Sood S, Friedman S. Sclerochoroidal calcification with optic nerve calcification in a patient with primary hyperparathyroidism and severe vision loss. Retin Cases Brief Rep. 2024;18(4):499-502. doi: 10.1097/ICB.0000000000001418.
7. Abouzaid M, Al-Sharefi A, Artham S, Masri I, Kotagiri A, Joshi A. A rare ophthalmic condition associated with primary hyperparathyroidism (PHPT): sclerochoroidal calcification (SC). Endocrinol Diab Metab Case Rep. 2019;2019(1):19-0003. doi: 10.1530/EDM-19-0003.
8. Lee DK, Eiferman RA. Ocular calcifications in primary hyperparathyroidism. Arch Ophthalmol. 2006;124(1):136-137. doi: 10.1001/archopht.124.1.136.

Copyright© AE&M all rights reserved.

9. Iwata S, Walker MD, Di Tullio MR, Hyodo E, Jin Z, Liu R, et al. Aortic valve calcification in mild primary hyperparathyroidism. J Clin Endocrinol Metab. 2012;97(1):132-137. doi: 10.1210/jc.2011-2107.
10. Carrai P, Camarri S, Pondrelli CR, Gonnelli S, Caffarelli C. Calcification of cardiac valves in metabolic bone disease: an updated review of clinical studies. Clin Interv Aging. 2020;15:1085-1095. doi: 10.2147/CIA.S244063.
11. Takahashi H, Aoki T, Fukumoto Y, Sugimura K, Nochioka K, Miura Y, et al. "Porcelain heart" a case of acute heart failure with massive myocardial calcification complicated with primary hyperparathyroidism. J Cardiol Cases. 2013;8(6):183-186. doi: 10.1016/j.jccase.2013.08.006.
12. Pepe J, Diacinti D, Fratini E, Nofroni I, D'Angelo A, Pilotto R, et al. High prevalence of abdominal aortic calcification in patients with primary hyperparathyroidism as evaluated by Kauppila score. Eur J Endocrinol. 2016;175(2):95-100. doi: 10.1530/EJE-15-1152.
13. Panchangam RB, Mahalaxmi V, Mayilvaganan S. Rare association of basal ganglia calcification and primary hyperparathyroidism: an interesting case report with review of literature. World J Surg Surgical Res. 2021;4:1276. doi: 10.25107/2637-4625.1276.
14. Xu H, Qin H, Zhong S, He Q, Chen S, Guan M. Hyperparathyroidism and cerebral calcifications: A case report. Neurocase. 2022;8(2):226-230. doi: 10.1080/13554794.2022.2071627.
15. Hyusein RR, Atsev S, Boyukliev A, Petrov PP, Velchev V, Penchev P. Cerebral calcifications as a result of primary hyperparathyroidism: A Report of a Rare Case. Cureus. 2024;16(4):e57826. doi: 10.7759/cureus.57826.
16. Landais A, Mallet G, Bourgeois-Beauvais Q, Parisi J, Mecharles S, Lannuzel A. Gyriform calcifications after ischemic stroke in a patient with primary hyperparathyroidism. Presse Med. 2018;47(7-8 Pt 1):690-692. doi: 10.1016/j.lpm.2018.04.005.
17. Sturdee SW, Bollen SR. Intra-articular calcification in primary hyperparathyroidism. Knee. 2004;11(4):323-325. doi: 10.1016/j.knee.2003.09.002.
18. Sun HM, Chen F, Yin HL, Xu XY, Liu HB, Zhao BL. Rapid development of metastatic pulmonary calcifications in primary hyperparathyroidism: a case report and literature review. Diagn Pathol. 2017;12(1):38. doi: 10.1186/s13000-017-0628-1.
19. Jia Y, Wang L, Yang G, Mao G, Cheng Y, Cao Y. Primary hyperparathyroidism characterized by diffuse homogeneous metastatic pulmonary calcification: A case report. Medicine (Baltimore). 2018;97(44):e13107. doi: 10.1097/MD.0000000000013107.
20. Xu W, Hu T, Lv S, Dong M, Yang J. Metastatic microcalcification in the lungs and stomach due to hyperparathyroidism: A case report. J Int Med Res. 2021;49(2):300060521994420. doi: 10.1177/0300060521994420.
21. Pradhan R, Gupta SK, Neyaz Z, Agarwal A. Pancreatic calcification in primary hyperparathyroidism. World J Endoc Surg. 2013;5(3):89. doi: 10.5005/jp-journals-10002-1137.
22. Khurram R, Khamar R, Mandumula S. Computed tomography findings of diffuse intracranial calcifications in a patient with primary hypoparathyroidism. J Radiol Clin Imag. 2020;3(1):033-037. doi: 10.26502/jrci.2809021.
23. Sommer G, Kopsa H, Zazgornik J, Salomonowitz E. Breast calcifications in renal hyperparathyroidism. AJR Am J Roentgenol. 1987;148(5):855-857. doi: 10.2214/ajr.148.5.855.
24. Castellanos M, Varma S, Ahern K, Grosso SJ, Buchbinder S, D'Angelo D, et al. Increased breast calcifications in women with ESRD on dialysis: implications for breast cancer screening. Am J Kidney Dis. 2006;48(2):301-306. doi: 10.1053/j.ajkd.2006.05.001.
25. Evans AJ, Cohen ME, Cohen GF. Patterns of breast calcification in patients on renal dialysis. Clin Radiol. 1992;45(5):343-344. doi: 10.1016/s0009-9260(05)80090-x.
26. Van Berkel B, Van Ongeval C, Van Craenenbroeck AH, Pottel H, De Vusser K, Evenepoel P. Prevalence, progression and implications of breast artery calcification in patients with chronic kidney disease. Clin Kidney J. 2021;15(2):295-302. doi: 10.1093/ckj/sfab178.
27. Sivakumar V, Rani ChS, Lakshmi AY, Lakshmi BV. Breast calcifications in women with end-stage renal disease on maintenance hemodialysis. Saudi J Kidney Dis Transpl. 2011;22(1):142-145. PMID: 21196633.
28. McDougal BA, Lukert BP. Resolution of breast pain and calcification with renal transplantation. Arch Intern Med. 1977:137(3):375-377. PMID: 320952.
29. Lee KM, Lee JE, Cha ES, Chung J, Kim JH, Moon BI. Dystrophic calcifications in the breast from secondary hyperparathyroidism. Breast Care (Basel). 2018;13(1):44-46. doi: 10.1159/000484198.
30. Cowlam TE, Bucknall TE. Cutaneous ectopic breast calcification in a haemodialysis patient. Breast. 2003;12(5):342-344. doi: 10.1016/s0960-9776(03)00104-8.
31. Resnikoff LB, Mendelson EB, Tobin CE. Hendrix TM. Breast imaging case of the day. Metastatic calcification in the breast from secondary hyperparathyroidism induced by chronic renal failure. Radiographics. 1996;16(6):1512-1513. doi: 10.1148/radiographics.16.6.8946553.
32. Michels KB, Xue F, Brandt L, Ekbom A. Hyperparathyroidism and subsequent incidence of breast cancer. Int J Cancer. 2004;110(3):449-451. doi: 10.1002/ijc.20155.
33. Oeffinger KC, Fontham ET, Etzioni R, Herzig A, Michaelson JS, Shih YC, et al. American Cancer Society: Breast cancer screening for women at average risk: 2015 guideline update From the American Cancer Society. JAMA. 2015;314(15):1599-1614. doi: 10.1001/jama.2015.12783. Erratum in: JAMA. 2016 Apr 5;315(13):1406. doi: 10.1001/jama.2016.3404.
34. D'Orsi CJ, Sickles EA, Mendelson EB, Morris EA, et al. ACR BI-RADS® Atlas: Breast Imaging Reporting and Data System. Reston (VA): American College of Radiology; 2013.
35. Tanaka Y. Primary hyperparathyroidism with breast carcinoma. Breast Cancer. 2010;17(4):265-268. doi: 10.1007/s12282-009-0158-0.
36. Minisola S, Pepe J, Piemonte S, Cipriani C. The diagnosis and management of hypercalcaemia. BMJ. 2015;350:h2723. doi: 10.1136/bmj.h2723.
37. Valentini V, Bucalo A, Conti G, Celli L, Porzio V, Capalbo C, et al. Gender-Specific Genetic Predisposition to Breast Cancer: BRCA Genes and Beyond. Cancers (Basel). 2024;16(3):579. doi: 10.3390/cancers16030579.
38. Axelrod DM, Bockman RS, Wong GY, Osborne MP, Kinne DW, Brennan MF. Distinguishing features of primary hyperparathyroidism in patients with breast cancer. Cancer. 1987;60:1624-1630. doi: 10.1002/1097-0142(19871001)60:7<1620::aid-cncr2820600733>3.0.co;2-3.
39. Nilsson IL, Zedenius J, Yin L, Ekbom A. The association between primary hyperparathyroidism and malignancy: nationwide cohort analysis on cancer incidence after parathyroidectomy. Endocr Relat Cancer. 2007;14(1):135-140. doi: 10.1677/erc.1.01261.
40. Norenstedt S, Granath F, Ekbom A, Bergh J, Lambe M, Adolfsson J, et al. Breast cancer associated with primary hyperparathyroidism: a nested case control study. Clin Epidemiol. 2011;3:103-106. doi: 10.2147/CLEP.S17298.
41. Fierabracci P, Pinchera A, Miccoli P, Conte PF, Vignali E, Zaccagnini M, et al. Increased prevalence of primary hyperparathyroidism in treated breast cancer. J Endocrinol Invest. 2001;24(5):315-320. doi: 10.1007/BF03343867.
42. Banerjee M, Kar A, Ahamed J, Bhattacharjee R, Maitra D, Maisnam I, et al. Renal Dysfunction in Primary Hyperparathyroidism is associated with nephrolithiasis, elevated serum calcium-phosphate product and parathormone levels. Endocrine. 2024;83(3):757-762. doi: 10.1007/s12020-023-03631-0.
43. Azam S, Eriksson M, Sjölander A, Gabrielson M, Hellgren R, Czene K, et al. Mammographic microcalcifications and risk of breast cancer. Br J Cancer. 2021;125(5):759-765. doi: 10.1038/s41416-021-01459-x.

Copyright© AE&M all rights reserved.

44. Victor F, Pereira Lemos AL, de Holanda Ribas AM, Bandeira L, Pimentel JH, de Andrade Damázio LO, et al. Occult renal calcifications in patients with normocalcemic primary hyperparathyroidism and their association with the parathyroid hormone-vitamin D axis. Int J Endocrinol. 2022;2022:4558236. doi: 10.1155/2022/4558236.
45. Perez AA, Schneider DF, Long KL, Pitt SC, Sippel RS. Timely evaluation and management of primary hyperparathyroidism in patients with kidney stones. J Surg Res. 2018;232:564-569. doi: 10.1016/j.jss.2018.07.028.
46. Ejlsmark-Svensson H, Bislev LS, Rolighed L, Sikjaer T Rejnmark L. Predictors of renal function and calcifications in primary hyperparathyroidism: A nested case-control study. J Clin Endocrinol Metab. 2018;103(9):3574-3583. doi: 10.1210/jc.2018-00923.
47. Matsunaga T, Nakamura Y, Umezu K, Fujii M, Kusama M, Koyanagi Y. Computerized image analysis of clustered microcalcifications on mammography: morphometric comparison between mammography and pathology. Breast Cancer. 1996;3:181-190. doi: 10.1007/BF02966982.
48. Seib CD, Ganesan C, Arnow KD, Pao AC, Leppert JT, Barreto NB, et al. Kidney stone events following parathyroidectomy vs nonoperative management for primary hyperparathyroidism. J Clin Endocrinol Metab. 2022;107(7):e2801-e2811. doi: 10.1210/clinem/dgac193.
49. Bilezikian JP, Khan AA, Silverberg SJ, Fuleihan GE, Marcocci C, Minisola S, et al. International Workshop on Primary Hyperparathyroidism.: Evaluation and management of primary hyperparathyroidism: Summary statement and guidelines from the Fifth International Workshop. J Bone Miner Res. 2022;37(11):2293-2314. doi: 10.1002/jbmr.4677.

Copyright© AE&M all rights reserved.

Archives of Endocrinology and Metabolism
ISSN 2359-4292
OFFICIAL JOURNAL OF THE BRAZILIAN SOCIETY OF ENDOCRINOLOGY AND METABOLISM

original

Evaluation of three inflammation-associated blood indices for predicting malignancy in thyroid nodules

Merve Çatak[1]
https://orcid.org/0000-0003-2654-3911

Bülent Koca[2]
https://orcid.org/0000-0001-7614-122X

Zeynep Çetin[3]
https://orcid.org/0000-0001-7824-4644

Özden Özdemir BAŞER[4]
https://orcid.org/0000-0001-8368-3182

[1] Tokat Gaziosmanpasa University, Faculty of Medicine, Department of Endocrinology and Metabolism, Tokat, Türkiye
[2] Tokat Gaziosmanpasa University, Faculty of Medicine, Department of General Surgery, Tokat, Türkiye
[3] Amasya Sabuncuoğlu Şerefeddin Training and Research Hospital, Amasya Şerefettin Sabuncuoğlu, Faculty of Medicine, Department of Endocrinology and Metabolism, Amasya, Türkiye
[4] Dokuz Eylul University, Faculty of Medicine, Department of Endocrinology and Metabolism, Izmir, Türkiye

ABSTRACT

Objective: Differentiated thyroid carcinoma (DTC) is the most common endocrine malignancy and usually has a favorable prognosis. However, both diagnostic and prognostic evaluations currently rely mainly on postoperative histopathological results. Systemic inflammation-based indices — such as the Systemic Immune-Inflammation Index (SII), Systemic Inflammation Response Index (SIRI), and Pan-Immune Inflammation Value (PIV) — have recently emerged as potential biomarkers in various cancers. This study aimed to evaluate the diagnostic and prognostic utility of these indices in patients undergoing thyroid surgery. **Subjects and methods:** This retrospective study included 554 patients who underwent total thyroidectomy between 2014 and 2021. Tumors were categorized as benign or malignant according to final histopathology. SII, SIRI, and PIV were calculated from preoperative complete blood counts. Multivariate logistic regression was performed and included age, sex, thyroid-stimulating hormone (TSH) level, glycated hemoglobin (HbA1c) level, and diabetes status. Receiver operating characteristic (ROC) analysis was used to determine diagnostic performance. **Results:** Among 554 patients, 366 had benign and 188 had malignant tumors. Among the systemic inflammatory markers, only the SII differed significantly between groups (p = 0.002) and remained an independent predictor of malignancy in multivariate analysis (OR = 0.85 per 100-unit increase, p = 0.007). ROC analysis revealed an AUC of 0.597, with 65.8% sensitivity and 58.2% specificity. None of the indices demonstrated prognostic value in the subgroup analyses. **Conclusion:** The SII demonstrated independent but clinically limited diagnostic value in differentiating malignant from benign thyroid lesions. Although its accuracy was poor (AUC <0.6), the SII may serve as a low-cost adjunct within multivariable preoperative models, particularly in indeterminate cytology cases.

Keywords: Differentiated thyroid carcinoma; systemic immune-inflammation index; systemic inflammation response index; pan-immune inflammation value; inflammation-based biomarkers; preoperative diagnosis; thyroid nodules

INTRODUCTION

Thyroid cancer is the most common endocrine malignancy worldwide, and its incidence has been steadily increasing in recent decades (1). The majority of cases are classified as differentiated thyroid carcinoma (DTC), which includes papillary thyroid carcinoma (PTC) and follicular thyroid carcinoma (FTC), both of which are generally associated with a favorable prognosis (2). While fine-needle aspiration biopsy (FNAB) is the gold standard for the preoperative evaluation of thyroid nodules, prognostic classification typically relies on postoperative histopathological features (3,4). However, both diagnostic and prognostic assessments in clinical practice currently depend heavily on invasive or postoperative procedures. There is a pressing need for accessible, noninvasive biomarkers that can assist in differentiating benign from malignant disease and support early risk prediction.

Received on July/20/2025
Accepted on Dec/11/2025
DOI: 10.20945/2359-4292-2026-0014

Correspondence to:
Merve Çatak
Tokat Gazıosmanpasa University,
Faculty of Medicine,
Department of Endocrinology and Metabolism
Gaziosmanpaşa Üniversite Hastanesi,
Kaleardi, 60030, Merkez Tokat, Turkey
merve.catak@gop.edu.tr

Associated editor:
Rosália do Prado Padovani
https://orcid.org/0000-0002-5497-6813

This is an open-access article distributed under the terms of the Creative Commons Attribution License

Copyright© AE&M all rights reserved.

Inflammation is recognized as a key player in tumor initiation, progression, and metastasis (5). In the context of cancer, tumor-associated inflammation involves not only local immune cell infiltration but also systemic immune responses that can be captured via hematologic indices derived from routine blood tests (5,6). Among these, the Systemic Immune-Inflammation Index (SII) — calculated using neutrophil, lymphocyte, and platelet counts — has demonstrated diagnostic utility and prognostic relevance in several malignancies, including hepatocellular carcinoma and gastrointestinal cancers (7,8). Similarly, the Systemic Inflammation Response Index (SIRI), which incorporates the levels of neutrophils, monocytes, and lymphocytes, has emerged as an alternative composite marker reflecting systemic immune balance (9).

More recently, the Pan-Immune Inflammation Value (PIV) has been introduced as a comprehensive biomarker that integrates four key circulating immune components: neutrophils, lymphocytes, platelets, and monocytes (10). Unlike traditional markers such as the neutrophil-to-lymphocyte ratio (NLR), these multiparameter indices aim to provide a broader and more robust representation of the host's inflammatory and immune status (10). These indices represent simple, reproducible, and cost-effective markers that can be readily derived from routine blood tests, which enhances their potential clinical applicability. In addition to being associated with cancer, the SII, SIRI, and PIV have been shown to be associated with disease activity in autoimmune, cardiovascular, and other chronic inflammatory conditions, highlighting their potential clinical versatility (11-13).

Although systemic inflammation indices have been investigated in patients with thyroid malignancies, most studies have focused primarily on the SII, whereas direct head-to-head comparisons of the SII, SIRI, and PIV in the same cohort remain scarce. Therefore, the incremental value of simultaneously evaluating these three indices under uniform clinical conditions has not been fully established (14).

Given the established link between chronic inflammation and tumorigenesis, metabolic conditions such as diabetes mellitus deserve particular attention. Diabetes mellitus is a chronic low-grade inflammatory condition that can alter systemic immune and metabolic pathways. Recent studies have shown that elevated inflammatory indices are associated with increased mortality in patients with type 2 diabetes, reflecting a sustained proinflammatory state (15). Moreover, diabetes itself has been identified as a potential risk factor for thyroid cancer, possibly through mechanisms involving insulin resistance, hyperinsulinemia, and chronic inflammation (16). Therefore, glucose and HbA1c levels were also assessed in our study to account for the potential metabolic and inflammatory effects of diabetes on systemic inflammation indices.

Although several studies have explored the prognostic utility of these indices in thyroid cancer, their diagnostic value — particularly in distinguishing benign from malignant nodules in the preoperative setting — is unclear. Therefore, this study was designed to assess both the diagnostic utility and potential prognostic significance of the SII, SIRI, and PIV in patients undergoing thyroid surgery.

SUBJECTS AND METHODS

This retrospective study was conducted at Tokat Gaziosmanpasa University Faculty of Medicine and included patients who underwent total thyroidectomy between January 2014 and December 2021. This study was approved by the Tokat Gaziosmanpasa University Clinical Research Ethics Committee (approval number: 21-KAEK-135) and was conducted in accordance with the principles of the Declaration of Helsinki. All patient data were anonymized to ensure confidentiality.

Patient selection

Patients aged 18 years or older with available preoperative laboratory results and postoperative histopathological diagnoses were considered eligible for inclusion. Indications for thyroidectomy included Bethesda IV–VI cytology results, Bethesda III nodules with suspicious ultrasound features or repeated Bethesda III results, nodules larger than 4 cm, nodules causing compressive symptoms, and hyperfunctioning nodules (toxic multinodular goiter or toxic adenoma).

Copyright© AE&M all rights reserved.

The exclusion criteria included a history of autoimmune thyroid diseases (such as Graves' disease and Hashimoto's thyroiditis or histopathological evidence of thyroiditis in the nontumoral thyroid parenchyma), pregnancy, rheumatologic or hematologic disorders, corticosteroid or immunosuppressive therapy, active infection, chronic liver or kidney disease, the presence of nonthyroidal malignancy, and incomplete laboratory data. Additionally, patients who were diagnosed with medullary or anaplastic thyroid carcinoma, noninvasive follicular thyroid neoplasms with papillary-like nuclear features (NIFTPs), tumors of uncertain malignant potential, or toxic nodular disease were excluded.

A flowchart showing the patient selection process is presented in **Figure 1**.

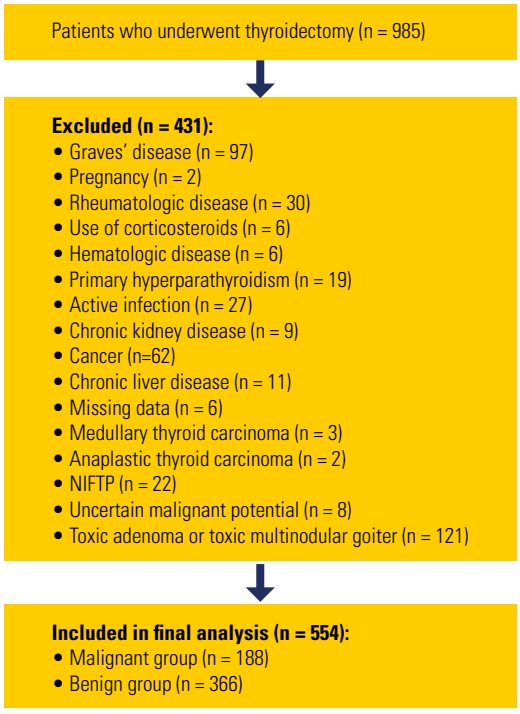


Figure 1. Patient selection flowchart.

Demographic and clinical data

Demographic information, including age and sex, was recorded for all included patients. On the basis of histopathological examination of the thyroidectomy specimens, patients were categorized into two groups: the benign group, consisting of individuals with nonneoplastic thyroid lesions, and the DTC group, consisting of patients diagnosed with papillary or follicular thyroid carcinoma.

Surgical and histopathological evaluation

Total thyroidectomy was performed as the standard surgical approach for all patients. In cases where preoperative cervical ultrasonography revealed pathological lymphadenopathy, either central or lateral neck lymph node dissection was performed according to clinical guidelines. In the DTC group, detailed histopathological features, including tumor size, histological subtype, capsular and vascular invasion, extrathyroidal extension, perineural invasion, and the presence of lymph node or distant metastases, were recorded. Tumor staging was conducted according to the 8th edition of the American Joint Committee on Cancer (AJCC) staging system (17).

Laboratory analysis

All laboratory data were obtained from fasting blood samples collected within one week before surgery. Since all patients were scheduled for elective operations, none had acute illness at the time of sampling. CBC parameters — including neutrophil, lymphocyte, monocyte, and platelet counts — were measured using a Sysmex XN-Series hematology analyzer (Sysmex Corp., Kobe, Japan). Fasting blood glucose levels were measured using the hexokinase enzymatic method, and HbA1c levels were assessed by high-performance liquid chromatography (HPLC). All analyses were performed in institutional biochemistry and hematology laboratories using standardized protocols.

Inflammatory index calculations

The following systemic inflammatory indices were calculated from the preoperative CBC parameters:

- **Systemic Immune-Inflammation Index (SII):** (neutrophil count × platelet count)/lymphocyte count.
- **Systemic Inflammation Response Index (SIRI):** (neutrophil count × monocyte count)/lymphocyte count.
- **Pan-Immune Inflammation Value (PIV):** (neutrophil count × monocyte count × platelet count)/lymphocyte count.

Statistical analyses

All the statistical analyses were performed using IBM SPSS Statistics for Windows, version 25.0 (IBM Corp.,

Copyright© AE&M all rights reserved.

Armonk, NY, USA). Continuous variables are presented as the mean ± standard deviation (SD) for normally distributed data or as the median (minimum–maximum) for nonnormally distributed data, while categorical variables are expressed as frequencies and percentages.

The distribution of continuous variables was assessed using the Kolmogorov–Smirnov and Shapiro–Wilk tests. For comparisons between the benign and DTC groups, the independent samples *t* test was used for normally distributed variables, and the Mann–Whitney U test was used for nonnormally distributed variables. Categorical variables were compared using Pearson's chi-square or Fisher's exact tests, as appropriate.

To evaluate the associations of systemic inflammatory indices (SII, SIRI, and PIV) with thyroid malignancy, univariate logistic regression analyses were initially performed. Variables with a p value < 0.10 in univariate analyses were included in multivariate logistic regression models using a backward stepwise method to identify independent predictors. The results are reported as odds ratios (ORs) with 95% confidence intervals (CIs).

In the DTC group, potential associations between inflammation indices and tumor-related features (such as tumor size, lymph node status, and disease stage) were further assessed using Pearson's or Spearman's correlation tests, depending on the data distribution.

Receiver operating characteristic (ROC) curve analysis was performed to evaluate the diagnostic performance of the systemic inflammation-based indices. The area under the curve (AUC), sensitivity, specificity, and optimal cutoff values (determined by the Youden index) are reported for indices that demonstrated statistically significant group differences.

A p value < 0.05 was considered to indicate statistical significance for all analyses.

RESULTS

A total of 985 patients who underwent thyroidectomy between January 2014 and December 2021 were initially screened. After the exclusion criteria were applied (as illustrated in **Figure 1**), 431 patients were excluded, resulting in a final cohort of 554 patients. These patients were categorized into two groups on the basis of postoperative histopathological findings: the malignant group (n = 188) and the benign group (n = 366). The mean age of the study population was 47.1 ± 11.9 years, with a female-to-male ratio of approximately 4:1.

Comparisons of demographic and laboratory characteristics between the two groups are presented in **Table 1**. The malignant group had a significantly younger mean age than the benign group did (45.10 ± 12.74 vs. 48.45 ± 11.15 years, p < 0.001). No statistically significant difference was observed in sex distribution (p = 0.204). Although the prevalence of diabetes

Table 1. Comparison of demographic and laboratory features between benign and malignant groups

Parameter	Benign group (n = 366)	Malignant group (n = 188)	p-value
Age (years)	48.45 ± 11.15	45.10 ± 12.74	**<0.001**
Sex (F/M)	287/79 (78.4/21.6%)	156/32 (83.0/17.0%)	0.204
DM presence (%)	39 (10.7%)	25 (13.3%)	0.151
TSH (mIU/L)	1.55 ± 1.30	1.98 ± 2.07	**0.009**
Free T4 (ng/dL)	1.22 ± 0.20	1.23 ± 0.22	0.392
Fasting glucose (mg/dL)	112.29 ± 31.40	115.28 ± 39.68	0.108
HbA1c (%)	5.98 ± 1.04	6.15 ± 1.26	0.134
SII	547.08 ± 302.05	654.75 ± 403.30	**0.002**
SIRI	1.13 ± 0.72	1.19 ± 0.86	0.438
PIV	309.91 ± 211.43	331.84 ± 265.21	0.218

Note: Values are presented as mean ± standard deviation or number (percentage), where appropriate.
F/M: female/male; DM: diabetes mellitus; TSH: thyroid-stimulating hormone; Free T4: free thyroxine; HbA1c: glycated hemoglobin; SII: systemic ımmune-ınflammation ındex; SIRI: systemic ınflammation response ındex; PIV: pan-ımmune-ınflammation value.

Copyright© AE&M all rights reserved.

mellitus was greater in the malignant group (13.3%) than in the benign group (10.7%), the difference was not statistically significant (p = 0.151). Serum TSH levels were significantly elevated in patients with malignancy compared with those with benign pathology (1.98 ± 2.07 vs. 1.55 ± 1.30 mIU/L, p = 0.009). No significant differences were observed in free T4, fasting glucose, or HbA1c levels.

The tumor characteristics of the malignant group are summarized in **Table 2**. The vast majority had papillary thyroid carcinoma (PTC, 95.2%), and the most common histological variant was classic PTC (59.8%), followed by follicular variant (25.7%), oncocytic (8.9%), and others (5.6%). Multifocal tumors were present in 43.6% of the patients, and bilateral involvement was observed in 33%. The mean tumor diameter was 16.54 ± 13.85 mm, and tumors < 1 cm in diameter were observed in 51.1% of the patients. Capsular invasion (29.8%), extrathyroidal extension (26.6%), and lymph node metastasis (13.8%) were relatively common, whereas vascular invasion (6.9%) and distant metastasis (4.0%) were less common. Radioactive iodine (RAI) therapy was administered to 43.6% of the patients.

With respect to preoperative inflammatory markers, the SII was significantly greater in the malignant group than in the benign group (654.75 ± 403.30 vs. 547.08 ± 302.05, p = 0.002). However, the SIRI and PIV values did not differ significantly between groups (p = 0.438 and p = 0.218, respectively).

Univariate analysis demonstrated that age (p = 0.002), TSH level (p = 0.009), and the SII (p = 0.002) were significantly associated with malignancy. In contrast, no significant associations were found for free T4 (p = 0.392), fasting glucose (p = 0.108), HbA1c (p = 0.134), sex (p = 0.204), or diabetes status (p = 0.151).

To identify independent predictors of malignancy, multivariate logistic regression analysis was conducted, including age, TSH level, SII, HbA1c level, sex, and diabetes status. Among these variables, only the Systemic Immune-Inflammation Index (SII) emerged as a statistically significant independent predictor (p = 0.007). Higher SII values were associated with increased odds of malignancy (OR = 1.002, 95% CI: 1.000–1.003). However, the effect size was minimal, as the odds ratio was very close to 1.0, indicating statistical significance but limited clinical relevance. In contrast, age (p = 0.844), TSH level (p = 0.096), HbA1c level (p = 0.389), sex (p = 0.787), and diabetes status (p = 0.849) were not significantly associated with malignancy according to the multivariate model. A detailed overview of the univariate and multivariate logistic regression results is provided in **Table 3**.

Table 2. Tumor characteristics in the malignant group

Tumor characteristics	Results
Papillary	179 (95.2%)
Follicular type	9 (4.8%)
PTC variant	
Classic	107 (59.8%)
Follicular	46 (25.7%)
Oncocytic	16 (8.9%)
Others	10 (5.6%)
Number of foci (Mean ± SD)	1.84 ± 1.26
Multifocality	
Yes	82 (43.6%)
No	106 (56.4%)
Laterality	
Unilateral	125 (66.5%)
Bilateral	62 (33.0%)
Tumor size (mm, Mean ± SD)	16.54 ± 13.85
Tumor Size Group	
< 1 cm	96 (51.1%)
1–4 cm	18 (9.6%)
> 4 cm	74 (39.4%)
Capsular invasion	
Yes	56 (29.8%)
No	132 (70.2%)
Lymph node metastasis	
Yes	26 (13.8%)
No	162 (86.2%)
Extrathyroidal extension	
Yes	50 (26.6%)
No	138 (73.4%)
Vascular invasion	
Yes	13 (6.9%)
No	175 (93.1%)
Distant metastasis	
Yes	7 (4.0%)
No	168 (96.0%)
RAI therapy	
Received	75 (43.6%)
Not received	97 (56.4%)

PTC: papillary thyroid carcinoma; RAI: radioactive iodine; SD: standard deviation.

Copyright© AE&M all rights reserved.

Table 3. Univariate and multivariate logistic regression analysis for predictors of malignancy

	Univariate OR (95% CI)	Univariate p-value	Multivariate OR (95% CI)	Multivariate p-value
Age	0.984 (0.969–0.998)	**0.025**	0.996 (0.962–1.032)	0.844
TSH	1.157 (1.038–1.289)	**0.009**	1.201 (0.968–1.491)	0.096
SII	1.001 (1.000–1.002)	**0.007**	1.002 (1.000–1.003)	**0.007**
HbA1c	1.086 (0.884–1.334)	0.446	1.221 (0.775–1.922)	0.389
Sex (F/M)	0.743 (0.464–1.190)	0.216	0.887 (0.371–2.118)	0.787
DM presence	1.273 (0.747–2.170)	0.372	1.112 (0.374–3.307)	0.849

OR: odds ratio; CI: confidence ınterval; TSH: thyroid-stimulating hormone; SII: systemic ımmune-ınflammation ındex; HbA1c: glycated hemoglobin; DM: diabetes mellitus; F/M: female/male.

To address the potential overlap between TSH and the SII, additional multicollinearity analyses were performed. The variance inflation factor (VIF) and tolerance values were within acceptable ranges (all VIF < 2.5, tolerance > 0.4), indicating no concerning collinearity. Furthermore, we compared two logistic regression models: In Model 1 (including age, sex, TSH level, HbA1c level, and diabetes status), none of the variables were significant predictors of malignancy. In Model 2 (Model 1 + SII), the SII remained an independent predictor (OR = 0.85 per 100-unit increase, p = 0.007), whereas the TSH level lost statistical significance (p = 0.096). These findings suggest that the predictive effect of the SII is independent of the TSH level.

Receiver operating characteristic (ROC) curve analysis was performed to evaluate the diagnostic performance of the Systemic Immune-Inflammation Index (SII) in distinguishing malignant from benign thyroid lesions. The optimal cutoff value for the SII was determined to be 487, with a sensitivity of 65.8% and a specificity of 58.2%. The area under the curve (AUC) was 0.597, indicating limited but statistically measurable discriminatory capacity. The area under the curve (AUC) was 0.597, indicating poor diagnostic accuracy despite statistical significance. The ROC curve of the SII is presented in Figure 2 to illustrate these findings.

In contrast, neither the Systemic Inflammation Response Index (SIRI) nor the Pan-Immune Inflammation Value (PIV) differed significantly between the benign and malignant groups; therefore, ROC curve analysis was not applicable for these indices.

In addition to evaluating their diagnostic utility, we also assessed the potential prognostic value of preoperative inflammatory indices, including the SII, SIRI, and PIV, within the malignant group. Specifically, their

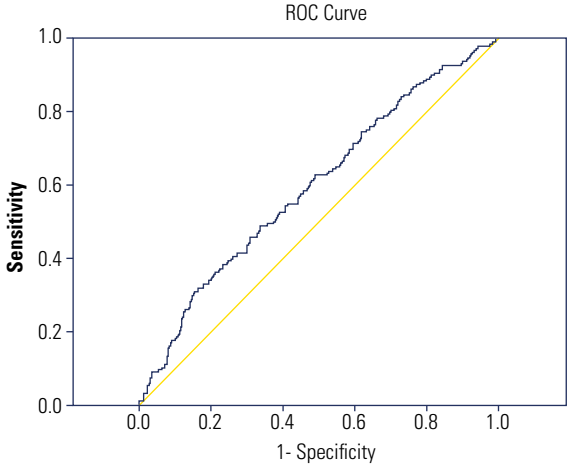


Figure 2. Receiver operating characteristic (ROC) curve of the Systemic Immune-Inflammation Index (SII) for predicting thyroid malignancy. The AUC was 0.597, indicating limited but measurable discriminative ability (cut-off: 487; sensitivity: 65.8%; specificity: 58.2%).

associations with established prognostic parameters such as tumor size (continuous and categorical), multifocality, laterality, lymph node metastasis, extrathyroidal extension, capsular invasion, vascular invasion, and distant metastasis were analyzed. However, all subgroup analyses yielded negative results, indicating that none of the indices demonstrated prognostic utility in relation to these histopathological features.

DISCUSSION

In this retrospective study, we assessed the diagnostic value of three systemic inflammatory indices — the Systemic Immune-Inflammation Index (SII), Systemic Inflammation Response Index (SIRI), and Pan-Immune Inflammation Value (PIV) — for differentiating malignant from benign thyroid nodules. Among 554 patients, only the SII was significantly associated with malignancy in both the univariate and multivariate analyses, although the effect size was very small (OR:

Copyright© AE&M all rights reserved.

0.85 per 100-unit increase; 95% CI: 0.75–0.96; p = 0.007), indicating that the clinical impact of this association is limited. In addition, compared with patients with benign nodules, patients with malignant nodules were significantly younger and had higher serum TSH levels, further supporting the known clinical patterns associated with thyroid cancer risk.

The interplay between inflammation and cancer has been the focus of intense research, with increasing evidence implicating the immune system in the initiation, progression, and prognosis of malignancies. The tumor microenvironment, which is composed of immune cells such as neutrophils, lymphocytes, and monocytes, influences tumor behavior through intricate mechanisms involving cytokines, chemokines, and transcription factors (5,18,19). Chronic inflammation contributes to genetic instability, immune evasion, angiogenesis, and metastasis (5). Consequently, systemic inflammatory markers derived from routine blood counts — such as the SII, SIRI, and PIV — have gained attention as potential surrogates for tumor–immune interactions in various cancers (20,21).

Several prior studies have explored these indices in the context of thyroid cancer. For instance, a cohort study demonstrated significantly elevated SII values in patients with DTC compared with those in healthy controls (22). Similarly, Vural and cols. found higher SII values in DTC patients than in those with multinodular goiter and lymphocytic thyroiditis, suggesting a possible role in distinguishing malignant from benign nodular disease (23). Zhao and cols. reported that the SII independently predicted lateral lymph node metastasis in papillary thyroid carcinoma (PTC) (24), whereas Pang and cols. employed machine learning algorithms to emphasize the predictive value of the SIRI for central lymph node metastasis (25). PIV has also been linked to distant metastasis and higher ATA risk categories in select cohorts (26).

Although the SII emerged as the only index independently associated with malignancy in our cohort, its overall diagnostic power was limited (AUC = 0.597; sensitivity, 65.8%; specificity, 58.2%), indicating that the SII cannot be considered a standalone diagnostic tool. Instead, it may function as a low-cost adjunct within multivariable preoperative models.

In contrast, evidence from previous studies suggests that for DTC, PIV may have more utility in prognostication than in diagnosis. In a cohort of 376 patients, Öztürk and cols. reported that elevated PIV was significantly associated with distant metastasis (AUC = 0.774), advanced TNM stage (OR > 7), and high ATA risk (OR > 29) (26). These findings suggest that PIV may reflect more aggressive tumor biology and could serve as a valuable prognostic marker in DTC. However, the inclusion of multiple immune cell types in the PIV formula — particularly monocytes — may introduce heterogeneity, potentially limiting its diagnostic performance in certain settings. In our study, the absence of a significant association between PIV and malignancy may be due to this complexity or study-specific factors such as cohort composition and exclusion criteria.

One of the key strengths of our study lies in its direct comparison of the SII, SIRI, and PIV under the same clinical conditions. Previous research has generally evaluated these indices in isolation; in contrast, our study provides a side-by-side assessment in a moderately large, single-center cohort (n = 554). While the SII remained statistically significant in the multivariate analysis, its effect size was minimal, and its diagnostic accuracy was poor, indicating limited clinical impact. SIRI and PIV, on the other hand, did not demonstrate independent associations with malignancy. The rigorous application of exclusion criteria enhances the internal validity of our findings, although the retrospective and single-center design limits their external validity and generalizability. However, subgroup analyses within the malignant cohort (tumor size, multifocality, lymph node metastasis, extrathyroidal extension, capsular invasion, vascular invasion, and distant metastasis) consistently yielded negative results, confirming that none of the evaluated indices demonstrated prognostic utility. This lack of prognostic relevance may be explained by the indolent course and relatively homogeneous biology of most differentiated thyroid cancers, where traditional histopathological factors (e.g., tumor size, extrathyroidal extension, and lymph node status) are more powerful predictors of outcome than systemic inflammatory markers are.

Copyright© AE&M all rights reserved.

Among the three indices evaluated, the SII emerged as the most promising marker, and its statistical significance despite its weak performance may be attributed to its unique composition. A first possible explanation lies in the exclusion of monocytes from the SII formula. The SII is calculated from the neutrophil, platelet, and lymphocyte counts, while both the SIRI and PIV incorporate monocytes. This distinction is particularly relevant given the complex and context-dependent role of monocytes in tumor biology (27). In the tumor microenvironment, monocytes can differentiate into tumor-associated macrophages (TAMs), which exert both tumor-promoting and tumor-suppressive effects depending on the immune context, tumor stage, and cytokine signaling (27,28). In thyroid cancer, the influence of TAMs is less well defined and may be less dominant than in other solid tumors (28). The exclusion of monocytes from the SII may thus provide a more stable and interpretable measure of systemic inflammation relevant to thyroid tumorigenesis.

A second possible explanation relates to the broader immunological mechanisms underlying thyroid cancer. While monocyte-macrophage lineage cells play a prominent role in several malignancies, thyroid cancer pathogenesis may be more closely linked to alterations in lymphocyte subsets, such as cytotoxic T cells and natural killer (NK) cells (29,30). SII reflects not only elevated neutrophil- and platelet-driven inflammation but also a relative suppression of lymphocyte-mediated immune surveillance. A lower lymphocyte count—potentially indicating impaired NK cell or T-cell function — may correspond to reduced antitumor immunity, which is better captured by the SII. In this context, the contribution of monocytes may be less relevant, as the dominant immune dysregulation involves lymphoid and myeloid balance rather than monocyte-derived effects alone. This mechanistic difference may help explain why the diagnostic ability of the SII was superior to that of monocyte-inclusive indices such as the SIRI and PIV in our cohort (29,30).

At the molecular level, the development and progression of DTC is shaped by a delicate balance between tumor-promoting inflammation and antitumor immune responses. NK cells and cytotoxic CD8+ T lymphocytes are central to immune surveillance (29-31). However, tumors may evade immune recognition by downregulating MHC class I molecules or inducing T-cell anergy and NK cell dysfunction (32). Indeed, MHC class I loss has been documented in papillary thyroid carcinoma and is associated with reduced tumor-infiltrating lymphocytes (33). Infiltrating immune cells in the thyroid tumor microenvironment often display an exhausted phenotype, marked by the expression of immune checkpoints such as PD-1 and CTLA-4 (31,33). Additionally, tumor-derived immunosuppressive cytokines promote regulatory T-cell differentiation and inhibit effector functions (34). These mechanisms, coupled with increased neutrophil and platelet activation — which support tumor angiogenesis and metastasis—underscore the multifaceted nature of the tumor–host interaction in thyroid cancer (35). In this context, systemic inflammatory indices such as the SII may function as integrative markers that reflect the overall immune-inflammatory status of the patient.

Our findings also revealed that patients with malignant thyroid nodules were significantly younger and had higher serum TSH levels than those with benign thyroid nodules. The inverse relationship between age and malignancy is consistent with the findings of earlier studies suggesting that DTC tends to present at younger ages, potentially because of increased surveillance and earlier detection (36). Elevated TSH levels in malignant cases may be explained by the trophic effects of these hormones on thyroid follicular cells, including the promotion of proliferation and inhibition of apoptosis (37). Notably, this association remained significant even after patients with hyperthyroid conditions such as Graves' disease and toxic multinodular goiter were excluded, supporting the notion that TSH may contribute directly to thyroid tumorigenesis, independent of functional thyroid status. Importantly, multicollinearity analyses confirmed that the SII retained its predictive significance independent of the TSH level, as the VIF values were < 2.5 and tolerance > 0.4. Moreover, in logistic regression models, the SII remained significant when it was added to a base model that included age, sex, TSH level, HbA1c level, and diabetes status, whereas the TSH level lost significance. These findings support the notion that the SII

Copyright© AE&M all rights reserved.

reflects an inflammatory dimension of thyroid tumorigenesis independent of the TSH level.

Despite the strengths of our study, including its structured design and stringent exclusion criteria, certain limitations must be acknowledged. The retrospective and single-center nature of the study may limit the generalizability of our findings. Another limitation is the lack of cytological data and standardized ultrasound features (such as TI-RADS), which would have provided a more comprehensive preoperative evaluation. Although glucose and HbA1c levels were included to account for the potential impact of diabetes on systemic inflammation, they were not significantly associated with malignancy in our cohort. Moreover, owing to the retrospective design, data on obesity and metabolic syndrome were not consistently available, and residual confounding by these comorbidities cannot be excluded. Finally, although all patients were scheduled for elective surgery and had no acute illness at the time of blood sampling, perioperative stress or subclinical factors within the week prior to surgery may still have influenced the systemic inflammatory indices.

From a clinical standpoint, the appeal of systemic inflammatory indices such as the SII lies not only in their diagnostic potential but also in their ease of implementation. These indices are calculated from standard complete blood count (CBC) parameters, which are routinely obtained during almost all preoperative evaluations. Unlike molecular tests or imaging modalities that may be costly or require specialized infrastructure, these indices are inexpensive and universally accessible and do not require additional procedures or add to the patient's burden. This makes them particularly attractive for use in resource-limited settings, as well as in routine practice where high-throughput risk stratification is needed. The incorporation of the SII into preoperative assessment models may provide a low-cost adjunct to existing diagnostic strategies, although further validation is warranted.

In conclusion, while the SII emerged as an independent predictor of malignancy, its effect size was minimal, and its diagnostic accuracy was poor (AUC < 0.6). Therefore, its clinical utility should be interpreted with caution, and the SII cannot be considered a standalone diagnostic tool. Instead, it may serve as a low-cost adjunct within multivariable preoperative models, particularly in challenging scenarios such as indeterminate cytology. Future multicenter, prospective studies are necessary to validate our findings and clarify the role of systemic inflammatory markers in thyroid cancer risk assessment.

Author contributions: MÇ – led the study, contributed to study design, data collection and processing, interpretation of findings, literature search and manuscript preparation and writing. BK – data collection and processing, Statistical Analyzes, interpretation of findings, critical revision of the manuscript. ZÇ – contributed to study design, interpretation of results, and critical revision of the manuscript. ÖÖB – contributed to study design, interpretation of findings, and critical revision of the manuscript. All authors have read and approved the final manuscript and agree to be accountable for all aspects of the work to ensure its accuracy and integrity.

Acknowledgments: the authors have no acknowledgments to declare.

Approval of the research protocol: this study was approved by Tokat Gaziosmanpasa University Ethics Committee Approval Number: 21-KAEK-135 and conducted in accordance with the Declaration of Helsinki.

Informed consent: informed consent was not needed because of the retrospective nature of the study.

Registry and the registration no. of the study/trial: N/A.

Animal studies: N/A.

Funding: the authors have no financial support.

Disclosure: no potential conflict of interest relevant to this article was reported.

Data availability: datasets related to this article will be available upon request to the corresponding author.

REFERENCES

1. Wiltshire JJ, Drake TM, Uttley L, Balasubramanian SP. Systematic Review of Trends in the Incidence Rates of Thyroid Cancer. Thyroid. 2016 Nov;26(11):1541-1552. doi: 10.1089/thy.2016.0100.
2. Haddad RI, Bischoff L, Ball D, Bernet V, Blomain E, Busaidy NL, et al. Thyroid Carcinoma, Version 2.2022, NCCN Clinical Practice Guidelines in Oncology. J Natl Compr Canc Netw. 2022 Aug;20(8):925-951. doi: 10.6004/jnccn.2022.0040.
3. Feldkamp J, Führer D, Luster M, Musholt TJ, Spitzweg C, Schott M. Fine Needle Aspiration in the Investigation of Thyroid Nodules. Dtsch Arztebl Int. 2016 May 20;113(20):353-9. doi: 10.3238/arztebl.2016.0353.
4. Haugen BR, Alexander EK, Bible KC, Doherty GM, Mandel SJ, Nikiforov YE, et al. 2015 American Thyroid Association Management Guidelines for Adult Patients with Thyroid Nodules and Differentiated Thyroid Cancer: The American Thyroid Association Guidelines Task Force on Thyroid Nodules and Differentiated Thyroid Cancer. Thyroid. 2016 Jan;26(1):1-133. doi: 10.1089/thy.2015.0020.

Copyright© AE&M all rights reserved.

5. Nishida A, Andoh A. The Role of Inflammation in Cancer: Mechanisms of Tumor Initiation, Progression, and Metastasis. Cells. 2025 Mar 25;14(7):488. doi: 10.3390/cells14070488.
6. Wang C, Shi Q, Zhang G, Wu X, Yan W, Wan A, et al. Two Hematological Markers Predicting the Efficacy and Prognosis of Neoadjuvant Chemotherapy Using Lobaplatin Against Triple-Negative Breast Cancer. Oncologist. 2024 May 3;29(5):e635-e642. doi: 10.1093/oncolo/oyae025.
7. He T, Xu B, Wang LN, Wang ZY, Shi HC, Zhong CJ, et al. The prognostic value of systemic immune-inflammation index in patients with unresectable hepatocellular carcinoma treated with immune-based therapy. Biomark Res. 2025 Jan 14;13(1):10. doi: 10.1186/s40364-024-00722-6.
8. Yang X, Wu C. Systemic immune inflammation index and gastric cancer prognosis: A systematic review and meta analysis. Exp Ther Med. 2024 Feb 1;27(3):122. doi: 10.3892/etm.2024.12410.
9. Gu L, Ma X, Wang L, Li H, Chen L, Li X, et al. Prognostic value of a systemic inflammatory response index in metastatic renal cell carcinoma and construction of a predictive model. Oncotarget. 2016 Jul 16;8(32):52094-52103. doi: 10.18632/oncotarget.10626.
10. Fucà G, Guarini V, Antoniotti C, Morano F, Moretto R, Corallo S, et al. The Pan-Immune-Inflammation Value is a new prognostic biomarker in metastatic colorectal cancer: results from a pooled-analysis of the Valentino and TRIBE first-line trials. Br J Cancer. 2020 Aug;123(3):403-409. doi: 10.1038/s41416-020-0894-7.
11. Atasoy MS, Guven H. Pan-Immune-Inflammation Value: A Novel Biomarker for Predicting Postoperative Atrial Fibrillation in Young Patients Undergoing Off-Pump CABG. J Cardiothorac Vasc Anesth. 2025 Jun;39(6):1464-1471. doi: 10.1053/j.jvca.2025.02.050.
12. Sargin G, Baris K, Gulen ST. Systemic immune-inflammation index in the evaluation of Sjogren's syndrome associated with interstitial lung disease, interstitial pneumonia with autoimmune features, and idiopathic pulmonary fibrosis. Adv Med Sci. 2025 Mar;70(1):57-61. doi: 10.1016/j.advms.2024.12.001.
13. Sahin R, Tanacan A, Serbetci H, Karagoz B, Agaoglu Z, Kara O, et al. First-trimester neutrophil-to-lymphocyte ratio (NLR), systemic immune-inflammation index (SII), and systemic immune-response index (SIRI) as predictors of composite adverse outcomes in pregnant women with Familial Mediterranean fever. Z Geburtshilfe Neonatol. 2024 Apr;228(2):156-160. doi: 10.1055/a-2125-0973.
14. Cao C, Li C, Li X, Sun W, Wang Y. Association of systemic immune-inflammation index (SII) and aggregate index of systemic inflammation (AISI) with thyroid nodules in patients with type 2 diabetes mellitus: a retrospective study. BMC Endocr Disord. 2023 Nov 20;23(1):251. doi: 10.1186/s12902-023-01509-w.
15. Zhang J, Fan X, Xu Y, Wang K, Xu T, Han T, et al. Association between inflammatory biomarkers and mortality in individuals with type 2 diabetes: NHANES 2005-2018. Diabetes Res Clin Pract. 2024 Mar;209:111575. doi: 10.1016/j.diabres.2024.111575.
16. Dong WW, Zhang DL, Wang ZH, Lv CZ, Zhang P, Zhang H. Different types of diabetes mellitus and risk of thyroid cancer: A meta-analysis of cohort studies. Front Endocrinol (Lausanne). 2022 Sep 23;13:971213. doi: 10.3389/fendo.2022.971213.
17. Amin MB, Greene FL, Edge SB, Compton CC, Gershenwald JE, Brookland RK, et al. The Eighth Edition AJCC Cancer Staging Manual: Continuing to build a bridge from a population-based to a more "personalized" approach to cancer staging. CA Cancer J Clin. 2017 Mar;67(2):93-99. doi: 10.3322/caac.21388.
18. Xie Y, Liu F, Wu Y, Zhu Y, Jiang Y, Wu Q, Dong Z, Liu K. Inflammation in cancer: therapeutic opportunities from new insights. Mol Cancer. 2025 Feb 24;24(1):51. doi: 10.1186/s12943-025-02243-8.
19. Chen C, Wang Z, Ding Y, Qin Y. Tumor microenvironment-mediated immune evasion in hepatocellular carcinoma. Front Immunol. 2023 Feb 10;14:1133308. doi: 10.3389/fimmu.2023.1133308.
20. Zhang Y, Wu J, Chen W, Liang X. Pretreatment System Inflammation Response Index (SIRI) is a Valuable Marker for Evaluating the Efficacy of Neoadjuvant Therapy in Breast Cancer Patients. Int J Gen Med. 2024 Sep 25;17:4359-4368. doi: 10.2147/IJGM.S478000.
21. Shi J, Liu C, Yang N, Qiu C. Pan-immune-inflammation value: a new prognostic index in operative laryngeal and pharyngeal carcinomas. Clin Transl Oncol. 2025 Jan;27(1):151-159. doi: 10.1007/s12094-024-03558-6.
22. Kars A, Sahin A, Kılıc K, Sakat MS, Bilen A. Systemic immune inflammation index in differentiated thyroid cancers. Acta Otorhinolaryngol Ital. 2022 Apr;42(2):150-154. doi: 10.14639/0392-100X-N1665.
23. Vural S, Muhtaroğlu A, Güngör M. Systemic immune-inflammation index: A new marker in differentiation of different thyroid diseases. Medicine (Baltimore). 2023 Aug 4;102(31):e34596. doi: 10.1097/MD.0000000000034596.
24. Zhao L, Zhou T, Zhang W, Wu F, Jiang K, Lin B, et al. Blood immune indexes can predict lateral lymph node metastasis of thyroid papillary carcinoma. Front Endocrinol (Lausanne). 2022 Aug 31;13:995630. doi: 10.3389/fendo.2022.995630.
25. Pang J, Yang M, Li J, Zhong X, Shen X, Chen T, et al. Interpretable machine learning model based on the systemic inflammation response index and ultrasound features can predict central lymph node metastasis in cN0T1-T2 papillary thyroid carcinoma. Gland Surg. 2023 Nov 24;12(11):1485-1499. doi: 10.21037/gs-23-349.
26. Öztürk Y, Kocabaş M, Karaköse M, Kulaksizoğlu M, Karakurt F. Prognostic significance of the pan-immune-inflammation value (PIV) in patients with differentiated thyroid carcinoma. Arch Endocrinol Metab. 2025 Apr 11;68:e240217. doi: 10.20945/2359-4292-2024-0217.
27. Wang K, Zhang X, Li A, Qiao X, Xu Y. The mechanism of action and therapeutic potential of tumor-associated macrophages in tumor immune evasion. Front Immunol. 2025 Apr 22;16:1545928. doi: 10.3389/fimmu.2025.1545928.
28. Zhu L, Li XJ, Gangadaran P, Jing X, Ahn BC. Tumor-associated macrophages as a potential therapeutic target in thyroid cancers. Cancer Immunol Immunother. 2023 Dec;72(12):3895-3917. doi: 10.1007/s00262-023-03549-6.
29. Li X, Wang K, Liu J, Li Y. A comprehensive analysis to reveal the underlying molecular mechanisms of natural killer cell in thyroid carcinoma based on single-cell RNA sequencing data. Discov Oncol. 2025 Jan 14;16(1):44. doi: 10.1007/s12672-025-01779-x.
30. Chen Z, Guo ML, Li YY, Yan K, Li L, Shen F, et al. Immune profiling identifies CD8+ T-cell subset signatures as prognostic markers for recurrence in papillary thyroid cancer. Front Immunol. 2022 Nov 7;13:894919. doi: 10.3389/fimmu.2022.894919.
31. Zheng X, Sun R, Wei T. Immune microenvironment in papillary thyroid carcinoma: roles of immune cells and checkpoints in disease progression and therapeutic implications. Front Immunol. 2024 Sep 3;15:1438235. doi: 10.3389/fimmu.2024.1438235.
32. Dhatchinamoorthy K, Colbert JD, Rock KL. Cancer Immune Evasion Through Loss of MHC Class I Antigen Presentation. Front Immunol. 2021 Mar 9;12:636568. doi: 10.3389/fimmu.2021.636568.
33. Anand N, Srivastava P, Husain N, Agarwal D, Gupta A, Pradhan R. Evaluation of CTLA-4 and PD-L1 Expression in Thyroid Carcinoma and Its Prognostic Significance. Cureus. 2024 Aug 16;16(8):e67004. doi: 10.7759/cureus.67004.
34. Ferrari SM, Fallahi P, Galdiero MR, Ruffilli I, Elia G, Ragusa F, et al. Immune and Inflammatory Cells in Thyroid Cancer Microenvironment. Int J Mol Sci. 2019 Sep 7;20(18):4413. doi: 10.3390/ijms20184413.
35. Anvari S, Osei E, Maftoon N. Interactions of platelets with circulating tumor cells contribute to cancer metastasis. Sci Rep. 2021 Jul 29;11(1):15477. doi: 10.1038/s41598-021-94735-y.
36. Leite-Almeida L, Silva RS, Vicente-Ferreira M, Costa C, Estevinho N, Castro-Correia C, et al. Age-related characteristics in differentiated thyroid cancer: a 20-year single-center retrospective analysis in pediatric and adolescent patients. Arch Endocrinol Metab. 2025 Apr 8;69(2):e240333. doi: 10.20945/2359-4292-2024-0333.
37. Wu Z, Xi Z, Xiao Y, Zhao X, Li J, Feng N, et al. TSH-TSHR axis promotes tumor immune evasion. J Immunother Cancer. 2022 Jan;10(1):e004049. doi: 10.1136/jitc-2021-004049.

Copyright© AE&M all rights reserved.

Archives of Endocrinology and Metabolism
ISSN 2359-4292
OFFICIAL JOURNAL OF THE BRAZILIAN SOCIETY OF ENDOCRINOLOGY AND METABOLISM

original

The decline of iodine therapy in the treatment of Graves' disease in a hospital center: a 20-year analysis

Isabela Busto Silva[1]
https://orcid.org/0000-0002-9213-4203
João Pedro Ignotti de Almeida[2]
https://orcid.org/0009-0004-6466-9464
Hans Graf[1]
https://orcid.org/0000-0001-8671-1556
Gisah Amaral de Carvalho[1]
https://orcid.org/0000-0002-2387-665X
Matheus Pessini Sousa[2]
https://orcid.org/0009-0004-7122-2011
Mariana Driesel Bertolin[2]
https://orcid.org/0009-0004-9183-6213
Fabíola Yukiko Miasaki[1]
https://orcid.org/0000-0001-6852-4300
Caio Pereira Mueller[2]
https://orcid.org/0009-0006-7101-1235
Cléo Otaviano Mesa Júnior[1]
https://orcid.org/0000-0002-9215-137X

[1] Departamento de Medicina Interna, Serviço de Endocrinologia e Metabologia (SEMPR), Universidade Federal do Paraná, Curitiba, PR, Brasil
[2] Universidade Federal do Paraná, Curitiba, PR, Brasil

ABSTRACT

Objective: To evaluate and describe the changes in the therapeutic approach to Graves' disease at a tertiary hospital center over a 20-year period, with an emphasis on the frequency of prescription and the timing of radioactive iodine indication. **Subjects and methods**: We conducted a retrospective analysis of data from medical records of patients recently diagnosed with Graves' disease (GD) and followed up at a single institution during two consecutive periods: Group A diagnosed between 2002 and 2010, and Group B between 2011 and 2022. We analyzed the percentage of patients who underwent iodine therapy and were considered to have failed therapy if they did not achieve hypothyroidism or euthyroidism, comparing the results between both groups. **Results**: A total of 597 GD patients were included, of which 223 underwent radioactive iodine (RAI) therapy (37.35%). In Group A, 176 patients (64%) received RAI treatment, whereas, in Group B, only 47 patients were given this therapeutic indication (14.6%) ($p < 0.001$). The reduction in RAI prescriptions between both periods was independent of the therapeutic indication. Interestingly, RAI prescription due to relapse after clinical treatment was uncommon in both study groups. There was a significant increase in the duration of antithyroid drug (ATD) therapy before RAI prescription in Group B compared to Group A. **Conclusion**: Significant changes were observed in GD treatment, with a decline in the use of RAI as a first-line or salvage therapy. Nonetheless, radioiodine therapy remained an effective and safe treatment modality with successful cure rates.

Keywords: Hyperthyroidism; Graves' disease; radioiodine

INTRODUCTION

Graves' disease (GD), the most common cause of hyperthyroidism, is associated with significant comorbidities and reduced quality of life (1). For over 70 years, three primary treatment options have been available: antithyroid drugs (ATD), radioactive iodine (RAI), and thyroidectomy. Preferences for first-line treatment vary across countries and regions, evolving over time based on new studies, updated evidence-based guidelines, or shifts in expert opinion (2). Thus, selecting the most suitable treatment for patients necessitates thoughtful discussions and active collaboration in decision-making (3).

Radioactive iodine is an effective treatment for managing hyperthyroidism in patients with GD, as iodine-131 is rapidly absorbed by the thyroid, with its beta emissions causing localized tissue destruction. Therapy is considered simple, safe, and often the most cost-effective option, offering rapid and definitive control of excess thyroid hormone effects (4). The ultimate goal of RAI therapy, as delineated in current American Thyroid Association guidelines, is to achieve near-complete ablation of the thyroid gland, leading to permanent hypothyroidism as the intended outcome (5).

In recent decades, there has been a noticeable shift in the strategies and trends regarding the use of RAI compared to ATD (6), particularly in the United States, where RAI therapy has been traditionally favored. A 2011 survey showed that over half of US clinicians

Received on Mar/20/2025
Accepted on Oct/2/2025
DOI: 10.20945/2359-4292-2026-0013

Correspondence to:
Isabela Busto Silva
isabelabustosilva@gmail.com

Associated editor:
Fernanda Vaisman Balieiro
https://orcid.org/0000-0002-6835-7108

This is an open-access article distributed under the terms of the Creative Commons Attribution License

Copyright© AE&M all rights reserved.

preferred RAI, whereas around 40% opted for initiating a one- to two-year course of ATD (7). However, by 2023, preferences had significantly shifted, with 91.5% of respondents favoring ATD and only 7% continuing to prefer RAI (8).

To further understand the evolving landscape of GD management, we conducted a study at our center to analyze current practices involving RAI and evaluate trends over the past 20 years. Our research aimed to assess key variables, including RAI prescription rates, prescribed activity levels, intervals between ATD use and RAI administration, and the effectiveness of this treatment modality. We then compared these variables across two decades to identify significant trends and changes in practice.

SUBJECTS AND METHODS

Our study is a retrospective analysis of medical records from patients diagnosed with GD and followed at a single institution during two distinct periods: Group A, consisting of patients diagnosed between 2002 and 2010, and Group B, comprising those diagnosed between 2011 and 2022. Diagnosis was based on suppressed thyroid-stimulating hormone (TSH) levels, elevated free thyroxine (FT4) or total T3 levels (TT3), positive thyrotropin receptor antibodies (TRAb), and/or thyroid scintigraphy showing diffuse increased tracer accumulation in an enlarged thyroid gland. As laboratory analyses were modified due to the extended follow-up period, adjustments to the methodological approach were necessary. Hence, TSH, FT4, and TT3 levels were measured with chemiluminescence assays (ABBOTT).

From July 2019 onward, analyses were conducted using the ALINITY system (TSH 0.35–4.94 mIU/mL; FT4 0.7–1.48 ng/dL; TT3 64–152 ng/dL). Between 2011 and July 2019, the ARCHITECT system was used (TSH: 0.4–4.5 IU/mL; FT4: 0.7–1.8 ng/dL; TT3: 80–180 ng/dL). Before 2011, TSH and thyroid hormones were measured using a microparticle enzyme immunoassay with the AXSYM system, also by ABBOTT (TSH: 0.4–4.0 IU/mL; FT4: 0.7–1.9 ng/dL; TT3: 80–200 ng/dL). The TRAb assay underwent several changes: from 2002 to 2005, it was performed using a first-generation radioimmunoassay, known as the TRAk human radioimmunoassay (BRAHMS Diagnostica, Germany), with results expressed as a percentage of inhibition of TSH binding, considering values ≥10% positive. Afterward, the TRAb assay was performed using chemiluminescence, deemed positive when levels exceeded 0.55 IU/L. From July 2019 onward, the TRAb assay method changed to using the Immulite 2000 equipment (Siemens, USA), with levels exceeding 1.5 IU/L considered positive.

We evaluated the percentage of patients undergoing iodine therapy who were deemed to have failed therapy if they did not achieve hypothyroidism or euthyroidism. Analyzed variables for this group included age, sex, smoking status, presence of thyroid eye disease (TED), therapeutic efficacy (defined as achieving hypothyroidism or euthyroidism within one year without the need for additional therapy), prescribed activity, maximum ATD dose, duration of ATD use before radioiodine administration, and time to progression to hypothyroidism. The RAI dose was empirically adjusted for each patient based on disease severity and goiter size, typically between 15–25 mCi, without a standardized protocol but rather through individualized clinical evaluation. Standard practice includes administering oral glucocorticoid prophylaxis (prednisone 0.5 mg/kg/day for 2–3 weeks, tapered thereafter) to all patients with active thyroid orbitopathy, those with moderate to severe inactive thyroid orbitopathy, and smokers with TRAb levels >3 times the upper limit of normal, even in the absence of evident orbital disease.

Data were analyzed using the IBM SPSS Statistics (v. 29.0) software. Associations between categorical variables were assessed using Fisher's exact test or the Chi-square test. Comparisons between both periods defined by the year of diagnosis (before 2010 or after) for quantitative variables employed the non-parametric Mann-Whitney test. The normality of continuous variables was evaluated using the Kolmogorov-Smirnov test, and *p*-values below 0.05 were deemed statistically significant.

RESULTS

A total of 597 patients with GD were included in the analysis, with 223 (37.35%) of them undergoing RAI treatment. Among these, 275 were diagnosed with

Copyright© AE&M all rights reserved.

GD between 2002 and 2010 (Group A), and 322 were diagnosed between 2010 and 2022 (Group B) (Figure 1). In Group A, 176 patients (64%) received RAI treatment, whereas in Group B, only 47 patients (14.6%) underwent this therapy ($p < 0.001$).

The baseline characteristics of both groups were generally similar, except for a higher prevalence of TED in Group A (Table 1). Due to changes in methodology and low testing rates at the beginning of the study, it was not possible to compare TRAb values between groups. The median TRAb values were 11.6 and 12.2 in Groups A and B, respectively. The sample was divided into two consecutive periods due to the notable decline in RAI therapy prescriptions over time. Furthermore, the increasing number of studies published in the last decade suggesting the safety of prolonged ATD use may have impacted clinical practice, supporting the rationale for analyzing the periods separately.

Our findings also revealed that RAI treatment prescription for GD has significantly declined in recent years, and this occurred consistently between both periods analyzed, regardless of the therapeutic indication (Figure 2).

Table 2 outlines the reasons for prescribing RAI in both groups, with the primary reason being treatment failure with ATD, which accounted for 57% during the earlier period (2002–2010) and 13.3% during the later period (2010–2022). Interestingly, relapses after clinical treatment were an uncommon reason for RAI prescription in both groups. Similarly, RAI as a first-line therapeutic option was infrequently observed across both periods and RAI following thyroidectomy was only observed in Group A (1.09%).

Among the analyzed variables, the maximum methimazole dose did not differ significantly between

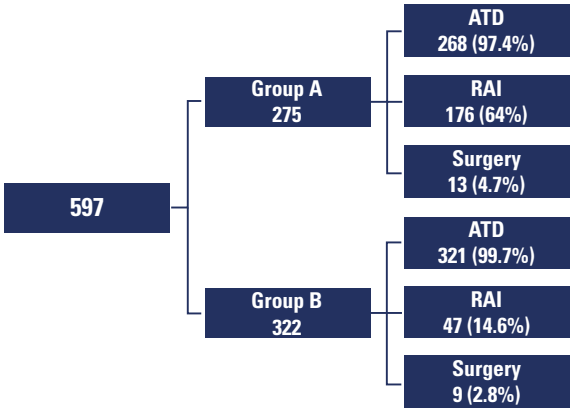


Figure 1. Flowchart illustrating the management of patients with Graves' disease and the therapeutic modalities indicated.

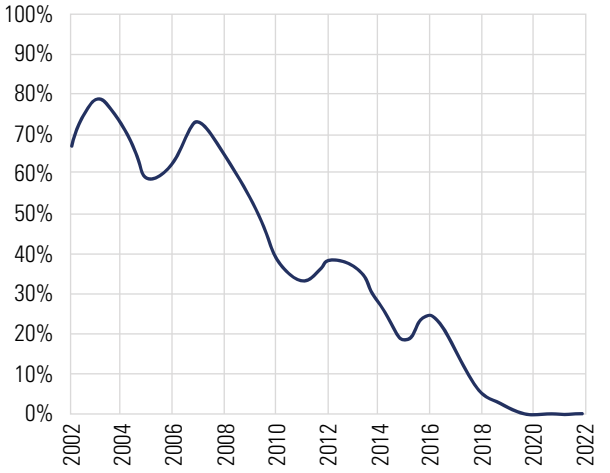


Figure 2. Percentage of patients with Graves' disease undergoing radioactive iodine treatment from 2002 to 2022.

Table 1. Baseline characteristics of participants undergoing radioactive iodine treatment

Variable	Group A (2002–2010)	Group B (2011–2022)	p-value
Patients (n)	176	47	–
Age (mean)	39.4	39.1	0.898
Female sex (%)	147 (83.5%)	43 (91.5%)	0.247
Active smoking (%)	63 (41.7%)	8 (21.1%)	0.062
Graves' ophthalmopathy (%)	90 (51.1%)	12 (25.5%)	0.002
TRAb			
Not tested	152 (48.4%)	15 (31.9%)	–
Positive	16 (9.1%)	28 (59.6%)	–
Negative	8 (4.5%)	4 (8.5%)	–
General follow up in years (median/standard deviation)*	8/5.1	6 / 2.8	< 0.001

TRAb: Positive thyrotropin receptor antibodies. *5 missing data on status or year of follow-up completion.

Copyright© AE&M all rights reserved.

Table 2. Indication for radioactive iodine treatment in patients with Graves' disease

RAI indication	Total n (%)	2002–2010 n (%)	2010–2022 n (%)
Received RAI indication	223 (37.36%)	176 (64%)	47 (14.6%)
Initial option	11 (1.84%)	9 (3.27%)	2 (0.62%)
Relapses after ATD treatment	9 (1.5%)	7 (2.5%)	2 (0.62%)
ATD treatment failure	200 (33.5%)	157 (57%)	43 (13.3%)
After thyroidectomy	3 (0.5%)	3 (1.09%)	0 (0%)
Total number of patients with GD	597 (100%)	275 (100%)	322 (100%)

RAI: radioactive iodine treatment; ATD: antithyroid drug; GD: Graves' disease.

groups, with a mean dose of 30.4 mg (SD ±13.3) in Group A and 30.8 mg (SD ±13.1) in Group B (p = 0.643). Nevertheless, the duration of methimazole treatment was significantly longer in Group B, with a median duration of 37.7 months (±33.7) compared to 23.2 months (±24.7) in Group A (p = 0.002).

The prescribed RAI activity was similar between groups, with a mean dose of 23.1 mCi (SD ±5.2) in Group A and 23.6 mCi (SD ±6.0) in Group B (p = 0.428). The necessity for additional RAI doses occurred in 12.3% of patients in Group A and 13.6% in Group B, indicating no significant difference (p = 0.801). Notably, treatment effectiveness was significantly higher in Group A, as 89.5% of patients achieved hypothyroidism or euthyroidism compared to 69.6% in Group B (p = 0.002). The median time to hypothyroidism following RAI therapy was identical for both groups at 4 months (p = 0.642). The prevalence of patients with TED undergoing RAI differed significantly between both groups. In Group A, 90 patients (51.1%) had TED, whereas only 12 patients (25.5%) had the diagnosis (p = 0.002) in Group B.

DISCUSSION

This study analyzed a cohort of nearly 600 patients with GD treated at a single institution over a 20-year period, with a particular focus on RAI therapy. The primary finding was a notable decrease in the utilization of RAI for treating GD, a trend that significantly accelerated over the last decade (**Figure 2**). Despite RAI's long-standing reputation as a straightforward, cost-effective, and rapid therapeutic option, its prescription has progressively declined.

Although we did not seek to identify the factors behind this shift, several plausible explanations exist. Concerns over the risk of developing new or worsening TED have likely played a role, as has evidence suggesting that prolonged ATD therapy may increase the likelihood of achieving remission in GD. Consequently, indications for RAI have gradually diminished in recent years, a stark contrast to the past when it was routinely recommended for patients who remained hyperthyroid after two years of ATD therapy. This trend also mirrors efforts to prevent permanent hypothyroidism and a move towards long-term medical management. In line with this shift, patients in our study who later transitioned to RAI had undergone ATD therapy for longer periods. Therefore, contemporary RAI candidates typically present with more severe diseases. Our analysis revealed these patients had significantly higher maximum methimazole doses compared to those receiving ATD therapy alone (30.4 vs. 24.3 mg; p < 0.001). Our findings align with research indicating ATD patients tend to be younger, possess fewer comorbidities, and include pregnant individuals, thereby reinforcing the preference for ATDs in these groups and (9), thereby reinforcing the reserved use of RAI for more challenging cases.

In our study, iodine therapy was initially chosen for a small proportion of patients in both groups (i.e., 3.3% in Group A and 0.6% in Group B). These rates are significantly lower than the 14.1% reported in a 2013 European survey and well below the 59% observed in a 2011 United States survey (7,10). Intriguingly, a recent international survey of clinical practice patterns published in 2024 (8), which garnered responses from endocrinologists across 85 countries, revealed a striking shift in the preference for RAI as primary therapy. Only 7.0% of respondents (95/1353) indicated RAI as their first-line treatment for GD, revealing a significant

Copyright© AE&M all rights reserved.

regional variation ranging from a minimum of 1.8% to a maximum of 13.1% and highlighting a global trend away from RAI as an initial treatment option. The treatment trends identified in this study deviate from the 2016 American Thyroid Association hyperthyroidism practice guideline, which recommends an average RAI dose of 10–15 mCi (5). These findings also contrast with a meta-analysis and systematic review that reported a mean RAI dose of 8.5 mCi (range 6.8–12.6) (11). In our analysis, RAI doses were consistently higher, exceeding 20 mCi in both groups.

This study provides a basis for comparison with a previous study conducted at the same institution, by Sztal-Mazer and cols. (12), which analyzed cases diagnosed between 1994 and 2009. During that period, the average initial RAI dose was 21.4 mCi, achieving an overall success rate of 86%. The authors concluded that higher doses were associated with more successful treatment outcomes and earlier achievement of therapeutic goals. Conversely, despite similar RAI doses across groups, we found significant differences in success rates (89.5% in Group A vs. 69.6% in Group B). This suggests that RAI is increasingly being reserved for patients with more severe illnesses. A meta-analysis of randomized controlled trials revealed an average cure rate of hyperthyroidism with RAI treatment of 77.8% (13). Nevertheless, predicting the timing for RAI effects poses challenges, complicating patient monitoring. Our findings are consistent with the association between higher RAI doses and shorter remission times, evidenced by our study's median time to hypothyroidism being 4 months—shorter than the 6-month median observed in other studies (14). The median time to hypothyroidism in our study was calculated from the first post-RAI therapy assessments, potentially introducing a bias due to the assessment timing and confirmation of outcomes. Numerous factors, including gland size, volume, administered dose, and the presence of positive anti-thyroid peroxidase antibodies, likely influence these outcomes (15). Further research should explore these variables to enhance the efficacy and monitoring strategies of RAI treatment.

Despite our promising findings, some limitations must be acknowledged, such as its retrospective design which restricts the ability to pinpoint factors responsible for the observed reduction in RAI prescriptions precisely. Additionally, samples were divided based on the year of diagnosis to investigate changes in diagnostic practices; as a result, Group A had an earlier diagnosis and consequently a longer follow-up time, which significantly limits our study as it may have impacted observed outcomes. Other limitations include potential data collection biases and challenges in determining causal relationships. Regardless, these drawbacks were crucial for interpreting results and crucial for validating the conclusions. Additionally, the TRAb test was conducted less frequently in Group A compared to Group B due to limited availability of testing methods during the earlier period. Nevertheless, these limitations, our study's primary finding remains unchanged: a significant decrease in the prescription of RAI for treating GD over the past two decades. The scarcity of large-scale Brazilian studies on changes in GD treatment practices over time further underscores the relevance of our findings, which reflect trends at a single reference center over a 20-year period and may not represent nationwide practices in Brazil.

In conclusion, our results demonstrate a significant decline in the use of iodine therapy for GD in recent years. Despite this decline, RAI therapy continues to be an effective and safe option, demonstrating high success rates in treating hyperthyroidism. The reasons behind this reduction are not fully understood, and contributing factors may include concerns about inducing hypothyroidism, the potential for worsening TED, and increased confidence in the long-term use of ATD. Future studies should explore the benefits and drawbacks of different therapeutic modalities for GD, with an emphasis on aspects such as mortality reduction, quality of life improvements, and other long-term outcomes. It is crucial to assess whether the growing preference for ATD as a primary treatment indeed offers superior benefits for GD patients.

Acknowledgements: the authors would like to express their sincere gratitude to Marcia Olandoski for her invaluable assistance with the statistical analysis and data interpretation. Her expertise was essential for the successful completion of this work.

Disclosure: no potential conflict of interest relevant to this article was reported.

Copyright© AE&M all rights reserved.

Data availability: datasets related to this article will be available upon request to the corresponding author.

REFERENCES

1. Brito JP, Payne S, Singh Ospina N, Rodriguez-Gutierrez R, Maraka S, Sangaralingham LR, et al. Patterns of Use, Efficacy, and Safety of Treatment Options for Patients with Graves' Disease: A Nationwide Population-Based Study. Thyroid. 2020;30(3):357-364. doi: 10.1089/thy.2019.0132. Epub 2020 Feb 26. Erratum in: Thyroid. 2020;30(6):938. doi: 10.1089/thy.2019.0132.correx.
2. Sjölin G, Holmberg M, Törring O, Byström K, Khamisi S, de Laval D, et al. The Long-Term Outcome of Treatment for Graves' Hyperthyroidism. Thyroid. 2019;29(11):1545-1557. doi: 10.1089/thy.2019.0085.
3. Rodriguez-Gutierrez R, Gionfriddo MR, Ospina NS, Maraka S, Tamhane S, Montori VM, et al. Shared decision making in endocrinology: present and future directions. Lancet Diabetes Endocrinol. 2016;4(8):706-716. doi: 10.1016/S2213-8587(15)00468-4.
4. Sundaresh V, Brito JP, Thapa P, Bahn RS, Stan MN. Comparative Effectiveness of Treatment Choices for Graves' Hyperthyroidism: A Historical Cohort Study. Thyroid. 2017;27(4):497-505. doi: 10.1089/thy.2016.0343.
5. Ross DS, Burch HB, Cooper DS, Greenlee MC, Laurberg P, Maia AL, et al. 2016 American Thyroid Association Guidelines for Diagnosis and Management of Hyperthyroidism and Other Causes of Thyrotoxicosis. Thyroid. 2016;26(10):1343-1421. doi: 10.1089/thy.2016.0229. Erratum in: Thyroid. 2017;27(11):1462. doi: 10.1089/thy.2016.0229.correx.
6. Solomon B, Glinoer D, Lagasse R, Wartofsky L. Current trends in the management of Graves' disease. J Clin Endocrinol Metab. 1990;70(6):1518-24. doi: 10.1210/jcem-70-6-1518.
7. Burch HB, Burman KD, Cooper DS. A 2011 survey of clinical practice patterns in the management of Graves' disease. J Clin Endocrinol Metab. 2012;97(12):4549-58. doi: 10.1210/jc.2012-2802.
8. Villagelin D, Cooper DS, Burch HB. A 2023 International Survey of Clinical Practice Patterns in the Management of Graves' Disease: A Decade of Change. J Clin Endocrinol Metab. 2024;109(11):2956-2966. doi: 10.1210/clinem/dgae222.
9. Azizi F, Malboosbaf R. Long-Term Antithyroid Drug Treatment: A Systematic Review and Meta-Analysis. Thyroid. 2017;27(10):1223-1231. doi: 10.1089/thy.2016.0652.
10. Andrade VA, Gross JL, Maia AL. Iodo radioativo no manejo do hipertireoidismo da doença de Graves [Radioactive iodine therapy in Graves' hyperthyroidism]. Arq Bras Endocrinol Metabol. 2004 Feb;48(1):159-65. Portuguese. doi: 10.1590/s0004-27302004000100017.
11. Sundaresh V, Brito JP, Wang Z, Prokop LJ, Stan MN, Murad MH, et al. Comparative effectiveness of therapies for Graves' hyperthyroidism: a systematic review and network meta-analysis. J Clin Endocrinol Metab. 2013;98(9):3671-7. doi: 10.1210/jc.2013-1954.
12. Sztal-Mazer S, Nakatani VY, Bortolini LG, Boguszewski CL, Graf H, de Carvalho GA. Evidence for higher success rates and successful treatment earlier in Graves' disease with higher radioactive iodine doses. Thyroid. 2012;22(10):991-5. doi: 10.1089/thy.2011.0362.
13. Wang J, Qin L. Radioiodine therapy versus antithyroid drugs in Graves' disease: a meta-analysis of randomized controlled trials. Br J Radiol. 2016;89(1064):20160418. doi: 10.1259/bjr.20160418.
14. Kanokwongnuwat W, Penpong N. Prospective study to evaluate radioactive iodine of 20 mCi vs 10–15 mCi in Graves' disease. BMC Endocr Disord. 2024;24(54). doi: 10.1186/s12902-024-01588-3.
15. Mahmoud HA, Alsanory AAAA, Mostafa HG, Hassan ER. Factors affecting timing of hypothyroidism following radioactive iodine therapy (RAIT) for patients with Graves' disease: A 12-month observational study. Nucl Med Commun. 2024;45(6):499-509. doi: 10.1097/MNM.0000000000001838.

Copyright© AE&M all rights reserved.

Archives of Endocrinology and Metabolism
ISSN 2359-4292
OFFICIAL JOURNAL OF THE BRAZILIAN SOCIETY OF ENDOCRINOLOGY AND METABOLISM

original

Role of insulin-regulated aminopeptidase as potential biomarker in insulin resistant polycystic ovary syndrome patients

Osman Köse[1]
https://orcid.org/0000-0001-5656-6853

Koray Gök[2]
https://orcid.org/0000-0002-7420-1484

Elif Köse[3]
https://orcid.org/0000-0002-2232-4538

Sezen Irmak Gözükara[4]
https://orcid.org/0000-0002-4825-4611

Abdullah Tüten[2]
https://orcid.org/0000-0002-8495-6426

Mehmet Sühha Bostancı[1]
https://orcid.org/0000-0002-4776-6244

1 Department of Obstetrics and Gynecology, Sakarya University Faculty of Medicine, Sakarya, Turkey.
[2] Department of Obstetrics and Gynecology, Cerrahpasa Faculty of Medicine, Istanbul University-Cerrahpasa, Istambul, Turkey.
[3] Department of Public Health, Sakarya University Faculty of Medicine, Adapazarı, Sakarya, Turkey.
[4] Clinic of Medical Biochemistry, Sakarya Training and Research Hospital, Adapazarı, Sakarya, Turkey.

ABSTRACT

Objective: To measure serum insulin-regulated aminopeptidase levels in women diagnosed with polycystic ovary syndrome and to investigate their potential contribution of these levels to the development of insulin resistance, which plays a central role in the pathophysiology of polycystic ovary syndrome. **Methods**: The study group, recruited between May and December 2021, consisted of 40 patients diagnosed with polycystic ovary syndrome and 40 age-matched healthy controls. Serum insulin-regulated aminopeptidase levels were compared between the groups using the ELISA method. **Results**: Serum insulin-regulated aminopeptidase levels were significantly lower in the polycystic ovary syndrome group compared with the control group ($p < 0.001$). Subparameter assessments revealed that insulin-regulated aminopeptidase levels were even lower in insulin-resistant polycystic ovary syndrome patients ($p = 0.001$). Moreover, insulin-regulated aminopeptidase levels demonstrated a statistically significant negative correlation with fasting blood glucose, insulin, glycated hemoglobin, and HOMA-IR values. **Conclusion**: Serum insulin-regulated aminopeptidase levels were found to be lower in women with polycystic ovary syndrome than those in healthy controls. Furthermore, these levels appear to reflect insulin resistance, a key factor in the pathogenesis of polycystic ovary syndrome. Overall, these findings suggest that insulin-regulated aminopeptidase may serve as a potential biomarker for the identififfication of insulin resistance in women with polycystic ovary syndrome.

Keywords: Polycystic ovary syndrome; Insulin; Insulin resistance

INTRODUCTION

Polycystic ovary syndrome (PCOS) is one of the most common endocrine disorder among women of reproductive age, affecting approximately 11 to 13% of the global female population (1,2). It is a heterogeneous condition characterized by three core diagnostic features – hyperandrogenism, chronic anovulation, and polycystic ovarian morphology – often accompanied by metabolic abnormalities such as insulin resistance (IR) and obesity (3). Although the pathophysiology of PCOS is not fullyunderstood, it is thought to involve a combination of genetic predisposition, environmental factors, oxidative stress, chronic low-grade inflammation, and metabolic dysregulation (3,4). Insulin resistance, which plays a central role in the etiology of the disease, is present in approximately 50 to 80% of patients and contributes to hyperandrogenemia and reproductive dysfunction through multiple mechanisms (5,6). However, the exact mechanisms underlying IR in PCOS remain unclear, warranting further research (4). It has long been established that alterations in glucose transporters (GLUT) are involved in the development of IR. The primary mechanism is insulin-stimulated cellular glucose uptake, which is facilitated by

Received on Jul/17/2025
Accepted on Oct/4/2025

DOI: 10.20945/2359-4292-2026-0011

Correspondence to:
Osman Köse
koseo@sakarya.edu.tr

Associated editor:
Letícia F. Gontijo Silveira
https://orcid.org/0000-0002-0053-9167

This is an open-access article distributed under the terms of the Creative Commons Attribution License

Copyright© AE&M all rights reserved.

the translocation of GLUT4-containing vesicles from the cytoplasm to the plasma membrane (7). Insulin-regulated aminopeptidase (IRAP), a cellular protein featuring both intracellular and extracellular functional sites, is essential for this translocation process and plays a critical role in insulin-mediated glucose uptake via GLUT-4 in skeletal muscle and adipose tissue. During this process, its extracellular domain is cleaved by metalloproteases and released into the bloodstream (8). Given these functions, circulating IRAP levels have been proposed as a potential biomarker for IR, as demonstrated in previous studies in patients with type 2 diabetes (8,9). However, a review of the existing literature indicates that this association has not yet been investigated in women with PCOS.

For these reasons, this study aimed to measure serum IRAP levels in women diagnosed with PCOS and to investigate their potential contribution of these levels to the development of IR, which plays a central role in the pathophysiology of PCOS.

METHODS

This case-control study was conducted between May and December 2021 at the Department of Obstetrics and Research Hospital. Ethical approval was obtained from the Ethics Committee of the Faculty of Medicine, Sakarya University (date: May 7, 2021, approval no: 90). The study was conducted in accordance with the principles of the Declaration of Helsinki, and written informed consent was obtained from all volunteers.

The study included 40 patients diagnosed with PCOS according to the Rotterdam criteria (2003). The control group consisted of 40 healthy women of similar age and body mass index (BMI) who presented to the clinic for routine gynecological examinations. The inclusion criteria for all participants were an age range of 18 to 40 years and a BMI between 20 to 35 kg/m². For the control group, the absence of any significant gynecological pathology was required; only minor complaints such as dysmenorrhea or premenstrual syndrome were permitted.

The exclusion criteria for all participants were as follows: a history of smoking; current pregnancy or lactation; previous ovarian surgery; a diagnosis of endometrioma or endometriosis; thyroid disorders or abnormal prolactin levels; use of hormonal therapy (e.g., oral contraceptives) within the past 6 months; use of medications known to affect carbohydrate metabolism (e.g., insulin, cortisol); a history of chronic disease (e.g., epilepsy, renal failure, heart disease); and a history of cancer.

Clinical data and laboratory results of the participants were retrospectively collected from medical records. The following parameters were recorded: age, height, weight, intermenstrual interval, and the presence of oligo-anovulation and hirsutism. Body mass index was calculated using the formula: BMI = weight (kg) / [height (m)]².

The diagnosis of PCOS was established according to the Rotterdam criteria, which requires the presence of at least two of the following three features:

- Oligo-ovulation or amenorrhea, defined as a menstrual cycle exceeding 35 days or the absence of menses for 3 consecutive months, respectively.
- Clinical hyperandrogenism, primarily evidenced by hirsutism. This was assessed using the modified Ferriman-Gallwey (mFG) scoring system, where nine androgen-sensitive body areas were assigned a score from zero (no terminal hair growth) to 4 (extensive hair growth). A total mFG score of ≥ 8 was considered diagnostic (11).
- Biochemical hyperandrogenism, defined as an elevated serum level of any of the following androgens: total testosterone (reference range: 0.04 to 4.18 ng/dL), dehydroepiandrosterone sulfate (DHEAS) (reference range: 10 to 248 µg/dL), or 17-OH-progesterone (reference range: 0.2 to 1.0 ng/mL) (12-14). All participants underwent routine gynecological and transvaginal ultrasonographic examinations during the early follicular phase (days 2 to 4) of a spontaneous menstrual cycle. For the diagnosis of PCOS, polycystic ovarian morphology was defined according to the Rotterdam criteria as the presence of ≥ 20 follicles (2 to 9 mm in diameter) per ovary and/or an ovarian volume > 10 mL (15). The control group consisted of healthy women with regular menstrual cycles (26 to 32 days), normal ovarian morphology, and no evidence of clinical or biochemical hyperandrogenism.

Copyright© AE&M all rights reserved.

Laboratory studies

Blood samples were obtained from the brachial vein during the early follicular phase (cycle days 2 to 4) following an 8-hour overnight fast. A total of 16 mL of venous blood was collected from each participant into two tubes in the early morning. From one tube, the following serum analyses were performed: anti-Müllerian hormone (AMH), follicle-stimulating hormone (FSH), luteinizing hormone (LH), thyroid-stimulating hormone (TSH), total testosterone, free testosterone, DHEAS, 17-hydroxyprogesterone (17-OHP), fasting glucose, and fasting insulin. Serum AMH levels were quantified using a chemiluminescent immunoassay (Access AMH kits, Beckman Coulter Access 2 analyzer). This assay had a measurement range of 0.02 to 24 ng/mL, with an intra-assay coefficient of variation (CV) of 1.7% and an inter-assay CV of 3.1%. FSH, LH, TSH, total testosterone, insulin, and DHEAS levels were measured by chemiluminescent immunoassay on an Abbott Architect i2000 analyzer (Abbott Diagnostics). The inter-assay CVs were as follows: ≤ 10% for FSH, ≤ 7% for LH, ≤ 10% for TSH, ≤ 10% for total testosterone, ≤ 7% for insulin, and ≤ 10% for DHEAS. Fasting glucose levels were determined via the hexokinase method on a Beckman Coulter AU5800 analyzer. The assay demonstrated an intra-assay CV of 0.7%, a total CV of 0.9%, and a measurement range of 10 to 800 mg/dL. Serum 17-OHP and free testosterone levels were measured using radioimmunoassays (RIA) with Diasource kits. For the 17-OHP assay, the intra-assay CV was 6.8%, the inter-assay CV was 8.7%, and the measurement range was 0.17 to 14 ng/mL. For the free testosterone assay, the intra-assay CV was 5.7%, the inter-assay CV was 7.3%, and the measurement range was 0.3 to 90 pg/mL. Insulin resistance was evaluated using the homeostasis model assessment of insulin resistance (HOMA-IR), calculated as [fasting insulin (μU/mL) × fasting glucose (mg/dL)] / 405. A HOMA-IR value ≥ 2.5 was defined as indicative of IR.

The blood samples taken with the second tube blood sample were centrifuged at 4,000 rpm for 10 minutes, then the serums were separated and put into a deep freezer to be stored at -80°C until the day of analysis. On the study day, all samples were thawed in the same month and Human ICE protease-activating factor (IRAP) levels were measured using ELISA kits (MyBioSource, San Diego, USA, Catalog no: MBS260922). The results were calculated using the Biotek ELX800 (USA) ELISA reader, while the intra-measurement CV was reported as < 8% and the inter-measurement coefficient of variation as < 12%.

Statistics

Descriptive statistics are presented as mean ± standard deviation for normally distributed continuous variables and median (first-third quartiles) for non-normally distributed variables. Comparisons between groups for parametric and non-parametric data were performed using the Student's *t*-test and the Mann-Whitney U test, respectively. Correlations between continuous variables were assessed using Pearson's correlation coefficient. The discriminatory power of IRAP for diagnosing PCOS was evaluated using Receiver Operating Characteristic (ROC) curve analysis. A p-value of less than 0.05 was considered statistically significant. All analyses were conducted using IBM Statitical Package for the Social Sciences (SPSS) statistics, Version 20.0.

RESULTS

The clinical and laboratory findings of the participants in the patient and control groups included in this study are shown in **Table 1**. Serum LH, total testosterone, AMH, DHEAS, fasting glucose, insulin, and HOMA-IR values were significantly higher in the PCOS group than the control group. In contrast, serum IRAP levels were significantly lower in the PCOS group compared to the control group. Laboratory data comparing PCOS patients with and without IR are shown in **Table 2**. Accordingly, serum IRAP levels were significantly lower in the insulin-resistant group. The correlation of serum IRAP levels with biochemical variables is presented in **Table 3**. IRAP levels show a significant negative correlation with insulin, HbA1c, fasting blood glucose levels, and HOMA-IR.

The ROC curve for IRAP concentrations in the PCOS group is shown in **Figure 1**. The area under the curve was 83.1% (95% confidence interval: 0.744-0.918). The optimal cut-off value was 0.655 ng/mL, and the rates below this value were 82.5% and 70.0% for sensitivity and specificity, respectively (p=0.001).

Copyright© AE&M all rights reserved.

Table 1. Comparison of the clinical and laboratory characteristics of the women with polycystic ovary syndrome and the control group

	PCOS Median (1.-3. Quarter)	Control Median (1.-3. Quarter)	p-value
Age, years	27,00 (25,00-29,00)	28,00 (24,00-30,00)	0.674*
BMI, kg/m	26,82 ± 4,08	25,00 ± 4,27	0.054†
Serum fasting glucose, mg/dL	95,98 ± 7,80	89,90 ± 7,98	0.001†
LH, mIU/mL	11,47 ± 3,94	6,98 ± 2,62	< 0.001†
AMH, ng/mL	10,11 (6,87-13,48)	7,22 (5,11-8,54)	< 0.001*
FSH, mIU/mL	6,03 (5,19-7,31)	5,67 (5,00-6,00)	0.023*
TSH, uIU/mL	1,76 (1,19-2,46)	1,78 (1,42-2,49)	0.893*
Prolactin, ng/mL	14,80 (10,33-19,50)	13,15 (9,71-18,43)	0.587*
HDL, mg/dL	56,00 (48,36-63,25)	51,22 (43,25-61,25)	0.178*
LDL, mg/dL	118,50 (100,25-145,00)	105,00 (98,00-121,50)	0.204*
Cholesterol, mg/dL	157,80 ± 28,98	154,18 ± 17,85	0.504†
Triglycerides, mg/dL	86,00 (66,50-119,75)	69,07 (54,25-95,00)	0.030*
17-OH Progesterone, ng/mL	1,28 (0-87-2,02)	0,70 (0,57-0,87)	< 0.001*
Free testosterone, pg/mL	2,20 (1,74-3,01)	1,84 (1,38-2,17)	0.001*
Total testosterone, ng/dL	35,75 (28,13-48,68)	24,95 (20,57-31,57)	< 0.001*
DHEAS, µg/dL	318,81 ± 90,08	233,19 ± 66,05	< 0.001†
F-G score	13,00 (11,00-15,75)	7,00 (6,00-8,00)	< 0.001*
HOMA-IR	3,45 ± 1,46	1,60 ± 0,93	< 0.001†
Insulin, µIU/mL	13,90 ± 4,94	7,19 ± 4,00	< 0.001*
HbA1c	5,83 ± 0,43	5,16 ± 0,35	< 0.001†
IRAP, ng/mL	0,47 ± 0,19	0,73 ± 0,17	< 0.001†

*Mann-Whitney U Test, †Student t-test.

Results expressed as mean ± standard deviation.

POCUS: polycystic ovary syndrome; BMI: body mass index; LH: luteinizing hormone; AMH: Anti-Müllerian hormone; FSH: follicle-stimulating hormone; TSH: thyroid-stimulating hormone; HDL: high-density lipoprotein; LDL: low-density lipoprotein; DHEAS: dehydroepiandrosterone sulfate; F-G score: Ferriman-Gallwey score; HOMA-IR: homeostatic model assessment for insulin resistance; HbA1c: glycated hemoglobin; IRAP: insulin-regulated aminopeptidase.

Table 2. Comparison of laboratory tests in insulin resistant and non-insulin resistant polycystic ovary syndrome patients according to the homeostatic model assessment for insulin resistance cut-off of 2.5

	PCOS Insulin resistance +	PCOS Insulin resistance -	p-value*
Serum fasting glucose, mg/dL	104,04 ± 6,01	90,21 ± 4,55	< 0.001
Serum fasting insulin, µIU/mL	17,09 ± 3,66	9,11 ± 1,50	< 0.001
HOMA-IR	4,41± 1,09	2,03 ± 0,34	< 0.001
HbA1c, %	6,11 ± 0,23	5,42 ± 0,32	< 0.001
IRAP, ng/mL	0,39 ± 0,16	0,59 ± 0,16	0.001

* Student t test.

POCUS: polycystic ovary syndrome; HOMA-IR: homeostatic model assessment for insulin resistance; HbA1c: glycated hemoglobin; IRAP: insulin-regulated aminopeptidase.

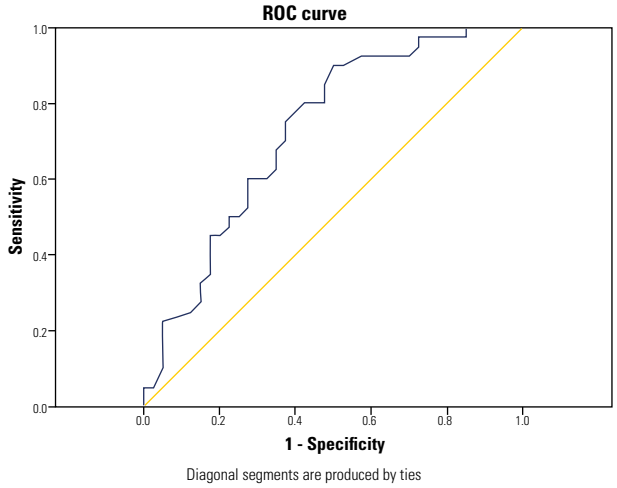
Table 3. Correlation of serum insulin-regulated aminopeptidase levels with biochemical variables in the polycystic ovary syndrome group

PCOS-IRAP	r	p-value
Serum fasting glucose, mg/dL	-0.604	< 0.001
HOMA-IR	-0.642	< 0.001
Insulin, µIU/mL	-0.617	< 0.001
HbA1c, %	-0.507	0.001
Free testosterone, pg/mL	-0.221	0.170
Total testosterone, ng/dL	-0.276	0.085
SDHEA, µg/dL	0.194	0.231

r: Pearson correlation coefficient.

HOMA-IR: homeostatic model assessment for insulin resistance; HbA1c: glycated hemoglobin; SDHEA: serum dehydroepiandrosterone sulfate.

Copyright© AE&M all rights reserved.



ROC: Receiver Operating Characteristic.

Figure 1. Receiver Operating Characteristic analysis of the discrimination of insulin-regulated aminopeptidase values of polycystic ovary syndrome cases.

DISCUSSION

Our results demonstrate that serum IRAP levels are significantly lower in the PCOS group than in the control group. Notably, a further reduction in IRAP levels was observed in PCOS patients with IR relative to those without, suggesting a significant influence of IR on IRAP expression. These findings suggest that IRAP may be associated not only with IR but also with hormonal disorders. Significant negative correlations were also observed between serum IRAP levels and fasting insulin, fasting glucose, HbA1c, and HOMA-IR. These correlations suggest that decreased IRAP levels are linked to IR and dysregulated glucose metabolism, positioning IRAP as a potential biomarker for IR. This finding aligns with existing literature. Furthermore, weak negative correlations were identified between IRAP levels and serum DHEAS, free testosterone, and total testosterone concentrations in PCOS patients. These findings suggest that IRAP may be associated not only with IR but also with hormonal disorders. The interactions between insulin, GLUT-4, and its closely associated protein, IRAP, are integral to regulating cellular glucose uptake, maintaining whole-body glucose homeostasis, and ensuring metabolic equilibrium. Disruptions in this intricate process can lead to IR. A review of the literature indicates that previous investigations into GLUT-4 and its role in IR in PCOS patients have relied on invasive methods, such as biopsies of adipocyte and endometrial tissue (16-18). As a less invasive alternative to these approaches, we hypothesized that measuring serum IRAP levels could serve as a surrogate marker for GLUT-4 translocation to the plasma membrane and, by extension, provide a reflection of IR in PCOS patients. This premise formed the rationale for the present study.

A review of the literature indicates that numerous studies have investigated the relationship between IR and IRAP. Research has demonstrated reduced IRAP translocation in both diabetic rats 19 and patients with type 2 diabetes mellitus (T2DM) (20,21). These foundational studies, which utilized invasive biopsy methods to analyze adipocyte (19,21) and skeletal muscle tissue (20), established a clear link between impaired IRAP activity and IR. Subsequent clinical investigations have employed a more practical, non-invasive approach by measuring serum IRAP levels. These studies consistently report decreased circulating IRAP levels in individuals with T2DM (8,9) and in pregnant women with gestational diabetes (22). Collectively, these findings from both tissue-based and serum-based analyses suggest that reduced IRAP levels may serve as a useful indicator of IR.

In our study, we found that the serum IRAP levels were significantly lower in the insulin-resistant group. It is well-established that insulin stimulation triggers the translocation of IRAP and GLUT4 to the plasma membrane as a complex. Subsequently, the extracellular domain of IRAP is cleaved by metalloproteases and released into the circulation (8,23). In states of IR, this physiological process is disrupted, leading to reduced cleavage and secretion of IRAP and, consequently, lower circulating levels. The findings of the present study are consistent with this mechanism and align with previous reports in the literature.

The PCOS group exhibited significantly higher levels of IR markers, including fasting insulin, fasting glucose, HbA1c, and HOMA-IR, relative to healthy controls. Consistent with this metabolic profile, serum IRAP levels showed a significant negative correlation with these indices. This inverse association provides important evidence linking lower IRAP levels to the development of IR in PCOS.

Copyright© AE&M all rights reserved.

As a result of our study, we found that serum IRAP levels were significantly lower in the insulin-resistant group. Moreover, IRAP levels demonstrated strong and statistically significant negative correlations with metabolic parameters, including fasting glucose, insulin, HOMA-IR, and HbA1c, indicating that higher IR and poorer glycemic control are associated with lower IRAP levels in PCOS patients. In contrast, IRAP levels showed weak and statistically non-significant correlations with hormonal parameters, including free and total testosterone and DHEA-S. Overall, these findings suggest that IRAP is more closely associated with metabolic disturbances than with androgen levels in PCOS, implying that circulating IRAP levels may primarily reflect IR, while their potential relationship with other hormonal parameters warrants further investigation in future studies.

The main limitations of this study include its case-control design, the relatively small sample size, the limited number of participants in the PCOS subgroups, and the use of the HOMA-IR index rather than the hyperinsulinemic-euglycemic clamp, which is considered the gold-standard method for assessing IR. An additional limitation is that the ACTH stimulation test was not performed to definitively rule out non-classical congenital adrenal hyperplasia (in patients with elevated 17-OH progesterone levels. Although clinical evaluation and DHEAS levels did not indicate non-classical congenital adrenal hyperplasia, future studies should incorporate this test to provide a more definitive differential diagnosis.

CONCLUSION

This study provides the first evidence linking reduced serum insulin-regulated aminopeptidase levels to polycystic ovary syndrome. Notably, insulin-regulated aminopeptidase levels were significantly lower in polycystic ovary syndrome patients both with and without insulin resistance compared to controls. The significant negative correlations observed between insulin-regulated aminopeptidase levels and indices of both insulin resistance and hyperandrogenemia indicate that insulin-regulated aminopeptidase may be involved in the core metabolic and endocrine disturbances characterizing the pathogenesis of polycystic ovary syndrome.

Author contributions: Conceptualization: Osman Köse, Mehmet Sühha Bostanci, Koray Gök; Methodology: Osman Köse, Mehmet Sühha Bostanci, Koray Gök; Software: Elif Köse; Validation: Elif Köse, Sezen Irmak Gözükara; Formal analysis: Elif Köse, Sezen Irmak Gözükara; Investigation: Osman Köse, Elif Köse, Abdullah Tüten, Mehmet Sühha Bostanci; Resources: Osman Köse, Elif Köse, Abdullah Tüten, Mehmet Sühha Bostanci; Data curation: Elif Köse, Sezen Irmak Gözükara; Writing – original draft preparation: Osman Köse, Elif Köse, Abdullah Tüten, Mehmet Sühha Bostanci; Writing – review & editing: Osman Köse, Elif Köse, Abdullah Tüten, Mehmet Sühha Bostanci, Koray Gök; Visualization: Osman Köse, Elif Köse; Supervision: Osman Köse, Elif Köse, Abdullah Tüten; Project administration: Osman Köse, Mehmet Sühha Bostanci, Koray Gök; Funding acquisition: Osman Köse, Elif Köse, Abdullah Tüten. We confirm that this work is original, has not been published previously, and is not under consideration for publication elsewhere.

Financial disclosure: the authors declare that this study received no financial support.

Disclosure: no potential conflict of interest relevant to this article was reported.

Data availability: datasets related to this article will be available upon request to the corresponding author.

REFERENCES

1. Stener-Victorin E, Teede H, Norman RJ, Legro R, Goodarzi MO, Dokras A, et al. Polycystic ovary syndrome. Nat Rev Dis Primers. 2024;10(1):27. doi: 10.1038/s41572-024-00511-3
2. Teede HJ, Tay CT, Laven J, Dokras A, Moran LJ, Piltonen TT, et al. International PCOS Network. Recommendations from the 2023 International Evidence-based Guideline for the Assessment and Management of Polycystic Ovary Syndrome. Fertil Steril. 2023;120(4):767-93. doi: 10.1016/j.fertnstert.2023.07.025
3. Sadeghi HM, Adeli I, Calina D, Docea AO, Mousavi T, Daniali M, et al. Polycystic ovary syndrome: a comprehensive review of pathogenesis, management, and drug repurposing. Int J Mol Sci. 2022;23(2):583. doi: 10.3390/ijms23020583
4. Zhao H, Zhang J, Cheng X, Nie X, He B. Insulin resistance in polycystic ovary syndrome across various tissues: an updated review of pathogenesis, evaluation, and treatment. J Ovarian Res. 2023;16(1):9. doi: 10.1186/s13048-022-01091-0
5. Chen W, Pang Y. Metabolic Syndrome and PCOS: Pathogenesis and the role of metabolites. Metabolites. 2021;11(12):869. doi: 10.3390/metabo11120869
6. Cassar S, Misso ML, Hopkins WG, Shaw CS, Teede HJ, Stepto NK. Insulin resistance in polycystic ovary syndrome: a systematic review and meta-analysis of euglycaemic-hyperinsulinaemic clamp studies. Hum Reprod. 2016;31(11):2619-31. doi: 10.1093/humrep/dew243
7. Bryant NJ, Govers R, James DE. Regulated transport of the glucose transporter GLUT4. Nat Rev Mol Cell Biol. 2002;3(4):267-77. doi: 10.1038/nrm782
8. Trocmé C, Gonnet N, Di Tommaso M, Samouda H, Cracowski JL, Cracowski C, et al. Serum IRAP, a novel direct biomarker of prediabetes and type 2 diabetes? Front Mol Biosci. 2021;7:596141. doi: 10.3389/fmolb.2020.596141
9. Mostafa TM, El-Gharbawy NM, Werida RH. Circulating IRAPe, Irisin, and IL-34 in relation to insulin resistance in patients with type 2 diabetes. Clin Ther. 2021;43(7): e230-e240. doi: 10.1016/j.clinthera.2021.05.003
10. Smet ME, McLennan A. Rotterdam criteria, the end. Australas J Ultrasound Med. 2018;21(2):59-60. doi: 10.1002/ajum.12096

Copyright© AE&M all rights reserved.

11. Ferriman D, Gallwey JD. Clinical assessment of body hair growth in women. J Clin Endocrinol Metab. 1961; 21:1440-7. doi: 10.1210/jcem-21-11-1440
12. Al Kindi MK, Al Essry FS, Al Essry FS, Mula-Abed WA. Validity of serum testosterone, free androgen index, and calculated free testosterone in women with suspected hyperandrogenism. Oman Med J. 2012;27(6):471-4. doi: 10.5001/omj.2012.112
13. Turpeinen U, Itkonen O, Ahola L, Stenman UH. Determination of 17alpha-hydroxyprogesterone in serum by liquid chromatography-tandem mass spectrometry and immunoassay. Scand J Clin Lab Invest. 2005;65(1):3-12. doi: 10.1080/00365510410008421
14. Haymond S, Gronowski AM. Reproductive related disorders. In: Burtis CA, Ashwood ER, Bruns DE, editors. Tietz textbook of clinical chemistry and molecular diagnostics. 4th ed. St. Louis, Missouri: Elsevier Inc.; 2006. p. 2132-4.
15. Teede HJ, Tay CT, Laven JJE, Dokras A, Moran LJ, Piltonen TT, et al. Recommendations from the 2023 International Evidence-based Guideline for the Assessment and Management of Polycystic Ovary Syndrome. J Clin Endocrinol Metab. 2023;108(10):2447-69. doi:10.1210/clinem/dgad463
16. Cabrera-Cruz H, Oróstica L, Plaza-Parrochia F, Torres-Pinto I, Romero C, Vega M. The insulin-sensitizing mechanism of myo-inositol is associated with AMPK activation and GLUT-4 expression in human endometrial cells exposed to a PCOS environment. Am J Physiol Endocrinol Metab. 2020;318(2): E237-E248. doi: 10.1152/ajpendo.00162.2019
17. Ezeh U, Chen IY, Chen YH, Azziz R. Adipocyte Insulin Resistance in PCOS: Relationship with GLUT-4 Expression and Whole-Body Glucose Disposal and β-Cell Function. J Clin Endocrinol Metab. 2020;105(7): e2408-20. doi: 10.1210/clinem/dgaa235
18. Li J, Chen S, Qin R, Liu X, Fan L, Wei M, et al. Talin1 regulates glucose metabolism and endometrial receptivity via GLUT-4 in patients with polycystic ovary syndrome and insulin resistance. Gynecol Endocrinol. 2023;39(1):2231085. doi: 10.1080/09513590.2023.2231085
19. Takeuchi M, Itakura A, Okada M, Mizutani S, Kikkawa F. Impaired insulin-regulated membrane aminopeptidase translocation to the plasma membrane in adipocytes of Otsuka Long Evans Tokushima Fatty rats. Nagoya J Med Sci. 2006;68(3-4):155-63.
20. Garvey WT, Maianu L, Zhu JH, Brechtel-Hook G, Wallace P, Baron AD. Evidence for defects in the trafficking and translocation of GLUT4 glucose transporters in skeletal muscle as a cause of human insulin resistance. J Clin Invest. 1998;101(11):2377-86. doi: 10.1172/JCI1557
21. Maianu L, Keller SR, Garvey WT. Adipocytes exhibit abnormal subcellular distribution and translocation of vesicles containing glucose transporter 4 and insulin-regulated aminopeptidase in type 2 diabetes mellitus: implications regarding defects in vesicle trafficking. J Clin Endocrinol Metab. 2001;86(11):5450-6. doi: 10.1210/jcem.86.11.8053
22. Tian C, Huang Z, Wen Z. Associations between serum placental leucine aminopeptidase and pregnancy outcomes. Int J Gynaecol Obstet. 2016;135(3):255-8. doi: 10.1016/j.ijgo.2016.05.016
23. Rubin BR, Bogan JS. Intracellular retention and insulin-stimulated mobilization of GLUT4 glucose transporters. Vitam Horm. 2009;80:155-92. doi: 10.1016/S0083-6729(08)00607-9

Copyright© AE&M all rights reserved.

Archives of Endocrinology and Metabolism
ISSN 2359-4292
OFFICIAL JOURNAL OF THE BRAZILIAN SOCIETY OF ENDOCRINOLOGY AND METABOLISM

case report

Immunotherapy response in microsatellite-stable poorly differentiated thyroid carcinoma with mismatch repair deficiency and high tumor mutational burden

João Henrique Feldmann[1]
https://orcid.org/0009-0006-7527-0285

João Felipe Feldmann[1]
https://orcid.org/0009-0005-6435-1349

Cassio Murilo Hidalgo-Filho[1]
https://orcid.org/0000-0002-7046-0059

Gustavo Luis Contado Alves[1]
https://orcid.org/0009-0006-4929-7206

Rafael Sarlo Vilela[2]
https://orcid.org/0000-0003-3054-0692

Sérgio Gonçalves[3]
https://orcid.org/0000-0001-6742-608X

Gilberto de Castro Júnior[1]
https://orcid.org/0000-0001-8765-3044

[1] Departamento de Oncologia Clínica, Hospital Sírio-Libanês, São Paulo, SP, Brasil
[2] Departamento de Patologia, Hospital Sírio-Libanês, São Paulo, SP, Brasil
[3] Departamento de Cirurgia de Cabeça e Pescoço, Hospital Sírio-Libanês, São Paulo, SP, Brasil

ABSTRACT

Poorly differentiated thyroid carcinoma (PDTC) is a rare and aggressive malignancy with a poor prognosis. Immunotherapy is typically guided by agnostic biomarkers such as microsatellite instability-high or high tumor mutational burden (TMB); however, these biomarkers are uncommon in PDTC. Therefore, identifying alternative predictive biomarkers remains an urgent necessity. We report the case of a 71-year-old woman who presented with life-threatening locoregional disease and was ineligible for radioiodine or tyrosine kinase inhibitors due to a prior subarachnoid hemorrhage. Molecular profiling of the resected tumor revealed a high TMB (10 mut/Mb), somatic mutations in MSH2 and ATM, and microsatellite stability (MSS). Immunohistochemistry demonstrated complete loss of MSH2/MSH6 expression, while PD-L1 expression was 20% (tumor proportion score). Based on these findings, pembrolizumab was initiated as first-line therapy. The patient experienced clinical improvement and maintained a sustained partial response for seven months, with excellent tolerability. This case represents one of the few documented reports of PDTC with MSS exhibiting marked responsiveness to immunotherapy. Our findings underscore that alternative biomarkers, such as somatic mutations in DNA repair genes including MSH2 and ATM, may predict unexpected responses to immune checkpoint blockade and inform therapeutic decisions, even in the context of MSS and borderline TMB. Broader implementation of molecular profiling is warranted to identify such patients.

Keywords: Thyroid cancer; poorly differentiated thyroid cancer; immunotherapy; MSH2; microsatellite stable

INTRODUCTION

Thyroid cancer (TC), the most prevalent endocrine malignancy, has experienced a 313% surge in global incidence over the past four decades. In the United States alone, 44,020 new cases are projected for 2025, with over 87% classified as well-differentiated thyroid carcinomas (WDTCs) (1). Poorly differentiated thyroid carcinoma (PDTC) accounts for only 2–15% of cases but contributes disproportionately to TC-related mortality. Originating from follicular cells, PDTC represents an intermediate clinicopathological entity between WDTC and anaplastic thyroid carcinoma (ATC) and is currently recognized as a distinct disease category by the World Health Organization. Although only 15% of PDTC patients present with metastases at diagnosis, distant metastatic disease develops in 37–85% of cases, and 60% of patients succumb to disease progression. Survival rates decline significantly, from 50–85% at 5 years, to 34–50% at 10 years, and ultimately to 0% at 15 years (2).

Received on Aug/4/2025
Accepted on Nov/5/2025
DOI: 10.20945/2359-4292-2026-0008

Correspondence to:
João Henrique Feldmann
Departamento de Oncologia Clínica,
Hospital Sírio-Libanês,
01308050 – São Paulo, SP, Brasil

Associated editor:
Rosália do Prado Padovani
https://orcid.org/0000-0002-5497-6813

This is an open-access article distributed under the terms of the Creative Commons Attribution License

Copyright© ACE&M all rights reserved.

The spectrum of genomic alterations in PDTC reflects a highly heterogeneous disease, mainly due to varying diagnostic criteria employed across studies (3). The molecular profile is characterized by mutations in *HRAS*, *KRAS*, and *NRAS* (25–35% combined), *BRAF* (15–33%), components of the PI3K/AKT/mTOR pathway (11%), *PTEN* (4–33%), *EIF1AX* (11%), *TERT* promoter (40%), *TP53* (16–28%), and *ATM* (7%), resulting in an intermediate mutational profile between WDTC and ATC (4,5). Compared to ATC, PDTC exhibits a higher frequency of gene fusions (10–14%) (5).

Regarding tumor mutational burden (TMB), PDTCs have a reported median of 2 mutations per megabase, and programmed death-ligand 1 (PD-L1) expression levels are similarly low (6). Although PDTC is not typically associated with classic biomarkers predictive of response to immunotherapy, the tumor microenvironment (TME) remains dynamic, with immune editing and tumor-cell interactions influencing cytotoxic or immunosuppressive phenotypes (6). Given the limited treatment options and absence of established therapeutic targets, next-generation sequencing (NGS) panels, as recommended by European Society for Medical Oncology guidelines, are essential (7).

Here, we present an exceptionally rare case of metastatic PDTC showing a remarkable and durable response to immunotherapy in a context traditionally considered unfavorable for such treatment due to microsatellite stability (MSS), borderline TMB, and urgent need for rapid therapeutic response given the risk of airway obstruction. To our knowledge, this is among the first reported cases to suggest that additional defects in DNA repair pathways, such as MSH2 and ATM mutations identified in our patient, may represent actionable biomarkers to guide clinical decision-making, with outcomes surpassing those observed in studies supporting biomarker-agnostic use of immunotherapy.

CASE REPORT

A 71-year-old self-identified White, Hispanic/Latina female with no significant medical, psychosocial, or family history presented with a painless, progressively enlarging left cervical mass over three months **(Figure 1A)**. Doppler ultrasound of the thyroid revealed a solid, expansive lesion in the left thyroid lobe and left cervical lymphadenopathy at levels IIA and IV. Contrast-enhanced computed tomography of the neck and chest demonstrated extensive local invasion, including tracheal narrowing, esophageal compression, obliteration of the left retropharyngeal space, and approximately 180° encasement of the left common carotid artery. The lesion measured 13.7 × 6.8 × 6.5 cm. Additional suspicious lymph nodes were identified at levels II, III, and the left supraclavicular region. Pulmonary parenchyma appeared unremarkable. Bronchoscopy and nasofibrolaryngoscopy confirmed tracheal stenosis due to extrinsic compression and mild asymmetry of the laryngeal region. Clinical staging, according to the 8th edition of the American Joint Committee on Cancer, was cT4bN1bM0.

Fine needle aspiration of the thyroid lesion and left supraclavicular lymph node revealed a proliferative epithelial lesion. Immunohistochemistry was positive for thyroglobulin, TTF-1, PAX8, and GATA3, and negative for calcitonin, supporting the suspicion of a neoplasm of follicular origin. The patient subsequently underwent total thyroidectomy, parathyroidectomy, and lymph node dissection at levels II–VII. Pathological analysis identified a PDTC, based on the latest World Health Organization pathology criteria, measuring 15 cm, with vascular invasion, multifocal disease, and gross extrathyroidal extension into adjacent tissues **(Figures 2A–C)**. Margins were involved, but sampled lymph nodes were negative for malignancy. In the postoperative period, the patient developed a subarachnoid hemorrhage (Fisher IV) with thoracic subdural extension, resulting in motor, speech, and swallowing deficits. This complication necessitated prolonged hospitalization and delayed oncologic follow-up.

Approximately one year after surgery, fluorodeoxyglucose-labeled positron emission tomography indicated a recurrent expansive lesion occupying the left retropharyngeal space, causing oropharyngeal bulging and partial obliteration of the left piriform sinus. Additional findings included lymphadenopathy at levels Ib and II on the left, with displacement of the trachea and esophagus, a right paratracheal lymph node, and distant fluorodeoxyglucose-avid lesions consistent with pulmonary nodules and a lesion in the left costal arch. Given concerns for systemic recurrence, a new lymph node biopsy

Copyright© AE&M all rights reserved.

was performed, and an NGS-based multigene somatic panel was conducted on the thyroidectomy specimen. This analysis involved DNA sequencing for single and multiple nucleotide variants and small insertions and deletions in 510 genes, as well as RNA sequencing for gene fusions in 55 genes, including detection of oncogenic isoforms and alternative splicing variants in 3 genes. These assays were performed using the Illumina TruSight Oncology 500 panel on the Illumina NextSeq 550 platform, utilizing a custom analysis pipeline within BaseSpace Variant Interpreter (v. 3.6.2.0).

Molecular analysis demonstrated microsatellite stability, a TMB of 10 mut/Mb, which is considered high according to the adopted cutoff of ≥10 mut/Mb, and somatic pathogenic variants in *MSH2* (c.1865del, p.(Pro622GlnfsTer13)) and *ATM* (c.5825C>T, p.(Ala1942Val)). Additional mutations were detected in *BCOR*, *CIC*, *DAXX*, *PPM1D*, *SPEN*, and *TP53*. Immunohistochemistry for DNA repair enzymes showed loss of *MSH2* and *MSH6* expression **(Figures 2D–E)**. PD-L1 expression, assessed using the SP263 clone, revealed a tumor proportion score (TPS) of 20% **(Figure 2F)**. Given the diagnosis of metastatic PDTC with DNA repair deficiency, high TMB, positive PD-L1 expression, and a somatic *MSH2* mutation, the patient was started on tumor-agnostic pembrolizumab monotherapy at a dose of 200 mg every three weeks, consistent with the KEYNOTE-158 study (8). The patient achieved symptomatic control, along with a partial response of the primary thyroid lesion, as evidenced by considerable reduction in size **(Figure 1B)**, and stable disease in the lymph nodes, lungs, and bones. Treatment was well tolerated, with immune-mediated hypophysitis and adrenal axis deficiency as the only observed immune-related toxicities; both were managed with physiological doses of glucocorticoids and mineralocorticoids. In February 2025, the patient experienced locoregional disease progression while maintaining excellent systemic disease control. Local radiotherapy was administered, and the patient achieved good disease control without the need for further therapy following discontinuation of immunotherapy, corresponding to a duration of response of approximately seven months.

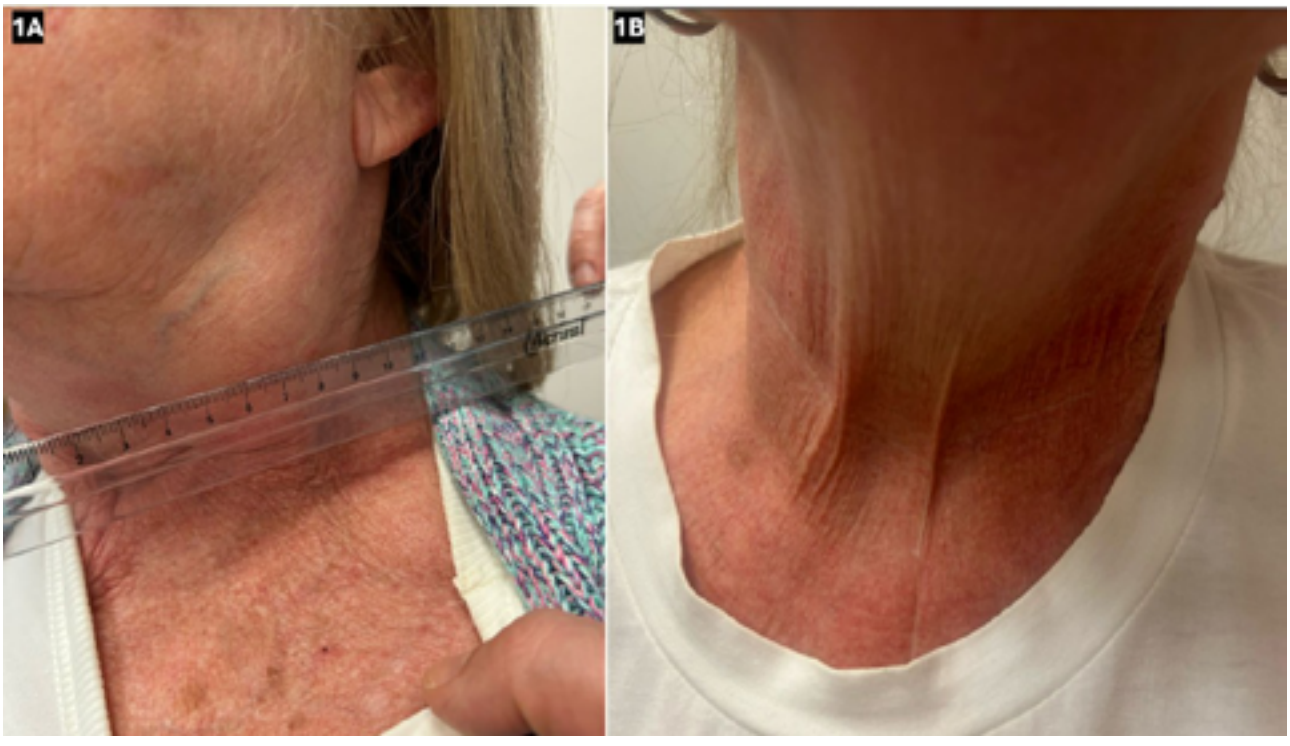


Figure 1. Rapid and marked early clinical response to pembrolizumab. **A**) Left-sided cervical mass, approximately 8 cm in its greatest dimension, noted to be fixed and firm upon palpation. **B**) Palpation and visual assessment of the left cervical mass showed marked tumor reduction following three cycles of pembrolizumab.

Copyright© AE&M all rights reserved.

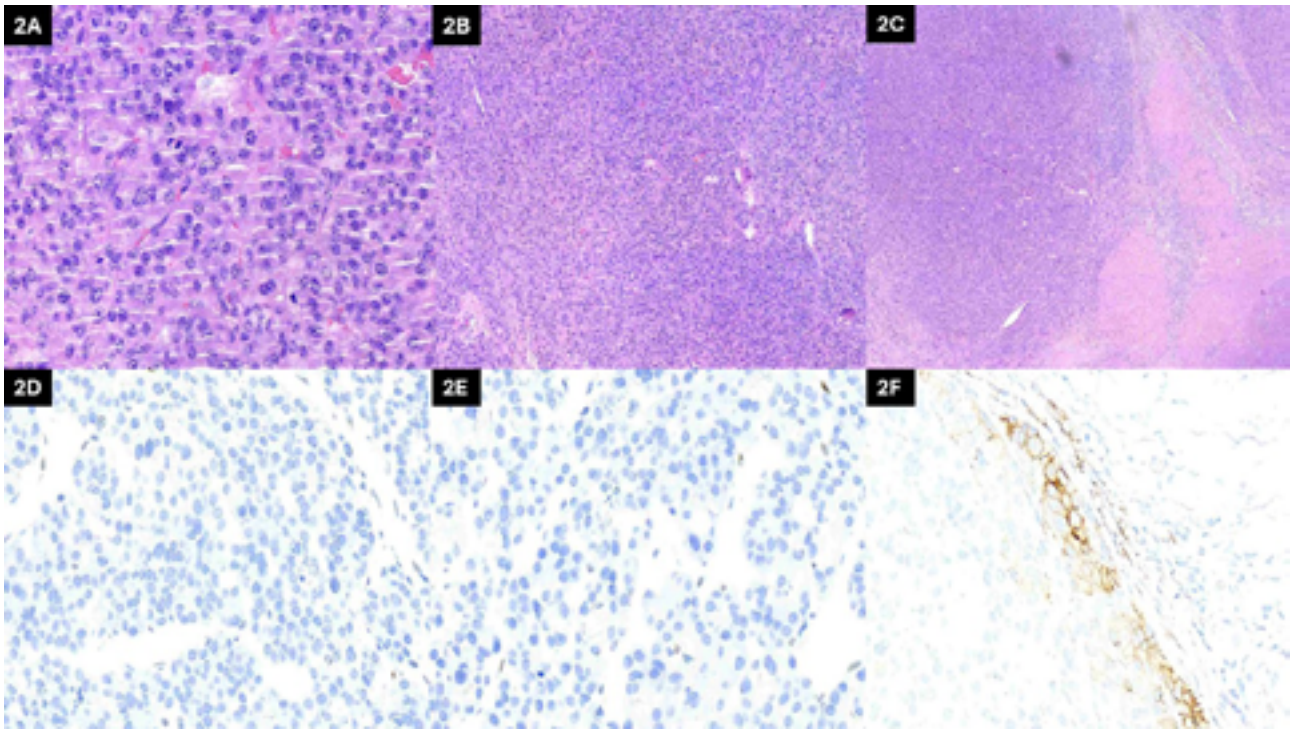


Figure 2. Pathological features of solid carcinoma with PD-L1 expression and MMR deficiency. **A**) hematoxylin and eosin (H&E), 40× magnification: solid-pattern carcinoma with atypical nuclei and frequent mitoses. **B**), H&E, 10× magnification: solid neoplasm with convoluted nuclei, irregular chromatin, and occasional nucleoli. **C**), H&E, 4× magnification: overview of the solid tumor; left side highlights nuclear details; right side indicates extensive necrosis. **D**), immunohistochemistry (IHC) MSH6 (SP93), 40× magnification: loss of nuclear expression. **E**) IHC MSH2 (G219-1129), 40× magnification: loss of nuclear expression. **F**), IHC PD-L1 (SP263), 40× magnification: ~20% tumor proportion score with membranous staining.

DISCUSSION

Poorly differentiated thyroid carcinoma is a rare and aggressive form of TC, with limited treatment options available in advanced stages. Our patient presented with locoregional invasion, pulmonary and osseous metastases, and a high tumor burden, necessitating prompt therapeutic intervention. Owing to a recent subarachnoid hemorrhage, standard systemic therapies such as tyrosine kinase inhibitors posed substantial risk, and radioiodine therapy was not indicated. In this context, pembrolizumab was considered based on a unique molecular profile suggestive of immunogenicity.

Systemic therapies for advanced TC, including sorafenib, lenvatinib, vandetanib, and cabozantinib, are associated with modest response rates and significant toxicity, particularly in poorly differentiated histologies. Specifically, in PDTC, sorafenib has demonstrated overall response rates of approximately 12%, while lenvatinib, cabozantinib, and vandetanib showed overall response rates between 30–35%, with hypertension and cardiovascular events occurring in up to 68% of patients (9-12). Given our patient's recent cerebrovascular event, the risk-benefit profile of tyrosine kinase inhibitors was deemed unfavorable. Moreover, radioiodine therapy was not recommended, given the lack of iodine uptake in PDTC and the urgent need for systemic disease control.

DNA mismatch repair (MMR) defects can be identified by the loss of expression of any MMR protein (e.g., MSH2, MSH6, MLH1, and PMS2) using immunohistochemistry (IHC), indicating deficient MMR status (dMMR); or by polymerase chain reaction or NGS to detect microsatellite instability, defined as microsatellite instability-high (MSI-H). MMR alterations are present in approximately 2–4% of solid tumors and may be discordant in a minority of cases (13,14). Although MSI-H is the prototypical marker of dMMR, growing evidence suggests that dMMR can confer tumor immunogenicity independently of detectable MSI-H. This effect may result from the accumulation of point mutations and frameshifts at non-classical

Copyright© AE&M all rights reserved.

microsatellite loci that results in the formation of immunogenic neoantigens, and by virtue of the engagement of cytosolic nucleic acids activation of innate immune circuits, such as cGAS-STING. Additionally, current MSI testing strategies may underestimate genomic instability within a subset of dMMR tumors, thereby underrepresenting their true immunogenic potential. Collectively, these findings support the concept that MMR deficiency itself, rather than MSI status alone, may be sufficient to render tumors responsive to immune checkpoint blockade (15,16).

Both MMR deficiency and MSI-H are exceedingly rare in TC, a topography not typically associated with Lynch syndrome (13,14). In a series of 485 TC patients, including 17 cases of PDTC, only four were classified as MSI-H with dMMR, all of whom had follicular thyroid carcinomas. Notably, whole-exome sequencing of two MSI-H tumors in that cohort revealed a hemizygous loss-of-function *MSH2* mutation in one case (17). In a separate Korean study including 15 patients with PDTC, three exhibited high TMB (>13 mut/Mb), and one harbored a somatic *MSH2* mutation (18).

In our patient, molecular profiling revealed a frameshift mutation in *MSH2* and concurrent loss of *MSH2/MSH6* expression by IHC, with MSS on NGS. Although not MSI-H, the TMB of 10 mut/Mb exceeds the PDTC median of 2 mut/Mb and the 7.5 mut/Mb mean observed in PDTCs harboring MMR alterations (6). These findings suggest that *MSH2* loss may drive immunogenicity even in MSS tumors, highlighting a potential immune oncology-responsive to immune oncology therapies.

The TME of PDTC is characteristically immune-cold, with low PD-L1 expression and limited immune infiltration. Cameselle García and cols. (8) evaluated the TME and PD-L1 status in 28 patients (15 with ATC and 13 with PDTC), finding that only one PDTC case surpassed the 1% TPS threshold by IHC (1). This outlier exhibited concurrent loss of *MLH1* and *PMS1*, a *TP53* mutation, and increased infiltration of CD3+CD8+ T lymphocytes, S100+ dendritic cells, and CD68+CD163+ macrophages, features characteristic of ATC. Our patient had a TPS of 20% in the context of an MSH2 mutation and dMMR/MSS status, suggesting convergence toward an ATC-like immune phenotype. This observation supports the hypothesis that MMR gene alterations may define a rare immunogenic molecular subgroup within PDTC (8).

Progressive dedifferentiation from WDTC to ATC occurs through the stepwise accumulation of molecular alterations (19). Mutations in *TP53* and ATM have been implicated in this process and are frequently associated with aggressive histologies. In PDTC, ATM mutations have been reported in approximately 7% of cases and up to 9% of ATCs, often co-occurring with *TP53* alterations (2,4). In our case, both mutations were present, supporting the interpretation that these genomic events may act as early drivers of dedifferentiation and underpin the clinically aggressive behavior observed, despite the absence of radioiodine refractoriness or previous systemic treatment. These findings also raise the possibility that such tumors may share therapeutic vulnerabilities with ATC.

Although clinical evidence supporting immune oncology in PDTC remains limited, it is mounting. In the phase 2 KEYNOTE-158 trial, pembrolizumab monotherapy produced objective responses in 7 out of 103 patients with advanced TC, including a complete response in one PDTC case. The median progression-free survival was 4.2 months (20). Another phase 2 trial evaluating ipilimumab plus nivolumab in aggressive TC included five PDTC cases, with a partial response in one patient (21). The ATLEP trial, which combined lenvatinib and pembrolizumab in 29 advanced TC cases, reported higher response rates in PDTC compared to ATC, regardless of PD-L1 expression (22). In our case, first-line pembrolizumab led to symptom resolution and a progression-free survival of approximately 7 months, exceeding historical controls and further supporting its potential role in biomarker-selected PDTC patients.

This report has some inherent limitations. First, pembrolizumab was administered as first-line therapy in a patient who had not received prior radioiodine therapy or tyrosine kinase inhibitors, limiting comparisons with standard therapeutic sequences. Second, although IHC confirmed the loss of *MSH2* and *MSH6*, we did not conduct additional analyses of tumor-infiltrating lymphocytes, regulatory T cells, or tumor-associated macrophages, which could have facilitated a

Copyright© AE&M all rights reserved.

more comprehensive characterization of the TME (6). Third, PDTCs harboring MMR gene mutations are exceptionally rare, which may introduce selection biases and limit the generalizability of findings from isolated reports. Nonetheless, this case possesses several strengths. It documents the use of pembrolizumab as upfront monotherapy in a molecularly defined PDTC with dMMR/MSS phenotype and intermediate TMB, resulting in rapid clinical improvement and a durable response. The report integrates genomic, pathological, and clinical data to bolster the rationale for checkpoint blockade in selected PDTCs, contributing valuable real-world evidence to a sparsely populated literature.

CONCLUSION

In summary we present a rare case of metastatic PDTC with a confirmed dMMR phenotype characterized by MSH2 mutation and loss of MSH2/MSH6 protein expression despite an MSS profile. The tumor demonstrated intermediate TMB and a durable clinical response to pembrolizumab administered as first-line therapy. This case underscores the significance of comprehensive molecular profiling in thyroid carcinomas, particularly in identifying biomarkers beyond histologic subtype, such as dMMR by IHC or NGS. Our findings support the consideration of checkpoint inhibitors in selected PDTC patients, even in the absence of MSI-H. Further studies are warranted to clarify the predictive value of MMR alterations and TMB in the immunotherapeutic management of PDTC.

Funding statement: none to declare.

Acknowledgments: the authors kindly acknowledge the patient and their family for providing data for this case report, as well as all the healthcare professionals from the Head and Neck Oncology and Radiology departments at *Hospital Sírio-Libanês* (São Paulo, Brazil).

Author contributions: JHF contributed to conceptualization and methodology and led project administration, data analysis, formal analysis, and drafting of the original manuscript. JFLF contributed equally to conceptualization, methodology, project administration, data analysis, formal analysis, drafting, and final approval. CMTHF and GLCA provided supporting contributions to conceptualization, methodology, project administration, data analysis, formal analysis, and drafting, and shared supervisory responsibilities. RSV and SG supported project administration, data analysis and interpretation, formal analysis, drafting, and final approval. GCJ led conceptualization, methodology, and supervision, contributed equally to project administration and final approval, and supported data analysis and interpretation. All authors approved the final manuscript.

Ethics and institutional review board approval: This study was approved by the Institutional Research Ethics Committee for Human Subjects (CEPesq-SP) and subsequently by the National Research Ethics Committee through Plataforma Brasil (CAAE no. 86424125.5.0000.5461). The research was conducted in accordance with the ethical standards outlined in the Declaration of Helsinki. The patient voluntarily provided written informed consent before participating in the study, including consent for the publication of clinical details and images, in compliance with institutional and ethical standards.

Disclosure: JHF, JFF, CMHF, GLCA, RSV, and SG declare no conflicts of interest. GCJ reports receiving honoraria from AstraZeneca, Pfizer, Merck Sharp & Dohme, Bristol Myers Squibb, Novartis, Roche, Amgen, Janssen, Merck Serono, Lilly, Takeda, and Daiichi Sankyo/UCB Japan; serving in consulting or advisory roles for Boehringer Ingelheim, Pfizer, Bayer, Roche, Merck Sharp & Dohme, Bristol Myers Squibb, AstraZeneca, Yuhan, Merck Serono, Janssen, Libbs, Sanofi, Novartis, Lilly, Takeda, and Daiichi Sankyo/UCB Japan; participating in speakers' bureaus for AstraZeneca, Bayer, Novartis, Roche, Merck Serono, Bristol Myers Squibb, Merck Sharp & Dohme, Boehringer Ingelheim, Pfizer, Janssen, Amgen, and Takeda; and receiving travel, accommodations, or other expenses from Merck Sharp & Dohme, Novartis, Pfizer, Roche, AstraZeneca, Boehringer Ingelheim, Bayer, Bristol Myers Squibb, Merck Serono, and Daiichi Sankyo/UCB Japan.

Data availability: all data generated or analyzed during this study are included in this published article.

REFERENCES

1. Siegel RL, Kratzer TB, Giaquinto AN, Sung H, Jemal A. Cancer statistics, 2025. CA Cancer J Clin. 2025 Jan-Feb;75(1):10-45. doi: 10.3322/caac.21871.
2. Tong J, Ruan M, Jin Y, Fu H, Cheng L, Luo Q, et al. Poorly differentiated thyroid carcinoma: a clinician's perspective. Eur Thyroid J. 2022 Mar 24;11(2):e220021. doi: 10.1530/ETJ-22-0021.
3. Kim JY, Myung JK, Kim S, Tae K, Choi YY, Lee SJ. Prognosis of Poorly Differentiated Thyroid Carcinoma: A Systematic Review and Meta-Analysis. Endocrinol Metab (Seoul). 2024 Aug;39(4):590-602. doi: 10.3803/EnM.2024.1927.
4. Landa I, Ibrahimpasic T, Boucai L, Sinha R, Knauf JA, Shah RH, et al. Genomic and transcriptomic hallmarks of poorly differentiated and anaplastic thyroid cancers. J Clin Invest. 2016 Mar 1;126(3):1052-66. doi: 10.1172/JCI85271.
5. Elia G, Patrizio A, Ragusa F, Paparo SR, Mazzi V, Balestri E, et al. Molecular features of aggressive thyroid cancer. Front Oncol. 2022 Dec 20;12:1099280. doi: 10.3389/fonc.2022.1099280.
6. Garcia-Alvarez A, Hernando J, Carmona-Alonso A, Capdevila J. What is the status of immunotherapy in thyroid neoplasms? Front Endocrinol (Lausanne). 2022 Aug 5;13:929091. doi: 10.3389/fendo.2022.929091.
7. Mosele MF, Westphalen CB, Stenzinger A, Barlesi F, Bayle A, Bièche I, et al. Recommendations for the use of next-generation sequencing (NGS) for patients with advanced cancer in 2024: a report from the ESMO Precision Medicine Working Group. Ann Oncol. 2024 Jul;35(7):588-606. doi: 10.1016/j.annonc.2024.04.005. Epub 2024 May 27. Erratum in: Ann Oncol. 2025 Apr;36(4):472. doi: 10.1016/j.annonc.2024.11.010.

Copyright© AE&M all rights reserved.

8. Cameselle-García S, Abdulkader-Sande S, Sánchez-Ares M, Rodríguez-Carnero G, Garcia-Gómez J, Gude-Sampedro F, et al. PD-L1 expression and immune cells in anaplastic carcinoma and poorly differentiated carcinoma of the human thyroid gland: A retrospective study. Oncol Lett. 2021 Jul;22(1):553.
9. Brose MS, Nutting CM, Jarzab B, Elisei R, Siena S, Bastholt L, et al.; DECISION investigators. Sorafenib in radioactive iodine-refractory, locally advanced or metastatic differentiated thyroid cancer: a randomised, double-blind, phase 3 trial. Lancet. 2014 Jul 26;384(9940):319-28. doi: 10.1016/S0140-6736(14)60421-9.
10. Schlumberger M, Tahara M, Wirth LJ, Robinson B, Brose MS, Elisei R, et al. Lenvatinib versus placebo in radioiodine-refractory thyroid cancer. N Engl J Med. 2015 Feb 12;372(7):621-30. doi: 10.1056/NEJMoa1406470.
11. Wells SA Jr, Robinson BG, Gagel RF, Dralle H, Fagin JA, Santoro M, et al. Vandetanib in patients with locally advanced or metastatic medullary thyroid cancer: a randomized, double-blind phase III trial. J Clin Oncol. 2012 Jan 10;30(2):134-41. doi: 10.1200/JCO.2011.35.5040. Epub 2011 Oct 24. Erratum in: J Clin Oncol. 2013 Aug 20;31(24):3049.
12. Brose MS, Robinson B, Sherman SI, Krajewska J, Lin CC, Vaisman F, et al. Cabozantinib for radioiodine-refractory differentiated thyroid cancer (COSMIC-311): a randomised, double-blind, placebo-controlled, phase 3 trial. Lancet Oncol. 2021 Aug;22(8):1126-1138. doi: 10.1016/S1470-2045(21)00332-6.
13. Latham Schwark A, Srinivasan P, Kemel Y, Shia J, Bandlamudi C, Mandelker D, et al. Pan-cancer microsatellite instability to predict for presence of Lynch syndrome. J Clin Oncol. 2018;36(18 Suppl):LBA1509. doi: 10.1200/JCO.2018.36.18_suppl.LBA1509.
14. Bonneville R, Krook MA, Kautto EA, Miya J, Wing MR, Chen HZ, et al. Landscape of Microsatellite Instability Across 39 Cancer Types. JCO Precis Oncol. 2017;2017:PO.17.00073. doi: 10.1200/PO.17.00073.
15. Baretti M, Le DT. DNA mismatch repair in cancer. Pharmacol Ther. 2018 Sep;189:45-62. doi: 10.1016/j.pharmthera.2018.04.004.
16. Le DT, Durham JN, Smith KN, Wang H, Bartlett BR, Aulakh LK, et al. Mismatch repair deficiency predicts response of solid tumors to PD-1 blockade. Science. 2017 Jul 28;357(6349):409-413. doi: 10.1126/science.aan6733.
17. Genutis LK, Tomsic J, Bundschuh RA, Brock PL, Williams MD, Roychowdhury S, et al. Microsatellite Instability Occurs in a Subset of Follicular Thyroid Cancers. Thyroid. 2019 Apr;29(4):523-529. doi: 10.1089/thy.2018.0655.
18. Lee Y, Moon S, Seok JY, Lee JH, Nam S, Chung YS. Characterization of the genomic alterations in poorly differentiated thyroid cancer. Sci Rep. 2023 Nov 6;13(1):19154. doi: 10.1038/s41598-023-46466-5.
19. Nikiforov YE. Genetic alterations involved in the transition from well-differentiated to poorly differentiated and anaplastic thyroid carcinomas. Endocr Pathol. 2004 Winter;15(4):319-27. doi: 10.1385/ep:15:4:319.
20. Marabelle A, Le DT, Ascierto PA, Di Giacomo AM, De Jesus-Acosta A, Delord JP, et al. Efficacy of Pembrolizumab in Patients With Noncolorectal High Microsatellite Instability/Mismatch Repair-Deficient Cancer: Results From the Phase II KEYNOTE-158 Study. J Clin Oncol. 2020 Jan 1;38(1):1-10. doi: 10.1200/JCO.19.02105.
21. Sehgal K, Pappa T, Shin KY, Schiantarelli J, Liu M, Ricker C, Besson NR, et al. Dual Immune Checkpoint Inhibition in Patients With Aggressive Thyroid Carcinoma: A Phase 2 Nonrandomized Clinical Trial. JAMA Oncol. 2024 Dec 1;10(12):1663-1671. doi: 10.1001/jamaoncol.2024.4019.
22. Dierks C, Ruf J, Seufert J, Kreissl M, Klein C, Spitzweg C, et al. 1646MO Phase II ATLEP trial: Final results for lenvatinib/pembrolizumab in metastasized anaplastic and poorly differentiated thyroid carcinoma. Ann Oncol. 2022 Sep 1;33:S1295-5. doi:10.1016/j.annonc.2022.07.1726

Copyright© AE&M all rights reserved.

Archives of Endocrinology and Metabolism
ISSN 2359-4292
OFFICIAL JOURNAL OF THE BRAZILIAN SOCIETY OF ENDOCRINOLOGY AND METABOLISM

case report

From amenorrhea to pregnancy: spontaneous recovery of the female athlete triad during the COVID-19 pandemic

Eduardo Medeiros Ferreira da Gama[1]
https://orcid.org/0000-0002-3485-1407

Francisco de Paula Paranhos-Neto[1]
https://orcid.org/0000-0001-6661-0993

Miguel Madeira[1]
https://orcid.org/0000-0001-6752-2880

Laura Maria Carvalho Mendonça[2]
https://orcid.org/0000-0003-2129-3546

Maria Lucia Fleiuss Farias[1]
https://orcid.org/0000-0003-0466-3250

[1] Divisão de Endocrinologia, Hospital Universitário Clementino Fraga Filho, Universidade Federal do Rio de Janeiro, Rio de Janeiro, RJ, Brasil
[2] Divisão de Reumatologia, Hospital Universitário Clementino Fraga Filho, Universidade Federal do Rio de Janeiro, Rio de Janeiro, RJ, Brasil

ABSTRACT

The Female Athlete Triad (Triad) and Relative Energy Deficiency in Sport (RED-S) are conditions associated with low energy availability (EA) that can lead to menstrual dysfunction, impaired bone health, and metabolic disturbances. This case report describes the remission of Triad in a professional triathlete during the COVID-19 pandemic. A 24-year-old female triathlete was evaluated in 2018. She reported bulimia nervosa from 12–15 years old and hypothalamic amenorrhea since she was 21 years old. Her training volume was approximately 20 hours per week (swimming, cycling, and running), and the amount of EA was critically low (<10 kcal/fat free mass/day). The athlete had lower than expected BMD at DXA scan (lumbar spine Z-score -2.3 SD) and lower cortical and trabecular vBMD and trabecular number by comparison with HR-pQCT normative data for young Brazilian women. During the 2020 pandemic, training centers were closed, leading to a decrease in exercise volume and a more balanced energy intake. Menstrual cycles resumed and she conceived spontaneously in the same year. Pregnancy and postpartum recovery were uneventful. She returned to competitions post pandemic, but no longer as a professional athlete. Chronic energy deficiency significantly affects the hypothalamic-pituitary-gonadal axis and bone health. A forced reduction in training intensity and improved dietary intake were key factors in the restoration of menstrual function and reproductive health. This case highlights the potential reversibility of the Female Athlete Triad when energy balance is restored. Awareness and early intervention are essential for preventing long-term consequences in female athletes.

Keywords: Female athlete triad syndrome; relative energy deficiency in sport; amenorrhea; bone density

INTRODUCTION

The Female Athlete Triad (Triad) was initially described as being associated with eating disorders, amenorrhea, and osteoporosis. Over time, this concept has evolved into the broader model of Relative Energy Deficiency in Sport (RED-S), which considers a wide range of systemic effects, such as endocrine, metabolic, and immune dysfunctions. Energy availability (EA) can be estimated as dietary intake minus exercise energy expenditure normalized to lean body mass or fat free mass (FFM). Low EA is a primary driver of these conditions, leading to repercussions on reproductive function and bone health (1,2).

In high-performance sports, female athletes often prioritize an optimal body composition for performance, which can result in chronic energy deficits. Less than 30 kcal/FFM/day may be insufficient to maintain menstrual function, whereas adequate EA is estimated as > 45 kcal/FFM/day (3,4).

This case report describes a professional triathlete with the Female Athlete Triad for several years, which was characterized by amenorrhea and changes in bone density and microstructure. This athlete

Received on Apr/30/2025
Accepted on Nov/11/2025
DOI: 10.20945/2359-4292-2026-0007

Correspondence to:
Eduardo Medeiros Ferreira da Gama
Divisão de Endocrinologia,
Hospital Universitário Clementino Fraga Filho,
Universidade Federal do Rio de Janeiro
Avenida Professor Rodolpho Paulo Rocco 255
21941-913 – Rio de Janeiro, RJ, Brasil
dudagama01@ufrj.br

Associated editor:
Marise Lazaretti-Castro
https://orcid.org/0000-0001-9186-2834

This is an open-access article distributed under the terms of the Creative Commons Attribution License

Copyright© ACE&M all rights reserved.

then developed spontaneous remission during the COVID-19 pandemic, which result in the return of menstrual function and a subsequent pregnancy.

CASE PRESENTATION

This patient was included in 2018 in a broad research project of Female Athletes approved by the Ethics Committee of HUCFF-UFRJ (CAAE: 64516117.9.0000.5257). Written informed consent was obtained from all volunteers who participated in the study.

The athletic career began when she was 16 years old, transitioning to professional status by age 20. The training regimen included 20 hours per week distributed among swimming (20 km), cycling (10–12 hours), and running (60 km). Despite achieving excellent competition results, she expressed persistent dissatisfaction with her body weight and felt, that it did not align with elite competition standards. At age 21, she developed oligomenorrhea and subsequent hypothalamic amenorrhea. She had a prior history of bulimia nervosa (ages 12–15) but denied the use of hormonal contraceptives, tobacco products, alcohol, or illicit drugs.

She was 24 years old during the study, reported amenorrhea since 22 years old and denied previous fractures. A full clinical, anthropometric, metabolic and imaging assessment was performed.

Biochemistry: Gonadotropins, estradiol, and prolactin levels were measured on multiple occasions during the period of menstrual dysfunction, and results consistently demonstrated normal prolactin levels. This endocrine profile is characteristic of functional hypothalamic amenorrhea secondary to low energy availability, as illustrated in **Figure 1**. The patient's fasting glucose = concentration was 96 mg/dL (70-99), vitamin B_{12} = concentration was 786 pg/mL (210-980), and folic acid concentration was 18.4 ng/mL (≥ 3.9). Other biochemical parameters, such as follow-up measurements obtained after menstrual recovery, are summarized in **Table 1**.

Dual energy absorptiometry (DXA) was used to evaluate areal bone mineral density (BMD, g/cm²) and Z-scores (differences between the patient's BMD and age-gender-matched healthy individuals) at the lumbar spine and hip, using a GE Lunar Prodigy Advance densitometer. In accordance with the 2023 International Society for Clinical Densitometry (ISCD) guidelines, a Z-score at or below −2.0 SD indicates "lower than expected BMD". Whole-body DXA scans were used to assess body composition, including total and regional fat mass and fat-free mass (FFM), following standard ISCD procedures (5). Results were as follows: body mass index = 20 kg/m² (normal range 18.5-24.9), total fat mass = 11.42 kg, fat mass index (total fat/height²) = 3.93 (NR 5-9) and fat free mass = 46.83 kg. Additionally, lumbar spine BMD = 0.893 g/cm² (LS Z-score -2.3 SD), and total hip BMD = 0.953 g/cm² (TH Z-score -0.3 SD).

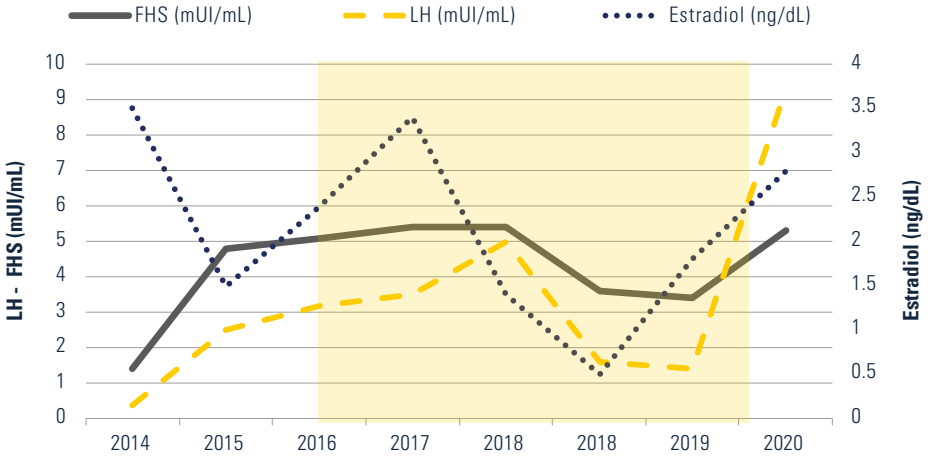


Figure 1. Longitudinal evolution of gonadotropic and ovarian hormones (LH, FSH, and estradiol) from 2014 to 2020. The progressive increase in estradiol concentrations paralleled the normalization of gonadotropins (FSH and LH) following the restoration of energy availability. The shaded area represents the amenorrheic period. Menstrual recovery occurred after a reduction in training volume and improvement in caloric intake.

Copyright© AE&M all rights reserved.

Table 1. Laboratory data obtained during the study visits conducted while the patient was under functional hypothalamic amenorrhea ("Amenorrheic period") and after menstrual and hormonal recovery in 2020 ("Recovery"). Reference ranges correspond to standard values for women of reproductive age

Parameter (unit)	Amenorrhea (2018)	Recovery (2020)	Reference range
FSH (mIU/mL)	3.6	5.3	3.5–12.5
LH (mIU/mL)	1.6	9.3	2.4–12.6
Estradiol (ng/mL)	< 0.5	2.8	30–120 Follicular
Prolactin (ng/mL)	7.0	13.9	5-25
Testosterone (ng/dL)	23	24	8.4–48.1
Insulin (µU/mL)	2.0	5.3	2–25
HOMA-IR	0.4	1.1	< 2.5
IGF-1 (ng/mL)	160	183	110–270
TSH (µIU/mL)	1.8	2.61	0.4–4.0
Free T_4 (ng/dL)	1.2	1.14	0.8–1.8
Reverse T_3 (ng/dL)	16	18.2	10–24
Vitamin D (25OHD, ng/mL)	32	40.0	≥20
PTH pg/dL	29	29	15–65
Calcium (mg/dL)	9.4	9.0	8.6–10.0
Phosphorus (mg/dL)	3.6	3.5	2.5–4.5
Magnesium (mg/dL)	1.8	2.0	1.6–2.6

High resolution peripheral quantitative computed tomography (HR-pQCT) was performed using a Scanco Xtreme CT, with a voxel size of 82 µm, and a standard distal radius and tibia protocol. Volumetric BMD and bone microstructure were measured at cortical and trabecular compartments, according to a recent consensus (6). All data were compared with normative data defined for age-matched Brazilian women, as published by Alvarenga and cols. (7). This athlete had lower than expected values for volumetric bone mineral density (vBMD) in the tibia, cortical and trabecular vBMD in the radius, and cortical vBMD in the tibia, as well as a lower trabecular number and greater trabecular separation in the radius **(Table 2)**.

The Eating Attitudes Test (EAT-26), Bulimic Investigatory Test of Edinburgh (BITE), and Body Shape Questionnaire (BSQ) were applied as validated Portuguese self-administered instruments to screen for disordered eating and body-image concerns. Results were as follows: EAT-26 = 37 points (positive); BITE = 27 points (positive); BSQ = 118 points (negative).

Assessment of energy availability: To estimate the athlete's daily energy consumption, a three-day food record was requested and, include two weekdays and one weekend day. Dietary data were analyzed using computer-based nutrition software (DietWin Personal). The average daily energy intake was then compared with international recommendations to determine whether the intake met the thresholds for adequate EA (≥45 kcal/kg FFM/day) or was critically low (<30 kcal/kg FFM/day) (8,9). It was determined that the patient's EA was critically low (<10 kcal/FFM/day).

Table 2. Bone assessment using HR-pQCT at baseline

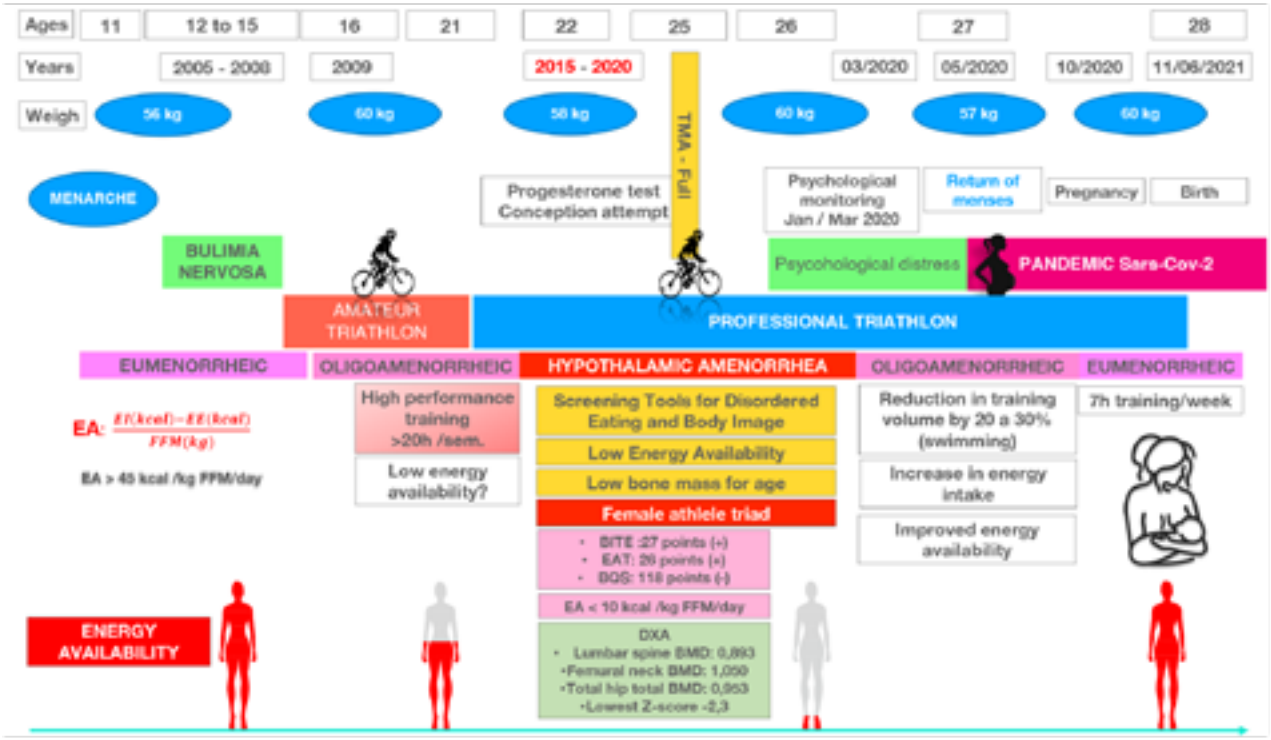
Variable	Athlete (24.8 yrs)	Reference – Alvarenga (20–29 yrs)
Distal Radius		
Total vBMD (mg HA/cm³)	352.9	331 (279–370)
Cortical vBMD (mg HA/cm³)	**955.8**	1,017 (974–1,053)
Cortical Thickness (mm)	0.93	0.86 (0.72–1.03)
Trabecular vBMD (mg HA/cm³)	**136.9**	172 (155–193)
Trabecular Number (1/mm)	**1.49**	2.02 (1.92–2.17)
Trabecular Thickness (mm)	0.077	0.069 (0.064–0.075)
Trabecular Separation (mm)	**0.595**	0.423 (0.387–0.454)
Distal Tibia		
Total vBMD (mg HA/cm³)	**304.0**	324 (309–365)
Cortical vBMD (mg HA/cm³)	**937.3**	1,015 (989–1,043)
Cortical Thickness (mm)	1.29	1.28 (1.05–1.43)
Trabecular vBMD (mg HA/cm³)	159.6	168 (152–194)
Trabecular Number (1/mm)	1.72	1.84 (1.61–2.03)
Trabecular Thickness (mm)	0.077	0.077 (0.072–0.088)
Trabecular Separation (mm)	0.503	0.466 (0.416–0.527)

Copyright© AE&M all rights reserved.

Nutritional Intake, Resting Metabolic Rate and Energy Expenditure Evaluation. The resting metabolic rate and total energy expenditure were estimated by indirect calorimetry to be 1403 kcal/day and 3241 kcal/day, respectively, whereas the patient average daily caloric intake was 2051 kcal/day, which confirmed a significant energy deficit. The distribution of macronutrients consisted of 49% carbohydrates (4.1 g/kg/day), 22% protein (2.4 g/kg/day), and 30% lipids. The daily calcium intake was 673 mg, which is below the recommended intake for optimal bone health.

Cardiopulmonary exercise testing (CPET) revealed a maximal oxygen uptake (VO_2 max) of 58.9 mL/kg/min, which corresponded to 146% of the predicted value. The achieved maximum metabolic equivalent (MET) was 16.8 and, indicated excellent aerobic capacity despite the energetic and hormonal imbalance.

Seven-year follow-up: The patient's body mass showed only minor variations throughout follow-up and, ranged from 56 kg at age 12 to 60 kg at age 26. At the onset of hypothalamic amenorrhea, the patient weighed was 58 kg. During the COVID-19 pandemic, the closure of training centers and cancellation of competitions led to a forced reduction in exercise intensity. The overall training volume markedly decreased — from 15–18 hours to approximately 6–8 hours per week. This, combined with a less restrictive dietary pattern, resulted in an improved energy balance despite no significant weight change. Psychological distress was also noted initially, and required counseling support. In May 2020, after more than five years of amenorrhea, her menstrual cycle resumed, and conception occurred in October, when she weighted 60 kg. This, suggests that the restoration of energy balance, rather than weight gain, was the key determinant of hypothalamic–pituitary–gonadal axis recovery. The pregnancy was uneventful and the baby was born healthy and full-term. Notably, the patient had attempted to conceive four years earlier, during the amenorrheic phase, but there was no withdrawal bleeding after oral progesterone challenge, which confirmed persistent functional hypothalamic suppression. The case is summarized in **Figure 2**.



Abbreviations: EA: energy availability; EI: energy intake; EE: energy expenditure; FFM: fat-free mass; BITE: Bulimic Investigatory Test of Edinburgh; EAT: Eating Attitudes Test; BSQ: Body Shape Questionnaire; DXA: dual-energy X-ray absorptiometry.

Figure 2. Timeline of the athlete's clinical and training history showing menstrual status, body mass evolution, and major life events. The figure highlights the period of hypothalamic amenorrhea (2015–2020), pandemic-related reduction in training volume, and spontaneous menstrual and reproductive recovery in 2020.

Copyright© AE&M all rights reserved.

She resumed training postpandemic and began participating in competitive triathlon but no longer as a professional athlete. Her menstrual cycles have remained regular since this time, and she had no fractures until 2025.

DISCUSSION

Chronic low levels of EA have profound effects on the hypothalamic-pituitary-gonadal axis and, lead to menstrual dysfunction and impaired bone health (4). This case illustrates these changes and shows how spontaneous energy balance restoration through reduced exercise volume and improved dietary intake can reverse these effects.

Laboratory findings throughout the follow-up confirmed the functional and reversible suppression of the hypothalamic–pituitary–gonadal (HPG) axis. During the amenorrheic period, gonadotropins and estradiol levels markedly decreased, which is consistent with hypogonadotropic hypogonadism secondary to energy deficiency. Reduced insulin levels reflected this energy-deficient state (10), whereas normal thyroid and IGF-1 profiles indicated metabolic adaptation. Chronic low EA reduce leptin, insulin, and IGF-1 signaling, which leads to decreased hypothalamic kisspeptin stimulation and suppression of GnRH pulsatility, as reviewed by Angelidi and cols. (11). These neuroendocrine adaptations result in reversible inhibition of ovarian function and contribute to altered bone remodeling. Furthermore, these findings illustrate the coordinated neuroendocrine response to chronic low EA, in which diminished GnRH pulsatility leads to temporary suppression of ovarian activity. The restoration of energy balance has been shown to normalize LH pulsatility and menstrual function in exercising women with functional hypothalamic amenorrhea (12).

This patient had a long history of disordered eating and body image concerns. To further investigate the presence of eating-related disturbances, we applied three validated Portuguese versions of self-administered questionnaires. The Eating Attitudes Test (EAT-26) (13), which evaluates behaviors that are typically associated with anorexia nervosa and their severity, showed a patient score of 37 points (positive); the Bulimic Investigatory Test of Edinburgh (BITE) (14), which is aimed at identifying bulimic symptoms and compensatory methods, showed a patient score of 27 points (positive), and the BSQ score (15), which measures dissatisfaction with body image, showed a patient score of 118 points (negative). Although not diagnostic tools, these questionnaires are widely used to screen individuals at risk for developing eating disorders.

Other screening instruments that are specifically designed for physically active populations, such as the Low EA in Females Questionnaire (LEAF-Q) (16), have been proposed to identify female athletes at risk for the Female Athlete Triad and related conditions. However, as no validated version of the LEAF-Q was available in Portuguese at the time of assessment, it was not used in this case.

The clinical significance of RED-S extends beyond menstrual function. Impaired bone health poses long-term risks, including increased fracture susceptibility. In this case, evaluation during the amenorrheic period revealed lower than expected areal BMD at the lumbar spine (Z-score below −2 SD), which agrees with reports in the literature on the Female Athlete Triad and functional hypothalamic amenorrhea, where bone loss is frequently observed. Compared with nonathletes, athletes in weight-bearing sports usually have 5%–15% higher BMD. Although weight-bearing exercise is generally associated with improved bone mass, a growing body of research has demonstrated that impaired bone health is common in endurance athletes (17). For example, as many as 41-45% of elite endurance athletes have low BMD (18). This apparent paradox is explained by the effects of chronically low EA and menstrual dysfunction, which may override the osteogenic stimulus of physical activity.

Compared with age-matched normal Brazilian women, this athlete also presented lower than expected volumetric BMD and bone structural parameters, as described by Alvarenga and cols. (7) These changes in bone microarchitecture have also been previously documented in the literature. Ackerman and colleagues were pioneers in demonstrating, through HR-pQCT, that athletes with amenorrhea present greater cortical porosity and reduced cortical thickness and density. This occurs, despite preserved or

Copyright© AE&M all rights reserved.

even increased bone strength, such as higher stiffness and estimated failure load. These findings suggest that exercise may lead to periosteal expansion, but amenorrhea offsets its benefits by favoring endocortical resorption and delays the mineralization of newly formed bone (19-21).

Prolonged hypoestrogenism, as observed during functional hypothalamic amenorrhea, may lead to decreased bone formation and increased resorption and, predispose patients to low bone mineral density and microarchitectural deterioration. The interplay among these hormonal pathways, as summarized in recent reviews (11), highlights how the restoration of EA and normalization of estradiol are crucial for skeletal health.

Similarly, in a recent study involving long-distance triathletes without evidence of hypoestrogenism, we demonstrated that low EA attenuates the positive skeletal effects of exercise, even in the absence of menstrual dysfunction. Compared with athletes with adequate EA, athletes with low EA had s significantly lower cortical volumetric BMD (tibia), reduced cortical area and thickness, and lower total vBMD (radius). In addition, stress fractures were more frequent in the low EA group (4 out of 12) than in the adequate EA group (2 out of 11), which reinforces the importance of early detection and nutritional management to preserve skeletal integrity in this population (22)

The observed menstrual recovery aligns with findings from the REFUEL study, which demonstrated that increasing energy intake in exercising women with menstrual disturbances effectively restored reproductive function (12). Furthermore, additional studies highlight that even in athletes with regular menstrual cycles, low EA can compromise bone density and microarchitecture (3).

A limitation of this study is the absence of leptin measurements, which would have provided an additional biomarker of EA and hypothalamic activation. Moreover, bone mineral density and microarchitectural assessments (DXA and HR-pQCT) were not repeated after menstrual and hormonal recovery.

CONCLUSION

This case highlights the reversibility of the Female Athlete Triad when EA is restored. The spontaneous remission observed in this triathlete underscores the critical role of exercise modulation and adequate nutritional intake in reversing endocrine disturbances. Preventive strategies, such as regular monitoring of energy availability, menstrual function, and bone health, are essential for mitigating the adverse effects of RED-S and ensuring long-term athletic performance and overall health in female athletes.

Funding: this research received no specific grant from any funding agency in the public, commercial, or not-for-profit sectors.

Disclosure: the authors declare no conflicts of interest related to this case report. No additional contributors were involved in data collection, analysis, or manuscript preparation beyond the listed authors.

Data availability: datasets related to this article will be available upon request to the corresponding author.

REFERENCES

1. De Souza MJ, Hontscharuk R, Olmsted M, Kerr G, Williams NI. Drive for thinness score is a proxy indicator of energy deficiency in exercising women. Appetite. 2007 May;48(3):359-67. doi: 10.1016/j.appet.2006.10.009.
2. Loucks AB. Energy availability and infertility. Curr Opin Endocrinol Diabetes Obes. 2007 Dec;14(6):470-4. doi: 10.1097/MED.0b013e3282f1cb6a.
3. Papageorgiou M, Dolan E, Elliott-Sale KJ, Sale C. Reduced energy availability: implications for bone health in physically active populations. Eur J Nutr. 2018 Apr;57(3):847-859. doi: 10.1007/s00394-017-1498-8.
4. De Souza MJ, Koltun KJ, Williams NI. The Role of Energy Availability in Reproductive Function in the Female Athlete Triad and Extension of its Effects to Men: An Initial Working Model of a Similar Syndrome in Male Athletes. Sports Med. 2019 Dec;49(Suppl 2):125-137. doi: 10.1007/s40279-019-01217-3.
5. Shuhart C, Cheung A, Gill R, Gani L, Goel H, Szalat A. Executive Summary of the 2023 Adult Position Development Conference of the International Society for Clinical Densitometry: DXA Reporting, Follow-up BMD Testing and Trabecular Bone Score Application and Reporting. J Clin Densitom. 2024 Jan-Mar;27(1):101435. doi: 10.1016/j.jocd.2023.101435.
6. Whittier DE, Boyd SK, Burghardt AJ, Paccou J, Ghasem-Zadeh A, Chapurlat R, et al. Guidelines for the assessment of bone density and microarchitecture in vivo using high-resolution peripheral quantitative computed tomography. Osteoporos Int. 2020 Sep;31(9):1607-1627. doi: 10.1007/s00198-020-05438-5.
7. Alvarenga JC, Fuller H, Pasoto SG, Pereira RM. Age-related reference curves of volumetric bone density, structure, and biomechanical parameters adjusted for weight and height in a population of healthy women: an HR-pQCT study. Osteoporos Int. 2017 Apr;28(4):1335-1346. doi: 10.1007/s00198-016-3876-0.
8. Papageorgiou M, Martin D, Colgan H, Cooper S, Greeves JP, Tang JCY, Fraser WD, Elliott-Sale KJ, Sale C. Bone metabolic responses to low energy availability achieved by diet or exercise in active eumenorrheic women. Bone. 2018 Sep;114:181-188. doi: 10.1016/j.bone.2018.06.016.
9. De Souza MJ, Koltun KJ, Strock NC, Williams NI. Rethinking the concept of an energy availability threshold and its role in the Female Athlete Triad. Curr Opin Physiol. 2019 Aug;10:35–42. doi:10.1016/j.cophys.2019.04.001.
10. Koehler K, Hoerner NR, Gibbs JC, Zinner C, Braun H, De Souza MJ, et al. Low energy availability in exercising men is associated with reduced

Copyright© AE&M all rights reserved.

leptin and insulin but not with changes in other metabolic hormones. J Sports Sci. 2016 Oct;34(20):1921-9. doi: 10.1080/02640414.2016.1142109.

11. Angelidi AM, Stefanakis K, Chou SH, Valenzuela-Vallejo L, Dipla K, Boutari C, et al. Relative Energy Deficiency in Sport (REDs): Endocrine Manifestations, Pathophysiology and Treatments. Endocr Rev. 2024 Sep 12;45(5):676-708. doi: 10.1210/endrev/bnae011.
12. De Souza MJ, Mallinson RJ, Strock NCA, Koltun KJ, Olmsted MP, Ricker EA, et al. Randomised controlled trial of the effects of increased energy intake on menstrual recovery in exercising women with menstrual disturbances: the 'REFUEL' study. Hum Reprod. 2021 Jul 19;36(8):2285-2297. doi: 10.1093/humrep/deab149.
13. Garner DM, Olmsted MP, Bohr Y, Garfinkel PE. The eating attitudes test: psychometric features and clinical correlates. Psychol Med. 1982 Nov;12(4):871-8. doi: 10.1017/s0033291700049163.
14. Henderson M, Freeman CP. A self-rating scale for bulimia. The 'BITE'. Br J Psychiatry. 1987 Jan;150:18-24. doi: 10.1192/bjp.150.1.18.
15. Cooper PJ, Taylor MJ, Cooper Z, Fairbum CG. The development and validation of the body shape questionnaire. Int J Eat Disord. 1987 Jul;6(4):485-94. doi: 10.1002/1098-108X(198707)6:4<485: AID-EAT2260060405>3.0.CO;2-O.
16. Melin A, Tornberg AB, Skouby S, Faber J, Ritz C, Sjödin A, Sundgot-Borgen J. The LEAF questionnaire: a screening tool for the identification of female athletes at risk for the female athlete triad. Br J Sports Med. 2014 Apr;48(7):540-5. doi: 10.1136/bjsports-2013-093240.
17. Nattiv A, Loucks AB, Manore MM, Sanborn CF, Sundgot-Borgen J, Warren MP; American College of Sports Medicine. American College of Sports Medicine position stand. The female athlete triad. Med Sci Sports Exerc. 2007 Oct;39(10):1867-82. doi: 10.1249/mss.0b013e318149f111.
18. Kelly AW, Hecht S. The female athlete triad. Ann Jt. 2022 Jan 15;7:6. doi: 10.21037/aoj-2020-03.
19. Ackerman KE, Nazem T, Chapko D, Russell M, Mendes N, Taylor AP, et al. Bone microarchitecture is impaired in adolescent amenorrheic athletes compared with eumenorrheic athletes and nonathletic controls. J Clin Endocrinol Metab. 2011 Oct;96(10):3123-33. doi: 10.1210/jc.2011-1614.
20. Ackerman KE, Putman M, Guereca G, Taylor AP, Pierce L, Herzog DB, et al. Cortical microstructure and estimated bone strength in young amenorrheic athletes, eumenorrheic athletes and non-athletes. Bone. 2012 Oct;51(4):680-7. doi: 10.1016/j.bone.2012.07.019.
21. Mitchell DM, Tuck P, Ackerman KE, Cano Sokoloff N, Woolley R, Slattery M, et al. Altered trabecular bone morphology in adolescent and young adult athletes with menstrual dysfunction. Bone. 2015 Dec;81:24-30. doi: 10.1016/j.bone.2015.06.021.
22. Gama E, Kasuki L, Paranhos-Neto FP, Madeira M, Mendonça L, Schtscherbyna A, et al. Low Energy Availability Interferes With Exercise-Associated Bone Effects in Female Long-Distance Triathletes as Detected by HR-pQCT. J Clin Densitom. 2022 Apr-Jun;25(2):160-167. doi: 10.1016/j.jocd.2021.01.013.

Copyright© ACE&M all rights reserved.

Archives of Endocrinology and Metabolism
ISSN 2359-4292
OFFICIAL JOURNAL OF THE BRAZILIAN SOCIETY OF ENDOCRINOLOGY AND METABOLISM

case report

Identification of a novel *THRB* mutation causing thyroid hormone resistance syndrome

Jing Yang[1,2,*]
https://orcid.org/0000-0001-5052-1857

Chuan Wang[3,*]
https://orcid.org/0009-0003-1280-0152

Li Quan[1,2]
https://orcid.org/0009-0006-8658-8168

Sheng Jiang[1,2]
https://orcid.org/0000-0003-3115-4347

[1] State Key Laboratory of Pathogenesis, Prevention and Treatment of High Incidence Diseases in Central Asia, Urumqi, China
[2] Department of Endocrinology, The First Affiliated Hospital of Xinjiang Medical University, Urumqi, China
[3] Department of Endocrinology, The Xinhua Hospital of Yili Kazakh Autonomous Prefecture, China

*These authors contributed equally.

ABSTRACT

Resistance to thyroid hormone syndrome (RTHS) is a rare disorder caused by mutations in the thyroid hormone receptor beta (*THRB*) gene, resulting in impaired action of thyroid hormones on target tissues and organs. We report a case of a 57-year-old Chinese male who presented with palpitations and hand tremors. Laboratory tests revealed elevated serum thyroid hormone levels, while serum thyroid-stimulating hormone (TSH) levels remained within the normal range. Enhanced magnetic resonance imaging of the pituitary gland showed no abnormalities. Through genetic testing, we identified a rare heterozygous point mutation in the *THRB* gene, specifically c.938T>C: p.M313T. To the best of our knowledge, this mutation site has not been previously reported in the literature. Clinically, RTHS is often misdiagnosed as hyperthyroidism, leading to inappropriate treatment and potential exacerbation of thyroid hormone resistance. Therefore, accurate diagnosis of this condition is crucial. Given the rarity of RTHS, we hope that this case report will enhance the understanding of its clinical manifestations and management, particularly in patients with *THRB* gene mutations.

Keywords: Thyroid hormone resistance; thyroid hormone receptor beta; mutation; thyroid hormone resistance syndrome; refetoff syndrome

INTRODUCTION

Resistance to thyroid hormone syndrome (RTHS) is a relatively rare disorder, primarily caused by mutations in the thyroid hormone receptor beta (*THRB*) gene. These mutations lead to impaired responsiveness of tissues and organs to thyroid hormones (1,2). In the human body, thyroid hormones regulate various physiological processes through two main receptor genes: the *THRB* and the thyroid hormone receptor alpha (*THRA*) (3). There are three receptor subtypes, namely THRα1, THRβ1, and THRβ2, which are predominantly expressed in different tissues. The prevalence of RTHS is approximately 1 in 40,000 individuals (4,5). Clinical manifestations of RTHS are diverse and may include palpitations, hand tremors, and other symptoms.

The majority of RTHS cases are associated with mutations in the *THRB* gene and are termed RTHβ (6). A minority of cases are related to mutations in the *THRA* gene, as well as defects in genes involved in thyroid hormone transport and metabolism. Laboratory tests typically reveal persistently elevated levels of free T3 and free T4, while serum thyroid-stimulating hormone (TSH) levels remain within the normal range (7-9). The genetic inheritance pattern is predominantly autosomal dominant, although autosomal recessive inheritance and sporadic cases have also been reported.

Received on Sept/21/2025
Accepted on Oct/20/2025
DOI: 10.20945/2359-4292-2026-0006

Correspondence to:
Li Quan and Sheng Jiang
xjjiangsheng@126.com

Associated editor:
Celia Regina Nogueira
https://orcid.org/0000-0002-4014-0660

This is an open-access article distributed under the terms of the Creative Commons Attribution License

Copyright© AE&M all rights reserved.

Notably, individuals with heterozygous *THRB* gene mutations often exhibit more severe symptoms compared with those with homozygous mutations.

Due to the varying degrees of thyroid hormone resistance in target tissues, patients with RTHβ exhibit high clinical phenotypic heterogeneity. They may present with symptoms of hyperthyroidism, hypothyroidism, or be entirely asymptomatic. However, most patients with RTHβ are asymptomatic, which can easily lead to missed or incorrect diagnoses in clinical practice, and subsequently exacerbate thyroid hormone resistance. Therefore, accurate diagnosis of this disease is of great significance.

In this study, through gene sequencing, we identified a rare mutation (p.M313T) in the *THRB* gene of a patient with RTHS. To the best of our knowledge, this is a novel gene mutation site, and there have been no previous reports of this mutation.

CASE REPORT

A 57-year-old male presented to our outpatient clinic with a 3-year history of palpitations and hand tremors. Previous thyroid ultrasound examinations had indicated the presence of thyroid nodules; however, the results of his thyroid function tests were unavailable. During this period, the patient had not received any specific treatment. On physical examination, the patient's height was 165 cm, weight was 83 kg, blood pressure was 113/72 mmHg, heart rate was 81 beats per minute, and respiratory rate was 18 breaths per minute. There was no exophthalmos or ophthalmic signs. The thyroid gland was not enlarged, no tremors were palpable, and no vascular murmurs were detected. The heart, lungs, and abdomen were normal, and there was no edema in the lower extremities. The patient had married at the age of 22 years and had two sons. His past medical history was unremarkable, and he had no other family members with similar problems.

Thyroid ultrasound revealed multiple bilateral benign nodules (TI-RADS category 3). Laboratory tests performed on March 6, 2024, demonstrated elevated thyroid hormone levels with a normal TSH level (**Table 1**). A repeat thyroid function test conducted in our hospital on March 16, 2024, yielded similar results (**Table 1**). To further rule out the influence of assay reagents, an additional thyroid function test using chemiluminescence immunoassay was performed in a different hospital on March 21, 2024, which again showed elevated thyroid hormone levels with a normal TSH level (**Table 1**). The iodine uptake rate of the thyroid gland was 25.4% at 3 hours (reference range: 6%–28%) and 58.1% at 24 hours (reference range: 16–50%). Magnetic resonance imaging (MRI) of the pituitary gland did not reveal any pituitary adenomas (**Figure 1**). Other pituitary axes showed normal function (**Table 2**). An electrocardiogram showed sinus rhythm. Based on the patient's medical history and examination, RTHS was suspected, and the patient was advised to undergo genetic testing.

Table 1. Results of the proband's thyroid function and antibody panel

Test (unit)	Result by Date		Normal range	Test (unit)	Result by Date	Normal range
	March 6, 2024	March 16, 2024			March 21, 2024	
TSH (mIU/L)	2.13	2.51	0.72–4.2	TSH (μIU/mL)	2.7082	0.3500–4.9400
FT4 (pmol/L)	57.1	52.4	12–22	FT4 (ng/dL)	2.13	0.70–1.48
TT4 (nmol/L)	193.00	171.00	66–181	TT4 (μg/dL)	15.53	4.87–11.72
FT3 (pmol/L)	14.4	13.00	3.1–6.8	FT3 (pg/mL)	6.41	1.58–3.91
TT3 (nmol/L)	3.71	3.31	1.2–3.1	TT3 (ng/mL)	1.78	0.64–1.52
TPOAb (IU/mL)	15.6	16.70	0–34	TPOAb (IU/mL)	2.42	<5.62
TgAb (IU/mL)	21.2	12.10	0–115	TGAb (IU/mL)	0.65	<4.11
TRAb (IU/L)	–	<0.80	0–1.75	TRAb (IU/L)	1.670	0.000–1.750
TG (ng/mL)	–	207.00	3.5–77	TG (ng/mL)	190.00	3.50–77.00
rT3 (U/L)	–	1.11	0.31–1.24	–	–	–

Abbreviations: FT3: free triiodothyronine; FT4: free thyroxine; rT3: reverse triiodothyronine; TG: thyroglobulin; TgAb: thyroglobulin antibody; TPOAb: thyroid peroxidase antibody; TRAb: thyrotropin receptor antibody; TSH: thyroid-stimulating hormone; TT3: total triiodothyronine; TT4: total thyroxine.

Copyright© AE&M all rights reserved.

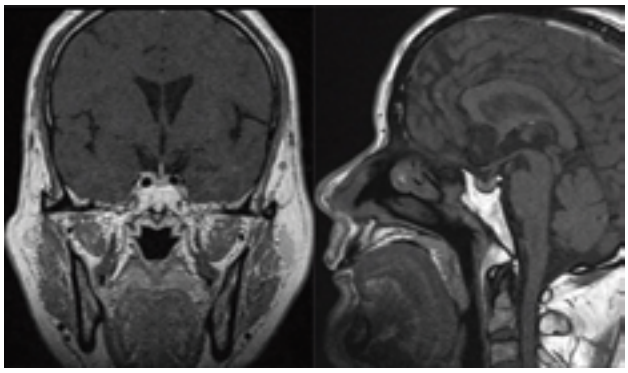


Figure 1. The proband underwent plain and enhanced magnetic resonance imaging of the pituitary gland. No abnormal signals were detected in the pituitary gland, and the pituitary stalk was centrally located. No abnormalities were observed in the morphology or signals of the optic chiasm and bilateral internal carotid arteries. On enhanced scanning, the enhancement of the pituitary tissue was relatively uniform and consistent, with no evidence of abnormal enhancement.

Table 2. Results of the proband's laboratory tests

Parameter (unit)	Result	Normal range
Potassium (mmol/L)	3.58	3.5–5.1
Sodium (mmol/L)	139.56	137–147
Calcium (mmol/L)	2.10	2.1–2.55
Magnesium (mmol/L)	0.89	0.7–1.0
Phosphorus (mmol/L)	0.94	0.81–1.45
Creatinine (mmol/L)	68.6	53–115
Fasting glucose (mmol/L)	4.83	3.9–6.1
Triglycerides (mmol/L)	0.92	0.29–1.83
Total cholesterol (mmol/L)	4.97	2.8–5.7
LDL-C (mmol/L)	3.5	2.7–3.1
Albumin (g/L)	43.9	40–55
AST (U/L)	26	15–40
ALT (U/L)	37.2	9–50
SHBG (nmol/L)	22	20.6–76.7
Growth hormone (ng/mL)	1.45	0.03–2.47
IGF-1 (ng/mL)	74.6	45–210
Cortisol at 10 AM (nmol/L)	139.6	101.2–535.7
Cortisol at 2 AM (nmol/L)	32.9	–
ACTH at 10 AM (pg/mL)	17.4	7.2–63.3
FSH (IU/L)	9.31	0.95–11.95
LH (IU/L)	4.75	0.57–12.07

Abbreviations: LDL-C: low-density lipoprotein cholesterol; AST: aspartate aminotransferase; ALT: alanine aminotransferase; SHBG: sex hormone-binding globulin; IGF-1: insulin-like growth factor-1; ACTH: adrenocorticotropic hormone; LH: luteinizing hormone; FSH: follicle-stimulating hormone.

In this study, whole-exome high-throughput sequencing (WES) was employed. The data were analyzed using the Verita Trekker variant detection system and the Enliven variant annotation and interpretation system, both of which were independently developed by Berry Genomics (Beijing, China). For suspected dynamic mutations identified by WES, a comprehensive analysis was conducted using polymerase chain reaction (PCR) and capillary electrophoresis. Based on the guidelines of the American College of Medical Genetics and Genomics (ACMG) and the application recommendations of the ClinGen Sequence Variant Interpretation (SVI) Expert Panel, as well as a review of public databases such as the Human Phenotype Ontology (HPO; https://hpo.jax.org/app/), Online Mendelian Inheritance in Man (OMIM; https://omim.org/), and Genetics Home Reference (https://medlineplus.gov/genetics/), the c.938T>C mutation in the *THRB* gene (**Figure 2**) was classified as a pathogenic mutation site.

DISCUSSION

First reported by Refetoff and cols. in 1967, RTHS is a rare endocrine disorder with an incidence of approximately 1 in 40,000 individuals. Here, we report a case of a 57-year-old male with RTHS. The patient presented with symptoms typical of hyperthyroidism, including palpitations and hand tremors. Thyroid function tests revealed elevated serum thyroid hormone levels, while TSH levels remained normal, consistent with the biochemical and clinical features commonly reported in RTHS (10,11). Genetic testing identified a novel mutation in the *THRB* gene. Specifically, a heterozygous point mutation was found at nucleotide position 938 in exon 9, where thymine was replaced by cytosine (c.938T>C). This mutation resulted in the substitution of methionine with threonine at amino acid position 313 (p.M313T). This mutation site is located in a key functional domain of the *THRB* gene, likely altering the receptor's conformation and affecting its affinity for thyroid hormones. This, in turn, interferes with the receptor's binding efficiency and transcriptional activity, ultimately leading to thyroid hormone resistance. This finding is consistent with previous studies showing that most RTHS cases are caused by *THRB* gene mutations and exhibit autosomal dominant inheritance (12,13). Functional studies of *THRB* gene mutations have provided strong evidence supporting this mechanism (14). To our knowledge, the specific

Copyright© AE&M all rights reserved.

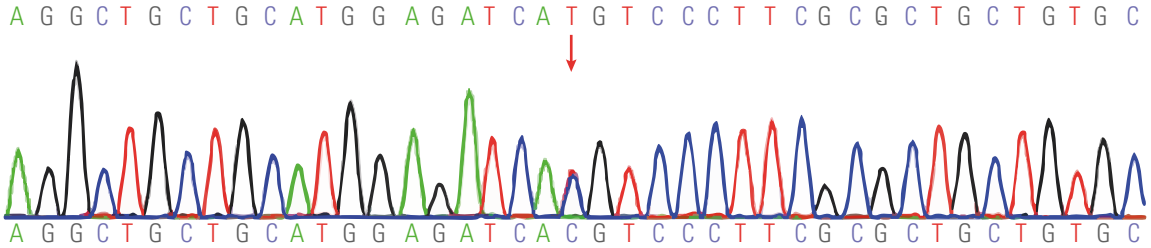


Figure 2. Sequencing analysis of the thyroid hormone receptor beta (*THRB*) gene in the proband. A heterozygous point mutation was identified in exon 9, where the nucleotide at position 938 was mutated from thymine to cytosine. This mutation resulted in the substitution of methionine with threonine at amino acid position 313. The arrow indicates the location of this point mutation.

mutation identified in this patient has not been previously reported.

Notably, RTHS is primarily driven by heterozygous pathogenic variants in the *THRB* gene, which account for over 80% of affected families. These mutations cluster in three critical hotspot regions (exons 7–10), including the segment encompassing codons 310–353, where our novel p.M313T variant is located (15). These regions are essential for ligand binding and signal transduction. Consequently, mutations like p.M313T are predicted to disrupt thyroid hormone binding affinity and subsequent transcriptional activity, leading to the clinical manifestation of hormone resistance. While *THRB* mutations represent the majority of cases, approximately 10% are attributed to other mechanisms, such as reduced number of thyroid hormone receptors or other unknown factors (16). The specific organ distribution of functional receptor isoforms (TRα1, TRβ1, and TRβ2) underlies the diverse clinical presentations observed in RTHS.

The clinical manifestations of RTHS are diverse and complex. Goiter is present in 66–95% of patients. Approximately 60% of patients have mood disorders, and 40–60% suffer from attention-deficit/hyperactivity disorder, presenting with behaviors such as inattentiveness, hyperactivity, and impulsivity. Additionally, 33–75% of patients exhibit tachycardia (17,18). Notably, goiter was absent in our patient.

Based on clinical manifestations, RTHS is classified into three main types: Generalized Resistance to Thyroid Hormone (GRTH), Pituitary Resistance to Thyroid Hormone (PRTH), and Peripheral Resistance to Thyroid Hormone (PRTH). Patients with GRTH usually have no obvious symptoms except for goiter. Patients with PRTH show mild to moderate manifestations of hyperthyroidism, such as hyperhidrosis, palpitations, and hand tremors, but may also present with symptoms of hypothyroidism. In our case, the patient presented with clinical symptoms of hyperthyroidism, including insomnia, tachycardia, and hand tremors. Therefore, the patient is considered to have PRTH. In addition to these symptoms, some patients may also experience growth retardation, decreased learning ability, hearing impairment, and abnormal bone development (19). The symptoms vary widely among different patients, and even among patients with the same mutation within the same family, the symptoms may not be identical. This clinical heterogeneity is likely due to the variable nature of the genetic mutations and the specific tissues affected.

Diagnosis of RTHS requires careful judgment by comprehensively considering clinical symptoms, physical signs, family history, and the results of other auxiliary examinations (20). Gene sequencing is the gold standard for diagnosis. In terms of differential diagnosis, RTHS has many similarities with other diseases that can lead to elevated thyroid hormone levels without TSH suppression and needs to be carefully distinguished. We retested the patient's thyroid function in another hospital using different reagents. The results of the retest were consistent with those obtained in our hospital, thereby ruling out potential detection errors. Under such circumstances, it was necessary to differentiate whether our patient had a thyrotropin-secreting pituitary adenoma (TSHoma). Ninety percent of patients with TSHomas show a blunted response to thyrotropin-releasing hormone (TRH) stimulation. An MRI of the sella turcica often

Copyright© AE&M all rights reserved.

reveals a pituitary adenoma. There are no *THRB* gene mutations, and the serum level of sex hormone-binding globulin (SHBG) is usually high. In contrast, in most patients with RTHS, TSH shows a normal response to TRH stimulation, there is no pituitary adenoma, and approximately 80% of them have *THRB* gene mutations, with a normal serum SHBG level. In addition, it is also necessary to differentiate from diseases caused by mutations in the *THRA* gene. In patients with *THRA* mutations, the levels of thyroid hormones and TSH are close to normal, but growth and gastrointestinal function abnormalities are present, while in RTHS, the main feature is the reduced responsiveness of tissues to thyroid hormones. Enhanced MRI of the pituitary gland in our patient did not detect any pituitary adenoma. Additionally, serum SHBG level was within the normal range. Therefore, the diagnosis of TSHoma was excluded in our patient.

Having established the diagnosis of RTHS through differential diagnosis, the focus shifts to its clinical management. Regarding the treatment strategy, there is currently no radical cure for RTHS. The main treatment principles focus on effectively relieving patients' symptoms and improving their quality of life. For patients with relatively mild symptoms, such as the one in this case, the use of beta blockers has achieved good results in relieving tachycardia. This is mainly because beta blockers can specifically block the excessive stimulation of thyroid hormones on cardiac β-receptors, thereby reducing the discomfort caused by a rapid heart rate and lowering the risk of cardiovascular events (21). Patients with RTHS must strictly avoid the use of antithyroid drugs (ATDs), primarily because the function of these drugs is to inhibit the synthesis of thyroid hormones, which is completely contrary to the compensatory mechanism of RTHS and would disrupt the body's fragile compensatory balance. If ATD is used, they further reduce circulating thyroid hormone levels. In patients with reduced tissue responsiveness to thyroid hormone, additional lowering of hormone levels can further limit the availability of thyroid hormones to target tissues, potentially exacerbating symptoms of hypothyroidism, such as fatigue and lethargy. Simultaneously, the reduction in thyroid hormone levels stimulates the pituitary gland to secrete a large amount of TSH through negative feedback, potentially leading to pituitary TSH cell hyperplasia or even pituitary adenoma in the long term. It will also mask the typical laboratory features of RTHS, complicating the diagnosis and subsequent treatment direction. This has been fully demonstrated by Lai and cols. in relevant research (22). For patients with symptoms of hypothyroidism or growth retardation, thyroid hormone replacement therapy can be considered on the premise of closely monitoring thyroid function indicators. Furthermore, for patients with mood disorders or attention-deficit/hyperactivity disorder, psychological counseling and drug interventions can be implemented. However, during the treatment process, it is necessary to closely monitor the dynamic changes of thyroid function to prevent overtreatment and avoid other adverse reactions (23). Throughout the treatment, it is essential to closely monitor indicators, including thyroid hormone levels, TSH, and liver and kidney function, to adjust the treatment plan in a timely manner. At the same time, genetic screening of the patient's relatives is helpful for early detection and treatment of potential patients.

Our study identified a novel heterozygous p.M313T mutation in the TRβ gene of a patient with generalized RTHβ. While the p.M313T variant itself has not been previously documented, its pathological relevance is strongly corroborated by a highly parallel finding in the literature. Notably, a study by Del Prete and cols. (2021) reported an identical methionine-to-threonine substitution — p.M310T — in a patient with a virtually identical phenotype of generalized RTHβ (24). This finding provides a crucial context for our discovery. The coexistence of pathogenic M→T mutations at adjacent codons 310 and 313 signifies that the M310–M313 segment constitutes a genuine and critical mutational hotspot within the ligand-binding domain of TRβ. The clustering of phenotypically identical missense mutations is a hallmark of functionally indispensable protein regions. The fact that both mutations involve the replacement of a bulky, hydrophobic methionine with a polar threonine suggests a common mechanistic basis for pathogenicity.

One limitation of the present study was the inability to perform genetic testing on the proband's family

Copyright© ACE&M all rights reserved.

members. This constraint has several important implications. First, it restricts our understanding of the inheritance pattern, as we cannot definitively distinguish whether the p.M313T variant is a *de novo* or an inherited mutation, which directly affects the assessment of its penetrance. Second, it introduces significant uncertainty into clinical genetic counseling, precluding accurate recurrence risk assessment for the patient's first-degree relatives and future offspring. Finally, potential strategies for early detection and preventive management cannot be implemented, as we are unable to identify other potentially asymptomatic family members who may carry the pathogenic variant.

Several critical challenges in the RTHS field warrant further investigation. A primary focus should be on establishing large-scale, international patient registries. These multicenter databases are crucial for collecting robust, longitudinal data on this rare disorder. Furthermore, detailed genotype-phenotype correlation studies are needed to elucidate how specific mutations influence disease severity, clinical presentation, and long-term outcomes. On the clinical front, research must prioritize the development of standardized strategies for early detection of RTHS, including genetic screening protocols for at-risk relatives and refined diagnostic algorithms for patients with unexplained thyroid function test abnormalities. Future research combining these clinical findings with foundational studies on molecular pathogenesis will be key to developing personalized management plans and improving overall patient prognosis and quality of life.

CONCLUSION

We report a case of a 57-year-old Chinese male with RTHS. A novel heterozygous point mutation — c.938T>C: p.M313T — in the *THRB* gene was discovered. This finding further enriches the clinical case data of RTHS in the Chinese population and is of great significance for improving clinicians' awareness and diagnostic capabilities regarding this disease.

Author contributions: Sheng Jiang and Li Quan were responsible for the conception, design, quality control, and proofreading of the manuscript, and are accountable for the entire manuscript. Jing Yang and Chuan Wang were in charge of writing and revising the manuscript. Sheng Jiang, Li Quan, Jing Yang, and Chuan Wang carried out the research and conducted the feasibility analysis. Jing Yang was responsible for collecting the case data. Chuan Wang was responsible for organizing the case data. Sheng Jiang, Li Quan, Jing Yang, and Chuan Wang were responsible for analyzing and interpreting the results.

Acknowledgements: none.

Funding: this study was supported by the Xinjiang Uygur Autonomous Region Science and Technology Innovation Team (Tianshan Innovation Team) project (grant no. 2022TSYCTD0014).

Ethics approval and consent to participate: the Ethics Committee of the First Affiliated Hospital of Xinjiang Medical University approved this research.

Patient consent for publication: written informed consent has been obtained from the patient for the publication of this case report and the accompanying images, as well as the use of the patient's data.

Disclosure: no potential conflict of interest relevant to this article was reported.

Data availability: datasets related to this article will be available upon request to the corresponding author.

REFERENCES

1. Refetoff S, Bassett JH, Beck-Peccoz P, Bernal J, Brent G, Chatterjee K, De Groot LJ, Dumitrescu AM, Jameson JL, Kopp PA, Murata Y, Persani L, Samarut J, Weiss RE, Williams GR, Yen PM. Classification and proposed nomenclature for inherited defects of thyroid hormone action, cell transport, and metabolism. J Clin Endocrinol Metab. 2014 Mar;99(3):768-70. doi: 10.1210/jc.2013-3393.
2. Pappa T, Anselmo J, Mamanasiri S, Dumitrescu AM, Weiss RE, Refetoff S. Prenatal Diagnosis of Resistance to Thyroid Hormone and Its Clinical Implications. J Clin Endocrinol Metab. 2017 Oct 1;102(10):3775-3782. doi: 10.1210/jc.2017-01251.
3. Pappa T, Refetoff S. Human Genetics of Thyroid Hormone Receptor Beta: Resistance to Thyroid Hormone Beta (RTHβ). Methods Mol Biol. 2018;1801:225-240. doi: 10.1007/978-1-4939-7902-8_18.
4. Persani L, Campi I. Syndromes of Resistance to Thyroid Hormone Action. Exp Suppl. 2019;111:55-84. doi: 10.1007/978-3-030-25905-1_5.
5. Sun H, Cao L, Zheng R, Xie S, Liu C. Update on resistance to thyroid hormone syndromeβ. Ital J Pediatr. 2020 Nov 11;46(1):168. doi: 10.1186/s13052-020-00929-x.
6. Yusufu A, Chen WJ, Zhang MC. Thyroid hormone resistance syndrome with P453T mutation in thyroid hormone receptor β gene: A pedigree report. Medicine (Baltimore). 2020 Oct 30;99(44):e22824. doi: 10.1097/MD.0000000000022824.
7. Concolino P, Costella A, Paragliola RM. Mutational Landscape of Resistance to Thyroid Hormone Beta (RTHβ). Mol Diagn Ther. 2019 Jun;23(3):353-368. doi: 10.1007/s40291-019-00399-w.
8. Zhao J, Xu L, Li C, Wang F, Liao L, Dong J. The clinical characteristics and gene mutations associated with thyroid hormone resistance syndrome coexisting with pituitary tumors. Front Endocrinol (Lausanne). 2023 Feb 10;14:1131044. doi: 10.3389/fendo.2023.1131044.
9. Pappa T, Refetoff S. Resistance to Thyroid Hormone Beta: A Focused Review. Front Endocrinol (Lausanne). 2021 Mar 31;12:656551. doi: 10.3389/fendo.2021.656551.
10. Refetoff S, Weiss RE, Usala SJ. The syndromes of resistance to thyroid hormone. Endocr Rev. 1993 Jun;14(3):348-99. doi: 10.1210/edrv-14-3-348.
11. Guo J, Xiang T, Wang Y, Yuan G. A rare mutation in *THRB* gene of resistance to thyroid hormone: a case report of a Chinese pedigree. QJM. 2024;117(7): 538-540. doi: 10.1093/qjmed/hcae057.

Copyright© AE&M all rights reserved.

12. Dumitrescu AM, Refetoff S. The syndromes of reduced sensitivity to thyroid hormone. Biochim Biophys Acta. 2013 Jul;1830(7):3987-4003. doi: 10.1016/j.bbagen.2012.08.005.
13. Agrawal NK, Goyal R, Rastogi A, Naik D, Singh SK. Thyroid hormone resistance. Postgrad Med J. 2008 Sep;84(995):473-7. doi: 10.1136/pgmj.2008.069740.
14. Adams M, Matthews C, Collingwood TN, Tone Y, Beck-Peccoz P, Chatterjee KK. Genetic analysis of 29 kindreds with generalized and pituitary resistance to thyroid hormone. Identification of thirteen novel mutations in the thyroid hormone receptor beta gene. J Clin Invest. 1994 Aug;94(2):506-15. doi: 10.1172/JCI117362.
15. Wang J, Lv H. Identification of a novel mutation in the thyroid hormone receptor β gene that causes thyroid hormone resistance syndrome: A case report. Mol Med Rep. 2019 Nov;20(5):4683-4687. doi: 10.3892/mmr.2019.10703.
16. Ortiga-Carvalho TM, Sidhaye AR, Wondisford FE. Thyroid hormone receptors and resistance to thyroid hormone disorders. Nat Rev Endocrinol. 2014 Oct;10(10):582-91. doi: 10.1038/nrendo.2014.143.
17. Tagami T. An overview of thyroid function tests in subjects with resistance to thyroid hormone and related disorders. Endocr J. 2021 May 28;68(5):509-517. doi: 10.1507/endocrj.EJ21-0059.
18. Rezgani I, Chihaoui M, Oueslati I, Chaker F, Nagi S, Yazidi M. Thyroid hormone resistance syndrome caused by a novel mutation in the thyroid hormone receptor-beta gene (*THRB*, GLU457LYS) treated with methimazole. Clin Case Rep. 2022;10(11):e6543. doi: 10.1002/ccr3.6543.
19. Ferrara AM, Onigata K, Ercan O, Woodhead H, Weiss RE, Refetoff S. Homozygous thyroid hormone receptor β-gene mutations in resistance to thyroid hormone: three new cases and review of the literature. J Clin Endocrinol Metab. 2012 Apr;97(4):1328-36. doi: 10.1210/jc.2011-2642.
20. Campi I, Covelli D, Moran C, Fugazzola L, Cacciatore C, Orlandi F, et al. The Differential Diagnosis of Discrepant Thyroid Function Tests: Insistent Pitfalls and Updated Flow-Chart Based on a Long-Standing Experience. Front Endocrinol (Lausanne). 2020 Jul 7;11:432. doi: 10.3389/fendo.2020.00432.
21. Illouz F, Briet C, Mirebeau-Prunier D, Bouhours-Nouet N, Coutant R, Sibilia P, et al. Cardiac complications of thyroid hormone resistance syndromes. Ann Endocrinol (Paris). 2021 Jun;82(3-4):167-169. doi: 10.1016/j.ando.2020.03.008.
22. Lai S, Zhang S, Wang L, Chen Z, Fu X, Jianhao P, et al. A Rare Mutation in Patients With Resistance to Thyroid Hormone and Review of Therapeutic Strategies. Am J Med Sci. 2015 Sep;350(3):167-74. doi: 10.1097/MAJ.0000000000000538.
23. Choi JH, Cho JH, Kim JH, Yoo EG, Kim GH, Yoo HW. Variable Clinical Characteristics and Molecular Spectrum of Patients with Syndromes of Reduced Sensitivity to Thyroid Hormone: Genetic Defects in the *THRB* and SLC16A2 Genes. Horm Res Paediatr. 2018;90(5):283-290. doi: 10.1159/000493468.
24. Del Prete M, Muratori F, Campi I, Di Sacco G, Vignati F, Pellegrino D, Persani L. A rare mutation of thyroid hormone receptor beta gene in thyroid hormone resistance syndrome. Endocrinol Diabetes Metab Case Rep. 2021:21-0023. doi: 10.1530/EDM-21-0023.

Copyright© AE&M all rights reserved.

Archives of Endocrinology and Metabolism
ISSN 2359-4292
OFFICIAL JOURNAL OF THE BRAZILIAN SOCIETY OF ENDOCRINOLOGY AND METABOLISM

brief communication

Challenging the recessive paradigm of Mahvash disease: heterozygous phenotypes from a novel splice-site variant

Francisco Martínez Bugallo[1]
https://orcid.org/0000-0002-0380-3488

Gema García de la Rosa[1]
https://orcid.org/0000-0003-0976-2653

Carol Prieto-Morín[1]
https://orcid.org/0000-0001-5789-3143

[1] Human Genetic Unit, Department of Clinical Analysis Laboratory, University Hospital Nuestra Señora de Candelaria, Santa Cruz de Tenerife, Spain

ABSTRACT

Mahvash disease is a rare autosomal recessive condition caused by biallelic inactivating variants in the *GCGR* gene, impairing glucagon signaling and leading to alpha-cell hyperplasia and pancreatic neuroendocrine tumors (PNETs). Fewer than 20 cases have been reported, and the clinical impact of heterozygous variants remains unclear. Case Presentation: We report a family with a novel GCGR splice-site variant (c.1176+1_1176+7delGTGCCCG). The index case, a 61-year-old woman, presented with extensive pancreatic cystic disease and was found to be homozygous for the variant. She developed well-differentiated PNETs and underwent total pancreatectomy. Her sister, also homozygous, had similar clinical features and surgical history. In contrast, the heterozygous brother and two sons showed mild biochemical changes, such as elevated glucagon levels and small pancreatic cysts, without overt disease. The two homozygous sisters required pancreatic surgery followed by insulin and enzyme replacement therapy, whereas heterozygous carriers are currently being managed with biochemical and imaging surveillance. This family's phenotype suggests a broader spectrum of GCGR-related disease. While homozygous individuals displayed classic Mahvash disease, heterozygotes exhibited subtle biochemical and structural pancreatic changes, indicating possible semidominant expression. These findings are consistent with emerging evidence that monoallelic receptor pathway mutations may produce mild or subclinical phenotypes. This case challenges the classical recessive model of Mahvash disease and highlights the potential for disease expression in heterozygous carriers. These findings suggest that heterozygosity is not entirely silent and underline the need to reconsider surveillance recommendations for GCGR heterozygotes.

Keywords: Glucagon receptor; pancreatic neoplasms; genetic predisposition to disease; splice site mutation; neuroendocrine tumors

INTRODUCTION

Mahvash disease is a rare autosomal recessive disorder caused by inactivating mutations in the glucagon receptor gene (*GCGR*), leading to impaired glucagon signaling and compensatory pancreatic alpha-cell hyperplasia. Although fewer than 20 clinically confirmed cases have been reported worldwide (1-3), large-scale genomic studies suggest that the prevalence may be as high as four cases per million persons (2). This indicates that the condition is likely underrecognized rather than truly absent in the general population. Cases have been described in Asia, Europe, and North America, without evidence of geographical clustering. However, several families arose from consanguineous backgrounds (4,5), and accumulation of *GCGR* pathogenic variants in certain regions has been hypothesized to reflect founder effects or parental consanguinity (6).

Affected individuals typically show elevated plasma glucagon levels, pancreatic neuroendocrine tumors

Received on Aug/15/2025
Accepted on Oct/7/2025
DOI: 10.20945/2359-4292-2026-0005

Correspondence to:
Francisco Martínez Bugallo
Human Genetic Unit,
Department of Clinical Analysis Laboratory,
University Hospital Nuestra Señora de Candelaria,
Carretera General del Rosario 145
38010 – Santa Cruz de Tenerife, Spain
fmarburg@gobiernodecanarias.org

Associated editor:
Maria Candida Barisson
https://orcid.org/0000-0001-6150-1915

This is an open-access article distributed under the terms of the Creative Commons Attribution License

Copyright© AE&M all rights reserved.

(PNETs) not associated with glucagonoma syndrome, and may develop diabetes, diarrhea, or pancreatitis (1-3). The clinical impact of heterozygous *GCGR* variants is unclear due to limited familial and experimental data. In murine models, *Gcgr*+/− animals display normal pancreatic morphology and do not develop α-cell hyperplasia or neuroendocrine tumors, in contrast to the fully penetrant phenotype observed in *Gcgr*−/− mice (1). However, in other recessive endocrine disorders, such as MC4R or CYP21A2 deficiency, heterozygous carriers have been shown to manifest subtle clinical or biochemical phenotypes, suggesting that heterozygous states may not always be clinically silent.

Here, we describe a novel splice-site variant (c.1176+1_1176+7delGTGCCCG) segregated with clear phenotypic differences by zygosity, underscoring a discrepancy between animal models and human observations. These findings raise the possibility that heterozygous *GCGR* loss-of-function may exert clinical effects in humans, with implications for disease penetrance, surveillance, and counseling.

CASE PRESENTATION

The index case, a 61-year-old woman, was initially evaluated due to the incidental discovery of extensive pancreatic cystic disease (over 50 cysts throughout the gland) along with radiological features suggestive of chronic pancreatitis. Despite these findings, she had no clinical signs of endocrine or exocrine pancreatic insufficiency. The imaging abnormalities and a family history of pancreatic neoplasia in her sister prompted further investigation. Initial genetic testing for CFTR and VHL was negative.

Genetic testing revealed homozygosity for a novel *GCGR* splice-site variant, NM_000160.5:c.1176+1_1176+7delGTGCCCG, identified via clinical exome sequencing. This 7-base deletion at the intron 12 donor site is predicted to disrupt splicing, leading to loss of receptor function. Absent from population databases and unpublished, its classification as likely pathogenic is supported by in silico predictions, familial segregation, and similarity to other *GCGR* loss-of-function variants (7,8).

The patient developed well-differentiated PNETs and underwent total pancreatectomy, splenectomy, and cholecystectomy. Histology confirmed well-differentiated neuroendocrine tumors. She required insulin and enzyme therapy, with suboptimal metabolic control. Serial biochemical follow-up revealed persistently elevated glucagon levels (208–219 pg/mL; normal range 50–150 pg/mL) and intermittently elevated chromogranin A (up to 196 ng/mL; normal range 0–100 ng/mL), consistent with the expected biochemical signature of Mahvash disease.

The 66-year-old sister, also homozygous for the *GCGR* variant, underwent duodenopancreatectomy, splenectomy, and cholecystectomy 14 years ago due to pancreatic tumors. She previously showed elevated chromogranin A levels and now remains on insulin and enzyme therapy with stable metabolic status. Both sisters exhibit the classic Mahvash disease phenotype, including PNETs and endocrine/exocrine dysfunction.

The brother of both affected women, a 56-year-old man, was found to be heterozygous for the variant. He remains asymptomatic but has been under surveillance due to imaging findings of a subcentimetric intraductal papillary mucinous neoplasm (IPMN) without high-risk features. Imaging by endoscopic ultrasound (EUS) revealed a 4 mm cystic lesion in the pancreas, with no communication with the main pancreatic duct (**Figure 1**). His biochemical profile revealed a mild elevation in glucagon (178 pg/mL), though other tumor markers, including chromogranin A and pancreatic polypeptide, were within normal range. Surveillance has been carried out in accordance with the Kyoto

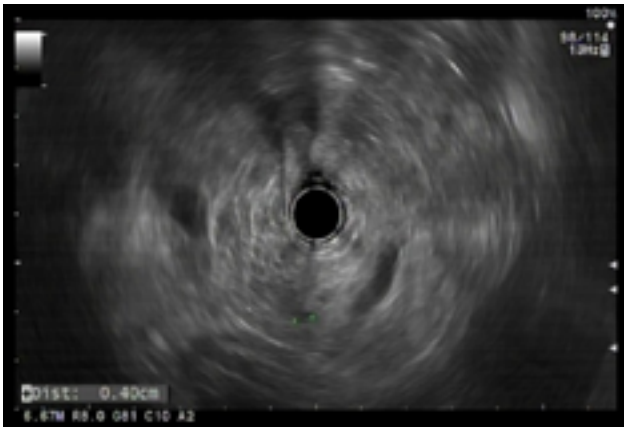


Figure 1. Endoscopic ultrasound of the heterozygous brother showing a 4 mm unilocular cyst in the posterior pancreatic body, with thin walls, no solid components, and no apparent communication with the main pancreatic duct.

Copyright© AE&M all rights reserved.

guidelines for IPMN (9). Although these guidelines allow discontinuation of follow-up after 5 years in stable lesions <20 mm, extended surveillance with annual MRI was chosen in this case, given the presence of a familial *GCGR* variant and its potential clinical implications.

The index patient's two sons, aged 36 and 31, are also heterozygous carriers. Both are clinically asymptomatic. The elder son had a normal MRI and normal biochemical parameters (glucagon 108 pg/mL; chromogranin A 60.31 ng/mL). In contrast, the younger son demonstrated a mild elevation in fasting glucagon levels (177 pg/mL), with normal chromogranin A and pancreatic polypeptide levels. Although no pancreatic lesions have been identified to date, this subtle increase in glucagon raises the possibility of early or subclinical alpha-cell proliferation in heterozygous carriers. He is currently undergoing conservative annual MRI, biochemical surveillance, and additional renal ultrasound to assess for possible cystic disease as observed in other relatives; however, the long-term monitoring strategy for heterozygous carriers has yet to be defined and may require adjustment as further data emerge.

The 86-year-old mother of the three siblings is heterozygous for the *GCGR* variant and, despite being asymptomatic, shows chronically elevated pancreatic enzymes without imaging evidence of lesions. No hormonal tests have been performed. Differential diagnoses such as chronic pancreatitis, subclinical ductal obstruction, medication effects, or age-related pancreatic changes were considered, although none were clinically suspected. Given her age and stable clinical course, further extensive investigations were not pursued. The deceased father was not genetically tested.

DISCUSSION

This family provides evidence that *GCGR*-related pathology may extend beyond the classical autosomal recessive model. While homozygous individuals clearly show the full Mahvash disease phenotype, the presence of pancreatic cysts and mildly elevated glucagon in heterozygotes suggests a possible semidominance effect. These findings align with emerging observations that some recessive conditions may manifest subtly in heterozygous carriers, particularly those involving receptor or hormonal pathways (10).

Consistent with previous reports describing *GCGR* variants in consanguineous families (6), the segregation pattern observed in this family — two homozygous daughters, a heterozygous mother, and an untested deceased father — strongly suggests paternal carrier status. Given the family's origin from a small, isolated village of around 400 inhabitants, distant consanguinity cannot be excluded.

The biochemical findings in this family support a spectrum of alpha-cell activity, even without evident neuroendocrine tumors. The index case and her homozygous sister showed significant elevations in glucagon and chromogranin A, consistent with Mahvash disease. Heterozygous relatives had mild glucagon increases, possibly indicating early or subclinical alpha-cell hyperplasia. Normal chromogranin A and pancreatic polypeptide levels in heterozygotes suggest no active tumor development. This pattern indicates that glucagon elevation may precede structural changes and could serve as an early marker for monitoring at-risk heterozygous individuals. Notably, while heterozygous *Gcgr*+/− mice show no pancreatic abnormalities, our findings in human carriers suggest that subtle biochemical or structural changes may still occur, highlighting an important divergence between animal models and human disease expression. Whether more subtle functional changes occur in heterozygous animals has not been systematically evaluated, and thus cannot be excluded.

Recent work by Kuiper and cols. (11) also described a family with a heterozygous *GCGR* variant (p.Ser152Phe) in which one carrier developed PNETs. Interestingly, somatic MEN1 mutations were identified in the tumors of that individual, suggesting that reduced glucagon receptor signaling may create a permissive state that, when combined with additional genetic events, promotes neoplastic transformation. This observation supports the notion that heterozygous *GCGR* loss-of-function alone may not invariably lead to clinically significant disease, but can predispose to pathological changes under specific conditions. A separate report by Deng and cols. (12) described a

Copyright© AE&M all rights reserved.

patient labelled as "heterozygous" who carried two *GCGR* variants (c.1345C>T and c.922C>T). One of these is a truncating variant likely to be pathogenic, while the other is a missense variant currently classified as a variant of uncertain significance, with limited evidence supporting a pathogenic role. In addition, segregation analysis was not performed, leaving it unclear whether the two variants are located on the same allele or on different alleles. Clinically, the patient showed a diffusely enlarged pancreas with heterogeneous enhancement on imaging and developed pancreatic neuroendocrine tumors. However, because the diagnosis relied primarily on clinical and imaging findings rather than on definitive genetic evidence, the underlying genetic status and mode of inheritance in this case remain highly uncertain, and it provides only limited insight into the potential consequences of *GCGR* heterozygosity.

These findings may suggest that clinical surveillance strategies for individuals heterozygous for *GCGR* pathogenic variants may need reconsideration. Although current guidelines assume complete recessivity and don't recommend follow-up for carriers, our observations in this family indicate that a cautious conservative monitoring approach could be considered. In particular, we propose—based on this limited experience—annual clinical and biochemical evaluation, with special attention to fasting glucagon levels, complemented by periodic pancreatic imaging using MRI or EUS. The optimal frequency and duration of imaging are not yet established, but an initial interval of 1–2 years appears reasonable and safe as a provisional approach until further evidence becomes available. This schedule could then be individualized over time according to the evolution of pancreatic findings and the patient's overall clinical course. From the radiological perspective, recent correspondence has emphasized the importance of carefully interpreting subtle cystic or ductal changes in carriers, as these may represent early or subclinical manifestations of disease (13). We emphasize that these recommendations are hypothetical and derived from a single family, and are intended mainly to stimulate further discussion and research on the management of heterozygous *GCGR* carriers.

Although the long-term risks for heterozygous carriers are not yet defined, our findings may suggest a potential for progression from isolated biochemical changes to structural pancreatic abnormalities. The development of clinically significant complications, such as α-cell hyperplasia or neuroendocrine tumors, appears uncommon but cannot be excluded, particularly if additional modifying factors are present. Thus, carriers should not be considered entirely unaffected, but their risk profile remains far lower and less predictable than that of homozygous individuals.

A recent case series by Gild and cols. (5) reviewed *GCGR* variants reported in Mahvash disease patients, including missense, nonsense, frameshift, and in-frame deletion mutations. These variants were observed in both homozygous and compound heterozygous states. These biallelic loss-of-function mutations often lead to the full disease phenotype. Our findings align with this and further suggest that even monoallelic loss of *GCGR* function may cause pancreatic or biochemical changes under certain conditions. Although the functional impact of this specific variant has not yet been confirmed, it is analogous to other loss-of-function mutations in *GCGR* that lead to absent receptor expression or activity (1,4).

As with many reports on rare genetic disorders, this study is inherently limited by the small number of affected individuals available for analysis — here restricted to a single family. The scarcity of published data on heterozygous *GCGR* carriers reflects a broader gap in the field rather than a shortcoming of this report. Another limitation is that alternative explanations for the incidence of pancreatic cysts in this family, such as unrelated genetic predispositions or shared environmental factors, cannot be fully excluded. However, the clear segregation of both biochemical abnormalities and cystic findings with *GCGR* zygosity argues in favor of a causal role of the variant, making these alternatives less likely. Taken together, these observations provide meaningful insights into the potential clinical impact of heterozygous variants. Rather than offering definitive conclusions, our report underscores the need for further investigations and may serve as a foundation for developing surveillance strategies in this previously overlooked group.

Copyright© AE&M all rights reserved.

CONCLUSION

In conclusion, this report describes a family with a novel *GCGR* splice-site variant segregated in both homozygous and heterozygous individuals, with phenotypes ranging from classic Mahvash disease to subtle biochemical or structural pancreatic changes. The consistent detection of mild hyperglucagonemia in heterozygotes, together with occasional cystic findings, suggests that *GCGR*-related pathology may extend beyond the strictly recessive model and include a broader phenotypic spectrum. Our observations raise the possibility that heterozygous carriers might manifest a mild phenotype compatible with a dominant pattern of low penetrance and variable expressivity, although additional studies are needed to confirm this hypothesis and better define its clinical implications, including surveillance strategies for carriers.

Authors' contribution: FMB: Conception and study design, data acquisition, data analysis, manuscript drafting, and final manuscript approval. GGR: Data acquisition, data analysis, manuscript drafting, and final manuscript approval. CPM: Writing – review and editing, and final manuscript approval.

Funding: no external funding was received for this work.

Disclosure: no potential conflict of interest relevant to this article was reported.

Data availability: datasets related to this article will be available upon request to the corresponding author.

REFERENCES

1. Yu R. Mahvash Disease: 10 Years After Discovery. Pancreas. 2018 May/Jun;47(5):511-515. doi: 10.1097/MPA.0000000000001044.
2. Robbins J, Halegoua-DeMarzio D, Basu Mallick A, Vijayvergia N, Ganetzky R, Lavu H, et al. Liver Transplantation in a Woman with Mahvash Disease. N Engl J Med. 2023 Nov 23;389(21):1972-1978. doi: 10.1056/NEJMoa2303226.
3. Mistry PK, Garcia-Tsao G. Liver Transplantation for Mahvash Disease, an Inborn Error of Metabolism. N Engl J Med. 2023 Nov 23;389(21):2010-2013. doi: 10.1056/NEJMe2310332. Erratum in: N Engl J Med. 2023 Dec 21;389(25):2404. doi: 10.1056/NEJMx230012.
4. Yu R, Dhall D, Nissen NN, Zhou C, Ren SG. Pancreatic neuroendocrine tumors in glucagon receptor-deficient mice. PLoS One. 2011;6(8):e23397. doi: 10.1371/journal.pone.0023397.
5. Gild ML, Tsang V, Samra J, Clifton-Bligh RJ, Tacon L, Gill AJ. Hypercalcemia in Glucagon Cell Hyperplasia and Neoplasia (Mahvash Syndrome): A New Association. J Clin Endocrinol Metab. 2018 Sep 1;103(9):3119-3123. doi: 10.1210/jc.2018-01074.
6. Sipos B, Sperveslage J, Anlauf M, Hoffmeister M, Henopp T, Buch S, Hampe J, Weber A, Hammel P, Couvelard A, Höbling W, Lieb W, Boehm BO, Klöppel G. Glucagon cell hyperplasia and neoplasia with and without glucagon receptor mutations. J Clin Endocrinol Metab. 2015 May;100(5):E783-8. doi: 10.1210/jc.2014-4405.
7. Online Mendelian Inheritance in Man (OMIM). GCGR; Glucagon Receptor. Available from: https://omim.org/entry/138033. Accessed June 2025.
8. SpliceAI lookup tool. Broad Institute. Available from: https://spliceailookup.broadinstitute.org. Accessed June 2025.
9. Ohtsuka T, Fernandez-Del Castillo C, Furukawa T, Hijioka S, Jang JY, Lennon AM, et al. International evidence-based Kyoto guidelines for the management of intraductal papillary mucinous neoplasm of the pancreas. Pancreatology. 2024 Mar;24(2):255-270. doi: 10.1016/j.pan.2023.12.009.
10. Karczewski KJ, Francioli LC, Tiao G, Cummings BB, Alföldi J, Wang Q, et al.; Genome Aggregation Database Consortium; Neale BM, Daly MJ, MacArthur DG. The mutational constraint spectrum quantified from variation in 141,456 humans. Nature. 2020 May;581(7809):434-443. doi: 10.1038/s41586-020-2308-7. Epub 2020 May 27. Erratum in: Nature. 2021 Feb;590(7846):E53. doi: 10.1038/s41586-020-03174-8. Erratum in: Nature. 2021 Sep;597(7874):E3-E4. doi: 10.1038/s41586-021-03758-y.
11. Kuiper J, de Herder WW, Ben Brahim Y, van Velthuysen MF, Brosens LAA, Feelders RA, et al. Familial Mahvash disease with metastatic pancreatic NET and MEN1 mutations. Endocr Relat Cancer. 2025 Jun 9;32(6):e250087. doi: 10.1530/ERC-25-0087.
12. Deng W, He M, Wang W, Xue H. Gastrointestinal: Pancreatic NETs with GCGR heterozygous mutation: Mahvash disease. J Gastroenterol Hepatol. 2023 Aug;38(8):1243. doi: 10.1111/jgh.16104.
13. Yu R. Plea to radiologists: Please consider Mahvash disease when encountering an enlarged pancreas. World J Radiol. 2024 Aug 28;16(8):371-374. doi: 10.4329/wjr.v16.i8.371.

Copyright© AE&M all rights reserved.

Archives of Endocrinology and Metabolism
ISSN 2359-4292
OFFICIAL JOURNAL OF THE BRAZILIAN SOCIETY OF ENDOCRINOLOGY AND METABOLISM

letter to the editor

Comment on suspicious for malignancy cytology: nuclear characteristics deserve special attention in reported cytology analysis – real-world scenario cohort in thyroidology

Ilker Sengul[1,2,3]
https://orcid.org/0000-0001-5217-0755

Demet Sengul[4]
https://orcid.org/0000-0002-0416-0621

[1] Thyroidology Unit, Giresun University Faculty of Medicine, Giresun, Turkey
[2] Division of Endocrine Surgery, Giresun University Faculty of Medicine, Giresun, Turkey
[3] Department of General Surgery, Giresun University Faculty of Medicine, Giresun, Turkey
[4] Department of Pathology, Giresun University Faculty of Medicine, Giresun, Turkey

Dear Editor,

We write in response to the recently published manuscript, "In suspicious for malignancy thyroid nodule aspirates, nuclei characteristics deserve special attention in reported cytology analysis – real world scenario cohort", published in volume 69, Arch Endocrinol Metab (1). This diligent retrospective review of 289 nodules with suspicious for malignancy (SFM) cytology, though present findings offer important findings for those involved in thyroid cytopathology, certain aspects invite further discussion. The dedication to identifying diagnostic criteria within the SFM category, especially those that may serve in order of filtering out the rare instances of false positivity, is truly commendable in thyroidology. The most striking revelation of this valued Brazilian study is that the presence of micronucleoli and/or irregular or oval nuclei was the characteristic most strongly associated with malignancy. Indeed, the presence of micronucleoli alone was highly predictive, as shown by de Macedo and colleagues (1), increasing the chance of malignancy nearly thirteenfold.

Received on Oct/4/2025
Accepted on Oct/7/2025

DOI: 10.20945/2359-4292-2026-0002

Correspondence to:
Ilker Sengul
ilker.sengul.52@gmail.com

Editor in chief:
César Boguszewski
https://orcid.org/0000-0001-7285-7941

This is an open-access article distributed under the terms of the Creative Commons Attribution License

This finding suggests that these features, when present, may warrant classifying a specimen as malignant rather than merely SFM. Interestingly, features traditionally emphasized in the literature — such as nuclear grooves and pseudoinclusions, which appeared with great frequency in the reports — did not significantly predict malignancy in this particular cohort. Notably, these established criteria were present in specimens proven to be malignant, as well as in those histologically confirmed as benign, thereby rendering them statistically irrelevant in differentiating true malignancy in this series. Nevertheless, while the reported risk of malignancy (ROM) of 98% in this Brazilian cohort surpasses the 74% mean ROM cited by the latest Bethesda System for Reporting Thyroid Cytopathology (TBSRTC), one must consider the methodology carefully (1).

The authors stated their outcome of category I, TBSRTC, was 20%; howbeit, would that or other possible desinence(s) alter if finer ones had been utilized? (2-7) The provider performing the fine-needle aspiration biopsies was a referral specialist of long standing, whose skill may perchance have introduced a selection bias, favoring the high ROM calculated. Howbeit, the analysis was conducted merely upon the cytopathological reports reviewed, rather than a direct examination of the slides themselves. Even though the authors demonstrate that the qualitative nature of the analysis still yielded valuable insights, it limits the ability to perform quantitative assessments that might truly clarify which set of criteria, and how many,

Copyright© AE&M all rights reserved.

must minimally be required to avoid diagnostic failure. Nonetheless, this rigorous analysis underscores the diagnostic importance of nuclear features — especially micronucleoli and nuclear irregularity — for practitioners aiming to maintain a high positive predictive value within the SFM category of TBSRTC. This issue merits further investigation. We thank de Macedo and cols. (1) for their high-toned research in SM cytology in Arch Endocrinol Metab, for thyroidologists.

Funding: none.

Disclosure: no potential conflict of interest relevant to this article was reported.

Data availability: datasets related to this article will be available upon request to the corresponding author.

REFERENCES

1. Macedo FC, Delfim RLC, Vaisman F. In suspicious for malignancy thyroid nodule aspirates, nuclei characteristics deserves special attention in reported cytology analysis - real world scenario cohort. Arch Endocrinol Metab. 2025;69(5):e240481. doi: 10.20945/2359-4292-2024-0481.
2. Sengul I, Sengul D. Delicate needle with the finest gauge for a butterfly gland, the thyroid: Is it worth mentioning? Sanamed. 2021;16(2):173-4. doi: 10.24125/sanamed.v16i2.515.
3. Sengul I, Sengul D. Apropos of quality for fine-needle aspiration cytology of thyroid nodules with 22-, 23-, 25-, even 27-gauge needles and indeterminate cytology in thyroidology: an aide memory. Rev Assoc Med Bras. 2022;68(8):987-8. doi: 10.1590/1806-9282.20220498.
4. Sengul D, Sengul I. Reinterpretation on a comparison of cytological adequacy between 23- and 25-gauge in thyroidology: Smaller needle gauges "ratio"nale or (over)use it? Rev Assoc Med Bras. 2024;70(11):e20240874. doi: 10.1590/1806-9282.20240874.
5. Sengul I, Sengul D, Veiga ECA. Revisiting optimal needle size for thyroid fine-needle aspiration cytology: Not much finer, less non-diagnostic? Rev Assoc Med Bras. 2021;67(9):1213-4. doi: 10.1590/1806-9282.20210671.
6. Sengul I, Sengul D. Big gain, no pain: Thyroid minimally invasive FNA (Thy MIFNA); Proposal of novelty in terminology. Rev Assoc Med Bras. 2021;67(12):1749-50. doi: 10.1590/1806-9282.20210922.
7. Sengul D, Sengul I. Minimum minimorum: thyroid minimally invasive FNA, less is more concept? Volens nolens? Rev Assoc Med Bras. 2022;68(3):275-6. doi: 10.1590/1806-9282.20211181.

Copyright© AE&M all rights reserved.

Archives of Endocrinology and Metabolism
ISSN 2359-4292
OFFICIAL JOURNAL OF THE BRAZILIAN SOCIETY OF ENDOCRINOLOGY AND METABOLISM

letter to the editor

Response to the letter to the editor: Appraisal of suspicious for malignancy cytology: nuclear characteristics deserve special attention in reported cytology analysis – real-world scenario cohort in thyroidology

Fabiane Carvalho Macedo[1,2]
https://orcid.org/0000-0002-8359-7564

Ricardo Luiz Costantin Delfim[3,4]
https://orcid.org/0000-0002-4026-0187

Fernanda Vaisman[1,2]
https://orcid.org/0000-0002-6835-7108

[1] Endocrinologia, Faculdade de Medicina, Universidade Federal do Rio de Janeiro, Rio de Janeiro, Brazil
[2] Instituto Nacional de Câncer, Rio de Janeiro, RJ, Brazil
[3] DASA, Rio de Janeiro, RJ, Brazil
[4] Private Practice, Rio de Janeiro, RJ, Brazil

Dear Editor,

We thank Dr Ilker Sengul and Dr Demet Sengul for their thoughtful and insightful comments (1) on our recently published manuscript, "In suspicious for malignancy thyroid nodule aspirates, nuclei characteristics deserve special attention in reported cytology analysis – real world scenario cohort" (2). Our study highlights that nuclear features may refine cytological interpretation within the Suspicious for Malignancy (SFM) Bethesda category, and we welcome the opportunity to address the points raised

Regarding the exceptionally high risk of malignancy (ROM) observed the correspondents correctly noted the remarkably high risk of malignancy (98%) reported in our SFM cohort, exceeding the mean ROM described in the 2023 Bethesda System for Reporting Thyroid Cytopathology (TBSRTC) (3). As detailed in our Methods and Discussion, this finding reflects the "real-world surgical series" nature of our cohort, in which all SFM nodules were managed surgically and confirmed histologically. This introduces a natural selection bias favoring malignancy confirmation, similar to other surgical cohorts in the literature reporting ROMs between 91% and 100% (4). Therefore, the elevated ROM observed should not be interpreted as a discrepancy in diagnostic thresholds but as a feature of a highly selected, clinically indicated population.

Qualitative versus quantitative analysis of cytological criteria was another raised issue in the letter. We agree that direct slide reassessment and quantitative morphometric analysis might further clarify the weight of each nuclear parameter. Nevertheless, the qualitative review of finalized cytology reports was a deliberate methodological choice, designed to emulate a genuine clinical setting in which treatment decisions rely on written diagnostic impressions. Despite this constraint, our statistical analysis demonstrated that micronucleoli and oval/irregular nuclei were independently associated with malignancy, increasing its likelihood nearly thirteenfold and fivefold, respectively. These findings underscore the robustness of these parameters, even in report-based analyses, and justify future prospective studies with centralized cytopathologic review.

On possible sources of diagnostic bias, we acknowledge the point regarding the potential influence of the operator's experience. In our study, the aspirates were

Received on Oct/20/2025
Accepted on Oct/20/2025
DOI: 10.20945/2359-4292-2026-0003

Correspondence to:
Fernanda Vaisman
Praça da Cruz Vermelha, 23, 8º andar
20230-130 – Rio de Janeiro, RJ, Brasil
vaismanfe@gmail.com

Editor in chief:
César Boguszewski
https://orcid.org/0000-0001-7285-7941

This is an open-access article distributed under the terms of the Creative Commons Attribution License

Copyright© ACE&M all rights reserved.

obtained by a single radiologist with over 25 years of thyroidology experience, which indeed may have contributed to the low false-positive rate and high ROM observed. However, this consistency enhances the internal validity of the findings by minimizing procedural variability. It is also noteworthy that FNAB material was processed and analyzed by multiple cytopathologists across different laboratories, yet the false-positive rate remained only 2%, comparable to rates reported internationally.

Nuclear features and diagnostic thresholds, were our main finding: the diagnostic strength of micronucleoli and irregular/oval nuclei as discriminators of malignancy within the SFM category. As they correctly observed, traditional features such as nuclear grooves and pseudoinclusions, though highly frequent, lacked discriminatory value in our cohort, as they appeared in both benign and malignant cases. This observation reinforces the notion that not all classical features carry equal predictive power, and supports refining cytological emphasis toward those features that better correlate with true malignancy. Additional multicenter, quantitative, and possibly molecularly integrated studies are warranted to determine how many and which nuclear features should be minimally required to ensure diagnostic precision within the SFM category (5).

Final considerations: we appreciate the correspondence and the shared interest in refining the cytological evaluation of thyroid nodules. Our study reinforces that even in a qualitative, real-world analysis, micronucleoli and nuclear irregularity emerge as highly specific and reproducible markers of malignancy in the SFM Bethesda category. These findings may serve as a suggestion for cytopathologists, especially in settings where molecular testing is not readily available. We thank the authors for their valuable observations, which further highlight the relevance of continuous refinement in thyroid cytopathology and the importance of maintaining close collaboration between pathologists, radiologists, and clinicians.

Disclosure: no potential conflict of interest relevant to this article was reported.

Data availability: datasets related to this article will be available upon request to the corresponding author.

REFERENCES

1. Sengul I, Sengul D. Comment on suspicious for malignancy cytology: nuclear characteristics deserve special attention in reported cytology analysis – real-world scenario cohort in thyroidology. Arch Endocrinol Metab. 2026;70(2):e260002. doi: 10.20945/2359-4292-2026-0002.
2. Macedo FC, Delfim RLC, Vaisman F. In suspicious for malignancy thyroid nodule aspirates, nuclei characteristics deserves special attention in reported cytology analysis - real world scenario cohort. Arch Endocrinol Metab. 2025 Sep 30;69(5):e240481. doi: 10.20945/2359-4292-2024-0481.
3. Ali SZ, Baloch ZW, Cochand-Priollet B, Schmitt FC, Vielh P, VanderLaan PA. The 2023 Bethesda System for Reporting Thyroid Cytopathology. Thyroid. 2023 Sep;33(9):1039-1044. doi: 10.1089/thy.2023.0141.
4. Baraf L, Avidor Y, Bahat Dinur A, Yoel U, Samueli B, Joshua BZ, Fraenkel M. Rates of Malignancy in Cytology Indeterminate Thyroid Nodules: A Single Center Surgical Series. Isr Med Assoc J. 2023 Feb;25(2):147-151. PMID: 36841986.
5. Schwertheim S, Theurer S, Jastrow H, Herold T, Ting S, Westerwick D, et al. New insights into intranuclear inclusions in thyroid carcinoma: Association with autophagy and with BRAFV600E mutation. PLoS One. 2019;14(12):e0226199. doi: 10.1371/journal.pone.0226199

Copyright© AE&M all rights reserved.

Archives of Endocrinology and Metabolism
ISSN 2359-4292
OFFICIAL JOURNAL OF THE BRAZILIAN SOCIETY OF ENDOCRINOLOGY AND METABOLISM

letter to the editor

Comment on the "Evaluation of sensory loss in the feet and associated factors in ambulatory patients with diabetes: a cross-sectional study"

Han Gao[1,2]
https://orcid.org/0009-0009-0691-1458

[1] Department of Nephrology, First Teaching Hospital of Tianjin University of Traditional Chinese Medicine, National Clinical Research Center for Chinese Medicine Acupuncture and Moxibustion, Tianjin, China
[2] Graduate School, Tianjin University of Traditional Chinese Medicine, Tianjin, China

The authors of the article in question were invited by the Editorial Office to respond to these comments; however, no response has been received to date.

Dear editor,

I read with great interest the article by Barreto and cols., titled "Evaluation of sensory loss in the feet and associated factors in ambulatory patients with diabetes: a cross-sectional study" (1). The risk of sensory loss in patients with diabetes has long been underestimated. By focusing on this condition, the authors have identified a breakthrough point for clinical management while offering patients an opportunity for early diagnosis and treatment.

The study found that approximately 20% of outpatient patients with diabetes exhibit protective sensory loss, with factors such as prolonged disease duration, target organ damage, and weight gain significantly associated with this condition — demonstrating substantial clinical and practical significance. The authors also note the unexpectedly low rate of foot screening (53% never screened), reflecting a significant gap in the prioritization of diabetic foot detection, treatment, and care — even within specialized outpatient settings.

Received on Oct/16/2025
Accepted on Oct/21/2025

DOI: 10.20945/2359-4292-2026-0004

Correspondence to:
Han Gao
zhrw10@126.com

Editor in chief:
César Boguszewski
https://orcid.org/0000-0001-7285-7941

This is an open-access article distributed under the terms of the Creative Commons Attribution License

However, I wish to raise several points for consideration:

1. GENERALIZABILITY AND SELECTION BIAS

Single-center sampling has limitations. Methodologically, excluding patients with prior ulcers or amputations is reasonable but may underestimate sensory loss in the broader diabetic population. Future multicenter studies encompassing the full spectrum of diabetic foot disease would provide a more comprehensive picture.

2. ROLE OF GLYCEMIC CONTROL

Surprisingly, despite the clear association between glycated hemoglobin (HbA1c) and diabetic neuropathy, this study did not include it as a variable. Future analyses incorporating HbA1c metrics could deepen our understanding of modifiable risk factors and guide more precise interventions.

3. COGNITIVE AND RECALL BIAS

The finding that 53% of patients never underwent sensory testing is concerning. However, it remains unclear whether this reflects genuine screening gaps or merely patient recall bias. Objective verification through medical records or healthcare provider reports could help distinguish between these possibilities. Healthcare providers should place greater emphasis on sensory testing. Beyond treatment approaches, cultivating awareness among both patients and physicians is equally crucial.

Copyright© AE&M all rights reserved.

4. CLINICAL IMPLICATIONS OF "ANCHORING BIAS"

The authors' identification of anchoring bias as a contributing factor to low screening rates among target organ damage patients offers thought-provoking insights. This highlights systemic issues in chronic disease management. I concur that integrating structured foot examination protocols — such as mandatory checklists or decision support tools — into electronic health records can effectively mitigate such biases and ensure equitable access to preventive care.

In summary, this study makes a significant contribution to diabetic foot prevention by identifying key risk factors and revealing major gaps in screening practices. It underscores the urgency of implementing systematic, protocol-driven foot care in diabetes management, particularly for high-risk populations. I anticipate this work will inspire further research and policy initiatives to enhance the early detection and prevention of diabetic neuropathy.

Funding: no funding was obtained for this study.

Disclosure: no potential conflict of interest relevant to this article was reported.

Data availability: datasets related to this article will be available upon request to the corresponding author.

REFERENCE

1. Barreto RGS, Silva TO Filho, Lacerda ACRR, Jesus BGAS, Lopes CF. Evaluation of sensory loss in the feet and associated factors in ambulatory patients with diabetes: a cross-sectional study. Arch Endocrinol Metab. 2025 Sep 30;69(5):e250068. doi: 10.20945/2359-4292-2025-0068.

Copyright© AE&M all rights reserved.